UNIVERSITÀ
DEGLI STUDI
DI PADOVA

Sede Amministrativa: Università degli Studi di Padova

Dipartimento di Ingegneria Industriale

SCUOLA DI DOTTORATO DI RICERCA IN: INGEGNERIA INDUSTRIALE
INDIRIZZO: INGEGNERIA CHIMICA, DEI MATERIALI E MECCANICA
CICLO XXVIII

IMPLEMENTING "QUALITY BY DESIGN" IN THE PHARMACEUTICAL INDUSTRY: A DATA-DRIVEN APPROACH

Direttore della Scuola: Ch.mo Prof. Paolo Colombo
Coordinatore d'indirizzo: Ch.mo Prof. Enrico Savio
Supervisore: Ch.mo Prof. Massimiliano Barolo

Dottoranda: Natascia Meneghetti

Foreword

The realization of the work included in this Dissertation involved the intellectual and financial support of many people and institutions, to whom the author is very grateful.
Most of the research activity that led to the results reported in this Dissertation has been carried out at CAPE-Lab, Computer-Aided Process Engineering Laboratory, at the Department of Industrial Engineering of the University of Padova (Italy), under the supervision of Prof. Massimiliano Barolo and Prof. Fabrizio Bezzo. Part of the work was carried out at Process Systems Enterprise, London (U.K.) during a 6-month stay under the supervision of Dr. Sean Bermingham, and part represents a collaboration with Dr. Simeone Zomer from GlaxoSmithKline, Ware (U.K.).
Financial support to this study has been provided by the University of Padova. The author is grateful also to "Fondazione Ing. Aldo Gini" (Padova, Italy) and to LLP/Erasmus Placement_SMP program (University of Padova, Italy) for their financial support for the project carried out at PSE.

All the material reported in this Dissertation is original, unless explicit references to studies carried out by other people are indicated. In the following, a list of the publications stemmed from this project is reported.

CONTRIBUTIONS IN PEER-REVIEWED JOURNALS

Facco, P., F. Dal Pastro, N. Meneghetti, F. Bezzo, M. Barolo (2015). Bracketing the design space within the knowledge space in pharmaceutical product development. *Ind. Eng. Chem. Res.*, **54**, 5128–5138.
Meneghetti, N., P. Facco, F. Bezzo, M. Barolo (2014). A methodology to diagnose process/model mismatch in first-principles models. *Ind. Eng. Chem. Res.*, **53**, 14002-14013

CONTRIBUTIONS IN PEER-REVIEWED JOURNALS (submitted)

Meneghetti N., P. Facco, F. Bezzo, C. Himawan, S. Zomer, M. Barolo (2016). Knowledge management in secondary pharmaceutical manufacturing by mining of data historians – A proof-of-concept study, submitted to: *Int. J. Pharm.*

CONTRIBUTIONS IN PEER-REVIEWED CONFERENCE PROCEEDINGS

Meneghetti N., P. Facco, F. Bezzo, C. Himawan, S. Zomer, M. Barolo (2016). Automated Data Review in Secondary Pharmaceutical Manufacturing by Pattern Recognition Techniques, to be presented at: ESCAPE 26, 26th European Symposium on Computer-Aided Process Engineering (Portorož, Slovenia, 12-15 June 2016).
Meneghetti, N., P. Facco, S. Bermingham, D. Slade, F. Bezzo, M. Barolo (2015). First-principles model diagnosis in batch systems by multivariate statistical modeling. In: *Computer-Aided Chemical Engineering 37, 12th International Symposium on Process Systems Engineering and 25th European Symposium on Computer Aided Process Engineering* (K.V. Gernaey, J.K. Huusom, R. Gani, Eds.), Elsevier, Amsterdam (The Netherlands), 437-442.
Meneghetti, N., P. Facco, F. Bezzo, M. Barolo (2014). Diagnosing process/model mismatch in first-principles models by latent variable modeling. In: *Computer-Aided Chemical Engineering 33, 24th*

European Symposium on Computer Aided Process Engineering (J.J. Klemeš, P.S. Varbanov, P.Y. Liew, Eds.), Elsevier, Amsterdam (The Netherlands) 1897-1902.

CONFERENCE PRESENTATIONS

Meneghetti, N., P. Facco, F. Bezzo, M. Barolo (2015) First-principles models enhancement by latent variable models. Oral presentation at: *Workshop Italiano di Chemiometria 2015,* February 25-27, Roma (Italy).

Meneghetti, N., P. Facco, F. Bezzo, M. Barolo (2014). Process/model mismatch diagnosis by latent variable modeling. Poster presentation at: *APM – Advanced Process Modelling Forum,* April 2-3*,* London (U.K.).

Abstract

Traditionally, the pharmaceutical industry is characterized by of peculiar characteristics (e.g., low production volumes, multi-products manufacturing based mainly on batch processes, strict regulatory framework) that make the implementation of modern quality principles more complex for this sector. However, the innovation gap with respect to other manufacturing industries is gradually reducing thanks to the introduction of the *Quality-by-Design* initiative by the Regulatory Agencies (such as the Food and Drug Administration, FDA and the European Medicines Agency, EMA). QbD is based on the concept that quality should be designed *into* a product, by a thorough understanding of product and processes features and risks. This initiative aims to support the transition of the pharmaceutical industry to a systematic approach based on scientific (rather than empiric) knowledge of products and processes, in order to facilitate the implementation of modern management tools, advanced technologies and innovative solutions.

Under this perspective, the application of Process Systems Engineering (PSE) solutions has rapidly grown. Despite the challenges encountered to adapt classical PSE approaches (mainly based on the use of mathematical modeling) to a pharmaceutical context, the benefits achieved by the use of PSE tools to support the implementation of QbD, opened the route to several studies in this field. Significant improvements have been observed in product quality and process capability and robustness thanks to the increase of process and product knowledge and understanding provided by modeling. This has allowed the pharmaceutical industries to accelerate the launch of new products into the market, to improve productivity and to reduce costs.

Although, in many PSE applications, first-principles models are preferred, the use of data-driven tools, such as latent variable modeling or pattern recognition techniques, is rapidly expanding. Thanks to the increasing availability of measurement data, these techniques have been demonstrated to be an optimal opportunity to address several problems that characterize pharmaceutical development and manufacturing activities.

The main objective of the research presented in this Dissertation is to demonstrate how these data-driven modeling techniques can be used to address some common issues that often affect the practical implementation of QbD paradigms in pharmaceutical development and manufacturing activities. Novel and general methodologies based on these techniques are presented with the aim of: *i*) supporting the diagnosis of first-principles models of pharmaceutical operations; *ii*) supporting the implementation of some fundamental QbD elements, such as the identification of the design space (DS) of a new pharmaceutical product, as well as continual improvement paradigms by periodic review of large manufacturing databases.

With respect to **first-principle models diagnosis**, a methodology is proposed to diagnose the root cause of the process/model mismatch (PMM) that may arise when a first-principles (FP) model is challenged against a set of historical experimental data. The objective is to identify which model equations or model parameters most contribute to the observed mismatch, without carrying out any additional experiment. The methodology exploits the available historical and simulated data, generated respectively by the process and by the FP model using the same set of inputs. A data-driven model (namely, a latent variable one) is used to analyze the correlation structure of the historical and simulated datasets, and information on where the PMM originates from is obtained using diagnostic indices and engineering judgment. The methodology is first tested on two simulated steady-state systems (a jacket-cooled continuous stirred reactor and a solids milling unit), and then it is extended to dynamic systems (a drying unit and a penicillin fermentation process). It is shown that the proposed methodology is able to pinpoint the model section(s) that actually originate the mismatch.

With respect to the **design space identification** issue, a methodology is proposed to limit the extension of the domain over which experiments are carried out to determine the DS of a new pharmaceutical product. In fact, for a new pharmaceutical product to be developed a reliable first-principles model is often not available. In this case, the DS is found using experiments carried out within a domain of input combinations (the so-called knowledge space; e.g. raw materials properties and process operating conditions) that result from products that have already been developed and are similar to the new one. The proposed methodology aims at segmenting the knowledge space in such a way as to identify a subspace of it (called the experiment space) that most likely brackets the DS, in order to limit the extension of the domain over which the new experiments should be carried out. The methodology is based on the inversion of the latent-variable model used to describe the system (accounting also for model prediction uncertainty) in order to identify a reduced area of the knowledge space wherein the design space is supposed to lie. Three different case studies are presented to demonstrate the effectiveness of the proposed methodology.

Finally, with respect to the **periodic review of large manufacturing databases**, a methodology is proposed to systematically extract operation-relevant information from data historians of secondary pharmaceutical manufacturing systems. This operation may result particularly burdensome, not only because of the very large dimension of the datasets (which may reach millions of data entries) but also because not even the number of the operations completed in a given time window may be known a priori. The proposed methodology permits not only to automatically identify the number of batches carried out in a given time window, but also to assess how many different products have been manufactured, and whether or not the features characterizing a batch have changed throughout a production campaign. The results achieved by

testing the proposed methodology on two six-month datasets of a commercial-scale drying unit demonstrate the potential of this approach, which can be easily extended to other manufacturing operations.

Riassunto

Negli anni, l'industria farmaceutica ha sviluppato un forte carattere bipolare: se da un lato è stata in grado di lanciare sul mercato prodotti sempre più avanzati, in grado di rispondere alle esigenze di una società in continua evoluzione, dall'altro ha conservato una filosofia di produzione basata soprattutto sull'esperienza più che sul rinnovamento e l'utilizzo di tecnologie avanzate. La motivazione risiede in parte nel fatto che l'industria farmaceutica è caratterizzata da una serie di fattori (ad esempio bassi volumi di produzione, processi prevalentemente di tipo batch e un quadro normativo rigido) che rendono effettivamente più difficile l'attuazione delle moderne filosofie di produzione basate su principi di rinnovamento continuo. Tuttavia, negli ultimi decenni, il divario con le industrie di produzione più mature si sta gradualmente riducendo grazie al lancio di una nuova iniziativa da parte delle agenzie regolatore internazionali, basata del concetto di *Quality by Design* (QbD). Questa iniziativa si fonda nella convinzione che la qualità di un prodotto dovrebbe essere concepita come parte integrante *della progettazione* del prodotto stesso e del suo processo produttivo, ottenuti grazie ad una conoscenza approfondita delle caratteristiche e dei rischi legati allo sviluppo del prodotto e del processo di produzione. L'iniziativa quindi, mira a sostenere la transizione dell'industria farmaceutica verso un approccio sistematico per favorire soluzioni innovative, l'applicazione di conoscenze scientifiche e tecniche avanzate, nonché di moderni sistemi di gestione della qualità nello sviluppo dei prodotti e dei processi produttivi. Questo rinnovamento dovrebbe garantire negli anni una serie di benefici sia economici (come la riduzione del tempo necessario per il lancio di nuovi prodotti sul mercato, il miglioramento della produttività e la riduzione dei costi di produzione) sia sociali (come la garanzia di fornire prodotti di qualità e assicurare tale qualità nel tempo).

In questo contesto, è di fondamentale importanza l'utilizzo di strumenti di modellazione matematica avanzata, già largamente utilizzati in altri e più maturi settori di produzione. Nonostante le difficoltà incontrate per adattare questi strumenti alle esigenze delle applicazioni farmaceutiche, i vantaggi dell'utilizzo della modellazione nell'attuazione dei principi di QbD hanno aperto la strada a diversi studi in questo campo. Negli anni, l'utilizzo di questi strumenti ha permesso di ottenere miglioramenti significativi sia nella qualità dei prodotti processati, sia nella capacità e affidabilità dei processi di produzione. La modellazione di processo si basa principalmente su due tipi di approcci: il primo (modelli a principi primi) riguarda la rappresentazione matematica delle leggi fisiche alla base di un sistema, ad esempio bilanci di materia ed energia, il secondo (modelli basati su dati o *data-driven*) si fonda sull'utilizzo dell'informazione contenuta nei dati ottenuti dal sistema stesso. Anche se in molte applicazioni si predilige l'utilizzo di modelli principi primi, non sempre questo tipo di modelli sono disponibili. Per questo, l'uso di modelli *data-driven*, come per esempio di tecniche di modellazione a variabili

latenti (LVM, *latent variable models*) o tecniche di riconoscimento di *pattern*, è in rapida espansione. Grazie alla crescente disponibilità di dati, queste tecniche sono state in grado di dimostrare la loro efficacia nel risolvere diversi problemi che caratterizzano le diverse attività farmaceutiche. L'obiettivo di questa Dissertazione è quello di dimostrare come queste tecniche possano essere utilizzate per risolvere alcuni problemi spesso riscontrati nell'implementazione pratica dei paradigmi di QbD nell'industria farmaceutica. A tal proposito, vengono presentate delle metodologie innovative e generali basate sull'impiego di modelli *data-driven* con l'obiettivo di: *i*) consentire il miglioramento dei modelli di principi primi per facilitare il loro impiego nella modellazione di sistemi farmaceutici; *ii*) condurre alcune delle attività nelle quali un approccio QbD può tradursi, come l'identificazione dello spazio di progetto (*design space*) di un prodotto farmaceutico e l'analisi critica di voluminose raccolte di dati storici di processo.

Per quanto riguarda il **miglioramento di modelli a principi primi**, è stata sviluppata una metodologia per identificare la causa principale delle differenze (o *process/model mismatches*) che possono presentarsi tra i dati storici sperimentali e le stime fornite da un modello a principi primi. L'obiettivo è di identificare quali equazioni o parametri del modello contribuiscano maggiormente alla differenza osservata, senza effettuare alcuna ulteriore esperimento. La metodologia sfrutta i dati storici disponibili e un set di dati simulati, generati dal modello a principi primi utilizzando le stesse condizioni alle quali sono stati ottenuti i dati storici. Grazie all'utilizzo di un modello a variabili latenti, viene analizzata e confrontata la struttura di correlazione dei due set di dati disponibili, quello storico e quello e simulato, in modo da ricavare informazioni utili ad identificare la causa della scarsa accuratezza del modello. Per valutare l'efficacia della metodologia, nel Capitolo 3 vengono considerati due sistemi simulati in stato stazionario: un reattore continuo agitato e incamiciato e un molino. Nel Capitolo 4 la metodologia viene estesa e adattata a sistemi dinamici, considerando altri due processi simulati: un'unità di essiccazione e un fermentatore per la produzione di penicillina. I risultati ottenuti dimostrano che la metodologia proposta è in grado di indicare un gruppo di termini molto correlati tra loro, o addirittura un solo termine, che effettivamente contengono la reale causa d'errore nel modello. Sebbene la metodologia proposta sia stata sviluppata per analizzare modelli a principi primi di processi farmaceutici, essa può essere facilmente estesa a qualsiasi altro modello in regime stazionario o dinamico.

Nel Capitolo 5, vengono discussi i problemi relativi **all'identificazione dello spazio di progetto** (*design space*, DS) per un nuovo prodotto farmaceutico caratterizzato da singola specifica di qualità, nel caso in cui non sia disponibile un modello a principi primi da utilizzare per determinare tale spazio. In questi casi, lo spazio di progetto viene spesso identificato utilizzando gli esperimenti effettuati in un dominio (*knowledge space*) costituito dalle combinazioni delle condizioni operative di processo e delle proprietà delle materie prime utilizzate per la produzione

di prodotti già sviluppati, e simili al nuovo prodotto. Spesso, il numero di esperimenti da effettuare per identificare lo spazio del progetto all'interno di tale dominio è elevato. Per questo motivo, viene proposta una metodologia per identificare uno spazio limitato all'interno di questo dominio, detto spazio degli esperimenti (*experiment space*), che contiene lo spazio di progetto, in modo da ridurre notevolmente il numero di nuovi esperimenti necessari. La metodologia si basa sull'inversione del modello a variabili latenti utilizzato per descrivere il sistema, tenendo conto anche dell'incertezza del modello stesso. Lo spazio degli esperimenti viene stimato per tre diversi sistemi (due simulati e uno reale), dimostrando in tutti i casi l'efficacia della metodologia proposta.

Infine, per quanto riguarda **l'analisi critica di set di dati di produzione**, nel Capitolo 6 viene proposta una metodologia per estrarre in modo sistematico informazioni dai dati di grandi database storici di impianti produttivi industriali. Queste informazioni, possono essere utilizzate per individuare rapidamente potenziali aree di miglioramento, in modo da favorirne l'implementazione di paradigmi di miglioramento continuo. Trasformare in conoscenza questi dati, è particolarmente difficile perché spesso non si conosce nemmeno il numero dei batch effettuati in un certo periodo di produzione. La metodologia presentata consente di determinare automaticamente il numero di batch effettuati in un determinato intervallo di tempo e il numero di prodotti processati, e se le caratteristiche che contraddistinguono una certa produzione siano cambiate nel corso di campagne diverse. La metodologia proposta, basata sull'utilizzo di tecniche di riconoscimento di *pattern*, è stata utilizzata per analizzare due set di dati industriali relativi a sei mesi di produzione ciascuno. I risultati ottenuti dimostrano chiaramente il potenziale dell'approccio proposto.

Table of contents

List of acronyms

CDER	=	Center for Drug Evaluation and Research
CFD	=	computational fluid dynamics
CPP	=	critical process parameter
CSTR	=	continuous stirred tank reactor
CQA	=	critical-to-quality attribute
DAE	=	differential algebraic equation
DEM	=	discrete element method
DD	=	data-driven
DB	=	data-based
DoE	=	design of experiments
DS	=	design space
EMA	=	European Medicines Agency
FDA	=	Food and Drug Administration
FP	=	first-principles
ICH	=	International Conference on Harmonization of Technical Requirements for Registration of Pharmaceuticals for Human Use
KD	=	knowledge-driven
k-NN	=	k-nearest neighbor
LV	=	latent variable
LVM	=	latent variable model
LVRM	=	latent variable regression model
MPCA	=	multiway principal component analysis
MBDoE	=	model-based design of experiments
MSPC	=	multivariate statistical process control
NIPALS	=	nonlinear iterative partial least squares
NME	=	new molecular entity
ODE	=	ordinary differential equation
OPQ	=	office of pharmaceutical quality
PAT	=	process analytical technology
PBM	=	population balance model
PC	=	principal component

PCA = principal component analysis
PDE = partial differential equation
PLS = projection to latent structures
PMM = process-model mismatch
PQS = pharmaceutical quality system
PSD = particle size distribution
PSE = process systems engineering
QbD = quality-by-design
QTPP = quality target product profile
RSM = response surface model
SPE = squared prediction error
SVD = singular value decomposition
TDS = true design space

Chapter 1.

Motivation and state of the art

This Chapter provides an overview of the background and the motivations of this Dissertation. First, the current situation of the pharmaceutical industry and the main aspects of Quality-by-Design (QbD) initiative, as well as its main contributions to pharmaceutical development and manufacturing, are presented. Then, the significance of this concept and the opportunities it gives for the process systems engineering community are discussed. Finally, the role of knowledge-driven and data-driven models, with particular attention to the latent variable models in the implementation of QbD paradigms are highlighted, providing the objectives of the Dissertation and a roadmap to its reading.

1.1 The implementation of a QbD approach in pharmaceutical industry: a big challenge

1.1.1 A snapshot of the pharmaceutical industry current situation

In the last decade, the pharmaceutical industry has been faced with unprecedented business scenario changes, caused by continued patent expiration, market changes, drug reimbursement, increasing costs and decreasing productivity in R&D, and regulatory pressure. This scenario caused a substantial transformation of pharma traditional approach forcing the big pharma companies to revamping their strategies to remain competitive (Gautam and Pan, 2015).

Economic evolution. It has been estimated that between 2009 and 2014, $120bn of sales were lost from patent expiries, and between 2015 and 2020 a total of $215bn sales are at risk (EvaluatePharma, 2015). Significant market changes have also been experienced. Many countries' public and private health care systems are moving from volume-based to value-based payment models, and the slowing revenue growth in developed countries is prompting entry and expansion in new, emerging markets (Deloitte, 2015). Consequently, the development of new products is shifted towards more complex therapeutic targets, for which the patient base is narrower than that of preceding blockbusters (Kukura and Paul Thien, 2011). Additionally, the sales of pharmaceuticals is now much more strongly affected than in the past by the means by which patients pay for medicine. In fact, one of the biggest hurdles for a new drug's success is

whether it would qualify for reimbursement from the payers (Sadat et al., 2014). Pharmaceutical companies are increasingly losing their control over drug pricing as governments around the world are taking radical measures to gain control over drug prices and determine reimbursement. Governments and other payers are instituting price controls and increasing their use of generics and biosimilars to contain drug and device costs. In fact, even if market for prescription drugs will grow by 4.8% per year to reach $987bn by 2020, this value is lower than the one trillion dollars predicted in the past (EvaluatePharma, 2015).

R&D evolution. From 2006 and 2013 a stagnant or declining number of new molecular entities (NME) and biologicals have been approved by regulators each year in spite of the increases in R&D expenditure (from $3.1-5bn per NME). However, despite the widespread perception that pharmaceutical R&D is facing a decline period (Rafols *et al*., 2014) the recent trends indicate a turnaround may be under way. In 2014, R&D expenditure was $2.8bn per NME, the lowest for at least the past seven years (EvaluatePharma, 2015). This demonstrates that the efforts of the companies to contain R&D costs, do not compromise the increasing of the productivity and the ability of meeting regulatory requirements (EvaluatePharma, 2015). In fact, pharma companies are asked to find innovative solutions to adapt the traditional R&D and manufacturing approach to the new market requirements: the current big pharma model is transitioning to that of a lean, focused company with a growing revenue stream from specialty products and biologics and emerging markets (Gautam and Pan, 2015). Rafols *et al*., (2014) highlights the shift of pharma R&D from the open science activities associated with drug discovery and towards a systems integrator role, which is focusing on a diversification of the knowledge base, focused more on computation, health services and clinical-related disciplines than on traditional expertise in biomedical sciences. Furthermore, many big pharma companies are joining forces with academic researchers as well as biotechnology and pharmaceutical companies to boost early stage drug discovery research and improve R&D productivity (Sadat et al., 2014). Moreover, shifting the locus of innovation from in-house R&D to collaborative networks with external (often academic) collaborations (Rafols *et al*., 2014). This latter trend is demonstrated by the fact that pharmaceutical firms have engaged in a series of major mergers with each other and of acquisitions involving smaller drug discovery firms, and European and American R&D are moved to emerging countries with large markets such as India and China (Rafols *et al*., 2014). Finally, more efforts should to be addressed in moving compounds onto commercialization, but focusing on improvements on R&D returns by maximizing the innovation and cost containment. (Deloitte, 2015).

Manufacturing issues. Although a cutting-edge R&D represents the basis for a pharmaceutical industry modernization, this cannot be achieved completely without a substantial renewal of the manufacturing activities. Product manufacturing costs largely exceed the R&D expenses, and

amount to about 27% of revenues (am Ende *et al*., 2011). Therefore, even a fractional improvement in the quality of the manufacturing processes can bring tremendous competitive advantages.

In general, the manufacturing activities are categorized as primary or secondary manufacturing. The first category consist of all the chemical stages up to and including the manufacture and purification of the active pharmaceutical ingredient. All the steps after purification (except in some cases milling) are usually included in secondary processing (Bennet and Cole, 2003). Pharmaceutical product manufacturing is often done batchwise, and it follows strictly freezed recipes. Due to improper process development, the factors affecting the final product are not entirely known and therefore often cannot be controlled appropriately, thus determining potential product quality risks; cycle times are very variable, because "out-of-specification" ("exceptions") need frequently to be dealt with. All of these factors contribute to significantly decrease productivity and increase product costs, leading an increase of drug shortages and recalls.

The role of regulatory Agencies. There are a number of factors that traditionally differentiate the pharmaceutical industry from other chemical sectors and impose significant challenges to implement innovative principles. Among them, the high cost and low success rate in the discovery of a new therapeutic drug, the major cost and time associated with the phase of clinical trials that is required in order to demonstrate the safety and efficacy of a new molecular entity and the heavy regulation to which any drug product is subjected over its entire life cycle (Laínez *et al*., 2012). Regarding the last point, while there are continuing efforts to harmonize the regulatory requirements and procedures, and to meet the pharmaceutical industry needs, the rigid regulatory framework is still perceived as one of the main hurdles for a product development. In 2002, the American FDA (Food and Drug Administration) announced a significant new initiative, pharmaceutical current Good Manufacturing Practice (cGMP) for the 21st Century, to enhance and modernize the regulation of pharmaceutical manufacturing and product quality. This initiative, which was finalized by issuing in 2004 the Pharmaceutical CGMPs for the 21st century – A risk based approach (FDA, 2004a) had a number of objectives, including encouraging early adoption of new technological advances in the pharmaceutical industry, facilitating industry application of modern quality management techniques, implementing risk-based approaches, and ensuring that regulatory policies and decisions are based on state-of-the-art pharmaceutical science (Woodcock, 2013). The transition to this new approach has been supported through a number of subsequent initiatives launched by FDA (FDA, 2004b; FDA 2006). The heart of these initiatives is the introduction of the concept of *Quality by Design* (QbD), which means designing and developing a product and associated manufacturing processes that will be used during product development to ensure that the product consistently attains a predefined quality at the end of the manufacturing process (FDA, 2006). This concept have been further developed with the collaboration of FDA with the International Conference on Harmonization of Technical

Requirements for Registration of Pharmaceuticals of Human Use (ICH*), by providing a number of guidances (ICH 2005, 2008, 2009, 2010, 2011) that have become the international foundation for Quality by Design (Woodcock, 2013). Finally, very recently FDA CDER (Center for Drug Evaluation and Research) has created the Office of Pharmaceutical Quality (OPQ), which centralizes functions for regulatory review, policy, research and science activities, project management, quality management systems, and administrative activities (Yu and Woodcock, 2015). OPQ represent the last effort of FDA to reduce the gap with the manufacturing industry, by enhancing transparency and communication related to manufacturing technologies, issues, and capabilities, thereby preventing drug shortages and ensuring the availability of high-quality drugs. (Yu and Woodcock, 2015).

1.1.2 Quality by design paradigms

The concept of Quality by design (QbD) was introduced by Juran (Juran, 1992), who believed that product features and failure rates are largely determined during planning of quality, where the planning of quality is the activity of establishing quality goals and developing the product and processes required to meet those goals. Taking inspiration from this concept, regulatory Agencies recognized that quality should be built into the product, and testing alone cannot be relied on to ensure product quality (FDA, 2006). The FDA fosters the implementation of QbD principles into pharmaceutical development and manufacturing, recognizing the potential of this new approach and that an increased testing does not necessarily improve product quality. The aim of QbD is to support the transition from an experience-based to a systematic and science-based approach guaranteeing at the same time high product quality from the patient's perspective. "Instead of being in a reactive mode and taking corrective actions once failures occur, QbD causes manufacturers to focus on developing process understanding and supporting proactive actions to avoid failures through vigilant lifecycle quality risk management" (Woodcock, 2013). A systematic product and process design and development permits not only to facilitate the achievement of the desired product quality, but also to reduce R&D and manufacturing costs.

A recent review provided by a collaboration between the FDA CDER and academic members, clarifies the main goals of pharmaceutical QbD (Yu *et al*., 2014): *i*) achieving meaningful product quality specifications that are based on clinical performance; *ii*) increasing process capability and reduce product variability and defects by enhancing product and process design, understanding, and control; *iii*) increasing product development and manufacturing efficiencies; *iv*) enhancing root cause analysis and post approval change management.

According to the QbD approach, a systematic strategy that starts with the identification of the characteristics of the product assuring the desired clinical performance, that translates them into

* ICH brings together the regulatory authorities of Europe, Japan and United States with experts from the pharmaceutical industry.

a product formulation, and then assures through the designing and developing a robust manufacturing the achievement of the desired product quality, may guarantee the achievement of these goals. The QbD guidelines identify and define different elements in order to support a practical implementation of these goals (Yu *et al*., 2014):

1. a quality target product profile (QTPP) that identifies the critical quality attributes (CQAs) of the drug product;
2. product design and understanding including the identification of critical material attributes (CMAs);
3. Process design and understanding including the identification of critical process parameters (CPPs) and a thorough understanding of scale-up principles, linking CMAs and CPPs to CQAs;
4. A control strategy that includes specifications for the drug substance(s), excipient(s), and drug products as well as controls for each step of the manufacturing process;
5. Process capability and continual improvement.

1.1.2.1 A quality target product profile (QTPP)

The heart of the QbD paradigms is the definition of quality: according to the ICH guidelines, quality is defined as the suitability of either a drug substance or drug product for its intended use (ICH, 1999). Under an industrial perspective, the definition of quality passes through the identification of the quality target product profile (QTPP), which forms the basis of design for the development of the product. The QTTP provides a prospective summary of the quality characteristics of a drug product that ideally will be achieved to ensure the desired quality, taking into account safety and efficacy of the drug product (ICH, 2009). To define the QTPP the route of administration, dosage form, bioavailability, strength, and stability of a product should to be considered. In turn QTPP is a starting point for identifying the potential critical quality attributes CQAs, which represent all the physical, chemical, biological, or microbiological property or characteristic that should be within an appropriate limit, range, or distribution to ensure the desired product quality (ICH, 2009). The evaluation of the impact of these properties or characteristics on the QTTP, can be performed on the base of prior knowledge or using an iterative process of quality risk management. The list of CQAs should be continually updated, not only when the formulation and manufacturing process are selected, but also during the product lifecycle, as product knowledge and process understanding increase (ICH, 2009).

1.1.2.2 Product design and understanding

The identification of the potential CQAs should guide the product and process development in a QbD framework (ICH, 2009). In order to assure the final desired quality, all possible sources of variability that can have an impact on the CQAs should be identified. These sources of variability can be related respectively to the raw/input materials used in product formulation (i.e., excipient,

intermediate, APIs) and to the manufacturing process (ICH, 2009). In particular, under a QbD perspective, the objective of product design and understanding is to develop a robust product that can deliver the desired QTPP over the product shelf life (Yu *et al*., 2014). To this purpose, FDA suggests to identify the properties and the characteristics of the components of the drug product that can have an influence on its performance or on its manufacturability, such as physiochemical and biological properties of the drug substances and of the excipient selected, as well as their concentrations and interactions (ICH, 2009). All the property or characteristic of an input material that should be within an appropriate limit, range, or distribution to ensure the desired quality of that drug substance, excipient, or in-process material can be called critical material attributes (CMAs, Yu *et al*., 2014). The identification of CMAs may be supported by risk assessment and scientific knowledge for the identification of potentially high risk attributes, then appropriate Design of Experiment (DoE) or, when possible, first-principles models may be used to determine if an attribute is critical and consequently to support the establishment of levels or ranges that assure the desired product quality (ICH, 2009, Yu *et al*., 2014).

1.1.2.3 Process design and understanding

A process is generally considered well-understood when *i*) all critical sources of variability are identified and explained*, ii*) variability is managed by the process, and *iii*) product quality attributes can be accurately and reliably predicted (FDA, 2004b). Therefore, in process design and understanding, it is necessary to identify not only CMAs, but also the critical process parameters (CPPs), namely those parameters whose variability has an impact on a critical quality attribute and therefore should be monitored or controlled to ensure the process produces the desired quality (ICH, 2009). When a process parameter is considered critical, it should be monitored or controlled and limits for these CPPs should be established within which the quality of drug product is assured (ICH, 2009). The analysis of the potential CPPs and CMAs, and of their impact on the CQAs permit the evaluation of the process robustness, namely the ability of a process to deliver acceptable drug product quality and performance while tolerating variability in the process and material inputs (ICH, 2009). As product understanding, also process understanding can be supported by risk assessment and scientific knowledge (by empirical or mechanistic models) to establish the linkage between potential critical process parameters and CQAs and establish appropriate levels or ranges for these (ICH, 2011).

FDA's regulations stress the importance on the use of risk assessment tools in evaluating the risk that a variation in a material or intermediate attribute or a process parameter has on product CQAs (ICH 2009). Risk assessment is typically performed early in the pharmaceutical development process and it is repeated as more information becomes available and greater knowledge is obtained. In particular, principles and examples of tools for quality risk management that can be applied to different aspects of pharmaceutical quality are provided in ICH Q9 guide (ICH, 2005).

1.1.2.4 Design space

Under a practical point of view, one of the main result of product and process understanding which has a direct influence on the manufacturing activities, is the *design space*. The design space is the multidimensional combination and interaction of input variables (e.g., material attributes) and process parameters that have been demonstrated to provide assurance of quality (ICH, 2009). According to the FDA's regulations, the design space is subject to regulatory assessment and approval, but once it has been defined, changes that occur within the design space are not subjected to further regulatory approvals (ICH, 2009). The introduction of the design space concept, is one of the example of the new approach of regulatory agencies with respect to pharma industry activities, requiring more efforts in the achievement of a deep product and process understanding, in return of a more flexibility in the manufacturing process improvement. ICH guidelines provide only *general* indications on how to define and identify a design space, for example, by using scientific first principles and/or empirical models, such as appropriate statistical DoE techniques (ICH, 2011). Although on the one hand this position provides greater flexibility to the companies, on the other hand it increases the uncertainties related to the establishment of the design space. This is due mainly to the multivariate nature of the design space, which required a comprehensive knowledge of both the effects on the product quality of the single material attributes or process parameters, and of their interactions and combined effects. This multivariate nature prevents the determination of the design space using a combination of proven acceptable ranges, namely ranges of the process parameters obtained for each single parameter while keeping the other constant, for which the operation resulted in producing a product meeting the relevant quality criteria (ICH, 2009). This is due to the fact proven acceptable ranges from only univariate experimentation may lack an understanding of interactions between the process parameters and/or material attributes. According to ICH (2009) the design space can be described in terms of ranges of material attributes and process parameters, or in terms of more complex mathematical relationships, time dependent functions, or as a combination of variables such as components of a multivariate model (ICH, 2009). When the design space is established for a manufacturing process, it may be developed for single unit operations or across a series of unit operations. Since separate design spaces for each unit operations is often simpler to develop, a design space that spans the entire process can provide more operational flexibility. For this reason a company can chose to establish independent design spaces for one or more unit operations, or to establish a single design space that spans multiple unit operations in a line (ICH, 2009). Furthermore, a design space can be developed at any scale, but the applicant should justify the relevance of a design space developed at small or pilot scale to the proposed production scale manufacturing process, and discuss the potential risks in the scale up operation (ICH, 2009).

1.1.2.5 A control strategy

Product and process understanding and design studies provide the basis for the establishment of a control strategy. The identification of the sources of variability, represented both by process parameters and input materials (drug substances and excipients), that can have an impact on product quality, permits the definition of appropriate ranges and of a set of control activities to ensure that a product of required quality will be produced consistently (ICH, 2009). According to the ICH guidelines a proper control strategy should include the controls both on parameters and attributes related to drug substance and drug product materials and components, and control on facility and equipment operating conditions, in-process controls, finished product specifications (ICH, 2009). Therefore a control strategy is not intended only for the control of unit operations (as usually under an engineering perspective), but should include *i*) the control of input material attributes (e.g., drug substance, excipients, primary packaging materials) based on an understanding of their impact on processability or product quality, *ii*) product specifications, *iii*) in-process or real-time release testing in lieu of end-product testing, *iv*) a monitoring program (e.g., full product testing at regular intervals) for verifying multivariate prediction models (ICH, 2009). One of the aim of control strategy is to minimize end-product testing shifting the controls upstream, and an appropriate control strategy should facilitate feedback/feedforward controls and appropriate corrective/preventive action (ICH, 2008). Moreover, one of the effect of an appropriate control strategy, is that a comprehensive understanding and control of the effect of the critical material attributes on the process performance permit the acceptance of less tight limits for the input materials, since corrective actions could be implemented to ensure consistent product quality (ICH, 2009).

1.1.2.6 Process capability and continual improvement

An appropriate control strategy should provide assurance of continued suitability and capability of the processes (ICH, 2008). Process capability measures the inherent variability of a stable process that is in a state of statistical control in relation to the established acceptance criteria (Yu *et al*., 2014). A set of process capability indices are usually used for monitoring the performance of pharmaceutical manufacturing processes, in order to estimate the inherent variability due to common cause of a stable process and process performance when the process has not been demonstrated to be in a state of statistical control (Yu *et al*., 2014). A process is in a state of statistical control when it is subject only to random or inherent variability, namely when no source of variation cause detectable patterns or trends. Process and product understating, should help the identification and quantification of the sources inherent variation of a process, thus providing the basis for establishing appropriate control strategy (ICH, 2008).

Process capability monitoring is an example of how throughout the product lifecycle, companies have opportunities to improve product quality and to identify areas for continual improvement (ICH, 2008). Continual improvement represents the ongoing activities to evaluate and positively

change products, processes, and the quality system to increase effectiveness (FDA, 2006). This is an essential element in a modern quality system in order to maintain high process performance, namely to assure that the process is working within the design space, or even improve it, through periodic maintenance of the design space model. Process performance monitoring could include trend analysis of the manufacturing process as additional experience and process knowledge is gained during routine manufacture. This can support the expansion, reduction or redefinition of the design space and can contribute to justifying proposals for post approval changes (ICH, 2008). Continual improvements typically have five phases as follows (Yu *et al*., 2014):

- definition of the problem and of the project goals;
- measurement of key aspects of the current process and collection of the relevant data;
- analysis of the data to investigate and verify cause and effect relationships, and identification of the root cause of the defect if any;
- improvement or optimization of the current process based upon data analysis;
- control of the future state process to ensure that any deviations from target are corrected before they result in defects and implementation of control systems.

For continual improvements purposes, continuous learning through data collection and analysis over the life cycle of a product is important, and opportunities need to be identified to improve the usefulness of available relevant product and process knowledge during regulatory decision making. Approaches and information technology systems that support knowledge acquisition from historical databases are valuable for the manufacturers and can also facilitate scientific communication with the Agencies (FDA, 2004b).

1.1.3 PAT tools

In 2004 FDA launched the process analytical technology tool (PAT) framework (FDA, 2004b). The framework is founded on process understanding to facilitate innovation and risk-based regulatory decisions by industry and the regulatory Agencies. The framework has two components: *i*) a set of scientific principles and tools supporting innovation and *ii*) a strategy for regulatory implementation that will accommodate innovation (FDA, 2004b). According to the FDA's definition, PAT is "a system for designing, analyzing and controlling manufacturing through timely measurements (i.e., during processing) of critical quality and performance attributes of raw and in - process materials and processes, with the goal of ensuring product quality". It is important to note that the term analytical in PAT is viewed broadly to include chemical, physical, microbiological, mathematical and risk analysis conducted in an integrated manner (FDA, 2004b).

Following the QbD concepts, the PAT guidance highlights the importance of the availability of advanced tools that permit to analyze the relevant multi-factorial relationships among material, manufacturing process, environmental variables, and their effects on quality, in order to provide

a basis for identifying and understanding relationships among various critical formulation and process factors and for developing effective risk mitigation strategies. In the PAT framework, these tools can be categorized according to the following (FDA, 2004b):

- multivariate tools for design, data acquisition and analysis;
- process analyzers;
- process control tools;
- continuous improvement and knowledge management tools.

All the multivariate mathematical approaches, such as statistical design of experiments, response surface methodologies, process simulation and pattern recognition tools, in conjunction with knowledge management systems, are considered as multivariate tools which allow a scientific understanding of the relevant multi-factorial relationships between formulation, process, and quality attributes as well as a means to evaluate the applicability of this knowledge in different scenarios (FDA, 2004b).

Process analyzers include all the tools used to collect process data. Thanks to process analyzers, data can be analyzed at-line, i.e. by removing, isolating and analyzing the sample in proximity to the process stream; on -line, i.e. by diverting the sample from the manufacturing process and returning it to the process stream after the measurement; in-line, i.e. by keeping the sample inside the process stream, while the measurement can be made invasively or not (FDA, 2004b).

Process control tools are intended to provide process monitoring and control strategies to monitor the state of a process and actively manipulate it to maintain a desired state. Strategies should accommodate the attributes of input materials, the ability and reliability of process analyzers to measure CQAs, and the achievement to process end points to ensure consistent quality of the output materials and the final product (FDA, 2004b). To this purpose, Multivariate Statistical Process Control (MSPC) is presented as a feasible and valuable tool to realize the full benefit of the measurements acquired by process control tools. Finally, the role of continuous improvement and knowledge management tools, in increasing process and product understanding through the data collected and analyzed over the lifecycle of the product and facilitating the communication with the Agency on a scientific basis, has been already highlighted in § 1.1.2.6. A recent multi-author review article (Simon *et. al*., 2015) reported some of the current trends in the field of process analytical technology (PAT) by summarizing each aspect of the subject (sensor development, PAT based process monitoring and control methods) and presenting applications both in industrial laboratories and in manufacture.

1.1.4 The pharmaceutical quality system

The efforts of the European and American regulatory Agencies in promoting the adoption of QbD paradigms through a more efficient interaction with pharmaceutical industry, demonstrate the clear purpose of supporting a radical renovation of the pharmaceutical development and

manufacturing towards the "*desired state*" mentioned in FDA (2004a). The ultimate aim of these efforts may be represented by the definition of a comprehensive model for a pharmaceutical quality system, which can be implemented throughout the different stages of a product lifecycle. This model (sketched in Figure 1.1) for an effective pharmaceutical quality system, is described in ICH Q10 (ICH, 2008) guidance. The model is based on International Standards Organization (ISO) quality concepts and includes applicable Good Manufacturing Practice (GMP) regulations and complements ICH Q8 "Pharmaceutical Development" and ICH Q9 "Quality Risk Management" (ICH, 2005).

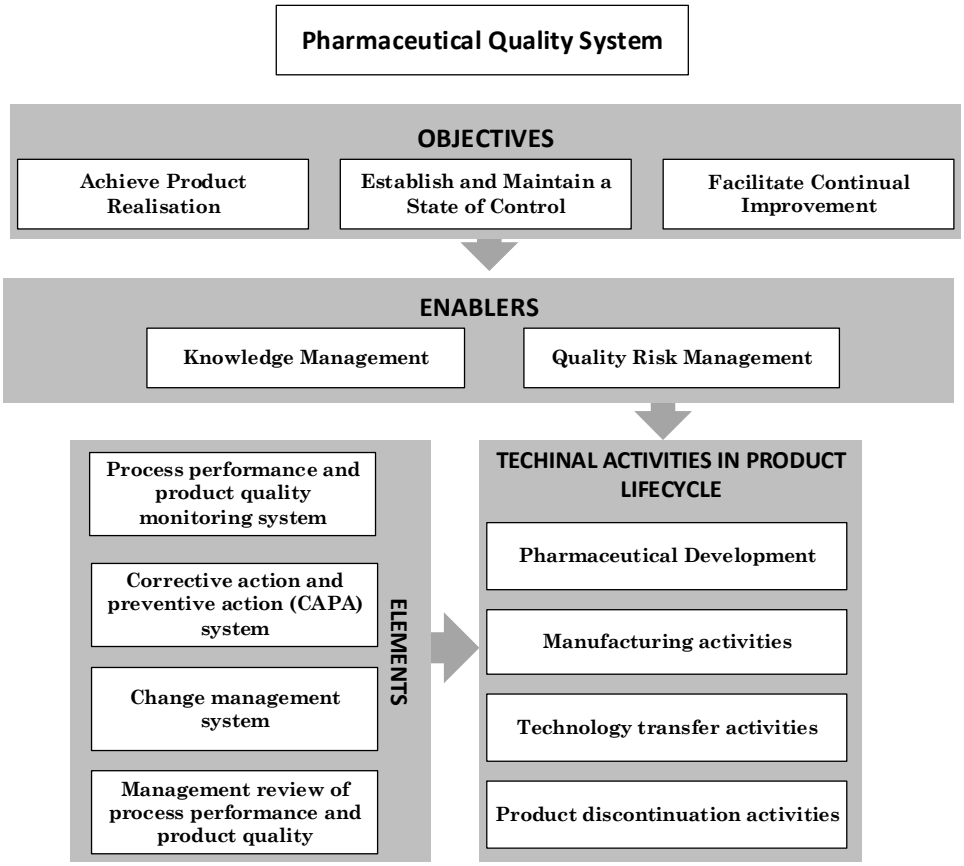

Figure 1.1. *Schematic representation of the Pharmaceutical Quality System model. Adapted from ICH10 guidance (ICH, 2008).*

Implementation of ICH Q10 throughout the product lifecycle should facilitate innovation and continual improvement and strengthen the link between pharmaceutical development and manufacturing activities. The diagram in Figure 1.1 illustrates the major features of the ICH Q10 Pharmaceutical Quality System (PQS) model. The three main objectives of the quality system model proposed are: *i*) achieving product realization, *ii*) establishing and maintaining a state of control and *iii*) facilitating continual improvement (ICH, 2008). The use of knowledge

management and quality risk management facilitate the achievement of these objectives by providing the means for science and risk based decisions related to product quality. Knowledge management is a systematic approach to acquiring, analyzing, storing and disseminating information related to products, manufacturing processes and components. Prior knowledge, pharmaceutical development studies, process validation studies over the product lifecycle, manufacturing experience and continual improvement represent some of the possible sources of knowledge. Quality risk management is integral to an effective pharmaceutical quality system. It can provide a proactive approach to identifying, scientifically evaluating and controlling potential risks to quality (ICH, 2008).

The pharmaceutical quality system covers the entire lifecycle of a product, which includes the following technical activities for new and existing products (ICH, 2008):

- *Pharmaceutical Development*, whose goal is to design a product and its manufacturing process to consistently deliver the intended performance, according to patients, regulatory authorities and internal customers' requirements;
- *Technology Transfer*, whose goal is to transfer product and process knowledge between development and manufacturing, and within or between manufacturing sites to achieve product realization. This knowledge forms the basis for the manufacturing process, *control strategy*, process validation approach and ongoing continual improvement;
- *Commercial Manufacturing,* whose goals are to achieve product realization, establish and maintain a state of control and facilitate continual improvement;
- *Product Discontinuation*, whose goal is to manage the terminal stage of the product lifecycle effectively.

In order to achieve the objectives of the pharmaceutical quality system, a set of elements should be applied appropriately to each lifecycle stage. The intent is to enhance these elements in order to promote the lifecycle approach to product quality (ICH, 2008):

- *Process performance and product quality monitoring system*: an effective monitoring system provides assurance of the continued capability of processes and controls to produce a product of desired quality and to identify areas for continual improvement.
- *Corrective action and preventive action (CAPA) system*: a system for implementing corrective actions and preventive actions resulting from the investigation of complaints, product rejections, non-conformances, recalls, deviations, audits, regulatory inspections and findings, and trends from process performance and product quality monitoring. A structured approach to the investigation process should be used with the objective of determining the root cause.
- *Change management system*: an effective change management system should evaluate, approve and implement changes of innovation, continual improvement, the outputs of process performance and product quality monitoring and CAPA drive. The change management

system ensures continual improvement is undertaken in a timely and effective manner. It should provide a high degree of assurance there are no unintended consequences of the change.

- *Management review of process performance and product quality*: management review should provide assurance that process performance and product quality are managed over the lifecycle. Depending on the size and complexity of the company, management review can be a series of reviews at various levels of management and should include a timely and effective communication and escalation process to raise appropriate quality issues to senior levels of management for review.

The implementation of a quality system throughout the product lifecycle, enables companies to evaluate opportunities for innovative approaches to improve the process and product quality and reduce the sources of variability that often cause wastes and reduce revenues.

1.1.5 Impact of QbD

"Potentially, the application of QbD paradigms should enhance development capability, speed, manufacturing robustness, as well as the manufacturer's ability to identify the root cause of manufacturing failures, as well as post-approval changes and scale-up operations" (Woodcock, 2013). In 2005 IBM estimated that improving new product and process development to design robust manufacturing processes through a QbD-based approach, could increase significantly the total revenues a drug product brings, from the discovery to the patent expiration. Traditionally, as reported in Figure 1.2 (solid line), after the pre-launch phase, in which investments in research and development are needed and which usually lasts around ten years, the product is launched and drug sales increase the revenues. Due to manufacturing process optimization usually required after the launch of the product, there is still not revenues for a certain period (one or two years). Afterwards, product sales start to increase, until reaching a peak usually ten years after the product launch, and then remains stable or even decreases due to the increase of market competition. In Figure 1.2 the dashed line shows the improvements that the adoption of the QbD-based approach prior to the launch of new products could provide, reducing the period from launch to peak sales by as much as five years.

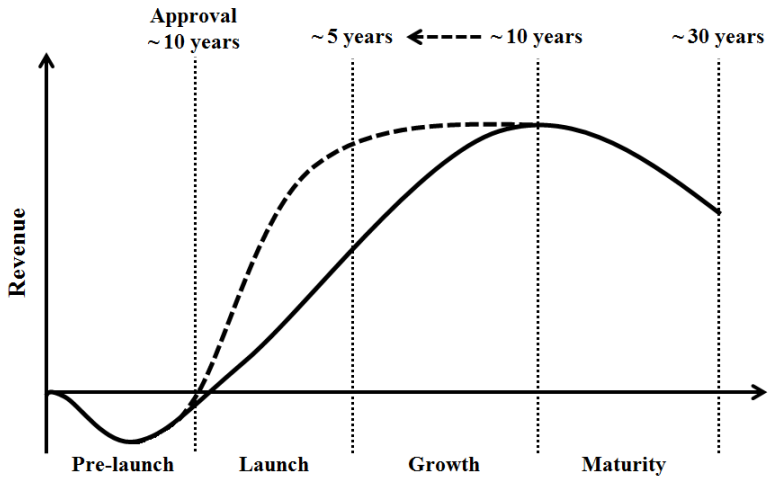

Figure 1.2. *Revenue trend for a drug product during its lifetime, if a traditional (solid line) or a QbD-based approach (dashed line) were used for pharmaceutical development and manufacturing (adapted from IBM, 2005; Tomba, 2013).*

A number of surveys have been performed to assess if after ten years from the introduction of the "Pharmaceutical cGMPs for the 21st Century", the transition from an experience-based to an innovative and modern industry has been completed, and if this transition has actually brought an increase of revenues. After a preliminary period of assessment, QbD and quality systems are beginning to gain ground in the pharmaceutical sector as reported by the International Society of Pharmaceutical Engineers Process Analytical Technology Community of Practice of United Kingdom/ Ireland (PAT COP UK/IR). The survey (Kourti and Davis, 2012), that contains the views of 12 pharmaceutical companies including biotech companies, indicated that significant benefits resulted from QbD-developed products, such as improved process and product knowledge and understanding, improved product quality and robustness, improved control strategy and increased process capability and robustness, which lead to a consistent decrease of batch failures. Moreover, significant improvements in development efficiency and in the formulation design, as well as significant reductions in the time required to develop a formulation have been also reported. Finally, most of the companies highlight also how these improvements lead to an effective cost reduction and leaner manufacturing.

Similar results were provided by the survey conducted by the Quality-by-Design and Product Performance Focus Group of AAPS (American Association of Pharmaceutical Scientists) to assess the state of adoption and perception of QbD. The survey (Cook *et al.*, 2013) collected the responses of 149 individuals from industry and academia about three main topics, regarding the frequency of application of QbD tools, the motivators of the application of QbD, and the benefits of the application of QbD. The results of the survey confirm that most of the companies are actually using several tools and most QbD elements, and over two thirds of respondents from industry have experienced the benefits of QbD regarding both the positive impact it can have on the patient, as well as on internal processes. However, the surveyed companies, affirmed that QbD

does not lead to a better return on investment. Finally, the survey highlights that there are contrasting views on the role of QbD in increased efficiency of the communication between industry and regulatory authorities (that is actually the aim of the introduction of the new OPQ). Therefore, according to the authors, the results of the survey indicate a broad adoption of QbD in pharmaceutical environment, but that the process of gathering all experience and metrics required for connecting and demonstrating QbD benefits to all stakeholders is still in progress (Cook *et al*., 2013).

1.2 The modeling contribution in the implementation of a QbD approach

The ICH guidances highlight the importance of using mathematical models to support every stage of pharmaceutical development and manufacturing (ICH, 2011). The same concept has been stressed by Gernaey and Gani (2010), which presented a model-based framework to support a systematic model-based design and analysis in pharmaceutical product and process development, discussing also the modeling issues related to model identification, adaptation and extension. Mathematical modeling represent a key element of Process Systems Engineering (PSE), a mature and well-established discipline of chemical engineering (Klatt and Marquardt, 2009), whose applications rapidly expanded also in the pharmaceutical industry. In a QbD context, PSE provides the pharma sector with the opportunity to benefits of advanced modeling tools that have already proved their effectiveness in other typical chemical sectors (García-Muñoz and Oksanen, 2010). Although some basic concepts described in the ICH guidances have been applied for quite a long time by several other industries (e.g. petrochemical, polymer and energy sectors), the challenge for PSE experts is to adapt these advanced modeling tools to the need of an industry characterized by a great variety of products, low volumes, mainly batch manufacturing plants with a strict regulatory environment (García-Muñoz and Oksanen, 2010).

An appropriate product and process understanding represents the minimum requirements of the QbD approach. Hence, the mathematical formulation of the relationships between CQAs, CPPs to product CQAs in a mathematical model can be used to support process/product development and design, to assure quality of the products, to support analytical procedure and process monitoring and control (ICH, 2011). Some direct outcomes of such an approach are for examples the reduction of the time usually required for the launch of a new product in the market, the improvement of the productivity and the reduction of the manufacturing costs. It is important to note that process modeling is not meant to be performed as a stand-alone activity; rather, it needs to be fully integrated with experimental strategy (García-Muñoz and Oksanen, 2010). This is should be intended as a mutual integration, where the results of modeling guide experimentation in order to reduce expensive experimental work, and the results of the experimentation are used to support model validation and continual improvement.

A model can derive from a mathematical representation of the physical laws underlying a system (such as mass and energy balances in knowledge driven models), or from data (in data-driven models), or from a combination of the two (in hybrid models). The selection of the type of model to be used depend on the existing knowledge about the system, the data available and the objective of the study (ICH, 2011). In particular, ICH guidelines emphasize the importance of the last aspect, offering a classification of the models based on the aim of the use of the model itself. Accordingly, models can be categorized for the purposes of regulatory submissions depending on the model's contribution in assuring the quality of the product, and for the purpose of implementation, depending on the intended outcome of the model. For the purpose of regulatory submission, models are categorized as *low*, *medium* and *high* impact models. Low impact models includes those models that are typically used to support product and/or process development (e.g., formulation optimization), medium impact models such models can be useful in assuring quality of the product but are not the sole indicators of product quality (e.g., most design space models, many in-process controls) and finally high impact model as those models whose prediction model is a significant indicator of quality of the product (e.g., a chemometric model for product assay, a surrogate model for dissolution). For the purpose of implementation, models can also be categorized on the basis of the intended outcome of the model (i.e., models to support process design, analytical procedures, process monitoring and control), but within each of these categories, models can be further classified, as low, medium or high, on the basis of their impact in assuring product quality (ICH, 2011).

Another important aspect that cannot be separated from model development, is model validation and verification. Model validation is an essential part of model development and implementation, and once a model is developed and implemented, verification should be performed throughout the lifecycle of the product (ICH, 2011). For model validation and verification, the ICH guidelines suggest to set acceptance criteria for the model relevant to the purpose of the model and to its expected performance, then to compare the accuracy of calibration and the accuracy of prediction, and to validate the model using external datasets. In the case of well-established first principles-driven models, prior knowledge can be leveraged to support model validation and verification, if applicable. The prediction accuracy of the model should be verified by parallel testing with the reference method during the initial stage of model implementation and can be repeated throughout the lifecycle (ICH, 2011).

Aside from the kind of model used, the increasing of interest of the PSE community to the pharmaceutical industry applications, demonstrates that this sector is actually undertaking a path of modernization. The use of PSE tools is increasing in process monitoring, quality control and process modeling as confirmed by the results reported by Troup and Georgakis (2012) regarding an industrial survey performed on this topic. For example, with respect to process monitoring, the survey results demonstrated an increasing trend in the use of multivariate statistical process control charting and of process monitoring software packages, most of which are based on the

use of chemometric models. In fact, these statistical multivariate tools are used by the 67% of the responding companies to analyze historical process and plant data. Regarding the use of process modeling, all of the companies surveyed indicated that response surface models ware routinely develop for unit operations, but when possible, fundamental models are preferred, especially in primary manufacturing. In secondary manufacturing, the use of first-principles models is more limited by the complexity of the mechanisms involved, forcing the employment of empirical models. As a consequence, a part from specific exceptions, the use of empirical models is broadly expanding (one third of the companies developed empirical models for 80-100% of the unit operations). Finally, process modeling is widely employed in the determination of a multivariate design space. More than two third of the companies surveyed report the use of design space strategies to identify a robust area of operation with respect to all major disturbances to the process (Troup and Georgakis, 2012). In summary, PSE tools are demonstrating their potential in supporting a radical change in pharmaceutical development and manufacturing approach. A new way of thinking is now developing, according to which "pharmaceutical ingredients, pharmaceutical products, the related manufacturing processes, and the biopharmaceutical properties are considered simultaneously and quantitatively" (Rantanen and Khinast, 2015).

An overview of the challenges associated with modeling common pharmaceutical processes, providing also a discussion of the recent developments in pharmaceutical process modeling, has been recently provided by Rogers and Ierapetritou (2015).

In Figure 1.3 a summary of the main contributions of knowledge-driven and data-driven models in the implementation of the elements that characterize the QbD approach (Section 1.1.1) is reported. A brief overview of these contributions is provided in the following, highlighting the advantages and drawbacks of the two modeling approaches and the efforts required in the future.

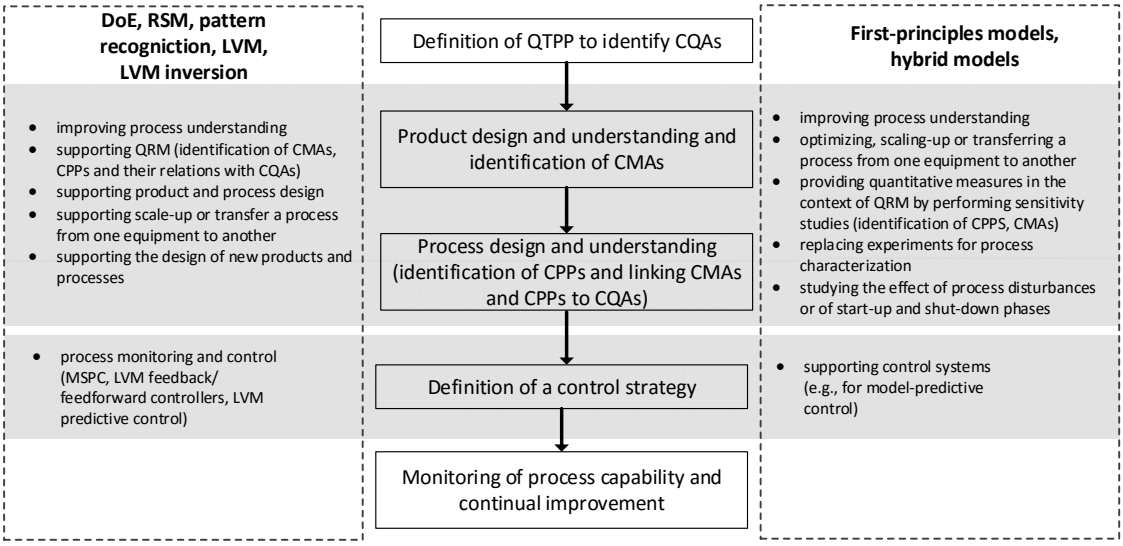

Figure 1.3. *Summary of the contribution of knowledge-driven and data-driven model to the elements that characterize a QBD approach.*

1.2.1 Knowledge-driven models

Knowledge-driven (KD) models, also called mechanistic (or first-principles, or fundamental models) describe the underlying functional mechanisms of the system under investigation, relaying on the use of fundamental knowledge typically in terms of mass, energy and momentum balances and of constitutive equations. Stated differently, KD models are a convenient representation of the available knowledge of a system. Under an industrial perspective, since first-principle models offer increased process understanding, enable a more flexibility in the incorporation of product physical properties, are often applicable for multiple products and allow extrapolation (under certain assumptions), these models are usually preferred to empirical models (Troup and Georgakis, 2010). Therefore, in the last years, the mechanistic modeling of pharmaceutical unit operations has made significant progress, thanks to the ability of these model to: *i*) improve the fundamental scientific understanding of a process, *ii*) optimize process scale-up and monitoring, *iii*) provide quantitative measures in the context of quality risk management, *iv*) replace experiments during a process characterization phase, *v*) study the effect of process disturbance or start-up and shut-down phases on the process performance (Rantanen and Khinast, 2015). However, it cannot be ignored that the time and efforts required to develop these type of models is often excessive for market requirements, especially in pharmaceutical environment, characterized by a production rates not comparable to that one of bulk chemical; moreover, the model assumptions are often not consistent with full scale process operating conditions (Troup and Georgakis, 2010).

Depending on the characteristics of physical phenomena underling a process, mechanistic models may lay on a systems of ordinary differential equations (ODEs), differential algebraic equations (DAEs) and partial differential equations (PDEs). In particular, the applications of PDEs models have rapidly expanded, due to the necessity of describing complex multi-phase dynamic systems, such as crystallization, drying and granulation processes. In this context, PDEs models are used in in the form of population balance models (PBM), to describe particle-size or crystal-size distributions, or computational fluid dynamics (CFD) to simulate fluidic systems, including multiphase flows (detailed reviews on the use the use of CFD for pharmaceutical unit operations, are provided by Kremer and Hancock, 2006 and by Wassgren and Curtis, 2006). CFD models may also be combined with different specific models to describe for example chemical reactions (e.g. Kashid *et a*l., 2007), or with PBM models to model the change of distributed properties as a function of spatial coordinates within a unit operation (Woo *et al*., 2009). Finally, the complex description of granular flows for example in powder blending, granulation, roller compaction, or tableting, may be assisted by the mechanistic simulation of particulate flows, using for example the discrete element method (DEM, Ketterhagen *et al*. (2009) reviewed a series of applications of these techniques in common pharmaceutical processes).

The availability of detailed model is essential to provide a deep understanding of the process and the assurance of the results obtained using the model for decision-making purposes. Anyway, when the implementation of a detailed mechanistic model is much computationally expensive (to be used for example to real-time applications), reduced order model represent an appropriate solution in order to reduce simulation times for CFD and PBM models (Gernaey *et al.*, 2012).
A second alternative that provides a compromise when full mechanistic models are not available, is the use of hybrid models, that rely on the combination of a mechanistic model with a data-driven model component. Often, in the interest of time, a hybrid approach will be preferred, where the mechanistic part of the model is gradually extended when more process knowledge becomes available, e.g. during process development (Gernaey *et al*., 2012).
For an extensive overview of the applications in the pharmaceutical industry of the above-mentioned categories of mechanistic, reduced-order and hybrid models, the reader is encouraged to refer to Gernaey *et al.* (2012) and Rantanen and Khinast (2015).

1.2.2 Data-driven models

Data-driven (DD) also called data-based (DB) or empirical models, do not require any prior knowledge of the physical mechanisms underlying a process, since the information useful to define mathematical relationships between its inputs and outputs is directly extracted by the analysis of the process data recorded. In a way, DD models are nothing more than a convenient representation of the available data. The empirical model category is very broad, including for example latent variable models (LVMs), statistical design of experiments (DoE) and response surface models (RSM), and pattern recognition techniques. The application of empirical models as PAT tools on pharmaceutical industry is rapidly growing, as reported by a recent survey according to which for most of the companies surveyed, more than one half of their unit operations are modelled empirically (Troup and Georgakis, 2013). Many aspects contribute to the success of DD models, such as the availability of an ever-increasing set of off-line and on-line process measurements and the possibility of providing a multivariate description of the systems with a significant time and effort saving with respect to mechanistic models. In this context, chemometric models have generated particular interest, demonstrating their ability in improving product and process knowledge especially in PAT applications (e.g. spectroscopy and image analysis). The use of multivariate data analysis methods like principal component analysis (PCA; Jackson, 1991), partial least-squares regression (PLS; Wold, 1983; Höskuldsson, 1988), statistical design of experiments (DoE; Montgomery, 2005) and pattern recognition techniques (Bishop, 2006; Duda *et al*., 2001) has rapidly extended after the PAT initiative. Many reviews are available on the use chemometric methods coupled with advanced characterization techniques, as for example the work of Roggo *et al.* (2007), which focuses on chemometric techniques and pharmaceutical NIRS applications, or the more extensive reviews provided by Rajalahti and

Kvalheim (2011) and Pomerantsev and Rodionova (2012) that consider not only NIR applications, but also applications of as infrared (IR), Raman spectroscopy, hyperspectral and digital imaging, and other tools as X-ray diffraction, chromatography or mass spectroscopy (MS). In particular, pattern recognition techniques are largely used coupled with analytical tools for qualitative analysis (e.g. Realpe and Velasquez, 2006), in order to control for example the product quality (color, surface characteristics, shape, particle size, etc.). However, in this Dissertation, an alternative use of these techniques will be provided in Chapter 6.

Similarly to mechanistic models, empirical model are also asked to describe not only the multivariate aspects of the relationships between CMAs, CPPs and CQAs, but also the non-linear and dynamic behavior that usually characterize the system. This is often achieved by the development of nonlinear DD such as quadratic response surface models (RSMs) usually related to design of experiments (DoE) methodologies (Montgomery, 2005; Box and Draper, 2007). Statistical design of experiments has been largely employed in pharmaceutical process and product development, especially for formulation design and product optimization, as highlighted by Gabrielsson *et al*. (2002) who reviewed several applications of DoE and multivariate analysis in pharmaceutical applications. There are also several applications about the use of DoE to explore the knowledge space and identify the regions within which parameter values are demonstrated to ensure the desired product CQAs, in order to support the definition of the design space (e.g., am Ende *et al*., 2007; Burt et al. 2011; Kapsi *et al*. 2012; Zacour *et al*., 2012a). Moreover, appropriate DoE permit the definition of reliable RSM models, that can be consider even higher than quadratic nonlinearities (including cubic, quartic, or higher terms). However, since the number of experiments increases very rapidly as the number of input variables or factors increases, the number of experiments that need to be performed to accurate estimate high nonlinearities is usually prohibitive. An alternative method to account for nonlinearities, is represented by the neural network models. However, although these models can describe even higher nonlinearities compared to RSM models, they require a similar large number of experiments and their predictions usually lack of transparency. Examples of the use of such data-driven models for the mapping of the design space of pharmaceutical processes, are provided by Boukouvala *et al*., (2010), which proposed three approaches based on different data-driven modeling techniques, using the ideas of process operability and flexibility under uncertainty.

While DoE and relating methods usually required large amount of new experiments, LVMs techniques are conceived to exploit and analyze the large amount of research and product data that usually derived from on-going manufacturing processes, experimental campaigns, data historians from different process units. The information extracted from these data can be useful not only to increase product and process understanding, but also to guide the development of new product and process or to support control strategies in manufacturing activities.

1.2.2.1 Latent variable modeling in QbD

LVMs are multivariate statistical models that, by analyzing large amounts of data, permits one to describe a system by using a reduced number of variables (called latent variables, LVs), obtained by a linear combination of the original (usually correlated) measurements.

The physical meaning of these new set of variables, is actually related to the forces driving the system and should be sought in the correlation existing between the original variables. Figure 1.3 reports a geometrical interpretation of the operation performed when a LVM is built on a dataset **X** [20×3], where 20 is the number of available samples and 3 is the number of measured variables ($\mathbf{x}_1$, $\mathbf{x}_2$, $\mathbf{x}_3$) for the collected samples.

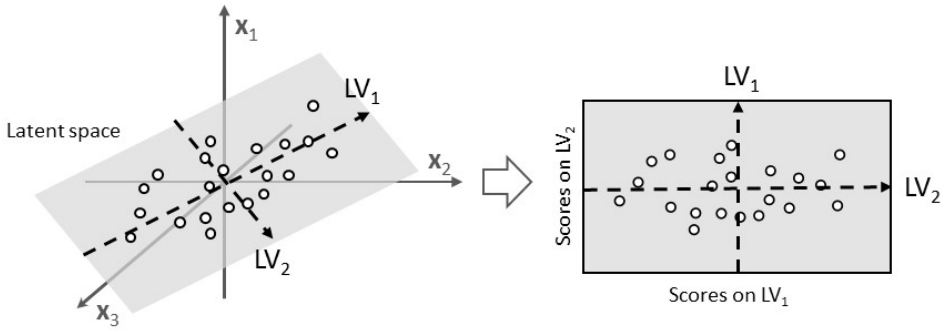

Figure 1.3. *Geometrical interpretation of an LVM (adapted from Tomba, 2013).*

As can be seen, the LVM transforms the three-dimensional space of the original variables into a two-dimensional space (called the latent space) defined by the two latent variables (LV_1, LV_2) whose directions correspond to the directions along which the variability of the data is higher. The projections of the original variables onto the latent space that describe the original space, are called scores and become the new variables defining the state of the system.

LVMs can be used also to relate data from different datasets (Burnham *et al*., 1996) using latent variable regression models (LVRMs). These models have been largely exploited coupled with analytical instruments to relate highly correlated input variables to response variables as product quality (examples of applications of LVMs on this topic, both in pharmaceutical and food industry can be found in Ottavian, 2013).

Besides LVMs application as predictive tools, their potential has been exploited also for different purposes. For example, given the statistical nature of LVMs, they can be employed for multivariate statistical process control (MSPC) in online process monitoring. This is a well-known and long-applied use of LVMs in several industrial sectors (Kourti, 2005). However, control systems based on the use of LVMs are usually not limited to process control (Flores-Cerrillo and MacGregor, 2004), process monitoring (MacGregor and Kourti, 1995) and eventually to the implementation of corrective actions, but are also used for the purpose of fault diagnosis (Wise and Gallagher, 1996; Birol *et al*., 2002; García-Muñoz *et al*., 2009). Moreover,

LVMs are used for process understanding and troubleshooting (García-Muñoz et al., 2003), for process operating conditions design (Jaeckle and MacGregor, 1998), process scale-up (García-Muñoz et al., 2005) and also for product design (Muteki et al., 2006) and optimization (Yacoub and MacGregor, 2004). A detailed review of pharmaceutical applications in these areas have been provided by Tomba *et al*. (2013a). For the purposes of this Disseration, only a summary of the main applications of LVM techniques will be provided in the following, in particular in relation the use of LVMs to support the definition of the *design space*. To this end, LVMs can be used to support pharmaceutical development activities in the selection of the materials to be included in a formulation or of the optimal operating conditions at which a process should operate. According to Tomba *et al*., (2013a), LVMs have found different applications to support the establishment of a design space:

- LVMs are coupled with DoE techniques to facilitate the choice of the parameters to include in a DoE analysis or to disclose the relationships between the input and output variables of a process. Moreover, these techniques are also ised to study the relationships between variables manipulated in a DoE plan and those which are only measured. Thanks to the use of LVMs, the information extracted by the analysis of the different kind of data (for example data measured on-line or spectra), usually highly correlated, was introduced in the analysis of the design space. Examples of these applications can be found in Huang et al. (2009), Streefland *et al*. (2009), Zacour *et al*. (2012b), Thirunahari *et al*. (2011) and Lourenço¸ *et al*. (2012). Moreover, starting from the concept that the design space in raw materials and in process parameters must be developed jointly, as changes in either one would affect the other, MacGregor and Bruwer (2008) proposed a framework for the development of design and control spaces or pharmaceutical operations. On the same topic, Souihi *et al*. (2013) proposed an application in which of DoE techniques combined with LVMs to identify the design space for a roller compaction process.
- LVMs are directly used to assist the identification of the design space through model inversion (Jaeckle and MacGregor, 1998 and 2000), by analyzing the data available from historical experiments and especially from already developed products. Used in this direct form, latent variable regression models (LVRM) are used to relate raw material CQAs, CPPs, which represent the inputs variables, to the product CQAs, which represent the response variables, using the historical available data of the process. In this case a product property can be estimated starting from a set of inputs (material properties and process parameters). Otherwise, in the inverse use of a LVRM, the raw materials properties/fractions and process parameters suitable to obtain the desired product properties are predicted starting from the desired product properties themselves, to support product or process design. However, as proposed by Kourti (2006) and demonstrated by García- Muñoz *et al*. (2010), an LVRM can be used to guide the experimentation in developmental studies or for the definition of the process design space in the LVM space. A general framework to perform LVRM inversion has been proposed by

Tomba *et al*. (2012), which consider different possible solutions to the inversion problem, depending on the design problem objectives and constraints. In the same work, it has been highlighted the analogy between the concepts of design space and of null space (Jaeckle and MacGregor, 1998). The null space, which arises from the LVM inversion under certain conditions, represents the space of the input variables that, according to the LVRM, correspond to the same sets of output variables. For this reason, according to the authors, the null space calculated from an LVRM inversion can be used as a starting point for the establishment of the design space of a process. Anyway, further research is needed to show how to use LVMs in the systematic identification of the design space of a process, especially focusing on a practical definition of design space limits (e.g., in the latent space of the model) usable not only to regulatory purposes but also to support ordinary manufacturing activities (Tomba, 2013a).

Many applications on the use of DoE and LVMs for process and product design purposes are reported in Tomba *et al*., (2013a), whereas an overview of the application of process modeling to determination of design space for pharmaceutical manufacturing processes has been recently provided by Rogers and Ierapetritou (2016).

1.2.3 Continuous improvement and knowledge management tools

The knowledge available for a process continually grows throughout the product lifecycle. Experiments conducted during product and process development and manufacturing, represent the basement of this knowledge (FDA, 2004b), but can also provide information to support the development of a knowledge system involving the overall production system. According to the pharmaceutical quality system model, monitoring data and information are essential to achieving problem resolution or problem prevention. In this context, multivariate tools can be used to review periodically historical data as more knowledge is acquired during process/product development and manufacturing, in order to assess possible changes in the relations between CMQ, CPPs and CQAs. An example on how LVMs can be used as part of a continuous quality verification approach for a new drug product is provided by Zomer *et al.*, 2010.

In general, due to the complexity of the problems to be addressed in pharmaceutical product-process design, an efficient and systematic knowledge base coupled with an inference system is essential (Gernaey *et al*., 2012). An example of the efforts performed to address this issue is represented by OntoCAPE, an overview of a general ontology for structuring knowledge in the chemical process engineering field (Morbach *et al*., 2007 and 2010). Moreover, Singh *et al*., (2010) described an ontology for knowledge representation and management, with the purpose of facilitating the selection of proper monitoring and analysis tools for a given application or process and permitting the identification of potential applications for a given monitoring technique or tool. An ontological information-centric infrastructure to support product and process

development in the pharmaceutical manufacturing domain was developed by Venkatasubramanian et al. (2006). Turning data into knowledge and managing that knowledge will remain one of the major challenges for the future (Gernaey *et al*., 2012). In fact, storage of historical data is usually managed by well established software product from an external supplier. However, the lack of appropriate tools to extract from these data the necessary process knowledge, for example in order to improve the performance of a process, is the actual bottleneck, and should be one of the focus points of future research.

1.3 Objectives of the research

In the last decade the number of studies on the application of modeling in pharmaceutical development and manufacturing has increased considerably, however, as acknowledged by several authors, there are still many open issues. The main objective of the research presented in this Dissertation is to demonstrate how LVMs and pattern recognition tools can be used to address some common issues that often affect the practical implementation of QbD paradigms in pharmaceutical development and manufacturing. The Dissertation presents novel and general methodologies based on the use of latent variable models and pattern recognition tools that can be employed to support the improvement of first-principles models, the identification of the design space, and the review of large manufacturing databases. The applications of the procedures proposed in this Dissertation and the innovative contributions they provide are summarized in the following.

- **Supporting first-principles model diagnosis.** The availability of a reliable first-principles model is often desirable to support process and product development and in the implementation of robust control strategy. However, the effort required to develop reliable models or to adapt the existing ones, represents the main hurdle to an extensive employment of these models. An FP model is constituted by equations and parameters. The appropriate set of equations represents the available knowledge on the underlying mechanisms driving the system. The values assigned to the parameters allow one to tune the general mechanism, described by the set of equations, to the actual physical/chemical system under investigation. When the FP model results do not match the available experimental data to a desired accuracy, a process/model mismatch (PMM) exists, that can be structural or parametric (or both). Tailored experiments can be designed to improve the model performance. Typically, model-based design of experiment (MBDoE) techniques or sensitivity studies can be used to this purpose, allowing either model discrimination among alternative set of equations, or parameter identification from a given set of equations. However, these solutions may be very demanding especially if the physical/chemical mechanisms driving the system are not known completely, since uncertainty may exist both on the model equations and on the model parameters. In this

Dissertation, a methodology based on the use of LVMs is proposed to pinpoint which term of the model is the most responsible for an observed PMM, both for steady-state and dynamic systems. The purpose is to analyze the reason of the poor performance of a FP model using only the available historical data, thus minimizing the overall experimental efforts usually needed to improve the FP model.

- **Supporting design space identification**. A key element of the Quality-by-Design initiative set forth by the pharmaceutical regulatory Agencies is the determination of the design space (DS) for a new pharmaceutical product. When the determination of the DS cannot be assisted by the use of a first-principles model, one must heavily rely on experiments. In many cases, the DS is found using experiments carried out within a domain of input combinations (e.g. raw materials properties and process operating conditions) that result from similar products already developed. This input domain is the knowledge space and the related experimentation can be very demanding, especially if the number of inputs is large. The objective is therefore to limit the extension of the domain over which the experiments are carried out hence, to reduce the experimental effort. To this purpose a methodology is presented to segment the knowledge space in such a way as to identify a subspace of it (called the experiment space) that most likely brackets the DS.

- **Supporting periodic review of historical datasets.** Thanks to the availability of fast, cheap and reliable on-line measurement devices, the use of advanced technologies to monitor and control pharmaceutical manufacturing processes has rapidly expanded. Large historical datasets spanning several years of manufacturing are usually available in the pharmaceutical industry. These datasets easily reach several millions of data entries. However, this data overload often hinders the possibility to effectively use of the information embedded in the data. Transforming data into knowledge may result particularly burdensome, considering that not even the number of the batches completed in a given time window is known a priori. In fact, data historians are usually recorded in a "passive" way, i.e. including in the same dataset data segments that possibly refer to temporary stalls of the equipment or to cleaning and maintenance operations. In this Dissertation, a methodology is proposed to systematically review large data historians of secondary pharmaceutical manufacturing systems in order to extract operation-relevant information, such as the number of batches carried out in a given time window, how many different products have been manufactured, and whether or not the features characterizing a batch have changed throughout a production campaign. The methodology proposed represent a valid PAT tool that can be coupled to existing data acquisition system to extract the information necessary to support the implementation of continual improvement paradigms.

The effectiveness of the general procedures proposed in this Dissertation is demonstrated by applying each of them to experimental (industrial scale) or simulated case studies. The next section presents a roadmap to the Dissertation.

1.4 Dissertation roadmap

In this Dissertation, data-driven modeling techniques are used to provide general solutions to support first-principles models enhancement, design space identification, and periodic review of historical datasets. A discussion of the recent evolution the pharmaceutical industry and of the use of process modeling in this sector has been provided in this Chapter, along with the main objectives of this Dissertation. The description of the data-driven modeling used in this Dissertation (namely LVMs and pattern recognitions techniques) is reported in Chapter 2.

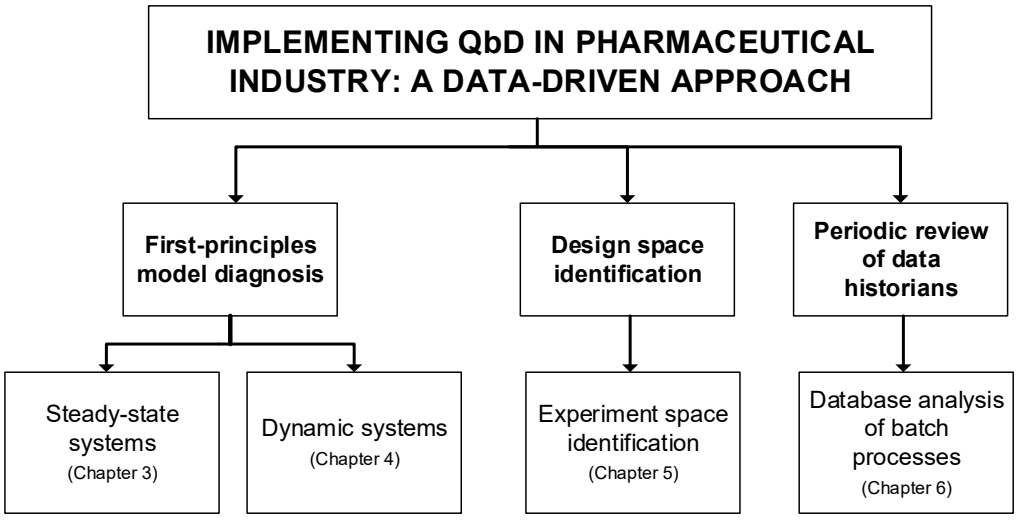

Figure 1.4. *Sketch of the research topics considered in this Dissertation.*

General methodologies based on the use of DD models are developed for each of the three areas analyzed. The pplications of these methodologies are presented in the following according to the sketch of Figure 1.4.

With respect to first-principles models diagnosis, in Chapter 3 and 4 a methodology is presented to diagnose the possible cause of a process/model mismatch, with the objective of reducing the experimental efforts usually needed to improve a first-principles model. The methodology relies on the use of the information extracted by means of latent variable models from the available data (namely, the historical process measurements and the first-principles model outputs). This information, coupled with engineering judgment, permits one to identify which sections of the

first-principles model mostly contribute to an observed process-model mismatch. In Chapter 3 two simulated steady-state systems are considered as test beds: a continuous jacketed stirred-tank reactor and a milling unit. In Chapter 4, the methodology is adapted to cope with dynamic systems. Two simulated case studies are considered: a dryer process and a penicillin fermentation process. Although the proposed methodology is developed to deal with pharmaceutical process models, it can be easily extended to any steady-state or dynamic model.

Chapter 5 focuses on the problems related to the identification of the design space (DS) for a new pharmaceutical product characterized by a single quality specification. A methodology is proposed to reduce the experiments needed to define the DS by exploiting the historical data of products similar to the new one (‘‘knowledge space’’). Through the inversion of the PLS model used to describe the system, a reduced area of the knowledge space wherein the design space is supposed to lie is identified (also accounting for model prediction uncertainty). Three case studies are presented to demonstrate the effectiveness of the proposed methodology.

Finally, Chapter 6 addresses the problem of the periodic review of large data historians to extract useful information for the implementation of continual improvement paradigms. A methodology based on the use of pattern recognition techniques (namely *k*-nearest neighbor and PCA models) is presented that allows analyzing large historical datasets of secondary manufacturing batch units. The effectiveness of the methodology in automatically isolating and analyzing meaningful data segments is shown for two large industrial datasets. The proposed approach permits one to monitor the evolution of the manufacturing campaigns over time and to detect possible exceptions in the manufacturing procedures.

In a concluding section, the summary of the main achievements is provided for each of the three areas analyzed along with the discussion of future investigations that may be carried out to improve the methodologies proposed in this Dissertation.

Chapter 2

Multivariate modeling background

This Chapter provides a general overview of the statistical and mathematical techniques applied in this Dissertation. First, a background on latent variable models (in particular principal component analysis and partial least-squares regression) is presented, focusing both on the algorithmic point of view and the practical one. Furthermore, the concepts of latent variable model inversion are introduced, and the fundamentals for their determination are provided, along with a brief introduction of the use of pattern recognition techniques for classification and clustering purposes.

The applications of the techniques described in this Chapter, have been performed in Matlab® (the MathWorks Inc., Natick, MA) using an in-house developed multivariate analysis toolbox (in Chapter 5, Facco *et al.*, 2015) and the PLS_Toolbox (Eigenvector Research, Inc., Wenatchee, WA, USA, 2015).

2.1 Latent variable modeling approaches

Latent variable models (LVMs) are statistical models that have been conceived to analyze large amounts of (usually correlated) data. The underlying concept of LVMs is that real data can be expressed as a liner combination of factors (called latent variables, LVs) that describe the major trend of the data and that can be interpreted based on the knowledge of the physical and chemical phenomena involved in the system. Hence, the theoretical foundation for the modeling of measured variables by means of latent variables (LV) is based on two principles (Eriksson *et al.*, 2006): *i*) the measurements, by definition, are sums of the underlying latent variables; *ii*) a set of measurements $\mathbf{X}$ [$N \times I$] generated by a function F (U,V), where each row $\mathbf{u}$ of $\mathbf{X}$ describes the change between observations and each column $\mathbf{v}$ describes the change between variables, can be transformed by the Taylor expansions of F in $\mathbf{u}$ direction, (after discretizing for n = observation and i = variable) in an LV model. The smaller the interval of $\mathbf{u}$ that is modelled, the fewer terms are needed in the Taylor expansion, and the fewer components are needed in the LV model. Under a practical point of view, the latent directions found by a LVM, represent the driving forces acting on the system and responsible for the variability of the data. Hence, LVMs are not only used for data compression, but also for data interpretation, assuming that essential information can be

extracted by analyzing how the variables co-vary, namely how they change with respect to one another.

In general, data can be categorized, depending on the nature of the variables, as factors and responses (Eriksson *et al*., 2006). The factors (also called predictors, parameters, regressors) are variables whose different levels might exert an influence on the system or on the process. These variables can be organized into a matrix **X** [$I \times N$] in which the N variables have been observed per I samples (or observations). The responses are variables which are measured to capture the performance of the system and can be organized in a matrix **Y** [$I \times M$] of M variables observed per I samples. In the analysis of the factors matrix, the objective of a LVM analysis is to explain the correlation structure of the N variables, in order to understand the relationships among them. Principal component analysis (PCA; Jackson, 1991) is one of the most useful techniques to this purpose. Alternatively, projection to latent structures (PLS, also called partial least-squares regression; Höskuldsson, 1988) is used in the combined analysis of the regressors and responses matrix to explain the cross-correlation structure of the variables in **X** and in **Y**, in order to study and quantify the relationships between regressors and response variables. Basic theory about PCA and PLS is reported in the following, largely based on the Dissertations of Tomba (2013) and Ottavian (2014).

2.1.1 Principal component analysis

Principal component analysis (PCA; Jackson, 1991) is a multivariate statistical method that summarizes the information embedded in a dataset **X** [$I \times N$] of I samples and N correlated variables (for example data on critical process parameters, initial conditions, process settings, critical quality attributes), by projecting the data through a linear transformation onto a new coordinate system of orthogonal (i.e., independent) principal components (PCs), which optimally capture the correlation between the variables, identifying the direction of maximum variability of the original data.

Principal component analysis permits to represent a dataset **X** as the sum of the R scores-loadings vectors outer products:

$$\mathbf{X} = \sum_{a=1}^{R} \mathbf{t}_a \mathbf{p}_a^{\mathrm{T}} \quad , \tag{2.1}$$

where: R = rank(**X**), $\mathbf{p}_a$ is the loading vector for PC a and contains information on how variables are related, $\mathbf{t}_a$ is called score vector for PC a and contains information on how samples are related to each other and ($^{\mathrm{T}}$) indicates the transpose operator. The computation of the model scores and loadings can be performed by solving the optimization problem (Burnham *et al.*, 1996) in Eq. (2.2). For one PC ($\mathbf{p}_1 = \mathbf{p}$):

$$\max_{\mathbf{p}} \left(\mathbf{p}^{\mathrm{T}} \mathbf{X}^{\mathrm{T}} \mathbf{X} \mathbf{p} \right) \quad \text{subject to } \mathbf{p}^{\mathrm{T}} \mathbf{p} = 1 \quad . \tag{2.2}$$

Vector **p** represents the latent direction of maximum variance in the data, where the original data can be projected, by obtaining the vector **t** of the coordinates into the PC space:

$$\mathbf{t} = \mathbf{X}\mathbf{p} \quad . \tag{2.3}$$

As a consequence, the problem in (2.2) can be reformulated as in (2.4), representing the maximization of the score vector length (Burnham *et al*., 1996):

$$\max_{\mathbf{p}} \left(\mathbf{t}^{\mathrm{T}} \mathbf{t} \right) \quad s.t. \ \mathbf{t} = \mathbf{X}\mathbf{p} \quad . \quad \mathbf{p}^{\mathrm{T}} \mathbf{p} = 1 \tag{2.4}$$

The analytical solution of this problem is readily obtained from its optimality conditions (López-Negrete de la Fuente *et al*., 2010) and is represented by the following eigenvalue problem:

$$\mathrm{cov}(\mathbf{X})\mathbf{p} = \mathbf{X}^{\mathrm{T}} \mathbf{X} \mathbf{p} = \lambda \mathbf{p} \quad , \tag{2.5}$$

where **p** is the eigenvector corresponding to the eigenvalue λ of the covariance matrix of **X**. Eq. (2.5) facilitates the geometrical interpretation of the optimization problem (2.2) whose aim is to maximize the variance captured by λ, which represents the variance explained by the product $\mathbf{t}\mathbf{p}^{\mathrm{T}}$. The eigenvector problem (2.5) can be used to determine the *N* loadings $\mathbf{p}_n$ of the PCA model, which correspond to the *N* orthonormal eigenvectors of the covariance matrix of **X**. As a consequence the resulting score vectors are orthogonal and they have a length equal to the eigenvalue λ associated to the *n*-th PC:

$$\begin{aligned} &\mathbf{p}_n^{\mathrm{T}} \mathbf{p}_r = \mathbf{t}_n^{\mathrm{T}} \mathbf{X}\mathbf{X}^{\mathrm{T}} \mathbf{t}_r = 0 \quad \text{for } n \neq r \quad \text{with } n, r = 1,...N \\ &\mathbf{p}_n^{\mathrm{T}} \mathbf{X}^{\mathrm{T}} \mathbf{X} \mathbf{p}_n = \mathbf{t}_n^{\mathrm{T}} \mathbf{t}_n = \lambda_n \quad \text{with } n = 1,...N \end{aligned} \quad . \tag{2.6}$$

As a result of the eigenvector problem[†] (2.4), the PCs are ordered in Eq. (2.1) according to the variance of the original dataset **X** that they capture. Usually, few principal components *A* are sufficient (i.e., $A << R$) to adequately describe **X** because correlated variables identify a common

[†] Note that the solution of the eigenvector problem Eq. (2.5) results in the first PCA loading **p**. In order to evaluate the remaining components, matrix **X** has to be deflated.

direction of variability that can be described by a single PC. Hence, assuming that only the first A PCs are retained to represent $\mathbf{X}$, Eq. (2.1) can be rewritten as:

$$\mathbf{X} = \sum_{a=1}^{A} \mathbf{t}_a \mathbf{p}_a^{\mathrm{T}} + \sum_{a=A+1}^{R} \mathbf{t}_a \mathbf{p}_a^{\mathrm{T}} = \mathbf{T}\mathbf{P}^{\mathrm{T}} + \mathbf{E} = \hat{\mathbf{X}} + \mathbf{E} \quad , \tag{2.7}$$

where $\mathbf{T} = [\mathbf{t}_1, \mathbf{t}_2, \ldots, \mathbf{t}_A]$ is the score matrix, $\mathbf{P} = [\mathbf{p}_1, \mathbf{p}_2, \ldots, \mathbf{p}_A]$ is the loading matrix, $\mathbf{E}$ is the $[I \times R]$ matrix of the residuals generated by the $(R - A)$ discarded PCs of the PCA model when $\mathbf{X}$ is reconstructed (i.e., approximated) by using only the first A PCs (i.e., $\hat{\mathbf{X}} = \mathbf{T}\mathbf{P}^{\mathrm{T}}$).

In general, using models the data are separated into two parts; the systematic part explained by the model, and the noise (or inherent variability) that usually characterizes the measurements (Eriksson *et al*., 2006). If the correct number of PCs are selected, $\hat{\mathbf{X}}$ should comprehend all the systematic part of the data, whereas the noise (and eventually the remaining un-modeled part of the data) is discarded in $\mathbf{E}$. Anyway, if data present strong non-linear characteristics the un-modeled variability of the data may include a part of systematic information that the PCA, which is basically a linear model, is not able to describe. Possible solution to this problem rely on appropriate data pretreatment (Section 2.1.1.1) and on the use of modified PCA algorithms (among others, NN-PCA, Dong and McAvoy, 1996; KPCA, Schölkopf *et al*., 1998; Mika *et al*., 1999).

A simplified graphical representation of the geometrical interpretation of the PCA model is provided in Figure 2.1. A dataset $\mathbf{X}$ of 7 samples and 2 variables ($\mathbf{x}_1$, $\mathbf{x}_2$) is considered. When a PCA model is applied, the direction of maximum variability of the data is identified by PC1, which represents the trend of the data in the (bidimensional) space of the original variables. This is an example of the ability of each single PC to capture the variability of all the variables which are correlated along that direction. This permit to describe the original dataset $\mathbf{X}$ by a lower number of variables, by projecting the data in $\mathbf{X}$ from the original variable space to the low - dimensional latent space of the PCs.

Under a geometrical point of view, the model loadings $p_{1,1}$ and $p_{1,2}$ represent the director cosines of $\mathbf{x}_1$ and $\mathbf{x}_2$ respectively, on PC1, namely the cosines of the angles between the latent direction of the model and the axes of the original variable space (gray area in Figure 2.1). Each score $t_{1,n}$ represents the coordinate of the n-th sample of matrix $\mathbf{X}$ in the new model space, represented by PC1. The distance of sample no. 1 to PC1, denoted by a dashed line perpendicular to the line indicating the first PC direction, represents the residual $e_{1,1}$, namely the information not captured by the model for this sample. However, if a second principal component (PC2) was considered (dashed gray line in Figure 2.1, orthogonal to PC1), it would account for the orthogonal distance of each projection from the PC1 direction, capturing a very limited variability of the data compared to PC1. Actually, in this case, a single PC is sufficient to adequately describe $\mathbf{X}$.

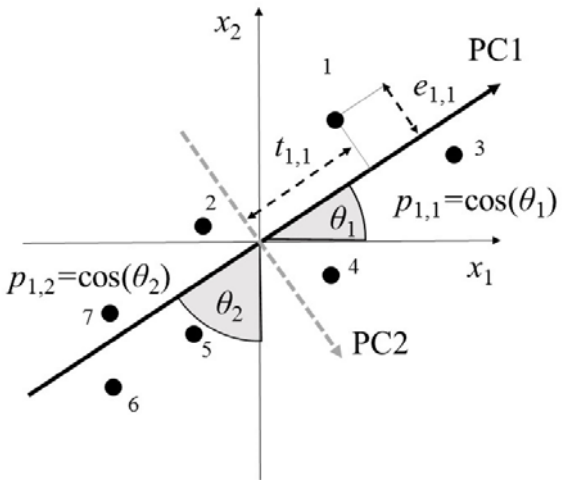

Figure 2.1. *Geometrical interpretation of the PCA scores and loadings for a dataset* **X** *[7×2]) (adapted from Tomba, 2013).*

The ability of representing a system with a reduced number of latent variables compared to the number of the original variables, is only a part of the advantages of the use of a PCA model. In fact, the graphical representation of the PCA model parameters (scores and loadings) is often used to gain understanding on the correlations among samples (through the scores) and variables (through the loadings). Additional details on the interpretation of scores and loadings plots are provided in Appendix A. For the computation of the model scores and loadings, the singular value decomposition[‡] (SVD; Meyer, 2000) of the covariance matrix of **X** ($\mathbf{X}^T\mathbf{X}$) or the nonlinear iterative partial least-squares algorithm (NIPALS; Wold, 1966) can be used.

2.1.1.1 Data pretreatment

Before building a PCA model, the data analyzed are usually pretreated. The appropriate pretreatment of **X** depends on the characteristics of the data and on the objectives of the analysis, and it may include filtering, denoising, transformations (e.g., logarithmic ones), advanced scaling and data compression (Eriksson *et al.,* 2006).

Usually, the datasets analyzed with LVMs (as process datasets), collects many variables of different type and physical meaning. To correctly analyzed their structure by a PCA model, it is important that variables are weighted in a similar way. The most common data pretreatment is autoscaling, i.e. mean-centering the data and scaling them to unit variance (Wise et al., 2006). Mean-centering (i.e., subtracting to each column $\mathbf{x}_n$ of **X** its mean values) avoids to detect the differences among the mean values of different variables as significant directions of variability. Scaling to unit variance (i.e., diving each column $\mathbf{x}_n$ of **X** by its standard deviation, so that the total variance of the column is equal to one) makes the analysis independent of the measurement

[‡] In this Dissertation the SVD has been used.

units, thus enabling the simultaneous analysis of variables with values of very different magnitudes, and has also the advantage of partially linearizing data. It is important to underline that when data in **X** are only mean-centered, matrix **Σ** represents the covariance matrix of **X**, while if data are auto-scaled, it becomes the correlation matrix of **X**. For this reason, correlations between variables can be identified from the loadings of a PCA model performed on auto-scaled data.

2.1.1.2 Selection of the number of PCs

As above-mentioned, usually the number (A) of PCs selected to adequately represent the original variable space, is smaller than the rank of **X**. The determination of the dimensionality of the latent space of the model, namely the selection of the number of PCs to be retained, is a critical aspect in the development of a PCA model, since it may affect its effectiveness and reliability. Several methods have been proposed in the literature (Valle *et al*., 1999) to deal with this issue. In general, PCA can be used simply to model a given dataset **X**, or to predict or compare external datasets using the information achieved by modeling the **X** dataset, called calibration set. Therefore, the selection of an appropriate number of PCs, is linked to the difference between the degree of fit and the predictive ability of the model, and depends on the purpose of the analysis performed. The fit tells how well the model is able to mathematically reproduce the data of the training set, whereas the predictive ability of the model is estimated by how accurately external **X**-data can be predicted (Eriksson *et al*., 2006). Therefore, to select the appropriate number of PCs different issues should be considered, as the number of samples, the total variance explained, the relative size of the eigenvalues (i.e. the variance explained per component), and the subject-matter interpretations of the PCs (Johnson and Wichern, 2007). In this Dissertation two of the several available methods have been applied:

- the scree test (Jackson et al., 1991);
- the eigenvalue-greater-than-one rule (Mardia et al., 1979);

The scree test is an empirical and graphical procedure, which is based on the analysis of the profile of an index indicating the variability of the original data captured by the PCA model per PC, in terms of explained variance R^2 per PC, eigenvalues (Eq. 2.5) or residual percent variance. The explained variance R^2 quantifies the amount of variability of the original data captured by the model:

$$R^2 = 1 - \frac{\sum_{i=1}^{I}\sum_{n=1}^{N}(x_{i,n} - \hat{x}_{i,n})^2}{\sum_{i=1}^{I}\sum_{n=1}^{N}(x_{i,n})^2} \quad , \tag{2.8}$$

where $x_{i,n}$ and $\hat{x}_{i,n}$ represent respectively the element in the *i*-th row and *n*-th column of the original matrix **X** and of the reconstructed matrix $\hat{\mathbf{X}}$. R^2 is calculated for each PCs included in the model. Its cumulative value is expressed as R^2_{CUM}.

The method is based on the idea that the variance described by the model should reaches a "steady-state", when additional PCs begin to describe the variability due to random errors. When a break point is found in the curve or when the profile stabilizes, that point corresponds to the number of PCs to be included in the model. The implementation of the method is relatively easy, but if the curve decreases smoothly it can be difficult to identify an "elbow" on it. The eigenvalue-greater-than-one rule is a simple rule for which all the PCs whose corresponding eigenvalues are lower than one are not considered in the model. The basic idea behind this method is that, if data are auto-scaled, the eigenvalue corresponding to a PC represents roughly the number of original variables whose variability is captured by the PC itself. If so, a PC capturing less than one original variable should not be included in the model. Although this method is very easy to implement and automate, in some cases PCs are discarded even if their eigenvalue is very close to one and their contribution to explain the systematic variability is significant. In these cases, it may be reasonable to lower the threshold in order to include PCs whose eigenvalue may be (slightly) lower than one.

In relation to the selection of the number of PCs to be retained, several diagnostics can be used to assess the performance of a PCA model. Further details and examples about this topic are provided for example in Eriksson *et al*. (2006).

2.1.2 Projection to latent structures (PLS)

Projection to latent structures (PLS; Wold et al., 1983; Höskuldsson, 1988) is a regression technique that relates a dataset of regressors **X** (e.g., initial conditions, process parameters, process measurements, critical process parameters), to a dataset of response variables **Y** (e.g., qualitative features, critical quality attributes) through the projection onto their latent structure. PLS allows modeling both the outer relations, that is the relations between the variables in **X** and **Y** individually, and the inner relations, that is the relations within the two matrixes (Geladi and Kowalski, 1986). PLS aims at finding a linear transformation of the **X** data in order to maximize the covariance of its latent space and that of **Y**. The optimization problem formalizing the search for the LVs can be converted into an eigenvector problem, namely the eigenvector decomposition of the joint covariance matrix $\mathbf{X}^T\mathbf{Y}\mathbf{Y}^T\mathbf{X}$:

$$\mathbf{X}^T\mathbf{Y}\mathbf{Y}^T\mathbf{X}\mathbf{w} = \lambda\mathbf{w} \quad , \tag{2.9}$$

being **w** the vector of weights representing the coefficient of the linear combination of **X**-variables determining the PLS scores **t**:

$$\mathbf{t} = \mathbf{Xw} \quad . \tag{2.10}$$

In order to obtain the weight vectors for the further LVs, the problem in Eq. (2.9) may be solved iteratively using the deflated $\mathbf{X}_a$ and $\mathbf{Y}_a$ matrices. In the deflation process at the a-th step, the reconstructions of each dataset ($\mathbf{X}_a$ and $\mathbf{Y}_a$) from the a-th estimated LV are subtracted to the datasets themselves assuming that A LVs have been retained. Eventually, the **X** and **Y** datasets are decomposed and related through their latent structures:

$$\mathbf{X} = \mathbf{TP}^{\mathrm{T}} + \mathbf{E} \quad , \tag{2.11}$$

$$\mathbf{Y} = \mathbf{TQ}^{\mathrm{T}} + \mathbf{F} \quad , \tag{2.12}$$

$$\mathbf{T} = \mathbf{XW}^{*} , \tag{2.13}$$

where **T** is the [I×A] score matrix, **P** and **Q** are the [N×A] and [M×A] loading matrices, **E** and **F** are the [I×N] and [I×M] residual matrices, which are minimized in the least-square sense, and $\mathbf{W}^{*}$ is the [N×A] weight matrix, which is calculated from the weights **W** to allow interpretation with respect to the original **X** matrix:

$$\mathbf{W}^{*} = \mathbf{W}(\mathbf{P}^{\mathrm{T}}\mathbf{W})^{-1} \quad . \tag{2.14}$$

The advantage in using PLS is that it provides a model for the correlation structure of **X**, a model for the correlation structure of **Y**, and a model of their mutual relation. The basic assumption is that the spaces identified by **X** and **Y** have a common latent structure, which can be employed to relate them. Note that oftentimes in (2.12) the score matrix **T** is substituted by the **Y** space score matrix **U**[I×A], with **U**=**TB** (called inner relation; Geladi and Kowalski, 1986).
This is explain in Figure 2.2 provides a geometrical interpretation of the PLS model: a dataset **X** [20×3] of regressors and a dataset **Y** [20×2] of response variables are considered. As can be seen, data in **X** arrange mainly on a plane, defined by two latent directions. Latent directions are identified in the **X** and in the **Y** space in order to best approximate the directions of maximum variability of the points in the original spaces and to provide a good correlation between the projections of the points themselves along these directions. As in the PCA case (Figure 2.1), the projections of the original points on these directions represent the PLS scores, while the loadings are the director cosines of the latent directions. Note that, while weights **W** are orthogonal in the **X** space, the loadings **Q** in the **Y** space may not necessarily be (Eriksson *et al*., 2006).

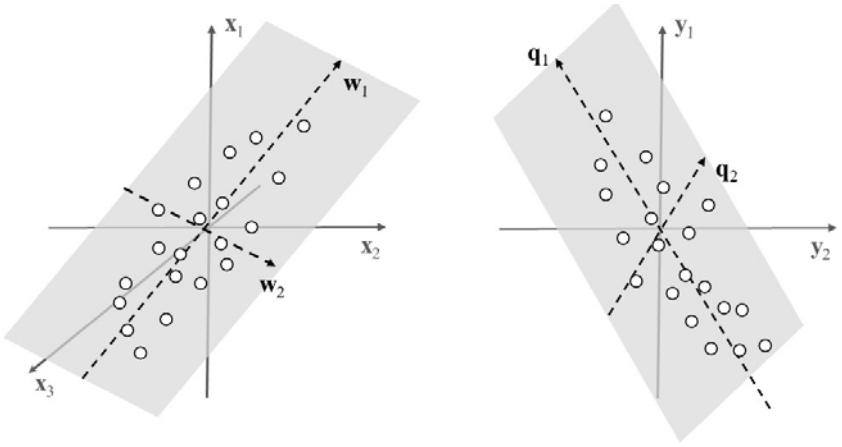

Figure 2.2. *Geometric interpretation of the PLS model decomposition in latent structures (adapted from Tomba, 2013).*

As for PCA, PLS model scores, weights and loadings can be interpreted to gain understanding on the similarity between different samples and on the correlation among variables within and between datasets. Further details on the interpretation of the PLS scores and weights/loadings are provided in Appendix A. Several algorithms have been proposed in the literature to calculate the parameters of a PLS model, in this Dissertation the NIPALS (Wold, 1966, Wold et al., 1983) algorithm has been used.

The selection of the number A of LVs to be retained is discussed by Wold (1978). The considerations on data pretreatment and model diagnostics reported for PCA are valid also for PLS. A thorough discussion of PLS modeling can be found in Wold *et al*. (1983), Höskuldsson (1988) and Burnham *et al*. (1996).

2.1.2.1 Statistics associated with the use of LVMs

When a LVM model is built, statistic indices can be calculated based on the data used for its calibration, in order to discover potential outliers or data that have a strong influence on the model. Two statistics are used to this purpose: the Hotelling's T^2 and the squared prediction error (SPE). The Hotelling's T^2 statistic (Hotelling, 1933) is a measure of the variation in each sample within the PCA model. It measures the overall distance of the projections of a sample of the **X** dataset from the PC space origin, weighted by the percentage of variance explained by each PC (Mardia et al., 1979):

$$T_i^2 = \sum_{a=1}^{A} \frac{t_{a,i}^2}{\lambda_a} \quad , \tag{2.15}$$

where $t_{a,i}$ represents the projection of the i-th observation on the a-th PC used to build the model and λ_a is the eigenvalue associated to the a-th PC. The T^2 statistic is used to assess the deviation of a sample from the average conditions (the PC space origin) represented in the dataset.

On the other hand, the representativeness of the observation by the model is quantified through the SPE statistic that is defined for the *i*-th sample as:

$$\mathrm{SPE}_i = \mathbf{e}_i^{\mathrm{T}}\mathbf{e}_i = \mathbf{x}_i(\mathbf{I} - \mathbf{P}\mathbf{P}^{\mathrm{T}})\mathbf{x}_i^{\mathrm{T}} \quad , \tag{2.16}$$

where $\mathbf{e}_i$ is the [N×1] residual vector for the reconstruction of the i-th observation $\mathbf{x}_i$ (i.e. the i-th row of the residual matrix **E**), and **I** the identity matrix of size [N×N]. SPE_i measures the orthogonal distance of the i-th observation from the latent space identified by the model, thus accounting for the model mismatch. This means that samples with high values of SPE are characterized by a different correlation structure with respect to the one described by the PCA model and, as a consequence, are not well-represented by the model.

Confidence limits can be set both for Hotelling's T^2 and for SPE, based on the values they assume for the data in model calibration, to evaluate possible outliers or analyze a new set of data ($\mathbf{X}^{\mathrm{PRED}}$). In particular, the scores have zero mean, variance equal to their associated eigenvalues and are orthogonal. Assuming that the data used to build the model are independent and identically distributed, scores are normally distributed. Therefore, for the scores on the a-th LV, a univariate confidence limit can be calculated from the critical value of the Student's t-distribution, with I-1 degrees of freedom at significance level α:

$$t_{(1-\alpha)\lim}(a) = \pm t_{I-1,\alpha/2} \cdot \sqrt{\lambda_a} \quad . \tag{2.17}$$

Under this assumption, the Hotelling's T^2 can be well-approximated as a Fisher's F- distribution, being it computed from the ratio of approximately normal variables. Its relevant confidence limit can therefore be estimated as (Mardia *et al.*, 1979):

$$T^2_{(1-\alpha)\lim}(A,I) = \frac{A\cdot(I^2-1)}{I\cdot(1-A)} \cdot F_{A,I-A,\alpha} \quad , \tag{2.18}$$

where $F_{A,I-A,\alpha}$ is the critical value of the F distribution with A and I - A degrees of freedom at significance level α. This determines in the A-dimensional score space an ellipsoidal confidence region, whose semi-axes are:

$$sa_a = \sqrt{\lambda_a T^2_{(1-\alpha)\lim}(A,I)} \quad \text{with } a = 1,....,A \quad . \tag{2.19}$$

In particular, to allow a visual representation, confidence ellipses can be determined through Eq. (2.19) for the projections of the scores of data in bi-dimensional planes.

The SPE statistic is a sum of squared errors, which can be assumed to follow a normal distribution. As a consequence, SPE can be approximated as a χ^2- distribution, and its relevant limit calculated as follows:

$$\text{SPE}_{(1-\alpha)\text{lim}} = [\nu/(2\cdot\mu)]\cdot\chi^2_{2\cdot\mu^2/\nu,a} \quad \text{with} \quad a = 1,....,\ A \quad , \tag{2.20}$$

where $\chi^2_{2\cdot\mu^2/\nu,a}$ is the critical value of the χ^2- distribution with $2\cdot\mu^2/\nu$ degrees of freedom at the significance level α; μ and ν are respectively the mean and the variance of the SPE values of the data used to build the model (Nomikos and MacGregor, 1995).

Once a LVM has been calibrated on the available datasets, the model can be used to assess the overall conformance of a new sample $\mathbf{x}^{\text{PRED}}$ to the data used to build the model (i.e. the historical data). This can be done by projecting $\mathbf{x}^{\text{PRED}}$ onto the PCA model space, in order to calculate the corresponding scores $\hat{\mathbf{t}}^{\text{PRED}}$ [A×1]:

$$\hat{\mathbf{t}}^{\text{PRED}\ \text{T}} = \mathbf{x}^{\text{PRED}\ \text{T}}\mathbf{P} \quad . \tag{2.21}$$

or, if a PLS model is used:

$$\hat{\mathbf{t}}^{\text{PRED}\ \text{T}} = \mathbf{x}^{\text{PRED}\ \text{T}}\mathbf{W}^{*} \quad . \tag{2.22}$$

The scores $\hat{\mathbf{t}}^{\text{PRED}}$ can be used to calculate the Hotelling's T^2 (Eq. 2.18) of the new sample ($T^2_{x^{\text{PRED}}}$) which provides a measure of the deviation of the new sample from the average conditions of the data used to build the model. Once the scores have been calculated, sample $\mathbf{x}^{\text{PRED}}$ can be reconstructed from the model for **X**:

$$\hat{\mathbf{x}}^{\text{PRED}} = \mathbf{P}\hat{\mathbf{t}}^{\text{PRED}} \quad . \tag{2.23}$$

which is valid both for a PCA or a PLS model. Furthermore, in the case of the PLS model, a prediction of the response variables can be obtained by reconstructing $\hat{\mathbf{y}}^{\text{PRED}}$ [M×1]:

$$\hat{\mathbf{y}}^{\text{PRED}} = \mathbf{Q}\hat{\mathbf{t}}^{\text{PRED}} \quad . \tag{2.24}$$

From $\hat{\mathbf{x}}^{\text{PRED}}$ the value of the squared prediction error for $\mathbf{x}^{\text{PRED}}$ ($\text{SPE}_{\mathbf{x}^{\text{PRED}}}$) can be obtained from Eq. (2.16). This statistic represents the model mismatch for the new incoming sample $\mathbf{x}^{\text{PRED}}$. The statistics $\hat{\mathbf{t}}^{\text{PRED}}$, $T^2_{\mathbf{x}^{\text{PRED}}}$ and $\text{SPE}_{\mathbf{x}^{\text{PRED}}}$ provide therefore measures of the conformance of $\mathbf{x}^{\text{PRED}}$ to the historical data. In particular the T^2 and SPE statistics calculated for the new sample are compared with the relevant confidence limits defined in Eq. (2.18) and Eq. (2.20) to judge the

similarity and the adherence of $\mathbf{x}^{PRED}$ to the data used to build the model (the same rationale is commonly used also to build monitoring charts for process monitoring purposes):

$$\begin{aligned} T^2_{\mathbf{x}^{PRED}} &\leq T^2_{(1-\alpha)\lim} \\ \mathrm{SPE}_{\mathbf{x}^{PRED}} &\leq \mathrm{SPE}_{(1-\alpha)\lim} \end{aligned} \quad . \tag{2.25}$$

If the conditions in (2.25) are satisfied, $\mathbf{x}^{PRED}$ the hypothesis that $\mathbf{x}^{PRED}$ complies with the calibration (i.e. historical) data with a 100(1-α)% probability is satisfied (Johnson and Wichern, 2007); otherwise a change in the mean conditions ($T^2_{\mathbf{x}^{PRED}} \leq T^2_{(1-\alpha)\lim}$) or in the representativeness of the model ($\mathrm{SPE}_{\mathbf{x}^{PRED}} \leq \mathrm{SPE}_{(1-\alpha)\lim}$) compared to the common cause data used to build the model may have occurred. If a problem is detected, the root cause can be identified by analyzing the relevant contributions of each variable in the **X** dataset to the T^2 and SPE statistics of the sample. These permit to identify the variables that are most responsible for the distance of a sample from the origin of the PC space or from the PC space itself. This can be done both for calibration data and for predicted data. In particular, the contributions to T^2 can be calculated as follows:

$$\mathbf{t}^{\mathrm{T}}_{\mathrm{CONT},i} = \mathbf{t}^{\mathrm{T}}_i \boldsymbol{\Lambda}^{-1/2} \mathbf{P}^{\mathrm{T}} \quad , \tag{2.26}$$

$\mathbf{t}_{\mathrm{CONT,i}}$ is a [N×1] vector of the contributions of each variable to the Hotelling's T^2 statistic and can be considered a scaled version of the data within the PCA model. The formulation in (2.26) has the property that the sum of the squared elements of $\mathbf{t}_{\mathrm{CONT,i}}$ gives T^2_i for the i-th observation. The contribution of each variable to the SPE_i statistic for the i-th sample coincides instead with the residuals in the reconstruction of the sample through the model (i.e. each single element $e_{i,n}$ of the i-th row of the residual matrix **E**):

$$\mathrm{SPE}_{\mathrm{CONT},i} = \mathbf{e}_{i,n} \quad . \tag{2.27}$$

The analysis of the variable contributions can reveal which variables mainly determine the position of a sample in the score space or out of it. This, together with physical knowledge on the system, may be useful especially when outliers are pinpointed, to understand the root cause of the problem. Procedures to calculate limits for the variable contributions have been proposed (Conlin *et al.*, 2000).

2.1.3 Model inversion

Latent variable model inversion was first introduced by Jaeckle and MacGregor (1998; 2000a and 2000b) and recently generalized by Tomba *et al*. (2012). The basic idea under LVM inversion is to exploit the relations between response variables and regressor variables, modelled by a LVRM,

in order to estimate a set of *input* variables $\mathbf{x}_{NEW}$ (e.g., initial conditions, process parameters, process settings, CPPs) starting from a desired set of response variables $\mathbf{y}_{DES}$ (target product profile). To estimate $\mathbf{x}_{NEW}$, the LVRM model is inverted as sketched in Figure 2.1.

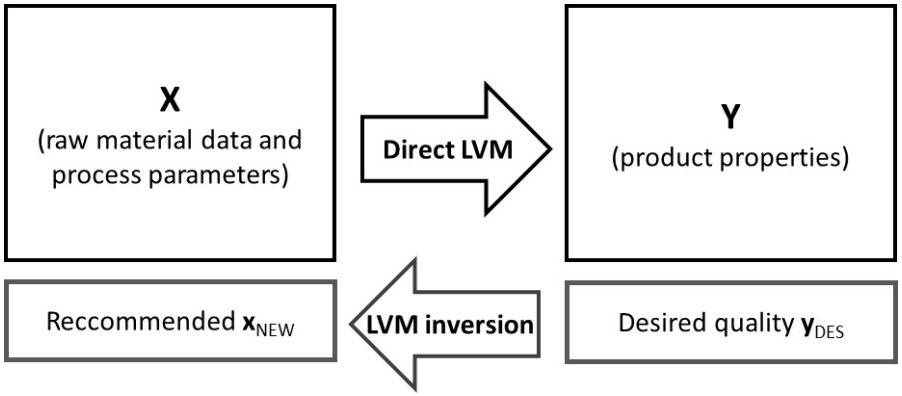

Figure 2.3. *Schematic of the direct use of LVM and of the LVM inversion (adapted from Ottavian et al., 2016)*

Assuming that the desired response $\mathbf{y}_{DES}$ has been defined, its projections $\hat{\mathbf{t}}_{NEW}$ onto the score latent space can be estimated by the LVRM inversion of the PLS model used to describe their relationship as (Jaeckle and MacGregor, 1998):

$$\hat{\mathbf{t}}_{NEW}^{T} = (\mathbf{Q}^{T}\mathbf{Q})^{-1}\mathbf{Q}^{T}\mathbf{y}_{DES} \quad . \tag{2.28}$$

The set of input variables $\hat{\mathbf{x}}_{NEW}$ corresponding to the desired product quality $\mathbf{y}_{DES}$ can be reconstructed from $\hat{\mathbf{t}}_{NEW}$ (2.28) using Eq. (2.23). This is called direct LVRM inversion, and $\hat{\mathbf{x}}_{NEW}$ follows the same covariance structure of the historical data (Jaeckle and MacGregor, 1998).
However, depending on the effective dimension of the latent spaces of **X** and **Y** (i.e., on their statistical rank) and on the number A of LVs retained to build the model, the solution to the inversion problem may not be unique. Assuming, $R_{\mathbf{X}}$ as the statistical rank of **X** and $R_{\mathbf{Y}}$ as the statistical rank of **Y**, the number of latent directions selected are usually A=max($R_{\mathbf{X}}$, $R_{\mathbf{Y}}$). Depending on the ranks of the datasets, three cases may arise (Jaeckle and MacGregor, 1998):

1. $A = R_{\mathbf{X}}$ ($R_{\mathbf{X}} > R_{\mathbf{Y}}$): this is the most common situation, where there are some LVs (or their combination) in the latent space of **X** statistically significant to describe the systematic variability in **X**, but which do not contribute in explaining the variability of the data in **Y**. In this case, part of the variability in the **X** space is not related to the **Y** space (Burnham *et al*., 1999) hence, the inversion exercise requires a projection from a lower dimensional **Y** space ($R_{\mathbf{Y}}$) to the higher dimensional **X** space ($R_{\mathbf{X}}$).
2. $A = R_{\mathbf{Y}}$ ($R_{\mathbf{Y}} \geq R_{\mathbf{X}}$): in this case, there is a substantial overlapping between the latent space of **X** and **Y** (Burnham *et al*., 1999), all the LVs of the **X** space potentially explain systematic

variability in **Y**. In this case, the model inversion corresponds to a projection from a higher dimensional **Y** space ($R_{\mathbf{Y}}$) to a lower dimensional **X** space ($R_{\mathbf{X}}$).

3. $A = R_{\mathbf{X}} = R_{\mathbf{Y}}$ but rank([**XY**]) > A: in this case, although the statistical rank of **X** and **Y** is equal, the rank $R_{\mathbf{XY}}$ is greater, therefore ($R_{\mathbf{XY}} - A$) latent dimensions do not overlap between the **X** and **Y** spaces. This situation is similar to the one where A = $R_{\mathbf{X}}$ ($R_{\mathbf{X}} > R_{\mathbf{Y}}$).

Only in the second case a unique solution exists by applying the direct model inversion. In the first and last cases, the number of solutions is infinite. Although the direct model inversion (Eq.2.28) provides the least-squares solution to the problem, this solution can be moved by changing $\hat{\mathbf{t}}_{\text{NEW}}$ along the directions of latent space that do not contribute to explain the variability of **Y**, namely which do not affect the response variables. These directions identify a *null space*, which represents the *locus* of the **X** projections not affecting the quality space of **Y** (Jaeckle and MacGregor, 1998). Therefore, the set $\mathbf{x}_{\text{NEW}}$ suggested by the direct inversion can be moved along the null space without affecting the product quality. In order to find the most suitable process conditions $\mathbf{x}_{\text{NEW}}$ along the null space that are necessary to achieve the desired quality $\mathbf{y}_{\text{DES}}$, an optimization problem have to be solved (Yacoub and MacGregor, 2011; García-Muñoz *et al*., 2006 and 2008). To this purpose, Tomba *et al*., (2012, 2013b) and Tomba (2013) proposed a general framework that allows one to find a solution $\hat{\mathbf{x}}_{\text{NEW}}$ that is coherent with the historical data used to build the underlying model, and also accounts for any experimental limitations or other constraints that may be present.

A thorough discussion on the inversion/optimization problem, is provided by Yacoub and MacGregor (2011), García-Muñoz *et al*. (2006, 2008) and Tomba *et al*. (2012, 2014).

2.1.3.1 Null space computation

As previously stated, when $R_{\mathbf{Y}} < R_{\mathbf{X}}$ a null space exists. Hence, the estimation $\hat{\mathbf{x}}_{\text{NEW}}$ and the reconstruction of $\hat{\mathbf{y}}_{\text{DES}}$ are formed by two latent contributions, $\mathbf{t}_{\text{NEW}}$ and $\mathbf{t}_{\text{NULL}}$, which accounts respectively for the effective scores of $\hat{\mathbf{y}}_{\text{DES}}$ in the latent space and for the translation of the scores along the null space in order to provide the reconstruction of $\hat{\mathbf{x}}_{\text{NEW}}$ at a minimum distance from the latent space (minimum SPE). Therefore, any solution of the inversion problem $\hat{\mathbf{x}}$ can be defined as:

$$\hat{\mathbf{x}} = \hat{\mathbf{x}}_{\text{NEW}} + \hat{\mathbf{x}}_{\text{NULL}} \quad , \tag{2.29}$$

where $\hat{\mathbf{x}}_{\text{NEW}} = \mathbf{P}\mathbf{t}_{\text{NEW}}$ $\hat{\mathbf{x}}_{\text{NULL}}$ and $\hat{\mathbf{x}}_{\text{NULL}} = \mathbf{P}\mathbf{t}_{\text{NULL}}$ (which falls on the remaining $R_{\mathbf{X}} - R_{\mathbf{Y}}$ directions). The null space is needed for the model to represent adequately the regressor variables, but it does not contribute in explaining the variability in the response variables, hence:

$$\mathbf{Q}\mathbf{t}_{\text{NULL}} = 0 \quad . \tag{2.30}$$

The null space represents the kernel of the loadings **Q** matrix and can be computed from the singular value decomposition of matrix **Q** (Jaeckle and MacGregor, 2000a):

$$\mathbf{Q} = \mathbf{U}_\mathbf{Q}\mathbf{S}_\mathbf{Q}\mathbf{V}_\mathbf{Q}^\mathrm{T} = \mathbf{U}_\mathbf{Q}\mathbf{S}_\mathbf{Q}[\mathbf{G}_1 \vdots \mathbf{G}_2]^\mathrm{T} \quad , \tag{2.31}$$

where $\mathbf{U}_\mathbf{Q}$ is the matrix of the left singular vectors of **Q**, $\mathbf{S}_\mathbf{Q}$ is the diagonal matrix of the singular values of **Q**, and $\mathbf{V}_\mathbf{Q}$ is the matrix of the right singular vectors of **Q**. In particular, the right singular vectors corresponding to the vanishing (zeros) singular values of **Q** span its null space. These are included in the columns of matrix $\mathbf{G}_2$ $[A\times(A - R_\mathbf{Y})]$, which therefore defines the null space of the model. Vector $\mathbf{t}_\mathrm{NULL}$ can therefore be moved arbitrarily along it, without affecting $\hat{\mathbf{y}}_\mathrm{DES}$, i.e.:

$$\mathbf{t}_\mathrm{NULL}^\mathrm{T} = \boldsymbol{\gamma}^\mathrm{T}\mathbf{G}_2^\mathrm{T} \quad . \tag{2.32}$$

In Eq. (2.32), which defines the model null space, $\boldsymbol{\gamma}$ is an $[(A - R_\mathbf{Y}) \times 1]$ vector arbitrary in magnitude and direction.

It should be observed that the concept of the null space can be related to the definition of the design space (ICH, 2009), namely to "the space of the input variable combinations that robustly ensure to obtain a defined product in output". As observed by Tomba *et al*. (2012) and Ottavian *et al*. (2016), the null space represents a useful basis for further experimentation to properly develop a DS, as will be shown in Chapter 5.

2.2 Pattern recognition techniques

Pattern recognition techniques are intended to devise ways and means of automating certain decision-making processes that lead to classification and recognition of common patterns and regularities in large sets of data (Pal and Mitra, 2004). Pattern recognition techniques present several advantages in the analysis of large datasets, namely: *i*) they are able to recognize those relationships that differentiate similar or not similar objects, thereby identifying the common properties that characterize different groups of objects; *ii*) they are able to handle multivariate data; *iii*) they facilitate the analysis of systems where the exact relationships are not fully understood, by extracting the important feature from the available datasets (Lavine and Davidson, 2006). The number and type of techniques that can be categorized in the big family of pattern recognition techniques are very broad, as well as are the application fields. In fact, thanks to their potential, pattern recognition techniques have been found many applications in engineering, as well as in medical, chemical pharmaceutical, social and economic sciences, both as classification (or clustering) tools and as regression/prediction tools.

In this Dissertation we are mainly interested in the use of pattern recognition techniques in their original acceptation, namely as classification tools. While regression methods model quantitative

responses on the basis of a set of regressor variables, classification techniques are quantitative methods for the modeling of qualitative responses, that attempt to find mathematical relationships between a set of descriptive variables and a qualitative variable (Ballabio and Todeschini, 2009). As mentioned above, pattern-recognition methods were originally designed to find classification rules (or empirical relationships) to classify new samples in relation to a specific property, according to the information extracted by a set of samples (called training or calibration set) for which the property of interest and the measurements indirectly related to that property are known. In this context, the term *pattern* indicates the set of measurements that describe each sample in the training set, for which the property of interest and measurements are known, whereas the assignment of a new sample to its respective class is called *recognition*, since it is performed by recognizing the property of interest (Lavine and Davidson, 2006).

Three main steps characterize a typical pattern recognition system: data acquisition, feature selection/extraction and classification/clustering. Once the data have been collected using a set of sensors, they are then passed on to the feature selection/extraction phase, where the dimensionality of the data is reduced by retaining only some characteristic features or properties. Finally, in the classification/clustering phase, the selected features are passed on to the classifying/clustering system that evaluates the incoming information and makes a final decision (Pal and Mitra, 2004).

In classification analysis, if I objects are considered, each described by M variables and divided into C categories (classes), they can be organized in a matrix $\mathbf{X}$, composed of I rows (the samples), and N columns (the explanatory variables). Each entry, $x_{i,n}$ represents the value of the n-th variable for the i-th object. The additional information concerning the class is collected into a vector $\mathbf{c}$ [$C \times 1$], constituted by C different labels or integers, each representing a class. Each sample $x_{i,n}$ can be considered as a point in a high-dimensional measurement space. Points representing objects from one class tend to cluster in a limited region of the measurement space separated from the others. Therefore, to solve a classification problem, the feature space should be partitioned into regions, namely one region for each category of input. This permits one to assign every data point in the entire feature space to one of the possible classes (region). However, usually the complete description of the classes is not known, since the available training set includes only a finite and usually small number of samples, which often provides only partial information for design a classifying/clustering system. On the basis of the information provided by the samples in the training set, the pattern recognition systems are designed, namely the values of the parameters of various pattern recognition methods are tuned to minimize the misclassification errors (Pal and Mitra, 2004).

Depending on the features of the available data, different type of classifiers can be designed. For example, the training set may include labeled or unlabeled data. In the first case, each new object is classified based on the information acquired on a set of objects with known classifications (i.e., labels); this classification method is called supervised. Otherwise, if no a priori information on

the set of samples that is used for classification purposes is available (unlabelled data), the method is called unsupervised. Supervised methods are used for classifying different objects, while clustering is performed through unsupervised methods. Principal components analysis represents an example of unsupervised methods. PCA does not focus on how many groups will be found, since it does not use information related to predefined classes of objects (Ballabio and Todeschini, 2009).

Then, distinctions can be made among the different classification techniques on the basis of the mathematical form of the decision boundary, i.e. on the basis of the ability of the method to detect linear or non-linear boundaries between the region in which the analyzed space is partitioned. Moreover, classification techniques can be probabilistic, if they are based on estimates of probability distributions, i.e. a specific underlying probability distribution in the data is assumed. Among probabilistic techniques, parametric and non-parametric methods can be distinguished, when probability distributions are characterized by location and dispersion parameters (e.g. mean, variance, covariance). Classification methods can also be defined as distance-based, if they require the calculation of distances between objects or between objects and models.

Examples of pattern-recognition methods that have been used to classification or clustering purposes include nearest neighbors, neural networks, discriminant analysis, clustering analysis, and principal component analysis. In this Dissertation, only the first and the last one are employed and described; further information and examples of application of other techniques can be found (among others) in Lavine and Davidson (2006) and Varmuza and Filmozer (2009), Pal and Mitra (2004).

2.2.1 K-nearest neighbors

k-nearest neighbor (*k*-NN) is a powerful classification technique. *k*-NN is a supervised method, namely a training set is required for the classification of new observations. The nearest neighbor classification rule (Cover and Hart, 1967) classifies an unclassified observation depending on the class attribution for an assigned number *k* of neighbors idecavolntified according to a given distance criterion. Therefore, *k*-NN is a distance-based method, since the classification is performed by calculating the distances between the new observation and all the observations of the training set.

In Figure 2.4a a graphical representation of the rationale underlying the *k*-NN method in the classification of a new sample (black star) is shown. Two different clusters are considered (Cluster 1 and Cluster 2), whose samples are denoted respectively as open triangles and squares. Assuming k=5, the k nearest neighbors to $x_{i,n}$, are identified as the closest 5 objects to the new sample that lie in the gray area around the sample. The predicted class membership $\hat{c}_{i,n}$ of the new object $x_{i,n}$ is obtained from the known class memberships $c(x(1)), \ldots, c(x(k))$ of the k nearest neighbors, and can be taken as the class that occurs most frequently among the k neighbors (Varmuza and

Filzmoser, 2009). Thus, the prediction corresponds to a majority vote among the neighbors, that with k=5, corresponds to Cluster 1, since 3 out of 5 closest samples belong to this cluster.

The decision boundary between different groups can be very rough, and it strongly depends on the parameter k. Thus, for small values of k, it is easily possible that classes do no longer form connected regions in the data space, but they can consist of isolated clouds. The classification of new objects can thus be poor if k is chosen too small or too large. In the former case, we are concerned with overfitting, and in the latter case with underfitting (Varmuza and Filzmoser, 2009). The importance of the selection of the parameter k is demonstrated in Figure 2.4b, where if k=11 is selected, the new sample is assigned to Cluster 2 instead of Cluster 1, since 6 out of 5 neighbors belong to this cluster.

Different methods to calculate the distance between the observation to be classified and the observations of the training set have been suggested, as well as different decision rules in case of ties. Since the decision boundary between different groups strongly depends on the parameter k (Varmuza and Filzmoser, 2009), cross-validation procedures should be implemented by testing a set of k values (e.g. from 1 to 10). Note that if the samples analysed are characterized by different variables measured in different units, similarly to the application of latent variables modeling, it is suggested that the data are first mean-centered and scaled to unit variance.

k-NN is a non-parametric classification method (i.e., it does not assume a form of the underlying probability density functions) and can handle multiclass problems. Another important advantage is that k-NN is a nonlinear method, since the Euclidean distance between two observations in the data space is a nonlinear function of the variables (Ballabio and Todeschini, 2009).

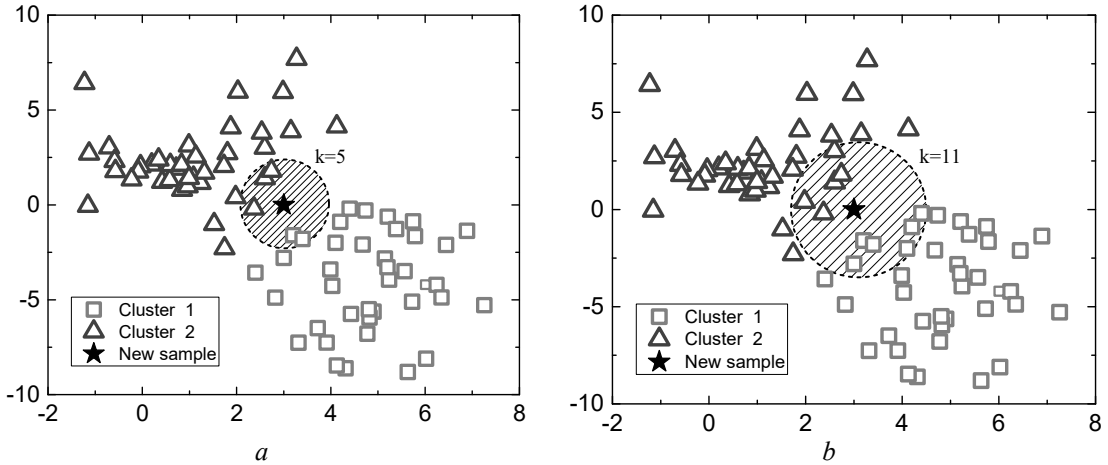

Figure 2.4. *Graphical interpretation of the k-NN classification of a new sample (★) considering (a) k=5 and (b) k=11.*

2.2.2 PCA for cluster analysis

Employed as a cluster analysis tool, principal component analysis has also been demonstrated to be a valid exploratory data analysis technique that is often very helpful in elucidating the complex

nature of multivariate relationships. Used for clustering purposes, this technique is employed to uncover relationships in large multivariate datasets without directly using the information about the class assignment of the samples. In fact, the latent variable space resulting from the application of the PCA, permits one to visualize the relative position of the data points of the original dataset, which usually group in different clusters. Hence, once the structure of a given dataset (called calibration or training set) is modelled, new samples can be projected onto the PCA model space built for that dataset, in order to recognize which cluster the new samples are most similar to. Usually, only two or three principal components are necessary to explain a significant fraction of the information present in multivariate data (Lavine and Davidson, 2006).

Clusters are usually defined intuitively, depending on the context, as shown in Figure 2.5. In this example three main clusters can be distinguished (marked by different open symbols), and the new projections (closed triangles) are clearly recognized as belonging to Cluster 3. However, notice that no measure of cluster validity can serve as a reliable indicator of the quality of a proposed partitioning of the data (Lavine and Davidson, 2006), even if some possible solutions are provided in the literature (Rousseeuw, 1987).

Used as a clustering technique, principal component analysis can be applied to multivariate data to identify outliers, to display data structure, and to classify samples.

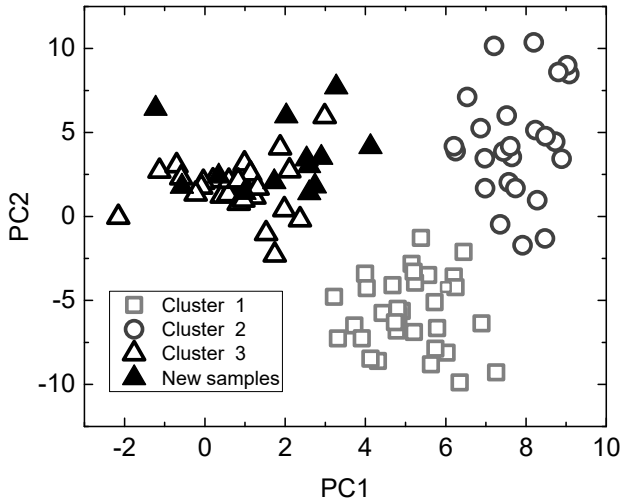

Figure 2.5. *Example of the discriminatory potential of the PCA model.*

Chapter 3

A methodology to diagnose process/model mismatch in first-principles models for steady-state systems*

In this Chapter a methodology is proposed to diagnose the root cause of the process/model mismatch (PMM) that may arise when a first-principles (FP) process model is challenged against a set of historical experimental data. The objective is to identify which model equations or model parameters most contribute to the observed mismatch, without carrying out any additional experiment. The methodology exploits the available data (namely, the historical dataset and a simulated one built by using the FP model) in order to analyze the correlation structure of the two datasets by means of a PCA model. Information on where the PMM originates from is obtained using diagnostic indices coupled to engineering judgment.

3.1 Introduction

Process modeling is an essential tool to support several process engineering activities (Stephanopoulos and Reklaitis, 2011; Gani, 2009; Pantelides and Urban, 2004). Mathematical modeling by first principles can be viewed as the best way to organize the available information about a process or a system in a meaningful way (Kiparissides *et al*., 2014). First-principles (FP) models are often preferred to data-driven (DD) ones, because they rely on a physical understanding on the system under investigation and allow some extrapolation beyond the range of data used to calibrate them (Pantelides and Renfro, 2013). On the other hand, DD (or data-based, DB) models are often easier to develop than FP ones, and may be computationally less intensive and more convenient for online use.

A model is made by equations and parameters. In an FP model, the equations represent the available knowledge on the underlying mechanisms driving the process, whereas the parameter values inform on how the general mechanisms are tuned to the actual system under investigation.

* Meneghetti, N., P. Facco, F. Bezzo, M. Barolo (2014). A methodology to diagnose process/model mismatch in first-principles models. *Ind. Eng. Chem. Res*., **53**, 14002-14013.

When the FP model of a process is challenged against a historical dataset, the model outputs may not match the historical evidence to a desired accuracy, and therefore process/model mismatch (PMM) occurs. This may be due to different reasons: *i*) the knowledge about the underlying process is limited, and therefore the model equations are (perhaps only partially) inappropriate; *ii*) the complexity of the physical phenomena involved in the process has been mathematically oversimplified, e.g. because the model has to be used online; *iii*) some of the model parameters have been assigned inappropriate values (for example, some of them may have been taken from the open literature, some other from proprietary information, some other from semi-theoretical studies). The occurrence of PMM can be critical when the model is used for design, optimization or control purposes.

The model adherence to reality can be enhanced by acting on the model equations (i.e., by formulating alternative mechanisms that describe the process under investigation) or on the model parameters. In both cases new experiments, i.e. experiments ranging over operating conditions not included in the historical database, are usually needed to speculate on the alternative mathematical formulations or to fine-tune the model parameters. To this purpose, model-based design of experiments (MBDoE) techniques can be used (Franceschini and Machietto, 2008; Marquardt 2005). MBDoE allows one to design experiments that can provide useful information for model discrimination among alternative set of equations, or for parameter identification in an assigned set of equations. Although effective, the MBDoE exercise may be quite demanding if one does not know in advance which equations or parameters are most responsible for the observed PMM. Additionally, carrying out new experiments is expensive by itself. Indeed, to enhance the model performance when PMM is detected, it would be very useful if the PMM could be diagnosed. This would amount to being able *i*) to assess whether the observed mismatch is due to the use of an inappropriate set of equations (structural mismatch) or to the inaccurate estimation of some parameters (parametric mismatch), and *ii*) to identify which equations or parameters are mostly responsible of the observed PMM. With this piece of information available, the MBDoE exercise could be sped up significantly, or perhaps even avoided.

The importance of diagnosing PMM has been recognized in process control applications (Wang *et al*., 2012; Badwe *et al.*, 2009) but has been somewhat overlooked with respect to general FP models. In this study, a methodology is proposed to diagnose the PMM originating when an FP model is challenged against a set of historical experimental data. “Synthetic” data are generated by running the FP model under the same input conditions characterizing the historical dataset. Then, using a DD model (namely, a multivariate statistical model), the correlation structure of this synthetic dataset is compared to that of the historical dataset, and information on where the PMM originates from is obtained using DD model diagnostic indices and engineering judgment. The proposed methodology uses only information included in the historical database and does not require any new experiment. Note that we are not interested in improving the FP model performance by complementing the FP model with a DD model section, as is done for example

in hybrid modeling. Rather, we would like to provide the modeler with a tool that can help him/her to detect which sections of the FP model are not performing well, thus targeting subsequent theoretical and experimental efforts (e.g., through an MBDoE exercise) or complementing other model analysis techniques (e.g., sensitivity analysis, Saltelli *et al*., 2000; Saltelli *et al*., 2008).
The proposed methodology is tested on two simulated systems of increasing complexity: a jacket-cooled chemical reactor and a solids milling unit.

3.2 Proposed methodology

It is assumed that a FP model describing the process is available and that PMM has been observed by comparing the model results to a set of historical steady-state process measurements. The rationale of the proposed methodology for PMM diagnosis is the following. First, a DD model, is developed to explain the correlation structure of appropriate nonlinear combinations of the simulated process variables, these combinations (called auxiliary variables) being suggested by the FP model structure. Then, it is assessed whether the same variable combinations, as calculated from the historical measurements, conform to this correlation structure. Finally, from the analysis of some model diagnostics, engineering knowledge is used to pinpoint the FP model equations or parameters that are mostly responsible for the observed PMM. To analyze the correlation structure of the datasets considered in this study, principal component analysis (PCA) is used (see Chapter 2, Section 2.1.1).

3.2.1 Diagnosing the process/model mismatch

The proposed methodology for PMM diagnosis consists of the following four steps, where subscripts Π and M refer to the process and to the model, respectively. It is assumed that a PMM has been observed by comparison of simulated and historical data.

1. Generation of the model matrix and of the process matrix. FP model simulations are run using the set of inputs of the historical dataset (one simulation for each of the available I steady state samples), and predictions of the measured outputs are obtained. We refer to this set of measured inputs/simulated outputs as to the set of "simulated measurements". On the other hand, the set of "historical measurements" (or simply measurements, averaged over possibly noisy steady state time series) corresponds to the historical dataset (i.e., measured inputs/measured outputs). For each sample, the simulated measurements, historical measurements and FP model parameters are appropriately combined to obtain two sets of V auxiliary variables each: one set refers to combinations of the simulated measurements and model parameters, and the other one to the same combinations, but using the historical measurements instead of the simulated ones. As will be clarified later, how the variables should be combined is suggested by the FP model structure. Note that each auxiliary variable

must include at least one input or one output variable, i.e. no auxiliary variable is obtained by combination of model parameters only, unless the model parameters change across the samples (e.g., when the parameters depend on material properties, and the processed material changes across the samples). The two sets of auxiliary variables are organized as columns of two matrices, $\mathbf{X}_{\mathrm{M}}$ [$I \times V$] and $\mathbf{X}_{\Pi}$ [$I \times V$], which are called the model matrix and the process matrix, respectively. Due to the existence of PMM, the correlation structure of $\mathbf{X}_{\Pi}$ is expected to be different from that of $\mathbf{X}_{\mathrm{M}}$.

2. Development of a PCA model for the model matrix. Both $\mathbf{X}_{\mathrm{M}}$ and $\mathbf{X}_{\Pi}$ are centered on the mean of $\mathbf{X}_{\mathrm{M}}$ and scaled on the standard deviation of $\mathbf{X}_{\mathrm{M}}$. Given that each auxiliary variable contains at least one input or one output measurement, after the scaling operations no columns in $\mathbf{X}_{\mathrm{M}}$ or $\mathbf{X}_{\Pi}$ result in null vectors. A PCA model is then built from $\mathbf{X}_{\mathrm{M}}$ and the residuals matrix $\mathbf{E}_{\mathrm{M}}$ is calculated:

$$\begin{aligned} \hat{\mathbf{X}}_{\mathrm{M}} &= \mathbf{T}_{\mathrm{M}}\mathbf{P}_{\mathrm{M}}^{\mathrm{T}} \\ \mathbf{E}_{\mathrm{M}} &= \mathbf{X}_{\mathrm{M}} - \hat{\mathbf{X}}_{\mathrm{M}} \end{aligned} \quad . \tag{3.1}$$

In 3.6 the meaning of the symbols is the same as Eq. 2.6 in Section 2.1.1 (Chapter 2).The PCA model describes the correlation structure of the data included in $\mathbf{X}_{\mathrm{M}}$. The number of PCs to be retained in the PCA model is determined by the eigenvalue-greater-than-one rule (Mardia *et al*., 1979).

3. Projection of the process matrix onto the PCA model. $\mathbf{X}_{\Pi}$ is projected onto the PCA model space and the residuals matrix $\mathbf{E}_{\Pi}$ is calculated:

$$\begin{aligned} \mathbf{T}_{\Pi} &= \mathbf{X}_{\Pi}\mathbf{P}_{\mathrm{M}} \\ \hat{\mathbf{X}}_{\Pi} &= \mathbf{T}_{\Pi}\mathbf{P}_{\mathrm{M}}^{\mathrm{T}} \\ \mathbf{E}_{\Pi} &= \mathbf{X}_{\Pi} - \hat{\mathbf{X}}_{\Pi} \end{aligned} \quad . \tag{3.2}$$

4. Analysis of the residuals matrices and diagnosis of the PMM. The two residuals matrices, $\mathbf{E}_{\Pi}$ and $\mathbf{E}_{\mathrm{M}}$, are analyzed to identify the auxiliary variables that most contribute to the inconsistency in the correlation structures of $\mathbf{X}_{\Pi}$ and $\mathbf{X}_{\mathrm{M}}$. These auxiliary variables, together with engineering judgment, are then used to pinpoint the FP model equations or parameters that most contribute to the observed PMM.

The residuals matrix reflects the data variability that is not captured by the model. If the elements $e_{i,v}$ of the v-th column $\mathbf{e}_v$ of $\mathbf{E}_{\mathrm{M}}$ follow a normal distribution, the variability not described by the model is deemed to be non-deterministic, and confidence limits can be set for $\mathbf{e}_v$ in the form:

$$CL_{\alpha,\mathbf{e}_m} = z_{\alpha/2} \cdot \sigma(\mathbf{e}_n) \quad , \tag{3.3}$$

where α is the significance level and typically takes a value of 0.01 or 0.05, $z_{\alpha/2}$ is the corresponding standard normal deviate and $\sigma(\mathbf{e}_v)$ is the standard deviation of $\mathbf{e}_v$. In this work, α = 0.05 (i.e. 95% confidence) is used, and $z_{\alpha/2}$ takes the approximate value of 1.96.
Note that $\mathbf{E}_\Pi$ accounts both for the mismatch between $\mathbf{X}_\Pi$ and $\mathbf{X}_M$, and for the fraction of the $\mathbf{X}_\Pi$ variability that is not described by the PCA model built on the $\mathbf{X}_M$ data. In order to account for the contribution due to the PMM only, the contribution related to the un-modeled variability of $\mathbf{X}_\Pi$ is removed from $\mathbf{E}_\Pi$. Hence, for each column v of $\mathbf{E}_\Pi$ the residuals analysis is done in terms of mean residuals-to-limit ratio ($MRLR_v$):

$$MRLR_v = \frac{\sum_{i=1}^{I}\left(\frac{\sqrt{(e_{\Pi\, i,v})^2}}{CL_{95\%,\mathbf{e}_{M\,v}}}\right)}{I} \quad , \tag{3.4}$$

that is the mean of the ratios between the residuals of each column of $\mathbf{E}_\Pi$ and the corresponding 95% confidence limit, calculated considering a normal distribution of residuals (see Eq. 3.3). In this study, the Anderson-Darling test (Anderson and Darling, 1952) was employed in order to check the null hypothesis that vector $\mathbf{e}_{\Pi,v}$ belongs to a population with a normal distribution of mean 0. Note that, if the residuals are not normally distributed, the confidence interval cannot be calculated from Eq. (3.3). Alternative expressions for the estimation of the confidence limits should be used if a different distribution of the residuals can be recognized (Martin and Morris, 1996; Doymaz *et al*., 2001).

3.3 Example 1: jacket-cooled reactor

3.3.1 Process and historical dataset

To illustrate the application of the proposed methodology, a jacket-cooled continuous stirred tank reactor (CSTR) is first considered. Two consecutive exothermic reactions take place in the reactor:

$$\text{reaction } 1: \ \mathrm{A} + \mathrm{B} \rightarrow 2\,\mathrm{C} \qquad R_1 = f_1(k_1, C_A^{out}, C_B^{out}, T^{out}) = k_1 C_A^{out} C_B^{out} \tag{3.5}$$

$$\text{reaction } 2: \ \mathrm{C} \rightarrow \mathrm{D} \qquad R_2 = f_2(k_2, C_C^{out}, T^{out}) = k_2 C_C^{out} \tag{3.6}$$

where A and B are the reactants, C is the desired product, D is the byproduct, R_r is the reaction rate expression for reaction r, C_s is the molar concentration of species s, T stands for temperature,

and superscript *out* refers to a variable at the reactor outlet. The kinetic constant k_r takes the Arrhenius form:

$$k_r = A_r \exp\left(\frac{-E_{a,r}}{RT^{out}}\right) \quad , \tag{3.7}$$

where R is the universal gas constant. The meaning of the other symbols is reported in Table 1. The process is described by the following set of equations (Luyben, 2007):

$$C_A^{out} - C_A^{in} - k_1 C_A^{out} C_B^{out} \cdot \frac{V_R}{F} = 0 \tag{3.8}$$

$$C_B^{out} - C_B^{in} - k_1 C_A^{out} C_B^{out} \cdot \frac{V_R}{F} = 0 \tag{3.9}$$

$$C_C^{out} - C_C^{in} + 2 \cdot k_1 C_A^{out} C_B^{out} \cdot \frac{V_R}{F} - k_2 C_C^{out} \cdot \frac{V_R}{F} = 0 \tag{3.10}$$

$$C_D^{out} - C_D^{in} + k_2 C_C^{out} \cdot \frac{V_R}{F} = 0 \tag{3.11}$$

$$\rho \cdot c_P \cdot \left(T^{out} - T^{in}\right) - \left(-Q_R - \frac{\dot{Q}}{V_R}\right) \cdot \frac{V_R}{F} = 0 \tag{3.12}$$

$$\rho_w \cdot c_{P,w} \cdot \left(T_j^{out} - T_j^{in}\right) - \left(\frac{\dot{Q}}{F_j}\right) = 0 \tag{3.13}$$

$$\dot{Q} = US\left(T^{out} - T_j^{out}\right) \tag{3.14}$$

$$Q_R = \Delta H_1 \cdot k_1 C_A^{out} C_B^{out} + \Delta H_2 \cdot k_2 C_C^{out} \tag{3.15}$$

where subscripts subscript *j* refers to the jacket and subscript *w* refers to the cooling utility.
As indicated in Table 3.1, it is assumed that measurements are available for 14 variables (8 inputs and 6 outputs). The nominal values of the parameters are reported in Table B.1 of Appendix B. The historical dataset consists of 25 sets of average measurements (samples) obtained for different combinations of the following input variables: C_A^{in}, C_B^{in}, T^{in}, T_j^{in}, V_R / F and F_j. The ranges of the input and output variables in the historical dataset are reported in Table B.2 of Appendix B.

Table 3.1. *Example 1: variables and parameters.*

Parameters and derived variables		**Measured variables in the historical dataset**			
		Inputs		**Outputs**	
A_r	Pre-exponential constant	C_A^{in}	Inlet molar concentration of A	C_A^{out}	Outlet molar concentration of A
c_p	Specific heat	C_B^{in}	Inlet molar concentration of B	C_B^{out}	Outlet molar concentration of B
$E_{a,r}$	Activation energy	C_C^{in}	Inlet molar concentration of C	C_C^{out}	Outlet molar concentration of C
S	Total area available for the heat exchange	C_D^{in}	Inlet molar concentration of D	C_D^{out}	Outlet molar concentration of D
U	Overall heat transfer coefficient	F	Feed flowrate	T_j^{out}	Outlet jacket temperature
V_R	Reactor volume	F_j	Cooling utility flowrate	T^{out}	Outlet reactor temperature
$\dot{Q}$	Heat exchange rate between the reactor and the jacket	T^{in}	Inlet reactor temperature		
Q_R	Heat rate generated by the reactions	T_j^{in}	Inlet jacket temperature		
ΔH	Enthalpy of reaction				
ρ	Density				

3.3.2 Application of the methodology and results

In order to test the effectiveness of the proposed methodology, three case studies are considered (Case study 1.A, 1.B and 1.C) that correspond to three different models M being built to represent process Π. Basically, the same set of equations as in Eqs. (3.8) - (3.15) is used in all case studies, but different parametric and structural PMM are included in each model (such as imprecise estimation of the heat exchange or kinetics parameters, or mis-modeling of the kinetic expression itself; Table 3. 2). However, it is assumed that one has no a-priori knowledge of the origin of mismatch. The objective is therefore to assess whether the observed PMM is structural or parametric, and to highlight which equation or parameter most contributes to the mismatch.

In order to build the process matrix and the model matrix (step 1 of the proposed methodology), the auxiliary variables are defined as appropriate (nonlinear) combinations of the process/model variables and of the model parameters, where the combinations are suggested by the model equations themselves. By looking at the structure of equation set (3.8) - (3.15), the model equations are partitioned in such a way as to define the following 11 auxiliary variables x_i:

$$
\begin{aligned}
&x_1 = C_A^{out} - C_A^{in}\ ; \quad x_5 = -R_1 \cdot \frac{V_R}{F}\ ; && x_9 = -\frac{V_R}{F} \cdot \left(\frac{-US\left(T^{out} - T_j^{\ out}\right)}{V_R} \right) \\
&x_2 = C_B^{out} - C_B^{in}\ ; \quad x_6 = -R_2 \cdot \frac{V_R}{F}; && x_{10} = \rho_w \cdot c_{P,w} \cdot \left(T_j^{out} - T_j^{in}\right) \\
&x_3 = C_C^{out} - C_C^{in}\ ; \quad x_7 = \rho \cdot c_P \cdot \left(T^{out} - T^{in}\right); && x_{11} = -\left[US\left(T^{out} - T_j^{\ out}\right)\right] \cdot F_j \\
&x_4 = C_D^{out} - C_D^{in}\ ; \quad x_8 = -Q_R \cdot \frac{V_R}{F}\ ;
\end{aligned}
\quad . \qquad (3.16)
$$

Note that each auxiliary variable includes at least one measurable variable. In the next subsections, the proposed methodology is applied to each case study and the results are discussed.

Table 3. 2. *Summary of the case studies considered in this study.*

Example	Case study	Type of mismatch	Model term involved	Applied variation
Example 1: CSTR	Case study 1.A	Parametric	U	+50%
	Case study 1.B	Structural	kinetics of the first reaction	$k_1 C_{A,\mathrm{M}}^{2/3} C_{B,\mathrm{M}}^{4/3}$
	Case study 1.C	Parametric	A_1	+50%
Example 2: mill	Case study 2.A	Parametric	$W_{m,\mathrm{kin}}$	–30%
	Case study 2.B	Parametric	f_{Mat}	–40%
	Case study 2.C	Parametric	q	+50%

3.3.1.1 Case study 1.A

Parametric mismatch is enforced by using a value U_M of the overall heat exchange coefficient in the model that is ~50% larger than the actual value (U_Π). Figure 3.1 provides a comparison between the historical and simulated outputs. Although the concentrations deviations (Figure 3.1a) and the temperature deviations (Figure 3.1b) are not large, they are systematic. Hence, PMM is observed, although its cause is not apparent from the inspection of Figure 3.1.

Following the definition of the auxiliary variables, the model matrix $\mathbf{X}_\mathrm{M}$ and the process matrix $\mathbf{X}_\Pi$ can be calculated (step 1). Note that the values taken by the auxiliary variables change according to whether simulated measurements or historical measurements are used in equation set (3.16). For example, in the calculation of x_5 for use in the model matrix, $R_1 = R_{1,\mathrm{M}} = f_1(C_{A,\mathrm{M}}^{out}, C_{B,\mathrm{M}}^{out}, T_\mathrm{M}^{out})$ is set. Instead, $R_1 = R_{1,\Pi} = f_1(C_{A,\Pi}^{out}, C_{B,\Pi}^{out}, T_\Pi^{out})$ is set in the calculation of the same variables for use in the process matrix. Also note that, since the actual values of the parameters are unknown, the model values are used both in $\mathbf{X}_\mathrm{M}$ and in $\mathbf{X}_\Pi$.

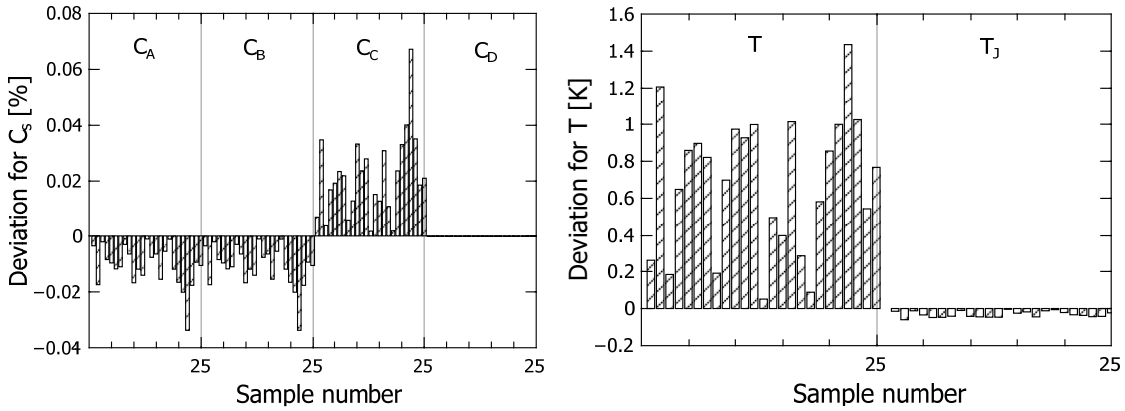

(a) (b)

Figure 3.1. *Case study 1.A. Deviations between historical and simulated outputs for (a) concentrations and (b) temperatures.*

A PCA model is then built on $\mathbf{X}_M$ (step 2). Table 3.3 reports the eigenvalues λ, the explained variance R^2 and its cumulated value R^2_{cum} for each PC of the model. Two PCs are selected, and they explain more than 99% of the variability of the $\mathbf{X}_M$ data. The model loadings in Figure 3.2 show that PC1, which captures most of the original variability (~72%), mainly describes the behavior of variables that are strongly correlated with the reactions (auxiliary variables $x_{1\text{-}6}$ and x_8), as well as that of x_7, whereas PC2 captures the variability of variables that are related to heat exchange (x_7 and $x_{9\text{-}11}$).

Table 3.3. *Case study 1.A. Diagnostics of the PCA model on* $\mathbf{X}_M$.

PC number	Eigenvalue of cov($\mathbf{X}_M$)	R^2	R^2_{cum}
1	7.88	71.60	71.60
2	3.02	27.46	99.06
3	0.08	0.71	99.77
4	0.02	0.23	100.00

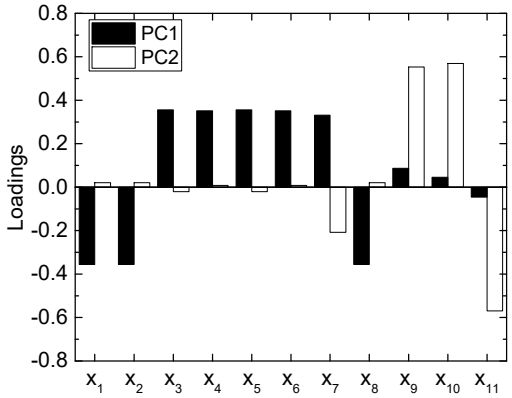

Figure 3.2. *Case study 1.A. Loadings on PC1 and PC2 for the PCA model on* $\mathbf{X}_M$.

After building the PCA model, $\mathbf{X}_{\Pi}$ is projected onto it (step 3). The projection results are shown in Figure 3.3: while the $\mathbf{X}_{M}$ samples lie very close to the plane formed by PC1 and PC2, the $\mathbf{X}_{\Pi}$ samples are far away from this plane. Hence, the two PCs optimally describing the variability of XM are not able to reliably represent also the correlation structure of the data in $\mathbf{X}_{\Pi}$, an issue that is related to the observed PMM. The distance of each sample from the plane represents the sum of the residuals of each auxiliary variable for that sample. The large residuals for $\mathbf{X}_{\Pi}$ confirm that the correlation structure of $\mathbf{X}_{\Pi}$ is not represented well by the PCA model built on $\mathbf{X}_{M}$.

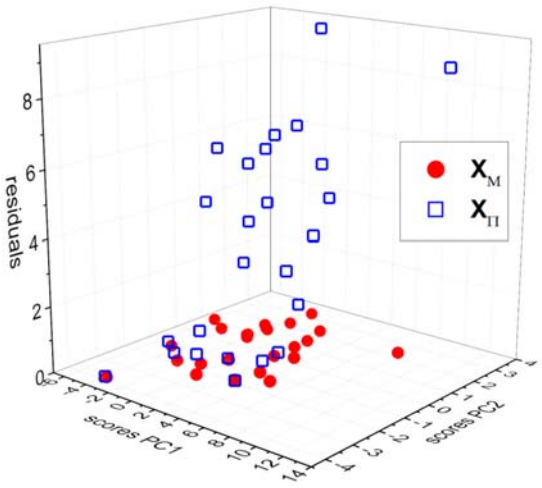

Figure 3.3. *Case study 1.A. Residuals in the scores space for each sample of the model matrix* $\mathbf{X}_{M}$ *and of the process matrix* $\mathbf{X}_{\Pi}$.

After confirming that the residuals obtained by the projection of $\mathbf{X}_{\Pi}$ are normally distributed, further insight on the origin of the PMM is gained by analyzing the $\mathbf{X}_{\Pi}$ sample projections in terms of $MRLR_v$ (step 4). The results are illustrated in Figure 3.4, from which one can see that the largest values of $MRLR_v$ are associated to auxiliary variables x_{10}, x_{11}, x_7 and x_9. Hence, it can be stated that these auxiliary variables mostly contribute to the observed PMM.

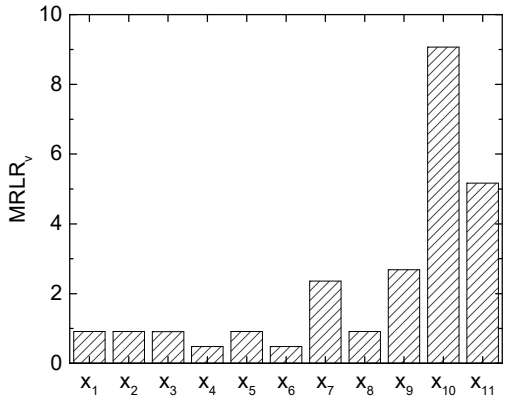

Figure 3.4. *Case study 1.A.* $MRLR_v$ *for each column of* $\mathbf{X}_{\Pi}$.

From Equation set (3.16), it can be noted that these auxiliary variables relate to the heat exchange system, and contain measurements (temperatures and flowrates) as well as model parameters (U, S, V_R, ρ and c_P). However, the other auxiliary variables that include the reactor temperature and the feed flow rate display significantly lower $MRLR_v$ values, and therefore we conclude that the observed PMM cannot be related to these measurements. On the other hand, it cannot be related to the reactor volume V_R either; in fact, if this were the case, an impact would be seen also on variables $x_{5\text{-}9}$, which all depend on θ. Hence, the derived variable $\dot{Q}=US\left(T^{out}-T_j^{out}\right)$ is one strong candidate source of the PMM, as it directly affects auxiliary variables x_{12} and x_{14}. From Eq. (3.14) one can see that the definition of $\dot{Q}$ includes two parameters: the heat exchange area S and the overall heat transfer coefficient U. Therefore, we conclude that the proposed methodology suggests that the observed PMM is most probably due to the fact that U or S have not been assigned an appropriate value in the FP model.

3.3.1.2 Case study 1.B

A structural error is enforced by assuming that the kinetics of the first reaction is represented by:

$$R_{1,\mathrm{M}} = k_1 C_{A,M}^{2/3} C_{B,M}^{4/3} \neq f_1(C_{A,\mathrm{M}}^{out}, C_{B,\mathrm{M}}^{out}, T_{\mathrm{M}}^{out}) \quad . \tag{3.17}$$

The deviation plots in Figure 3.5 clearly point to a PMM: all the simulated outputs (but the jacket temperature) show very large deviations from the historical values. Again, the source of the mismatch is not apparent from these plots, although engineering judgment suggests that the PMM is probably due to a wrong modeling of one or both kinetic terms.

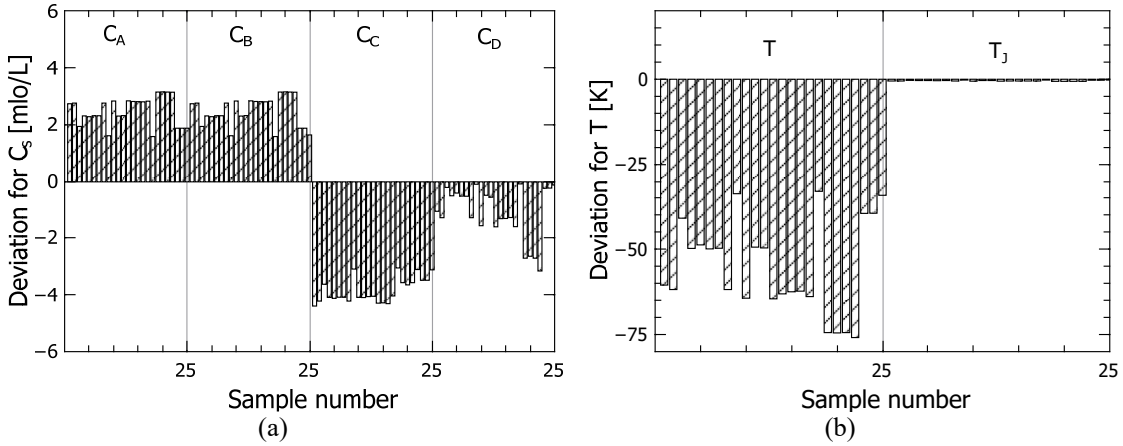

Figure 3.5. *Case study 1.B. Deviations between historical and simulated outputs for (a) concentrations and (b) temperatures.*

After calculating the model matrix $\mathbf{X}_{\mathrm{M}}$, a PCA model is built from it and 2 PCs are selected (Table 3.4). From the loadings reported in Figure 3.6 it can be observed that the correlation structure of

$\mathbf{X}_M$ is significantly different from that of the previous model. In this case, the first PC explains mainly the variability of auxiliary variables involved in the first reaction and in the heat exchange system ($x_{1\text{-}2}$, x_5, $x_{7\text{-}11}$; note that the values of the loadings of the variables involved in the second reaction are slightly smaller than those of the other variables), whereas the second PC explains the variability of auxiliary variables involved only in the second reaction ($x_{3\text{-}4}$, x_6).

Table 3.4. *Case study 1.B. Diagnostics of the PCA model on* $\mathbf{X}_M$.

PC number	Eigenvalue of cov($\mathbf{X}_M$)	R^2	R^2_{cum}
1	9.98	90.74	90.74
2	0.98	8.90	99.65
3	0.03	0.24	99.89
4	0.01	0.11	100.00

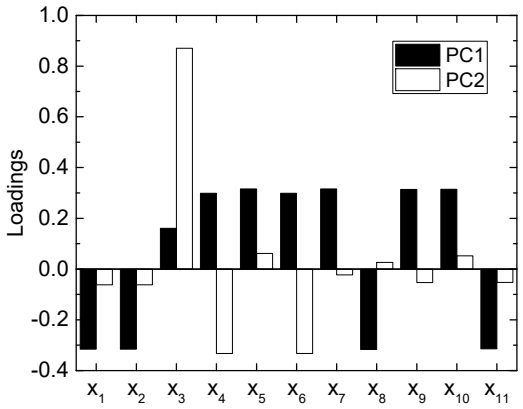

Figure 3.6. *Case study 1.B. Loadings on PC1 and PC2 for the PCA model on* $\mathbf{X}_M$.

After projecting $\mathbf{X}_\Pi$ onto the PCA model and confirming the normality of the residuals distributions of $\mathbf{X}_M$, the $MRLR_v$ are calculated and analyzed. The results are reported in Figure 3.7. The auxiliary variable that shows the greatest contribution to $MRLR_v$ is x_5, which is directly related to R_1 and V_R / F. However, since V_R / F also contributes to x_6 and x_9 and these auxiliary variables do not exhibit large $MRLR_v$ values, the reason for the observed PMM is attributed to an erroneous modeling of the first reaction kinetics. This conjecture is also supported by the large $MRLR_v$ value for x_8, an auxiliary variable involving the heat of reaction Q_R (hence, strongly correlated to R_1). Other auxiliary variables (e.g., $x_{1\text{-}4}$) show intermediate $MRLR_v$ values, and this is due to their correlation with R_1. Finally, note that $x_{9\text{-}11}$ provide negligible contributions to $MRLR_v$, meaning that the heat exchange section of the model is not a source of PMM.

Although the analysis done so far suggests that the first reaction is not modeled properly, it is still not possible to state whether the observed mismatch is parametric or structural, i.e. whether Eq. (3.17) is structurally wrong or the parameters therein are inaccurate.

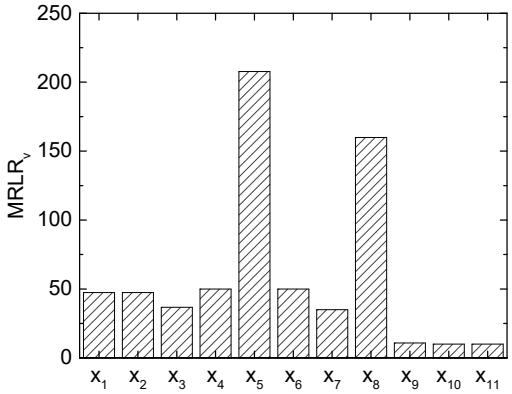

Figure 3.7. *Case study 1.B. MRLR$_v$ for each column of* $\mathbf{X}_{\Pi}$.

The mismatch diagnosis can be refined by defining a new set of auxiliary variables:

$$x'_1 = A_1 \exp\left(\frac{-E_{a,1}}{RT}\right); \quad x'_2 = \frac{E_{a,1}}{RT}; \quad x'_3 = C_A^{2/3}; \quad x'_4 = C_B^{4/3} \quad , \tag{3.18}$$

which derives from convenient partitioning of Eq. (3.17). The proposed methodology is iterated by defining a new model matrix $\mathbf{X}'_{M}$ [25×4] and a new process matrix $\mathbf{X}'_{\Pi}$ [25×4] (where the new set of auxiliary variables replaces the original one), and by building a PCA model on $\mathbf{X}'_{M}$. Two PCs are retained in the new model, which capture more than the 90% of the variability of the data. As shown by Figure 3.8, PC1 captures the variability of the first three new auxiliary variables (kinetic parameters and functional dependence of the (kinetic parameters and functional dependence of the kinetic expression on T and on C_A), whereas PC2 mainly captures the variability of x'_3 and x'_4 (functional dependence of the kinetic expression on C_A and C_B).

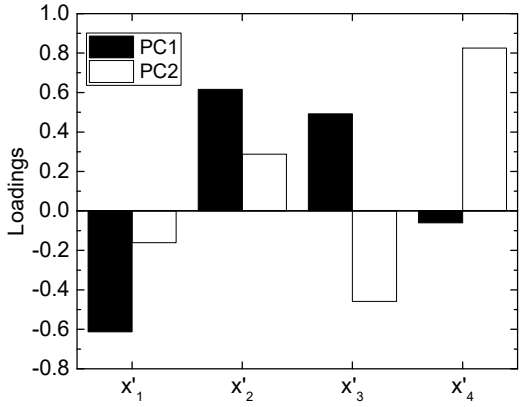

Figure 3.8. *Case study 1.B. Second iteration: loadings on PC1 and PC2 for the PCA model on* $\mathbf{X}'_{M}$.

With a word of caution on the normality of the residuals (which is not completely satisfied in this case), the $MRLR_v$ diagnostic index in Figure 3.9 pinpoints x_3 and x_4 as the main causes of the mismatch. Hence, we conclude that a structural mismatch on the kinetic expression for the first reaction is finally diagnosed as the root cause of the observed PMM.

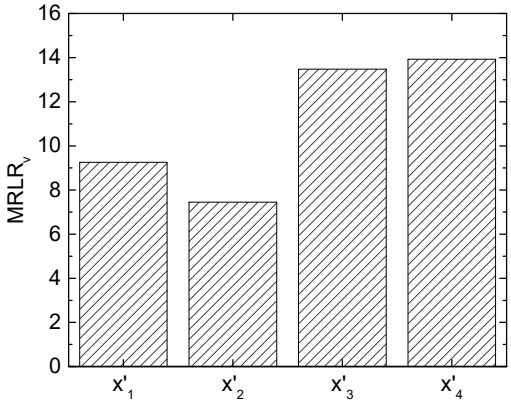

Figure 3.9. *Case study 1. Second iteration: $MRLR_v$ for each column of* $\mathbf{X}'_{\Pi}$.

3.3.1.3 Case study 1.C

Parametric mismatch is enforced by assigning the pre-exponential coefficient of the first reaction a value ($A_{1,M}$) that is 50% smaller than the correct one. This results in the deviation plots of Figure 3.10.

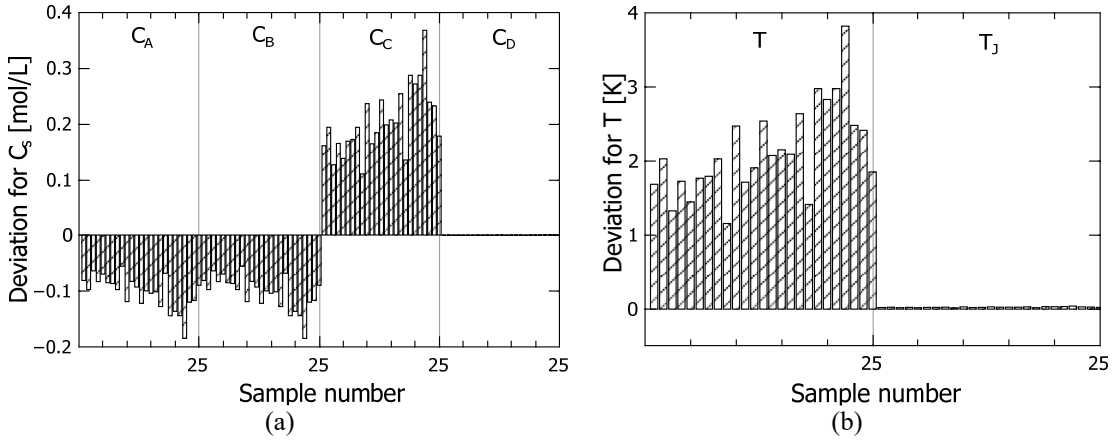

Figure 3.10. *Case study 1.C. Deviations between historical and simulated outputs for (a) concentrations and (b) temperatures.*

The PCA model needs 2 PCs to account for almost all of the variability of $\mathbf{X}_M$. Although not shown here for the sake of conciseness, the analysis of the model loadings provides results similar to those discussed in Case study 1.A.

After projection of $\mathbf{X}_{\Pi}$ and assessment of the normality of the residuals, the results reported in Figure 3.11 are obtained. The largest values of $MRLR_v$ are encountered for auxiliary variables x_5

and x_8, which both depend on R_1 as well as on V_R / F ; however, the mismatch cannot be attributed to V_R / F because $MRLR_v$ is not large for either x_6 or x_9. Therefore, it can be concluded that the observed PMM is most probably caused by mismodeling of the first reaction kinetics. Whether this is a parametric or a structural mismatch is impossible to state at this point.

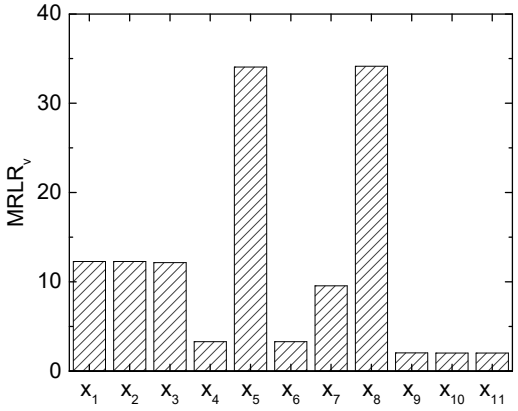

Figure 3.11. *Case study 1.C. $MRLR_v$ for each column of* $\mathbf{X}_{\Pi}$.

To provide further insight, the following new set of auxiliary variables is defined on the basis of the first reaction kinetic expression:

$$x'_1 = A_1 \exp\left(\frac{-E_{a,1}}{RT}\right); \quad x'_2 = \frac{E_{a,1}}{RT}; \quad x'_3 = C_A; \quad x'_4 = C_B \tag{3.19}$$

and new model matrix $\mathbf{X}'_{\mathrm{M}}$ [25×4] and process matrix $\mathbf{X}'_{\Pi}$ [25×4] are built. The loadings of the PCA model on $\mathbf{X}'_{\mathrm{M}}$ and the $MRLR_v$ values are shown in Figure 3.12.

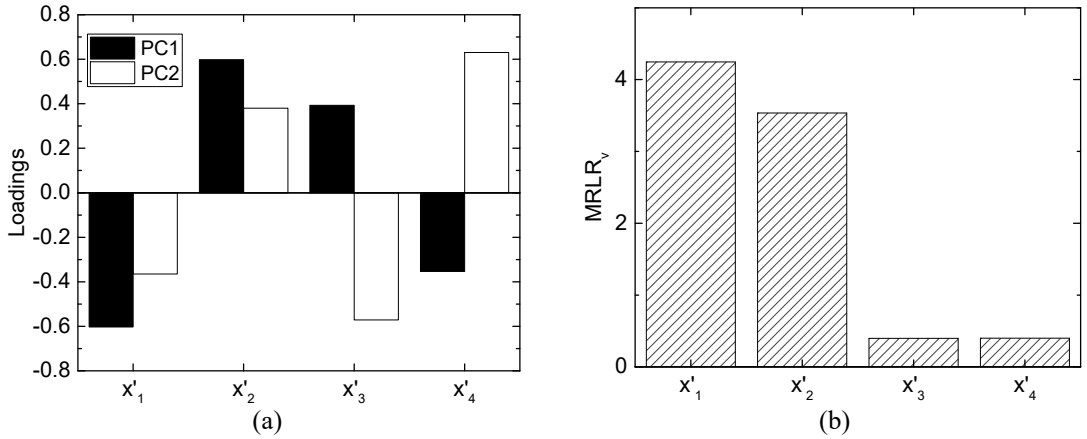

Figure 3.12. *Case study 1.C. Second iteration: (a) loadings on PC1 and PC2 and (b) $MRLR_v$ for each column of* $\mathbf{X}'_{\Pi}$.

The results in Figure 12b clearly show that x'_3 and x'_4 negligibly contribute to the mismatch. Hence, the mismatch is not due to a structural inadequacy of the kinetic expression; conversely, it is due to a parametric error, as shown by the large contributions provided by x'_1 and x'_2. However, since the latter two auxiliary variables are strongly correlated, it is not possible to decouple the effect of A_1 from that of $E_{a,1}$. In conclusion, the proposed diagnosing methodology correctly points to a parametric mismatch in the first kinetic expression, although the correlation between parameters hinders unambiguous detection of the PPM origin.

3.4 Example 2: solids milling unit

3.4.1 Process and historical dataset

A solids milling unit is considered as the second test bed for the proposed methodology, where the mill is used to reduce the mean particles size of a granulated polymer.
The process is described by the mass and population balances on the solid distributed phase. Assuming to process a given amount of material, with an inlet particle size distribution PSD_{in}, the population balance equation on mass basis is (Vogel and Peukert, 2005):

$$\frac{\partial M(y,t)}{\partial y} = \int_0^{y_{\max}} P_B(z)\, b(y,z)\, M(z,t)\, \mathrm{d}z - P_B(y)\, M(y,t) \quad , \tag{3.20}$$

where the change of the particle mass M of a certain size y is given by the mass leaving the size band as fragments (second addendum on the right term in (3.20) and the mass entering the size band as fragments from larger size z (integral term in Eq. 3.20). Two key quantities are considered: the grinding rate selection function P_B and the breakage function b. Different empirical formulations for the breakage and selection functions are available in the literature. The one suggested by Vogel and Peukert (2005) is used in this study:

$$B = \left(\frac{z}{y}\right)^q \frac{1}{2}\left(1 + \tanh\left(\frac{y-y'}{y'}\right)\right), \qquad \frac{\partial B(z,y)}{\partial y} = b(z,y) \tag{3.21}$$

$$P_B = 1 - \exp\left[-f_{\mathrm{Mat}}\, z\, k\, \left(W_{m,\mathrm{kin}} - W_{m,\min}\right)\right] \tag{3.22}$$

$$q = cv + d\,. \tag{3.23}$$

Note that P_B and b depend on several parameters (f_{Mat}, $W_{m,\mathrm{kin}}$, $W_{m,\min}$, q, k; Table 3.5), which are specific of the type of the polymer involved. The parameter values used to obtain the process

results are those reported by Vogel and Peukert (2005) and their values are listed in Table B.4 of Appendix B. The gSOLIDS® 3.0 (Process Systems Enterprise Ltd, London, UK, 2013) package is used to simulate the system.

Table 3.5. *Example 2: variables and parameters.*

Parameters and derived variables		**Measured variables in the historical dataset**			
		Inputs		**Outputs**	
c	Parameter	PSD_{in}	Inlet particle size distribution	PSD_{out}	Outlet particle size distribution
d	Parameter	v	Mill rotational velocity		
f_{Mat}	Mass based material strength parameter	ρ_{bulk}	Bulk density		
k	Number of impacts				
q	Power law exponent				
y'	Fragment size for additional fading				
$W_{m,\mathrm{kin}}$	Mass specific impact energy				
$W_{m,\mathrm{min}}$	Mass specific threshold energy				

The historical dataset consists of $N = 15$ samples obtained for different combinations of the following variables: inlet material particle size distribution PSD_{in} (in terms of mean particle diameter D_{in} and standard deviation σ_{in}), bulk density ρ_{bulk}, mill rotational velocity v. Different the values of the parameters f_{Mat}, $W_{m,\mathrm{kin}}$, $W_{m,\mathrm{min}}$ are also considered, assuming to process 4 different solid-phase polymers. The only measured output is the outlet PSD (PSD_{out}). The range of the input and output variables in the historical dataset are reported in Table B.3 of Appendix B.

3.4.2 Application of the methodology and results

As discussed previously, the only measured output is the outlet PSD, and diagnosing the PMM by looking at a single output represents an additional challenge for the proposed methodology. Note that the solution of Eq. (3.20) for this distributed-parameter system requires discretizing the integration range. To this purpose, the analyzed size range (from 10·μm to 8000·μm) is partitioned into $B = 40$ bins, each one corresponding to a different particle size. Therefore, the change of particle mass in the discrete size band b (Δm_b) during a grinding step is (Vogel and Peukert, 2005):

$$\Delta m_b = \sum_{j=1}^{i-1} m_j b_{b,j} P_{B,j} - m_b P_{B,i} \quad \text{with } b_{b,j} = B_{b-1,j} - B_{b,j} \quad , \tag{3.24}$$

where $k = 1$ is assumed. The particle size distribution vector $\mathbf{m}$ is obtained by considering all size bands. The final particle size distribution $\mathbf{m}_{out}$ resulting after a grinding step is calculated from:

$$\mathbf{m}_{out} = \mathbf{m}_{in} + \Delta\mathbf{m} \quad , \tag{3.25}$$

where $\mathbf{m}_{in}$ is estimated from the known PSD_{in}.
By inspection of Eq. (3.24), $V = 5$ auxiliary variables are defined for each bin b as:

$$\begin{aligned} \mathbf{x}_1(b) &= P_{B,b} & \mathbf{x}_4(b) &= m_b P_{B,b} \\ \mathbf{x}_2(b) &= \sum_{j=1}^{b-1} b_{b,j} & \mathbf{x}_5(b) &= PSD_{out} \\ \mathbf{x}_3(b) &= \sum_{j=1}^{b-1} m_j b_{b,j} P_{B,j} \end{aligned} \quad . \tag{3.26}$$

Note that the auxiliary variables are vectors of dimension B, because each of them takes a different value within each bin. Also note that, generally speaking, the definition of the auxiliary variables may change according to how the model equations are solved numerically.
Since, for each auxiliary variable, all B bins and all I samples are spanned, the process and the model matrices take the form of three-way arrays of dimension $[I \times V \times B]$, as illustrated in Figure 3.13. These arrays are denoted with $\underline{\mathbf{X}}_{\Pi}$ and $\underline{\mathbf{X}}_{M}$, respectively.

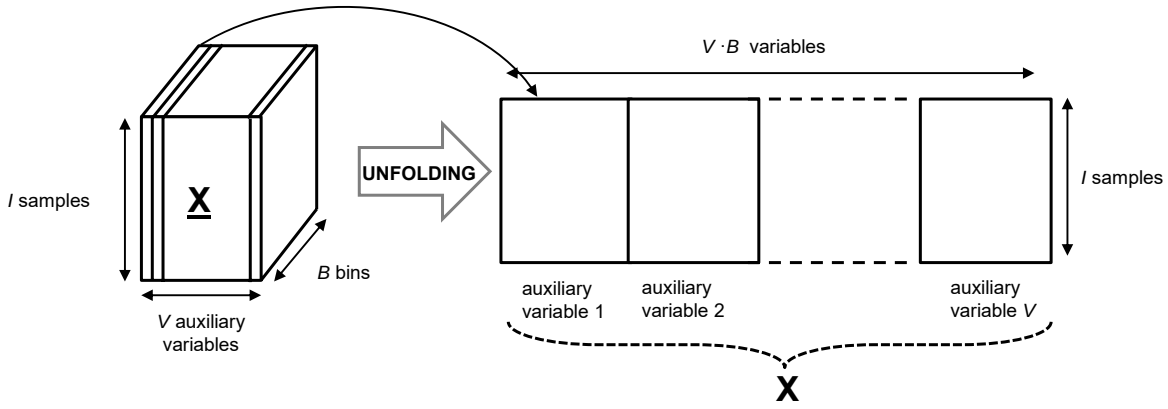

Figure 3.13. *Example 2: unfolding of the three-way array* $\underline{\mathbf{X}}$ *resulting from the auxiliary variables in Equation set (30).*

In order to account for the contribution of each bin simultaneously, multi-way PCA (MPCA, Nomikos and MacGregor, 1994) is employed instead of PCA. MPCA is equivalent to performing a PCA on the two-dimensional (2D) matrix $\mathbf{X}$ formed by unfolding $\underline{\mathbf{X}}$ sample-wise, i.e. by putting side by side each vertical slice of $\underline{\mathbf{X}}$, where each slice corresponds to a different auxiliary variable

(Figure 3.13). The resulting 2D matrix $\mathbf{X}$ has dimension [$I \times (V \cdot B)$], and each column of $\mathbf{X}$ represents the value of a given auxiliary variable within a given bin across all samples. This unfolding procedure is applied to both $\underline{\mathbf{X}}_{\Pi}$ and $\underline{\mathbf{X}}_{M}$, so that $\mathbf{X}_{\Pi}$ and $\mathbf{X}_{M}$ are obtained; both matrices have dimension [15×200]. Note that, since PSD_{out} is the only measured output, the process and model matrices turn out to be equal except for the columns that correspond to auxiliary variable. Three case studies are considered in the following, including three different sources of parametric mismatch (Table 3. ***2***).

3.4.1.1 Case study 2.A

Parametric mismatch is enforced by assigning parameter $W_{m,\mathrm{kin}}$ values that are 30% smaller than the actual values (Table B.3 of Appendix B). Note that $W_{m,\mathrm{kin}}$, which is related to the mass specific impact energy, affects the grinding rate selection function and depends on the type of material processed.

An MPCA model is built on $\mathbf{X}_{M}$ (step 2), using 9 PCs (however, 8 PCs might also be appropriate; Table B.5 of Appendix B). After projecting $\mathbf{X}_{\Pi}$ onto this model and assessing the normality of distribution of the residuals of $\mathbf{X}_{M}$, $MRLR_v$ is calculated for each column of $\mathbf{X}_{\Pi}$. The results obtained are illustrated in Figure 3.14, where, in order to simplify the graphical interpretation of the results, the $MRLR_v$ values are grouped according to the auxiliary variables they originate from.

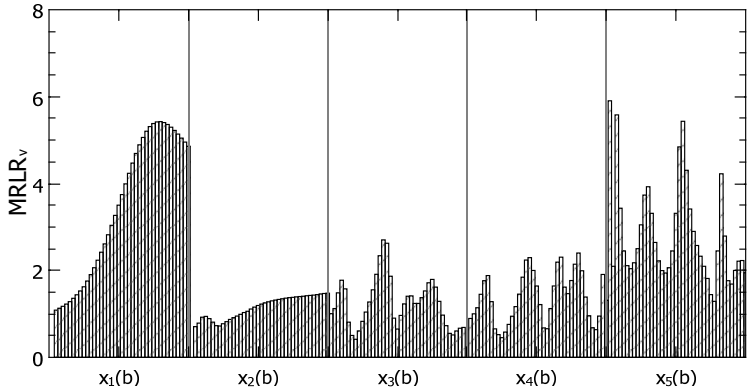

Figure 3.14. *Case study 2.A. $MRLR_c$ for each column of $\mathbf{X}_{\Pi}$. The columns are grouped according to the auxiliary variables they originate from; each bar within an auxiliary variable refers to a different bin.*

Figure 3.14 shows that auxiliary variables $\mathbf{x}_1$ and $\mathbf{x}_5$ have the largest $MRLR_v$ values. Since $\mathbf{x}_5$ directly relates to values of PSD_{out} in each bin (Eq. set 3.26), its high residuals simply indicate the existence of PMM. Auxiliary variable $\mathbf{x}_1$ directly relates to the grinding rate selection function. Hence, it is diagnosed that the observed PMM is due to an inconsistent grinding rate selection function, but it is not possible to identify whether the mismatch is due to a wrong estimation of some of the parameters included in this function or to an inappropriate function itself. In the

following, we look for some indication on the possibility that the observed PMM originates from incorrect parameter estimation.

From Eq. (3.22) it can be observed that auxiliary variable $\mathbf{x}_1$ implicitly depends on three material-specific parameters: f_{Mat}, $W_{m,\mathrm{kin}}$, $W_{m,\mathrm{min}}$. To get some insight on the contribution of these parameters to the PMM, the diagnosis methodology is iterated by defining a new set of auxiliary variables:

$$\begin{aligned} &\mathbf{x}'_1(b) = \ln(f_{\mathrm{Mat}}); \quad \mathbf{x}'_3(b) = \ln(W_{m,\mathrm{min}}); \quad \mathbf{x}'_5(b) = f(PSD_{out}) \\ &\mathbf{x}'_2(b) = \ln(W_{m,\mathrm{kin}}); \quad \mathbf{x}'_4(b) = \exp(q_{\mathrm{M}}) \end{aligned} \quad . \tag{3.27}$$

Three considerations are appropriate at this point: *i*) the logarithmic and exponential functions are used to linearize the relationship between the parameters and the outlet PSD; *ii*) although the values of each auxiliary variable is formally calculated within each bin, only $\mathbf{x}'_5(b)$ actually takes values that differ from bin to bin, because $\mathbf{x}'_{1-4}(b)$ are calculated from model parameters only; *iii*) since the samples included in the historical dataset refer to different materials, none of the mean-centered and scaled auxiliary variables correspond to a null vector.

The resulting matrices $\underline{\mathbf{X}}'_{\mathrm{M}}$ and $\underline{\mathbf{X}}'_{\Pi}$ have dimension [15×5×40], and 7 PCs are used to build the MPCA model on $\underline{\mathbf{X}}'_{\mathrm{M}}$. The high $MRLR_v$ values related to $\mathbf{x}'_2$ (Figure 3.15) allow one to recognize parameter $W_{m,\mathrm{kin}}$ as the probable cause of the mismatch, even though also $\mathbf{x}'_1$ (i.e. f_{Mat}) may point to a possible alternative cause.

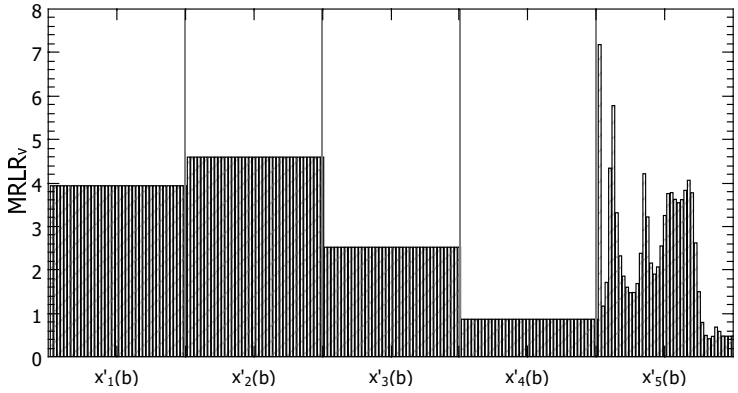

Figure 3.15. *Case study 2.A. Second iteration: $MRLR_v$ for each column of $\mathbf{X}'_{\Pi}$. The columns are grouped according to the auxiliary variables they originate from; each bar within an auxiliary variable refers to a different bin.*

Note that the results in Figure 3.15 slightly depend on the number of PCs used to build the MPCA model. If the analysis does not unambiguously point to one auxiliary variable, it may turn useful to build the MPCA model with a different number of PCs (i.e., by including one additional PC or removing one PC) to see whether some auxiliary variables are singled out more clearly. For

example, in this case study reducing to 6 the number of PCs pointed much more clearly to $\mathbf{x}'_2$ as the most important contributor to the $\mathbf{X}'_{\Pi}$ residuals.

3.4.1.2 Case study 2.B

Parametric mismatch is enforced by underestimating parameter f_{Mat} (values ~40% smaller than the true values are used in the FP model). Recall that f_{Mat} is a dimensionless number that relates to the strength of the material processed.

The resulting three-way array $\underline{\mathbf{X}}_M$ [15×5×40] is used to build the MPCA model using 8 PCs, and this results in normally-distributed $\mathbf{X}_M$ residuals. After the projection of $\mathbf{X}_{\Pi}$ onto the model, the analysis of the $MRLR_v$ values clearly shows that $\mathbf{x}_1$ provides the greatest contribution to the mismatch (Figure 3.16). Hence, $P_{B,i}$ is the variable to which the observed PMM can probably be ascribed.

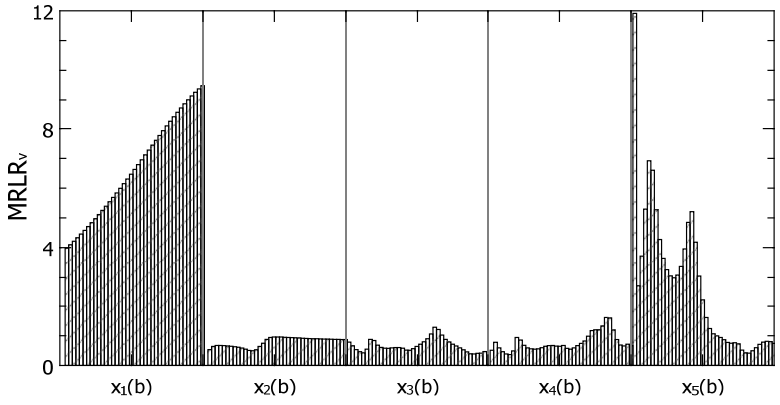

Figure 3.16. *Case study 2.B $MRLR_v$ for each column of $\mathbf{X}_{\Pi}$. The columns are grouped according to the auxiliary variables they originate from; each bar within an auxiliary variable refers to a different bin.*

As in Case study 2.A, to get more insight the diagnosing procedure is iterated by defining a new set of auxiliary variables; the same set as in Eq. (3.27) is used to this purpose. By building an MPCA model on 7 PCs, the results reported in Figure 3.17 are obtained. It appears that $\mathbf{x}'_1$ (which is related to f_{Mat}) and $\mathbf{x}'_4$ (which is related to q_M) are the two auxiliary variables that most contribute to the $\mathbf{X}'_{\Pi}$ residuals. Since Figure 3.16 indicates that $\mathbf{x}_1$ is by far the auxiliary variable that most contributes to the residuals, but $\mathbf{x}'_4$ does not include variables that are included also in $\mathbf{x}_1$, and it can be concluded that the proposed methodology diagnoses f_{Mat} as the root cause of the observed PMM.

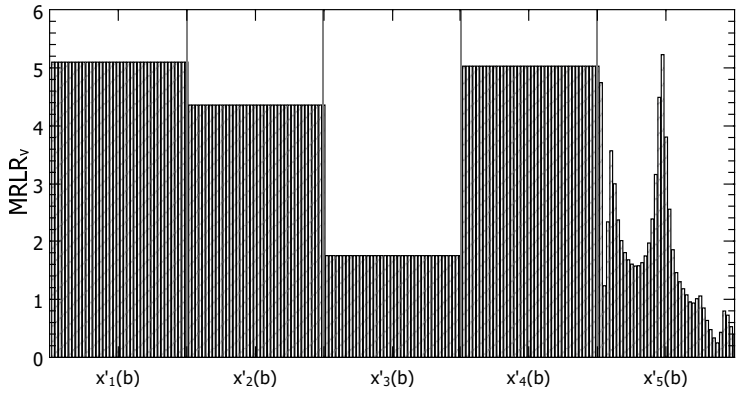

Figure 3.17. *Case study 2.B. Second iteration: $MRLR_v$ for each column of $\mathbf{X'}_{\Pi}$. The columns are grouped according to the auxiliary variables they originate from; each bar within an auxiliary variable refers to a different bin.*

3.4.1.3 Case study 2.C

Parametric mismatch is enforced by overestimating (by ~50%) the true *q* parameter. Note that q denotes the power law exponent within the breakage function, and it depends on the mill rotational velocity.

Application of the proposed methodology (with 9 PCs used to build the MPCA model) leads to the results illustrated in Figure 3.18. Again, $\mathbf{x}_1$ is identified as the strongest contributor to the $\mathbf{X}_{\Pi}$ residuals. However note that, differently from Case studies 2.A and 2.B, auxiliary variable $\mathbf{x}_5$, which is the variable on which the PMM is expected to show up, does not exhibit a significant contribution to the residuals. Hence, this first iteration of the diagnosing methodology suggests that for this case study the $MRLR_v$ index may not be able to identify the origin of the PPM, as the PPM itself is not clearly noticeable from the residuals.

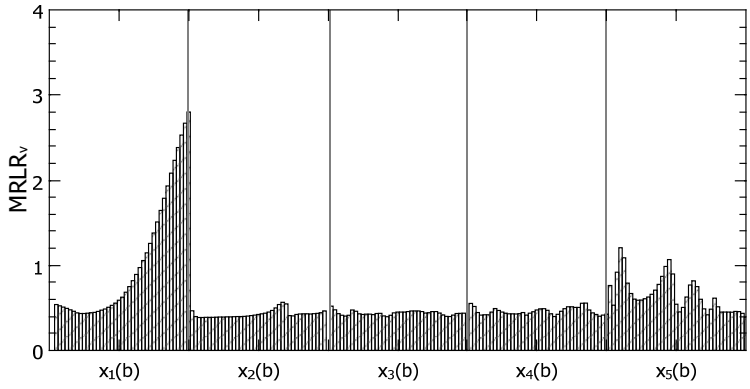

Figure 3.18. *Case study 2.C $MRLR_c$ for each column of $\mathbf{X}_{\Pi}$. The columns are grouped according to the auxiliary variables they originate from; each bar within an auxiliary variable refers to a different bin.*

In fact, after building an MPCA model (on 7 PCs) on $\underline{\mathbf{X}}'_{M}$ and projecting $\mathbf{X}'_{\Pi}$ onto it results in Figure 3.19, no definitive conclusions can be taken in this case with respect to the origin of the PMM: although the contribution of $\mathbf{x}'_4$ (hence q_M) is somewhat larger than that of the other auxiliary variables, this is not enough to unambiguously point to that parameter as the one that needs to be adjusted to enhance the FP model performance. It is worth noticing that q_M has a smaller impact on the outlet PSD with respect to the other parameters analyzed, and this makes the PMM diagnosis harder in this case study.

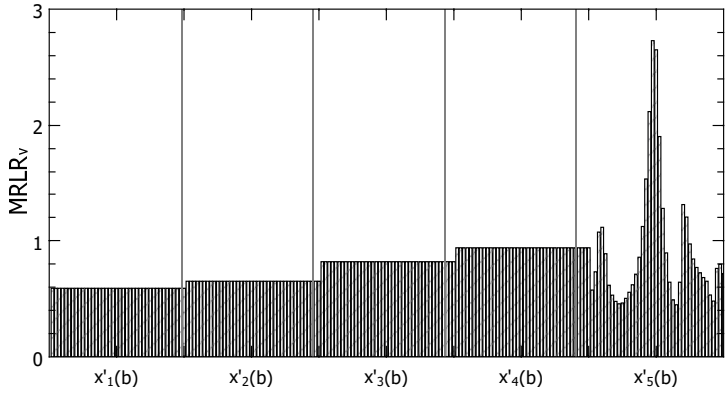

Figure 3.19. *Case study 2.C. Second iteration: $MRLR_c$ for each column of $\mathbf{X}'_{\Pi}$. The columns are grouped according to the auxiliary variables they originate from; each bar within an auxiliary variable refers to a different bin.*

3.5 Conclusions

In this Chapter, a methodology has been proposed to diagnose the causes of the process/model mismatch that may arise when a first-principles process model is challenged against a set of historical experimental data. The objective was to identify which model equations or model parameters most contribute to the mismatch, without carrying out any additional experiment.

The methodology exploited the available historical dataset and a simulated dataset, generated by the FP model using the same inputs as those of the historical dataset. Auxiliary variables were defined as appropriate nonlinear combinations of the model variables and parameters and of the process variables. The auxiliary variables were collected in two matrices, whose correlation structure was compared using a multivariate statistical technique, namely principal component analysis. Diagnostic indices were coupled to engineering judgment to pinpoint the model equations or model parameters that most contributed to make the correlation structures of the two matrices inconsistent, hence to determine the observed PMM.

Two simulated case studies at increasing level of complexity were used to assess the effectiveness of the proposed methodology: a jacketed continuos stirred tank reactor and a solids milling unit.

In both cases, the proposed methodology was generally effective in diagnosing the root cause of the observed mismatch.

There are several areas where further investigation should be carried out. First, appropriate confidence limits should be defined when the residuals distribution is not found to be normal. Additionally, the $MRLR_v$ index could be complemented with other diagnostic indices. Furthermore, analyzing the shape of the $MRLR_v$ profiles (and not only their average values) might prove useful to gain additional diagnostic indications. Finally, the effectiveness of the proposed methodology should be assessed for a wider range of structural mismatches, as well as for a combination of parametric and structural mismatches, and the methodology itself should be challenged against real-world systems. Nevertheless, the proposed methodology provides a very promising approach to the enhancement of FP models by systematic use of the information that is hidden within historical databases. By facilitating the diagnosis of the PMM root causes, any additional experimental effort, which may be needed to enhance the FP model performance, can be targeted much more appropriately, and the overall need for experimental campaigns can therefore be reduced.

Chapter 4

First-Principles Model Diagnosis in Batch Systems by Multivariate Statistical Modeling*

In this Chapter, the methodology proposed in Chapter 3 to diagnose the root cause of the mismatch in steady-states models is extended to dynamic models, considering a simulated batch drying process and a simulated penicillin fermentation process to test the proposed methodology. The likely sources of the mismatch are identified using a multivariate statistical model and analyzing the model residuals as well as the scores shifts. The importance of considering the entire evolution of a process in the diagnosis of a PMM is also discussed. Different examples are reported to demonstrate the effectiveness of the proposed methodology.

4.1 Introduction

When a first-principles (FP) model is challenged against a historical dataset, the model outputs may not match the historical evidence with the desired accuracy, and process/model mismatch (PMM) occurs. In Chapter 3, a methodology has been proposed to diagnose the root causes of PMM by exploiting the available historical dataset and a simulated dataset, generated by the FP model using the same inputs as those of the historical dataset. A data-driven (DD) model (namely, a multivariate statistical model) is used to analyze the correlation structure of the historical and simulated datasets, and information about from where the PMM originates is obtained using diagnostic indices and engineering judgment. The methodology was developed for steady-states processes. However, for dynamic processes the diagnosis of an observed PMM is more difficult because of the time-varying nature of the measurements, which imply data auto-correlation and cross-correlation, as well as a more strongly nonlinear behavior that may be difficult to capture using a linear multivariate model.

* Excerpts from this Chapter have been published in :Meneghetti, N., P. Facco, S. Bermingham, D. Slade, F. Bezzo, M. Barolo (2015). First-principles model diagnosis in batch systems by multivariate statistical modeling. In: *Computer-Aided Chemical Engineering 37* (K.V. Gernaey, J.K. Huusom, R. Gani, Eds.), Elsevier, Amsterdam (The Netherlands), 437-442.

In this Chapter, the PMM diagnosis methodology is extended to batch systems, using a simulated semi-batch solids drying process and a simulated penicillin fermentation process as test beds. In the first case study, multi-way principal component analysis (MPCA; Nomikos and MacGregor, 1994) is employed as a DD model, enhancing it with an orthogonal rotation (VARIMAX rotation) of the principal directions (Magnus and Neudecker, 1999; Wang et al., 2005). In the second case study, the comparison of the results obtained considering only the final measurements of a batch or the entire trajectories is also provided. Two different examples for both case studies are analyzed to discuss the ability of the proposed methodology to point to the FP model sections needing improvement.

4.2 Case study 1

4.2.1 Process description and available data

A simulated lab-scale drying process is considered, in which hot dry air flows through a bed of wet solid alumina granules, partially evaporating the water contained in the particles. The model equations derive from the work of Burgschweiger and Tsostas (2002), and are solved in the gSOLIDS® modeling environment (gSOLIDS®, Process Systems Enterprise Ltd, London, UK, 2014). The particle size distribution is discretized in 10 bins and no shrinkage of particles is considered. The global mass and energy balances for the particulate phase and vapor phase (indicated by subscripts *p* and *vap*, respectively) are:

$$\frac{dM_{i,p}}{dt} = F_p^{in} x_{i,p}^{in} - F_p^{out} x_{i,p}^{out} - R_{drying,i,p} \quad , \tag{4.1}$$

$$\frac{dH_p}{dt} = F_p^{in} h_p^{in} - F_p^{out} h_p^{out} - \Delta H_{drying,p} \quad , \tag{4.2}$$

$$\frac{dM_{i,vap}}{dt} = F_{vap}^{in} x_{i,vap}^{in} - F_{vap}^{out} x_{i,vap}^{out} + R_{drying,i,p} \quad , \tag{4.3}$$

$$\frac{dH_{vap}}{dt} = F_{vap}^{in} h_{vap}^{in} - F_{vap}^{out} h_{vap}^{out} + \Delta H_{drying,p} \quad , \tag{4.4}$$

where F is the mass flowrate, h is the specific enthalpy, x_i is the mass fraction of species i in the solid phase (alumina or water) or in the vapor phase (dry air or water), and superscripts *in* and *out* refer to the bed inlet and outlet, respectively. The drying rate $R_{drying,i,p}$ is given by:

$$R_{drying,i,p} = A_p \nu_i \rho_i k_{c,i} \left(Y_{eq,i} - Y_{bulk,i} \right) \quad , \tag{4.5}$$

and $\Delta H_{drying,p}$ is the enthalpy change rate due to drying. In (4.5), A_p is the particle surface area available for drying, ρ_i is the density of the gas phase, k_c is the mass transfer coefficient, and $Y_{eq,i}$ and $Y_{bulk,i}$ are respectively the equilibrium and actual dry-basis moisture content of the water in the gas phase. Finally, v_i is the normalized single-particle drying rate, which can be estimated from the experimental drying curve. The latter is a function of the normalized moisture content η_i, which is in turn calculated from the dry basis moisture content X_i, the equilibrium dry-basis moisture content $X_{eq,i}$ (which is a function of the relative humidity ϕ_i), and the critical dry basis moisture content $X_{cr,i}$. Details on the values of model parameters are reported in the original work of Burgschweiger and Tsostas (2002). This FP model will be referred to as "the process" in the following.

A set of N = 25 batches, representing the historical dataset, are simulated using different combinations of the following measurable inputs: inlet solid mass flowrate (F_p^{in}), initial moisture content (X^{in}), inlet mass flowrate (F_{vap}^{in}), and air temperature (T_{vap}^{in}). It is assumed that four measurable outputs exist: moisture content in the granules (X_i), granules temperature (T_p^{out}), outlet air temperature (T_{vap}^{out}), and outlet air relative humidity (ϕ_i). The batch length is 1420s and the measurement interval is 30 s; hence, T = 48 samples are available for each measured variable in each batch.

The PMM diagnosis methodology is tested by considering two process models that use the same set of equations as described above, but where two different parametric mismatches are purposely introduced. These sets of equations and (wrong) parameters will be referred to as "the model" in the following.

4.2.2 Proposed methodology

In order to diagnose the root-cause of an observed PMM, the framework proposed by in Chapter 3 is applied. However, appropriate adjustments are introduced to deal with dynamic data. According to the proposed rationale, a DD model (namely, a latent variable model) is first developed to model the correlation structure of appropriate combinations of the simulated process variables, these combinations being suggested by the FP model structure. Then, it is assessed whether the combinations of the same variables, but calculated from the historical measurements, conform to this correlation structure. Finally, from the analysis of some model diagnostic indices, engineering knowledge is used pinpoint the FP model sections that are mostly responsible for the observed PMM. In detail, the following steps are followed (subscripts Π and M refer to the process and to the model, respectively).

1. Auxiliary data designation. A set of V= 9 auxiliary variables is defined considering the model equation terms that, according to engineering judgment, are expected to be possibly related to the observed PMM:

$$\begin{array}{lll} x_1(n,t) = A_P & x_4(n,t) = \eta_i & x_7(n,t) = T^{vap} \\ x_2(n,t) = \nu_i & x_5(n,t) = k_{c,i} & x_8(n,t) = X_i \\ x_3(n,t) = X_{eq} & x_6(n,t) = \alpha_i & x_9(n,t) = \phi_i \end{array} \quad , \tag{4.6}$$

where (n, t) of the $[N \times T]$ matrix $\mathbf{X}_v$ is indicated by $x_v(n,t)$ and represents the v-th auxiliary variable evaluated at time t for batch n. In (4.6) i refers to water and α is the heat transfer coefficient involved in the calculation of the energy balances. The simulated and historical datasets are separately used to estimate the values of the auxiliary variables. The values taken by the auxiliary variables throughout the whole batches are arranged in the $[N \times V \times T]$ arrays $\underline{\mathbf{X}}_{\mathrm{M}}$ and $\underline{\mathbf{X}}_{\Pi}$, which are the model matrix and the process matrix, respectively.

Note that the values taken by some auxiliary variables (x_1, x_2, x_4, x_5 and x_6) are bin-dependent. However, only the bin including the largest number of particles is considered for their calculation. Also note that variables T^{vap}, X_i and ϕ_i (which can be measured) are purposely included in the auxiliary variable set (x_7, x_8 and x_9) to make the available measurements directly affect the correlation structures of $\underline{\mathbf{X}}_{\mathrm{M}}$ and $\underline{\mathbf{X}}_{\Pi}$.

2. Data-driven model development. An MPCA model (Nomikos and MacGregor, 1994) is built from $\underline{\mathbf{X}}_{\mathrm{M}}$. MPCA is equivalent to performing PCA (Jackson, 1991) on the $[N \times (V \cdot T)]$ matrix $\mathbf{X}_{\mathrm{M}}$ obtained by unfolding $\underline{\mathbf{X}}_{\mathrm{M}}$ batch-wise. Also $\underline{\mathbf{X}}_{\Pi}$ is unfolded (to $\mathbf{X}_{\Pi}$), and both $\mathbf{X}_{\mathrm{M}}$ and $\mathbf{X}_{\Pi}$ are autoscaled on the mean and standard deviation of $\mathbf{X}_{\mathrm{M}}$. PCA decomposes $\mathbf{X}_{\mathrm{M}}$ as the sum of A scores $\mathbf{t}_i$ and A loadings $\mathbf{p}_i$, where A is the number of principal components (PCs) that describe an adequate percentage of the dataset variability:

$$\mathbf{X}_{\mathrm{M}} = \mathbf{t}_{1,\mathrm{M}}\mathbf{p}_{1,\mathrm{M}} + \mathbf{t}_{2,\mathrm{M}}\mathbf{p}_{2,\mathrm{M}} + \cdots + \mathbf{t}_{A,\mathrm{M}}\mathbf{p}_{A,\mathrm{M}} + \mathbf{E}_{\mathrm{M}} = \mathbf{T}_{\mathrm{M}}\mathbf{P}_{\mathrm{M}}{}^{\mathrm{T}} + \mathbf{E}_{\mathrm{M}} \quad , \tag{4.7}$$

where $\mathbf{T}_{\mathrm{M}}$ $[N \times A]$ is the scores matrix and $\mathbf{P}_{\mathrm{M}}$ $[(V \cdot T) \times A]$ is the loadings matrix In both examples, 4 PCs are selected. Note however that the selected number of PCs can affect the ability of the methodology to effectively diagnose an observed PMM. How to provide a general guideline for the selection of A is still under investigation.

In this challenging case study, most of the auxiliary variables are very strongly correlated and provide similar contributions along all latent directions, thus confounding the analysis. In order to amplify the contribution of each auxiliary variable on one latent direction only, the VARIMAX rotation is applied (Magnus and Neudecker 1999; Wang et al., 2005). This technique uses an orthogonal rotation to transform the MPCA model space so that only a subset of the auxiliary variables show high weight values along each PC. Upon VARIMAX application, the residuals matrix $\mathbf{E}_{\mathrm{M}}$ is not modified, but can be calculated also from:

$$\mathbf{X}_{\mathrm{M}} - \mathbf{T}_{\mathrm{var,M}}\mathbf{P}_{\mathrm{var,M}}^{\mathrm{T}} = \mathbf{E}_{\mathrm{M}} \quad , \tag{4.8}$$

where $\mathbf{T}_{var,M}$ and $\mathbf{P}_{var,M}$ are (respectively) the scores and loadings matrices obtained by application of the VARIMAX rotation.

3. Process matrix projection. $\mathbf{X}_{\Pi}$ is projected onto the rotated MPCA model space and the residuals matrix $\mathbf{E}_{\Pi}$ is calculated as:

$$\mathbf{T}_{var,\Pi} = \mathbf{X}_{\Pi}\mathbf{P}_{var,M}, \quad \mathbf{X}_{\Pi} - \mathbf{T}_{var,\Pi}\mathbf{P}_{var,M}^{T} = \mathbf{E}_{\Pi} \quad , \tag{4.9}$$

4. Mismatch diagnosis. The mismatch may appear in the MPCA model as a large residual value or as a shift in the scores space (or both). For this reason, a mismatch analysis should evaluate both these aspects.

   The residuals analysis is performed by comparing $\mathbf{E}_M$ and $\mathbf{E}_{\Pi}$ to identify the auxiliary variables that are most responsible for the inconsistency in the correlation structures of $\mathbf{U}_M$ and $\mathbf{U}_{\Pi}$. These auxiliary variables, together with engineering judgment, are used to pinpoint which model sections are likely the cause of the observed PMM. In order to reduce the residuals contribution due to the fraction of data variability not described by the MPCA model, the results of residuals analysis are expressed using the mean residuals-to-limit ratio (MRLR), i.e. the mean of the ratios between the residuals of each column of $\mathbf{E}_{\Pi}$ and the corresponding 95 % confidence limit, calculated considering a normal distribution of the residuals for each variable (Eq. 3.4, Chapter 3; Choi and Lee, 2005).

   An analysis of the scores shift can be performed by jointly analyzing $\mathbf{T}_{var,M}$, $\mathbf{T}_{var,\Pi}$ and $\mathbf{P}_{var,M}$. For each PC, the scores shift is calculated as $(\mathbf{t}_{a,M,var} - \mathbf{t}_{a,\Pi,var})$, i.e., as the difference between the model matrix scores and the process matrix scores. The rationale beyond this approach is to identify the auxiliary variables that most affect the scores shift. These variables are identified by analyzing the MPCA model loadings along the direction that most contributes to the shift. To this purpose, the use of the VARIMAX rotation is particularly effective, as it allows one to emphasize the contribution of a single auxiliary variable (or very few of them) along each PC. The information obtained by this analysis may reveal particularly useful when a small-dimension historical dataset is available.

4.2.2.1 Results for Example 1.A

The mismatch is forced by altering the value of the critical moisture content (which is involved in the calculation of η_i) and results in a relative error of 1.6-17 % in the simulated final dry-basis particle moisture content. Hence, to correctly diagnose the PMM, the proposed methodology should point to auxiliary variable $\mathbf{X}_4$.

The residuals analysis (not reported for the sake of conciseness) cannot clearly point to the root cause of the mismatch, since all auxiliary variables have similar and low values of MRLR (high residuals are actually seen in $\mathbf{X}_3$ and $\mathbf{X}_9$, but this happens at the very beginning of the batch only). The scores shift analysis is more effective, instead.

Figure 4.1a reports the scores shifts for each batch together with the mean shifts through all batches along each PC. By far the largest shifts are seen along PC2; hence, the auxiliary variables having a significant weight along this direction are possibly related to the observed PMM. The [1×(V·T)] loadings $\mathbf{p}_{a,\mathrm{M,var}}$ are shown as black bars in Figure 4.1b. It can be seen that PC2 mainly captures the variability due to model terms $\mathbf{X}_2$ and $\mathbf{X}_3$, as well as that due to outputs $\mathbf{X}_7$ and $\mathbf{X}_9$. Hence, further investigation on the FP model should focus on the $\mathbf{X}_2$ and $\mathbf{X}_3$ terms. Model inspection suggests that their values are strongly and directly correlated to $\mathbf{X}_4$. Therefore, according to these considerations, to improve the FP model further investigation on model sections $\mathbf{X}_2$, $\mathbf{X}_3$ and $\mathbf{X}_4$ should be done. The other model sections (including those representing heat and mass transfer phenomena) are not likely sources of the observed PMM.

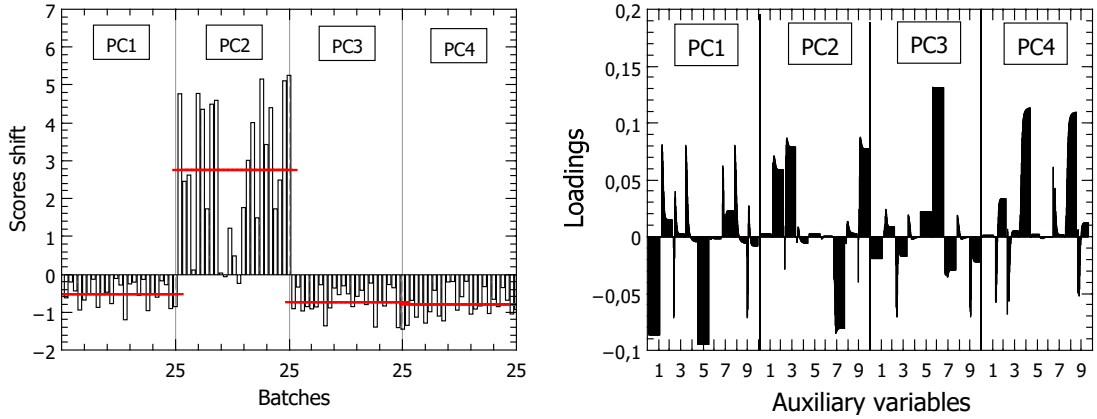

(a) (b)

Figure 4.1. *Example 1. (a) Shift of $\mathbf{t}_{a,M,var}$ from $\mathbf{t}_{a,II,var}$ for each batch (bars) and mean value of these differences (lines) for each PC. (b) Loadings for each PC obtained by applying the VARIMAX rotation to the MPCA model built on $\mathbf{X}_M$.*

4.2.2.2 Results for Example 1.B

The mismatch is forced by changing the mass transfer coefficient *kc*, and results in a 1.3-37 % error in the simulated final dry-basis particle moisture content. Hence, to correctly diagnose the PMM, the proposed methodology should point to auxiliary variable $\mathbf{X}_5$.

Figure 4.2a reports the results obtained by the residuals analysis. Although, at the very beginning of the batches, MRLR peaks for auxiliary variables $\mathbf{X}_3$ and $\mathbf{X}_9$, consistently high MRLR values along the entire batch lengths are seen only on $\mathbf{X}_1$, $\mathbf{X}_5$ and $\mathbf{X}_6$. These latter auxiliary variables are therefore regarded as the most responsible ones for the observed PMM. As $\mathbf{X}_1$, $\mathbf{X}_5$ and $\mathbf{X}_6$ refer to the contact area and to the mass and heat transfer coefficients, their values are strongly correlated, so that it is difficult to further discriminate their contribution to the PMM.

Figure 4.2b reports the scores shift for each PC. Although the main direction of the scores shift is along PC1, this is clearly not dominant, because significant shifts occur also along the other

principal directions. We conclude that several auxiliary variables concur to the shift occurrence, and the scores shift analysis does not effectively identify a likely PMM source.

To summarize, according to proposed methodology the observed mismatch is not related to model sections $\mathbf{X}_2$, $\mathbf{X}_3$ or $\mathbf{X}_4$. Conversely, model sections $\mathbf{X}_1$, $\mathbf{X}_5$ and $\mathbf{X}_6$ should be investigated to improve the FP model performance.

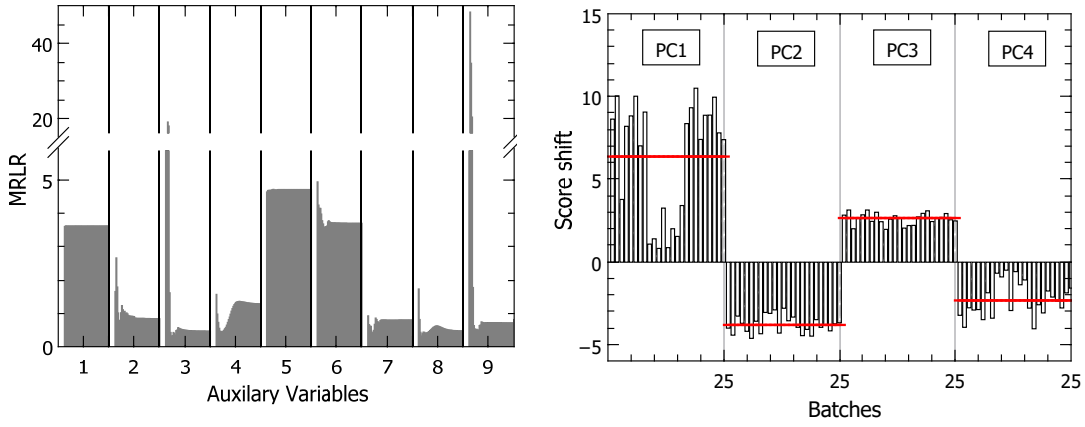

Figure 4.2. *Example 2. (a) MRLR values for each auxiliary variable. (b) Shift of* $\mathbf{t}_{a,M,var}$ *from* $\mathbf{t}_{a,\Pi,var}$ *for each batch (bars) and mean value of these differences (lines) for each PC.*

4.3 Case study 2

4.3.1 Process description and available data

The second case study concerns a simulated fed-batch fermentation process, developed by using a realistic dynamic model of penicillin fermentation. A detailed description of the process is provided by Birol *et al.* (2002) and Çinar *et al.* (2003). The process involves two operating stages: in the first stage the microorganisms grow in a batch culture (consuming oxygen and the initial substrate) then, in the second stage, the synthesis of the penicillin is performed by operating in a fed-batch mode. The penicillin is produced in a well-mixed bioreactor, where a control system keeps the reactor temperature and pH at desired values. The mass balance for each element (indicated by subscripts *p* for penicillin, *s* for substrate, *x* for biomass and *l* for dissolved oxygen) and energy balance of the system are:

$$\frac{dC_p}{dt} = \mu_{pp} C_x - K \cdot C_p - \frac{C_p}{V}\frac{dV}{dt} \quad , \tag{4.10}$$

$$\frac{dC_s}{dt} = -\frac{\mu}{Y_{x/s}} C_x - \frac{\mu_{pp}}{Y_{p/s}} C_x - m_x C_x + \frac{F_s}{V} - \frac{C_s}{V}\frac{dV}{dt} \quad , \tag{4.11}$$

$$\frac{dC_x}{dt} = \mu C_x - \frac{C_x}{V}\frac{dV}{dt} \quad , \tag{4.12}$$

$$\frac{dC_l}{dt} = -\frac{\mu}{Y_{x/o}}C_x - \frac{\mu_{pp}}{Y_{p/o}}C_x - m_o C_x + k_l a \cdot \left(C_l^* - C_{l,fin}\right) - \frac{C_l}{V}\frac{dV}{dt} \quad , \tag{4.13}$$

$$\frac{dQ}{dt} = r_{q1}\frac{C_x}{V}\frac{dV}{dt} + r_{q2} \cdot C_x \cdot V \quad , \tag{4.14}$$

where C stands for concentration, F for flowrate and V for volume. The specific growth rate μ and the specific penicillin production rate μ_{pp} are expressed as:

$$\mu_{pp} = \mu_p \cdot \left(\frac{C_{s,fin}}{k_p + C_{s,fin} + {C_{s,fin}}^2 / k_I}\right)\cdot\left(\frac{{C_{l,fin}}^p}{k_{op} \cdot C_{x,fin} + {C_{l,fin}}^p}\right) \quad , \tag{4.15}$$

$$\mu = \left(\frac{\mu_x}{1 + \frac{k_1}{[H_+]} + \frac{[H_+]}{k_2}} \cdot \frac{C_{s,fin}}{k_x \cdot C_{x,fin} + C_{s,fin}} \cdot \frac{C_{l,fin}}{k_{ox} \cdot C_{x,fin} + C_{l,fin}}\right)\cdot\left(k_g e^{\left(\frac{-E_g}{RT}\right)}\right) - k_d e^{\left(\frac{-E_d}{RT}\right)} \quad . \tag{4.16}$$

Details on the values of model parameters are reported in the original work of Birol *et al.* (2002). Note that, this set of differential-algebraic equations represents only a part of the model implemented in the simulator used to obtain the data (PenSim[§]) which also includes the pH and temperature control algorithms. However, in this study it is assumed that the control system is not affected by errors.

Two plants of different scales are considered. Plant A is a laboratory-scale plant with a culture volume of 10 L, whereas plant B is a pilot-scale plant with an average culture volume of 100 L. The two plants have been scaled maintaining the ratio P/V constant. The fermenter temperature and pH are maintained at the desired value by a PID controller in both plants, and they use the same settings as indicated by Birol *et al.* (2002). The reactor temperature is controlled by manipulating the heating/cooling water flowrate in the reactor jacket, while pH is controlled by adjusting the concentrated acid/base flowrate entering the reactor. Different initial conditions are used to simulate the two plants in terms of substrate feed concentration and initial substrate concentration, aeration rate, and agitation power (Table 4.1), whereas for all the other inputs the values suggested by Birol *et al.* (2002) are considered.

It is assumed that the model used validated on the laboratory-scale plant, and that has poor performance in the representation of the pilot-scale plant. In fact, two different errors have been

§ http://simulator.iit.edu/web/pensim/index.html

introduced in the FP model used to describe the pilot-scale plant to force the presence of a PMM (Example 2.a and 2.b).

Table 4.1. *Case study 2: Values of the input variables used to generate the historical and simulated datasets.*

Variables	Measurement unit	Initial values
Substrate feed rate concentration	[g/L]	0.0431; 0.035; 0.037; 0.039; 0.045
Initial substrate concentration	[g/L]	5; 8; 11; 17; 20
Aeration rate	[L/h]	3; 4.4; 5.8; 7.2; 10
Agitation Power	[W]	20; 32; 38; 44; 50

The trajectories of 26 different batches, carried out under different initial conditions in the pilot-scale plant (namely by the model that simulates the real conditions of the system), have been compared with the trajectories provided by the model under the same conditions (namely by the model where an error has been introduced) actually revealing the presence of a PMM. Note that if the same duration for each batch is maintained, different final concentrations of penicillin are achieved for the 26 batches considered. Also note that, all the available measurements (C_x, C_p, C_s, C_l, P (agitation power), V, T, H_+(hydrogen ion concentration), F_s) are affected by noise.
For both examples, the analysis have been divided into two steps: first, only the measurements at the end of the batches have been considered, thus reducing the analysis of the mismatch to that of a steady-state system; then, the entire trajectories have been analyzed (Figure 4.3). This approach permits one to assess the importance of considering the process dynamics. For both steps, the same set of V= 10 auxiliary variables is considered:

$$\begin{aligned}
x_1(n,t) &= k_l a \cdot \left(C_l^* - C_l\right) & x_6(n,t) &= C_x \cdot \left(m_x\right) \\
x_2(n,t) &= K \cdot C_p; & x_7(n,t) &= C_x \cdot k_d e^{\left(\frac{-E_d}{RT}\right)} \\
x_3(n,t) &= \mu_{pp} C_x & x_8(n,t) &= C_l \\
x_4(n,t) &= C_x \cdot \left(\frac{\mu_x}{1 + \frac{k_1}{[H_+]} + \frac{[H_+]}{k_2}} \cdot \frac{C_{s,fin}}{k_x \cdot C_{x,fin} + C_{s,fin}} \cdot \frac{C_{l,fin}}{k_{ox} \cdot C_{x,fin} + C_{l,fin}} \right) \cdot k_g e^{\left(\frac{-E_g}{RT}\right)} & x_9(n,t) &= C_{s,0} - C_s \\
x_5(n,t) &= C_x \cdot \left(m_o\right) & x_{10}(n,t) &= C_x
\end{aligned} \quad ,(4.17)$$

where element (n, t) of the [N×T] matrix $\mathbf{X}_v$ is indicated by $x_v(n,t)$ and represents the v-th auxiliary variable evaluated at time t for batch n. The simulated and historical datasets are separately used to estimate the values of the auxiliary variables. The values taken by the auxiliary variables throughout the whole batches are arranged in the [N×V×T] arrays $\underline{\mathbf{X}}_{\mathrm{M}}$ and $\underline{\mathbf{X}}_{\Pi}$, which are the model matrix and the process matrix, respectively.

Note that some auxiliary variables (x_8, x_9 and x_{10}) are constituted only by input and output measurements, and are included in the dataset only to strengthen a different correlation structure between $\underline{\mathbf{X}}_M$ and $\underline{\mathbf{X}}_\Pi$. Finally, since the temperature is maintained constant during the entire process, the terms involved in Eq. (4.14) are not considered in the auxiliary variables set.

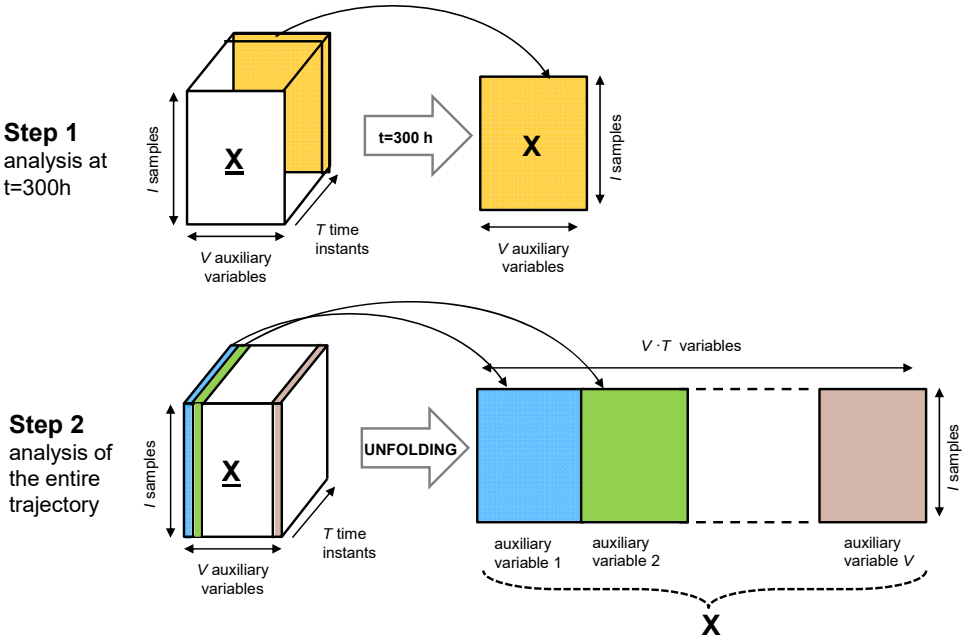

Figure 4.3. *Case study 2.A. The analysis of the mismatch is split into two steps: in the first step only the measurements at the end of the batches have been considered, whereas in the second step the entire trajectories have been analyzed, by an MPCA model.*

4.3.1.1 Results for Example 2.A

In this first example, it is assumed that a mismatch is forced by changing the parameter α (Eq. 4.18) in the calculation of mass transfer coefficient k_{la}, thus assuming that the model underestimates the mass transfer effectiveness (4.10).

$$k_{la} = \alpha \sqrt{f_g} \left(\frac{P}{V} \right)^{\beta} \quad . \tag{4.18}$$

An average change of 90% of this coefficient leads to a variation in the final penicillin concentration of the batches considered from 1 to 25%. However, note that in the calculation of x_1 of Eq. (4.17), parameter α is that assumed for the model, only the measured variables are different in $\underline{\mathbf{X}}_M$ and $\underline{\mathbf{X}}_\Pi$.

In the first step of the analysis, $\mathbf{X}_M$ and $\mathbf{X}_\Pi$ result to be 2-dimensional matrices [$N \times V \times 1$], since they are calculated considering the final measurements (t=300 h) available for the model and the

process, respectively. Following the procedure proposed in Chapter 3 (Section 3.2), a PCA model is built from $\mathbf{X}_M$ (previously autoscaled), considering 2 PCs able to capture more than 90 % of the variability of the data. Then $\mathbf{X}_\Pi$ (scaled on the mean and standard deviation of $\mathbf{X}_M$) is projected onto the latent space described by $\mathbf{X}_M$. As stated in Section 4.3, the mismatch may appear in the PCA model as a large residual value and/or as a shift in the scores space as shown in Figure 4.4a. This representation clearly shows the different position of the two datasets, both *on* the score plane (score shift) and *from* the score plane (high prediction residuals). The results of the residuals analysis performed by comparing $\mathbf{E}_M$ and $\mathbf{E}_\Pi$ through the MRLR index are shown in Figure 4.4b. The first auxiliary variable ($\mathbf{X}_1$), which presents a value of the MRLR index significantly higher than the other variables, is correctly identified as a possible cause of the mismatch (4.17).
In this case, the shift analysis (not reported for the sake of conciseness) does not permit to clearly point to the root cause of the mismatch; not even the application of the VARIMAX rotation prevents all auxiliary variables to have similar loadings on the first latent direction presenting the higher scores shift.

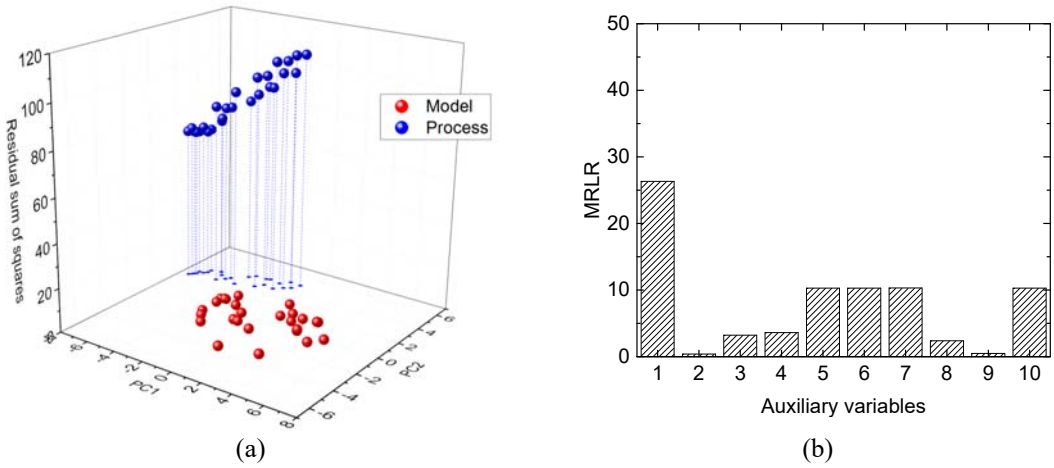

(a) (b)

Figure 4.4. *Case study 2.A. (a) Residuals in the scores space for each sample of the model matrix* $\boldsymbol{X}_M$ *and of the process matrix* $\boldsymbol{X}_\Pi$ *and (b)* $MRLR_v$ *for each column of* $\mathbf{X}_\Pi$, *calculated considering only the final measurements of each batch.*

In the second step, $\underline{\mathbf{X}}_M$ and $\underline{\mathbf{X}}_\Pi$ result to be 3-dimensional matrices [$N \times V \times T$], since they are calculated considering the entire trajectories of the samples available for the model and the process, respectively. Since the process involves a batch and a fed-batch stage, it has been considered more appropriate to split the analysis of the batch trajectories into two parts, each corresponding to the two operating stages. However, the time instant, where the switch from batch mode to fed-batch mode occurs, differs from batch to batch. Therefore, a synchronization of the batch trajectories before and after the switch point may be useful to adequately compare the correlation structure of $\underline{\mathbf{X}}_M$ and $\underline{\mathbf{X}}_\Pi$. There are several synchronization techniques available in

literature (Kourti, 2003), however this specific case study and the purpose of the analysis, a simple synchronization has been performed according to the following procedure:

1. the batch with the minimum duration of the batch phase is considered as the reference one for the first stage of the process;
2. the difference (in terms of number of samples) between the duration of the first stage of the process of each batch to the reference one is calculated. This number of samples is removed from each batch by selecting the samples randomly and uniformly throughout the first stage;
3. among the resulting batches, the one with the minimum duration of the fed-batch phase is considered as the reference one for the second stage of the process;
4. point 3 is repeated for the second stage of the process.

Finally, the same procedure explained in Section 4.3 has been applied both for the first and the second stage: first, an MPCA model is built from $\underline{\mathbf{X}}_M$, from the batch-wise unfolded and autoscaled matrix $\mathbf{X}_M$, then $\underline{\mathbf{X}}_\Pi$ (unfolded and scaled on the mean and standard deviation of $\mathbf{X}_M$), has been projected onto the latent space built on $\mathbf{X}_M$. Also in this case the application of VARIMAX rotation does not permit one to improve the analysis of the score shift. Finally, the residual matrices $\mathbf{E}_M$ and $\mathbf{E}_\Pi$ are calculated and compared through the MRLR index. The results are shown in Figure 4.4a and Figure 4.4b for the first and second phase of the process respectively. Although in both cases the first auxiliary variable is pinpointed as the reason of the mismatch, the shape and the magnitude of the residuals differ along the process, especially in the second stage (Figure 4.4b). For example, variables x_5, x_6 and x_7, directly linked to the biomass concentration x_{10}, show a similar trend that significantly increases in the first part of the second stage, and then settles to lower values by the end of it. This type of information can be very useful to support the modeler to validate the assumption that the PMM is caused by a wrong estimation of the mass transfer coefficient k_{la}.

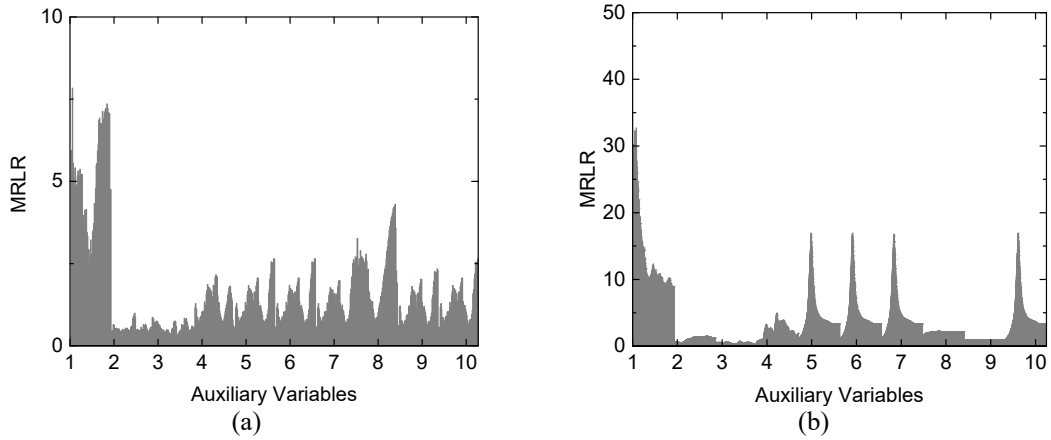

Figure 4.5. *Example 2.A (a) MRLR values for each auxiliary variable calculated considering the measurements related to the first phase of the process and (b) to the second phase of the process.*

Therefore, even if in this example the methodology is able to clearly pinpoint the reason of the mismatch without considering the dynamics of the system, this cannot be considered a general result. This issue is particularly true when the effect of the mismatch mostly manifests itself *during* the process instead than at the end of it.

4.3.1.2 Results for Example 2.B

In this second example, it is assumed that a mismatch is forced by changing parameter $Y_{s/x}$ (from 0.45 [-] to 0.2 [-]), which represents the yield constant involved in the calculation of the substrate utilization for the biomass production (Eq. 4.11)

This is a more complex example than the previous one, for two main reasons: the parameter affected by error is constant for all the batches considered, and its variation causes a significant change in most of the measured variables. In this case, the average variation of the final penicillin concentration is equal to 31%.

The same two-step procedure followed in Section 4.3.3 is repeated for this second example. The result of the analysis of the bi-dimensional matrices $\mathbf{X}_{\mathrm{M}}$ and $\mathbf{X}_{\Pi}$, performed by considering 3 PCs (R^2_{CUM} =98%), is reported in Figure 4.5. It can be observed that variables x_4 and x_9 present the highest values of the MRLR index, but also x_2 and x_3 present values comparable to them. By observing the auxiliary variables in 4.17 the results obtained suggest that the error may be related to μ (Eq. 4.16) which includes x_4. In particular, since only the substrate concentration (x_9) presents very high residuals, it can be concluded that the error might be associated to the relation between μ and C_s, that is actually provided by $Y_{s/x}$. In this context, the high values presented by x_2 and x_3 are related to their correlation with x_4 and x_9.

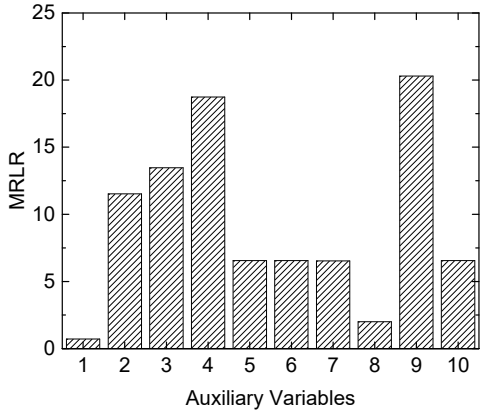

Figure 4.6. *Case study 2.B. $MRLR_v$ for each column of $\mathbf{X}_{\Pi}$, calculated considering only the final measurements of each batch.*

The analysis of the three-dimensional matrices $\underline{\mathbf{X}}_{\mathrm{M}}$ and $\underline{\mathbf{X}}_{\Pi}$ by an MPCA model built considering 2 PCs (R^2_{CUM} =89%), confirms that the diagnosis of the mismatch is less clear in this second example than in the previous one. As shown in Figure 4.7, the MRLR values confirms that the

mismatch clearly affects x_9, but neither in the first (Figure 4.7a) nor in the second phase (Figure 4.7b) of the process, a single term of the model can be unambiguously identified as the most responsible of the PMM. However, the analysis of the MRLR values trend confirms that x_5, x_6, and x_7 are highly correlated (even collinear) with x_{10}, and that, due the high values presented by x_4 and the end of the second phase, this variable may be most related to the PMM. Anyway, in this case, further investigations are needed to validate this conclusion. In Appendix 4, a different approach under investigation to solve this problem is presented.

Similar conclusions can be drown also when an error is introduced in the estimation of $Y_{s/p}$. Due to the strong correlation existing among the variables considered, it is very difficult to identify a single cause of the PMM.

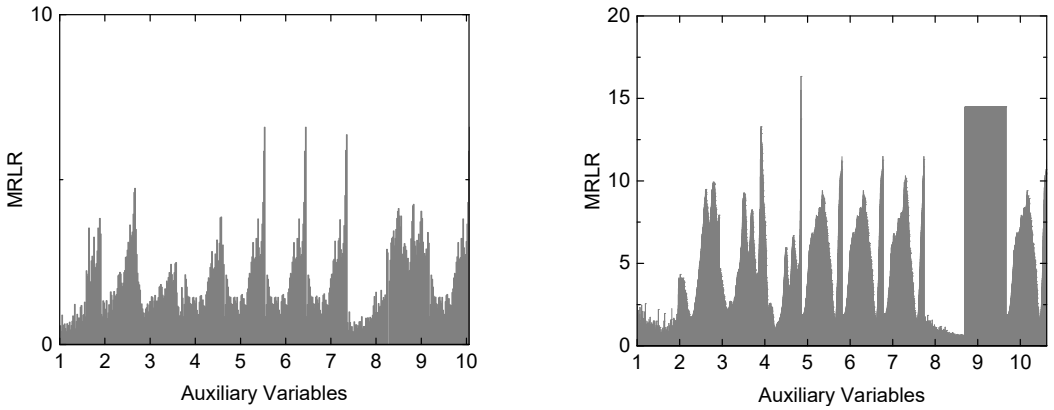

Figure 4.7. *Example 2.B. (a) MRLR values for each auxiliary variable calculated considering the measurements related to the first phase of the process and (b) to the second phase of the process.*

4.4 Conclusions

In this study, the methodology proposed in Chapter 3 to diagnose process/model mismatch has been extended to dynamic systems using two realistic models as test beds: one for a batch drying process and one for a penicillin fermentation process. The methodology exploits a set of historical data and a simulated dataset, generated by the first-principles model using the same inputs as those of the historical data set. Auxiliary variables were defined as appropriate nonlinear combinations of the model variables and parameters, as well as of process measurements. A multiway principal component analysis model was used to analyze the correlation structure of the historical and simulated datasets. In the first case study, information on the root cause of the PMM was obtained by the combined analysis of two diagnostic indices: the data-driven model residuals and the data-driven model scores shifts. With respect to the scores shifts, an orthogonal rotation of the principal axes was carried out in order to magnify the contribution of the most significant auxiliary variables to the shifts. In the second case study, a combined analysis of the whole

trajectories of the available batches and of the measurements taken at the end of each batch, revealed the importance of considering the dynamics of the system in order to validate the results obtained by the application of the methodology.

The results obtained show that the proposed methodology is able to direct the first-principles model improvement efforts towards the model sections that are truly affected by modeling errors. Further improvements should be directed to solve the problems encountered with strongly correlated variables, which often make the diagnosis of the mismatch less clear.

Chapter 5

Bracketing the design space within the knowledge space in pharmaceutical product development*

When a reliable first-principles model is not available for a new pharmaceutical product to be developed, the design space (DS) is often found using experiments carried out within a domain of input combinations (the so-called knowledge space; e.g. raw materials properties and process operating conditions) that result from products that are similar to the new one, but have already been developed. In this Chapter, a methodology is proposed that aims at segmenting the knowledge space in such a way as to identify a subspace of it (called the experiment space) that most likely brackets the DS, in order to limit the extension of the domain over which the experiments should be carried out. The methodology relies on the exploitation of historical information on products that have already been developed and are similar to the new one, and is based on the inversion of a latent-variable model. Products characterized by a single equality constraint specification are considered, and the effect of model prediction uncertainty is explicitly accounted for.

5.1 Introduction

The Quality-by-Design (QbD) initiative launched by the United States Food and Drug Administration (FDA) (FDA, 2004a) fosters the adoption of science-based (as opposed to experience-based) methodologies to support the development of new pharmaceutical products, with the purpose of building quality "by design" into the desired product, i.e. to consistently deliver a product with the intended performance. The ultimate objective of the QbD initiative is to promote product and process understanding in pharmaceutical development, in order to increase both manufacturing flexibility and process robustness (intended as the ability of the process to tolerate variability of materials and changes in the process conditions and equipment without negative impact on product quality). Deep understanding on how the critical quality

* Facco, P., F. Dal Pastro, N. Meneghetti, F. Bezzo, M. Barolo (2015). Bracketing the design space within the knowledge space in pharmaceutical product development. *Ind. Eng. Chem. Res*., **54**, 5128–5138.

attributes and critical process parameters interact is required to achieve this ambitious objective, and the key concept of design space (DS) was introduced to provide a science-based platform where this interaction can be investigated.

According to the International Conference on Harmonization (ICH) Q8(R2) Guidance (ICH, 2009), the DS is "the multidimensional combination and interaction of input variables (e.g., material attributes) and process parameters that have been demonstrated to provide assurance of quality". The DS of the process that manufactures a given product (in short, the DS of that product) is optionally proposed by the pharmaceutical company at the time of submission of that product to the regulatory agency, and it is subject to regulatory assessment and approval. "Working within the design space is not considered as a change" (ICH, 2009), and as such does not require any further regulatory approval. This is a very important aspect, which offers a pharmaceutical company the opportunity to continuously improve its manufacturing processes by reducing the regulatory oversight. In fact, the materials properties and process parameters can be changed by the company with no restrictions to maximize some performance metric, provided that their combination falls within the approved DS. Moving outside the design space would initiate a regulatory post-approval process, instead.

Some additional aspects of the ICH definition of DS are worth emphasizing. Firstly, the DS space refers to *multidimensional* combinations of material attributes and process parameters (in this study, material attributes and process parameters will be generally referred to as process inputs). The fact that these input combinations are multidimensional implies that the DS should not be described in terms of proven acceptable ranges for each input[**]. Instead, how these ranges interact in a multidimensional space is the very matter of interest of the DS. Second, the input combinations belonging to the DS should be *demonstrated* to fulfill some requirements. "Demonstration" calls for the direct or indirect use of mathematical models to guide some form of experimental activity, or to interpret or correlate the results obtained from experiments. Models (either knowledge-driven or data-driven) are the battle-horse of process systems engineering, which can therefore play a tremendously important role in pharmaceutical product and process development (Gernaey *et al*., 2012 and Troup, and Georgakis 2013). Finally, ICH refers to *assurance* of quality. Peterson (2008) and Pantelides *et al.* (2009) noted that, as the DS of a product is calculated from a model and the model itself is subject to uncertainty, the DS calculation is *probabilistic.* Any model-based technique used to calculate the DS of a product can only determine the probability of a given combination of inputs to belong to the DS. Therefore, it should be stated what probability is deemed sufficient to provide "assurance" of quality.

How the DS should be determined (or "developed", following the ICH parlance) and how it should be described in a submission is not strictly stated or recommended by the FDA. Graphical

[**] Interestingly, the regulatory documents are not entirely clear in this respect. In fact, while they state that "A combination of proven acceptable ranges does not constitute a design space", they also state that in a submission "A design space can be described in terms of ranges of material attributes and process parameters" (ICH, 2009).

representations in the space of the inputs (such as response surface plots or contour plots) are reported as demonstrating examples, but "more complex mathematical relationships (…) such as components of a multivariate model" are accepted as well (ICH, 2009). It should be noted that representing the DS by means of diagrams in the true input space sets a strong limitation with respect to the multivariate nature of the DS. In fact, while a bivariate space can be easily captured by a diagram, a trivariate one would be much harder to interpret at a glance, whereas an input space of dimension larger than three would be impossible to represent graphically in the input space. How to calculate the DS have been discussed in some studies. For example, Peterson (2008) determined the DS using a multiple-response surface prediction model, and he discussed the DS reliability using a Bayesian approach to account for both the model parameter uncertainty and the correlation structure of the data. Pantelides *et al.* (2010) used a first-principles model to identify the probabilistic DS for a batch reactor with input uncertainty. Following the same ideas, Close *et al.* (2014) used a first-principles model coupled with stochastic simulations to generate probabilistic process design spaces for a chromatography process. Chatzizacharia and Hatziavramidis (2014) compared three different approaches (response surface, Bayesian, and artificial neural network) to determine the DS under different data characteristics (complete data with no uncertainty, data with high uncertainty, and missing data).

Knowledge-driven (i.e., first-principles) models can be extremely useful to describe the complex and nonlinear relationships between materials properties, process conditions and critical quality attributes that set the basis for the calculation of the DS. However, developing a reliable first-principles model can be very challenging in a pharmaceutical industry context. In many cases, the DS calculation exercise heavily relies on experimentation: a set of experiments is designed and carried out, and a response (hyper)surface model is then used to fit the experimental evidence (Troup, and Georgakis 2013; Chatzizacharia and Hatziavramidis, 2014). On some occasions, the input domain for the designed experiments may be the same used for a set of historical products that have already been developed and that are in some sense similar to the one under investigation. This domain corresponds to the so-called knowledge space (MacGregor and Bruwer, 2008; Jaeckle and Macgregor 1998) of the products already developed and is expected to include the design space of the new product.[††] Spanning by experiments the entire knowledge space may be very demanding, especially if the number of inputs is large. The experimental effort would be significantly reduced if one were able to find within which portion of the knowledge space the DS is likely to lie. In fact, in this case a set of experiments would be designed and carried out spanning the input combinations that belong to this subspace only. In this Chapter, a methodology

[††] However, it should be acknowledged that a set of input combinations may exist, which are very different from any combination used in the manufacturing of historical products, but which would anyway ensure the desired product quality. This set would therefore belong to the DS of the new product, but not to the knowledge space of the historical products. The data-driven approach discussed in this study cannot provide information on this subset of the DS (Jaeckle and Macgregor 1998)

is proposed that aims at segmenting the knowledge space in such a way as to define a subspace wherein the DS is likely to be included, thus providing the developer a way to target his/her experimental efforts within a much smaller domain of input combinations. This subspace will be called the experiment space. Therefore, the objective is to develop a methodology that can return an experiment space that is likely to bracket the design space, but is conveniently narrower than the knowledge space.

To achieve this goal, a data-driven modeling approach is employed. Data-driven models are usually much simpler to develop than knowledge-driven (first-principles) ones, but their development requires a fairly large amount of data. This may not be an issue in pharmaceutical development environments, where historical datasets on products already developed are often available. Latent-variable (LV) modeling techniques, such as principal component analysis (PCA Chapter 2, Section 2.1.1) and projection to latent structures (PLS, Chapter 2, Section 2.1.1), are multivariate statistical tools that can optimally exploit historical datasets. Although these techniques have long been used as process analytical technology tools only, their potential is much greater than that. In fact, they are particularly useful to assist the practical implementation of QbD paradigms, with several successful applications of interest for the pharmaceutical industry (Tomba *et al*., 2013a). One particularly useful LV modeling approach is LV model inversion (Jaeckle and Macgregor 1998; Jaeckle and Macgregor 2000). By inverting an LV model (say, a PLS model) one can determine the set of inputs (namely, materials properties and process conditions) that enable one to obtain an assigned output (namely, a product quality property). Hence, PLS model inversion is strongly related to the determination of the DS of a given product and could provide an indication of where the experiment space is located (Tomba *et al*., 2012). However, since models are subject to uncertainty (Faber and Kowalski, 1997; Zhang and García-Muñoz 2009), when a PLS model is inverted the uncertainty is backpropagated to the calculated inputs, hence to the designated experiment space. In this study, we use a latent variable approach based on PLS model inversion to locate the experiment space inside the knowledge space, under uncertainty in the PLS model predictions and under the assumption that the desired new product is characterized by one equality constraint specification. Note that the experiment space will be identified in the latent variable space, which may enable a clear graphical representation of the experiment space also when the number of process inputs is large. Within the context of this study, the model inversion problem will be referred to as a product development problem.

The proposed methodology is tested on three simulated case studies. A nonlinear one-equation model is first used to provide a clear representation of the true design space and its relationship with the null space. Then, two systems of greater complexity (large number of inputs) and specific interest for the pharmaceutical industry are investigated: a dry granulation process by roller compaction and a wet granulation process.

5.2 Mathematical background

5.2.1 PLS model inversion

Usually a PLS model is used in its direct form (Chapter 2, Section 2.1.2); namely, given a set of input data **X** [$I \times N$] of I observations (samples) and N variables (e.g., raw materials properties, process settings, operating conditions), the PLS model is used to predict an associated response variable **Y** [$I \times M$] of M responses (e.g., a product quality attribute) according the following model structure:

$$\mathbf{X} = \sum_{a=1}^{A} \mathbf{t}_a \mathbf{p}_a^{\mathrm{T}} + \sum_{a=A+1}^{R} \mathbf{t}_a \mathbf{p}_a^{\mathrm{T}} = \mathbf{T}\mathbf{P}^{\mathrm{T}} + \mathbf{E} \quad , \tag{5.1}$$

$$\mathbf{Y} = \sum_{a=1}^{A} \mathbf{t}_a \mathbf{p}_a^{\mathrm{T}} + \sum_{a=A+1}^{R} \mathbf{t}_a \mathbf{p}_a^{\mathrm{T}} = \mathbf{T}\mathbf{Q}^{\mathrm{T}} + \mathbf{F} \quad , \tag{5.2}$$

$$\mathbf{T} = \frac{\mathbf{X}\mathbf{W}}{\mathbf{P}^{\mathrm{T}}\mathbf{W}} \quad . \tag{5.3}$$

Where the meaning of the symbol is the same of Eqs. (2.10-14) of Chapter 2. When the i-th observation $\mathbf{x}_i$ [$1 \times V$] of **X** is projected onto the model, its score vector is:

$$\mathbf{t}_i = \frac{\mathbf{x}_i \mathbf{W}}{\mathbf{P}^{\mathrm{T}}\mathbf{W}} \quad . \tag{5.4}$$

Its prediction and the associated model residual are:

$$\hat{\mathbf{x}}_i = \mathbf{t}_i \mathbf{P}^{\mathrm{T}} \quad , \tag{5.5}$$

$$\mathbf{e}_i = \mathbf{u}_i - \hat{\mathbf{u}}_i \quad . \tag{5.6}$$

Two indices are used to assess the model performance when this observation is projected: the Hotelling T_i^2 statistic (Eq. 2.15) and and the residual SPE_i statistic (Eq. 2.16). Under the assumption of multinormally distributed observations, whether or not $\mathbf{u}_i$ conforms to the observations of the calibration dataset can be assessed by comparing T_i^2 and SPE_i to the respective confidence limits $T_{\lim}^2$ (Eq. 2.18) and $\mathrm{SPE}_{\lim}$ (Eq. 2.20). In this study, 95% confidence limits for the T2 and SPE statistics are always used. Confidence limits can be also considered in the latent space of the scores in the shape of an ellipsoid whose semi-axis of the a-th LV can be calculated as in Eq. (2.18).

In this study, univariate responses (M=1) only are considered. Hence, matrix **Y** degenerates to a vector **y** of dimension [$N \times 1$], **Q** degenerates to **q** [$1 \times A$], and **F** to **f** [$N \times 1$].

In its inverse form (Chapter 2, Section 2.1.3) , the model can be used to suggest the combination $\mathbf{x}_{NEW}$ of inputs that are needed to obtain a product of desired quality y_{DES} , provided that the desired quality is (in some sense) similar to the quality of the products included in the historical dataset (Jaeckle and MacGregor 1998; Jaeckle and MacGregor 2000b). The similarity can be assessed by testing that y_{DES} conforms to the correlation/covariance structure available in the historical database that identifies the knowledge space (Jaeckle and MacGregor 2000a) and lies within the region of variability spanned by the knowledge space (Jaeckle and MacGregor 2000b). In this study, the analysis is limited to products characterized by a single quality attribute (i.e., $\text{rank}(\mathbf{y}) = 1$) assigned through an equality constraint (i.e., $y = y_{DES}$ is the required quality specification; extension to the case of inequality constraints is straightforward). As explained in Chapter 2 (Section 2.1.3) assumed as $R_{\mathbf{X}}$ the rank of the input matrix **X**, two cases can be outlined: the dimension of the latent space of **X** is the same as the dimension of **y** (i.e., $R_{\mathbf{X}}=1$) or the dimension of the latent space of **X** is greater than the one of **y** (i.e., $R_{\mathbf{X}}>1$; this is the most frequent occurrence). In the first case, a unique solution $\mathbf{x}_{NEW}$ to the model inversion problem (Eq. 2.28) exists $\mathbf{x}_{NEW} = \mathbf{t}_{NEW}\mathbf{P}^T$, and from Eq. (5.5-6) $\mathbf{x}_{NEW} = \hat{\mathbf{x}}_{NEW}$ and $\mathbf{e}_{NEW} = 0$. In the second case, the inversion problem is underdetermined and multiple solutions exist, that give rise to the null space of dimension ($R_{\mathbf{X}}$ - 1), which can be calculated analytically (Jaeckle and MacGregor 2000b) as reported in Section 2.1.3.1. All the problems considered in this study are characterized by the existence of a null space. A graphical interpretation of a one-dimensional null space is shown in Figure 5.1, where the score space for the first two latent variables is reported. The circles represent the historical data, and the dashed ellipse is the 95% confidence limit obtained from Eq. (2.18). The projection $\mathbf{t}_{NEW}$ of the direct model inversion solution is represented by the triangle. The null space projection onto the score diagram is a straight line passing through $\mathbf{t}_{NEW}$: if the model is not affected by uncertainty, all input combinations projecting onto this line are expected to yield a product with the same quality y_{DES} .

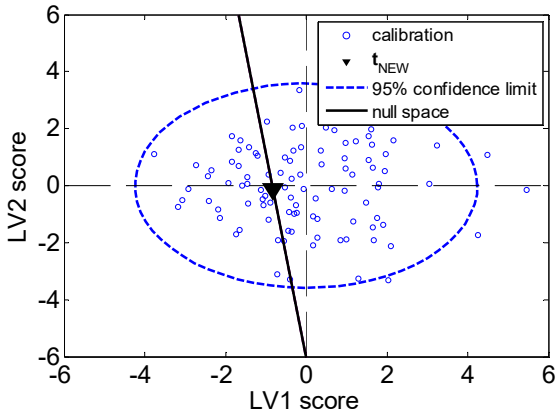

Figure 5.1. *Graphical interpretation of the null space in the score space of the first two latent variables of a PLS model. The example model has V = 5 input variables and N = 100 observations.*

The latent space spanned by the input combination projections that yield the products already manufactured is the knowledge space. It is assumed that a likely projection of the knowledge space onto the space of the first two LVs is the interior of the confidence ellipse shown in Figure 5.1. The input combinations that lie on the null space line, but do not belong to the knowledge space, are not represented appropriately by the model. In the following, the words null space will be referred to the subspace of it that is included within the knowledge space (in Figure 5.1, the segment included within the ellipse).

Tomba *et al.* (2012) observed that there is a strong relation between the mathematical concept of null space and the FDA concept of DS. If the product quality is characterized by equality constraints only and no uncertainty affects the PLS model, from a practical standpoint the two concepts are the same. However, if the PLS model is affected by uncertainty, when the model is inverted the uncertainty is backpropagated to the calculated inputs, i.e. to the calculated null space. Hence, the existence of uncertainty should be accounted for in the determination of the experiment space.

5.2.2 Prediction uncertainty in PLS models

Consider a new observation $\mathbf{x}_{obs}$. Its regression through a PLS model generates the predicted output $\hat{y}_{obs}$, which suffers from a mismatch with respect to the actual value y_{obs} that would be obtained by application of the input combination $\mathbf{x}_{obs}$ to the real process. This mismatch is due to the uncertainty that lie in the model. The main sources of uncertainty are the uncertainty on the parameters in the model calibration (Martens and Martens, 2000), on the calibration data (Reis and Saraiva, 2005), and on the predictions (Fernández Pierna *et al*., 2003; Bu *et al*., 2013). In this study, only the prediction uncertainty is considered, although alternative methods exist (Faber, 2002; Reis and Saraiva 2012, Vanlaer *et al*., 2013).

To characterize the prediction uncertainty on $\hat{y}_{obs}$, the approach proposed by Faber and Kowalski (1997) is followed, who accounted for the errors in the inputs, the errors in the responses, and the bias in the calculation of the mean-squared prediction error. The same approach was lately drawn on by Zhang and García-Muñoz (2009).

First, an estimation of the standard deviation s of the prediction error is calculated. Then, assuming that the estimation error follows a t-statistic, the $100(1-\delta)\%$ confidence interval (CI) on $\hat{y}_{obs}$ is calculated as:

$$\mathrm{CI} = \hat{y}_{obs} \pm \mathrm{t}_{\delta/2,I-d}\, s \quad , \tag{5.7}$$

where I is the number of the PLS model calibration samples, d is the number of degrees of freedom used by the model, and δ is the significance level for the confidence interval. The wider the CI at

a given significance level, the larger the prediction uncertainty. In this study, we refer to a 95 % CI. The standard deviation s can be estimated as (Faber and Kowalski, 1997):

$$s = \mathrm{SE}\sqrt{1 + h_{obs} + \frac{1}{I}} \quad , \tag{5.8}$$

where h_{obs} is the leverage of the observation:

$$h_{obs} = \frac{\mathbf{t}_{obs}\Lambda^{-1}\mathbf{t}_{obs}^{\mathrm{T}}}{I-1} \quad , \tag{5.9}$$

SE is the standard error of calibration, which is evaluated as in Zhang and García-Muñoz (2009):

$$\mathrm{SE} = \sqrt{\frac{\sum_{i=1}^{I}\left(y_i - \hat{y}_i\right)^2}{I-d}} \quad , \tag{5.10}$$

and y_i and $\hat{y}_i$ are (respectively) the i-th measured output and the i-th estimated output of the model calibration dataset. In this study, the number of degrees of freedom is set equal to the number of latent variables of the PLS model, i.e. $d = A$ (Krämer and Sugiyama, 2011). Other degrees of freedom selection methods were tested (Van der Voet, 1999; Ye, 1998), with no major changes in the results.

5.3 Bracketing the design space

Assume that historical datasets **X** and **y** are available, where **X** includes the input combinations that have been used to manufacture products with quality characteristic **y**. It is required to estimate the set $\mathbf{x}_{\mathrm{REAL}}$ of process inputs leading to a new product of quality y_{DES} not included in **y**. Several different input combinations $\mathbf{x}_{\mathrm{REAL}}$ may yield this product and, according to the ICH definition and to the univariate equality constraint $y = y_{DES}$, the set $\overline{\mathbf{X}}_{\mathrm{REAL}}$ including all of these combinations is the DS of product y_{DES}. We indicate with $\mathbf{X}_{\mathrm{REAL}}$ the subset of $\overline{\mathbf{X}}_{\mathrm{REAL}}$ whose projections fall within the knowledge space and therefore that can in principle be described by the PLS model relating **X** to **y**. We would like to estimate $\mathbf{X}_{\mathrm{REAL}}$ by inverting the model. The model estimate of a true input combination $\mathbf{x}_{\mathrm{REAL}} \in \mathbf{X}_{\mathrm{REAL}}$ is $\mathbf{x}_{\mathrm{NEW}}$.

If the model is not affected by uncertainty, the direct model inversion solution projects onto a score vector $\mathbf{t}_{\mathrm{NEW}}$ that can move along the null space without affecting the product quality. Stated differently, according to the PLS model there is an infinite number of input combinations $\mathbf{x}_{\mathrm{NEW}}$ that can lead to a product with the same desired quality, and their projections all lie in the null

space. Hence, according to the PLS model, the DS of product y_{DES} would be identified with the null space. However, if the PLS model is affected by prediction uncertainty, y_{DES} is predicted with uncertainty; when the model is inverted, the prediction uncertainty is backpropagated to the calculated inputs and therefore the null space calculation itself is affected by prediction uncertainty. Hence, when prediction uncertainty is present, the DS is not necessarily the null space.

From a practical point of view, the DS could be determined by carrying out a set of experiments designed within the knowledge space, and then correlating the experimental results with (say) a response surface model. However, determining the DS by experimentation within the entire knowledge space would be impractical due to the number of experiments that may be needed to account for the variability in all accessible inputs. The experimental effort could be significantly reduced if the experimental domain were restricted to a subspace of the knowledge space within which the DS is likely to lie. We call this subspace the experiment space, and in the following we describe a methodology that is able to return an experiment space that is likely to bracket the design space, but is conveniently narrower than the knowledge space.

5.3.1 Proposed knowledge space segmentation methodology

The knowledge space segmentation is carried out through the following steps.

- Step 1. A PLS model relating **X** to **y** trough A latent variables is built using Eqs. (5.1) - (5.3). Figure 5.1 provides a graphical representation of this model in the space of the first two latent variables.
- Step 2. Using Eqs. (2.28), the PLS model is inverted to determine the input variable combination $\mathbf{x}_{NEW}$ (from Eq. 5.5) that is expected to yield a product having the desired quality y_{DES} under no prediction uncertainty. The solution of the inversion problem is obtained in terms of the score vector $\mathbf{t}_{NEW}$ (triangle in Figure 5.1).
- Step 3. The prediction uncertainty on y_{DES} is evaluated as in Eqs. (5.7-5.10) at significance level $\delta = 0.05$, corresponding to $\Delta = 100(1-\delta) = 95\%$ confidence. Figure 5.2*a* shows the probability density function of the t distribution centered on y_{DES} with $(I - A)$ degrees of freedom. The 95% CI for y_{DES} is highlighted.
- Step 4. The PLS model is inverted by direct inversion to project the y values belonging to the 95% CI onto the latent space of the inputs. For convenience, the CI is discretized in a subset whose scores $\mathbf{T}_{NEW}$ are represented with magenta circles in Figure 5.2b.
- Step 5. The null spaces associated to each score vector belonging to $\mathbf{T}_{NEW}$ are calculated (magenta lines in Figure 5.2c). The DS is expected to lie within the intersection between these null spaces and the knowledge space (gray-shaded area in Figure 5.2d). This segmented region of the knowledge space is therefore the designated experiment space. Note that the wider the experiment space at a given confidence level, the wider the input

space that needs to be explored to correctly locate the DS by experimentation. Additionally note that, as also advocated by the regulatory agencies (ICH, 2009), the experiment space is designated in the latent variable space and not in the true input space, which is very convenient when a large number of (correlated) process inputs need to be accounted for.

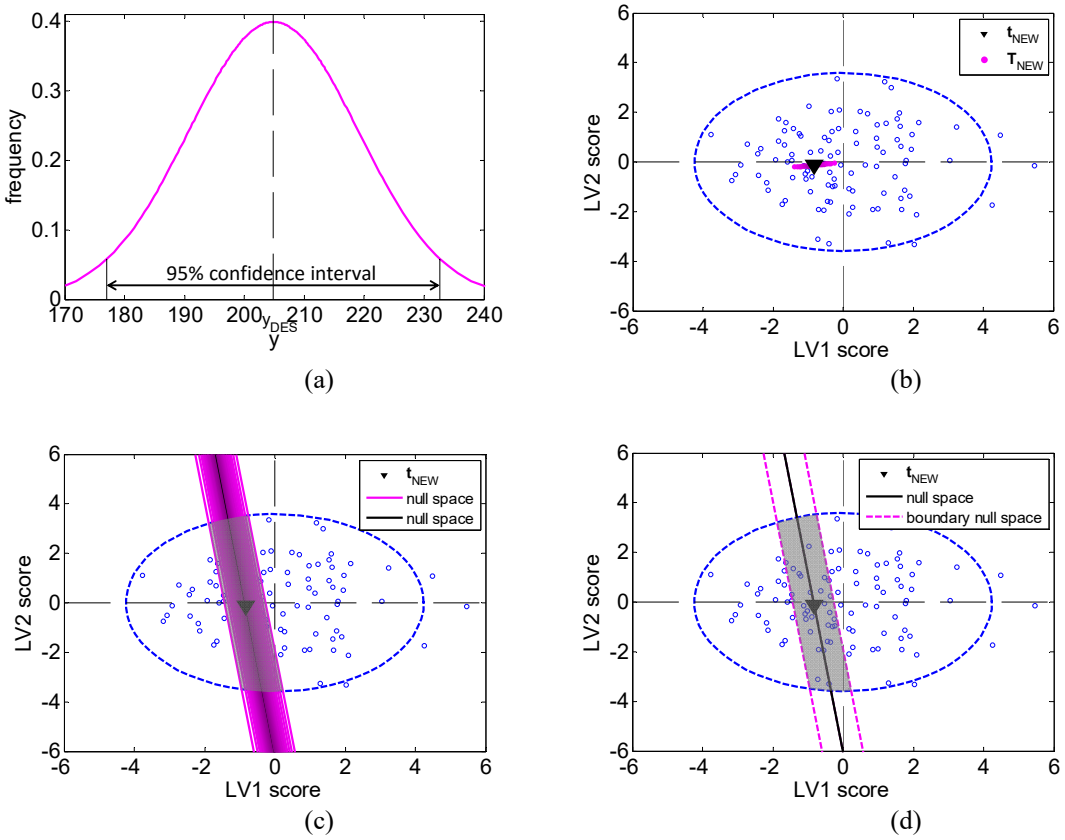

Figure 5.2. *Experiment space determination by segmentation of the knowledge space. (a) Determination of the model prediction uncertainty; (b) projection of the prediction uncertainty onto the knowledge space; (c) calculation of the null spaces for the outputs belonging to the prediction confidence interval; (d) designation of the experiment space (grey-shaded area).*

5.4 Case studies

5.4.1 Case study 1: mathematical example

A nonlinear mathematical model is used as a first illustrative case study. The calibration input dataset $\mathbf{X} = [\mathbf{x}_1, \mathbf{x}_2, \mathbf{x}_3, \mathbf{x}_4, \mathbf{x}_5]$ of dimension [1000×5] is made of 1000 calibration (i.e., "historical") observations on 5 variables. Matrix $\mathbf{X}$ collects both the independent inputs and the dependent

inputs. The independent inputs $\mathbf{x}_1$ and $\mathbf{x}_2$ are random Gaussian distributions. For any observation n, the dependent inputs $x_{n,3}$, $x_{n,4}$ and $x_{n,5}$ are defined as:

$$\begin{aligned} x_{n,3} &= x_{n,1}^2 \\ x_{n,4} &= x_{n,2}^2 \\ x_{n,5} &= x_{n,1} x_{n,2} \end{aligned} \tag{5.11}$$

The calibration response dataset $\mathbf{y}$ [1000×1] is built on the following model:

$$\mathbf{y} = k_0 + k_1\mathbf{x}_1 + k_2\mathbf{x}_2 + k_3\mathbf{x}_3 + k_4\mathbf{x}_4 + k_5\mathbf{x}_5 \quad , \tag{5.12}$$

where: $[k_0; k_1; k_2; k_3; k_4; k_5; k_6] = [-21.0; 4.3; 0.022; -0.0064; 1.1; -0.12]$.

Table 5.1 reports the calculated means and standard deviations for the $\mathbf{x}$'s and for $\mathbf{y}$ included in the historical datasets.

Table 5.1. *Case study 1: characterization of the input and output calibration datasets.*

Variable	Mean	Std. dev.
$\mathbf{x}_1$	41.73	16.07
$\mathbf{x}_2$	11.13	2.97
$\mathbf{x}_3$	1999.15	1408.07
$\mathbf{x}_4$	132.63	66.93
$\mathbf{x}_5$	464.85	227.38
$\mathbf{y}$	235.99	71.35

To assess the effectiveness of the knowledge space segmentation methodology, validation datasets $\mathbf{X}^*$ and $\mathbf{y}^*$ are used, with $\mathbf{X}^*$ [1000×5] and $\mathbf{y}^*$ [1000×1].

5.4.2 Case study 2: dry granulation by roller compaction

The second case study concerns a simulated granulation process of microcrystalline cellulose by roller compaction. "Historical" data from the roller compactor are obtained by simulating the process with the model proposed by Johanson (1965) under the gSOLIDS® modeling environment (Process Systems Enterprise Ltd, London, UK, 2013). The model predicts the intra-void fraction of the solids out of the roller compactor (which is the product quality property y) by accounting for the agglomeration between particles obtained from the mechanical pressure of two counter-rotating rolls. Details on the roller compactor model can be found in the original reference (Johanson, 1965).

The calibration and validation input matrices are $\mathbf{X}$ [90×8] and $\mathbf{X}^*$ [22×8], respectively. The inputs include raw materials properties (compressibility factor, friction angle between solid granulate

and roller compactor, effective angle of friction, and springback factor) as well as some characteristics and settings of the roller compactor (roller diameter, roller width, roller speed and pressure force). A summary of the input variables characteristics is reported in Table 5.2. Note that eight process inputs are considered, and they take discrete values.
The product quality data are collected in vectors $\mathbf{y}$ [90×1] and $\mathbf{y}^*$ [22×1], respectively for the calibration and the validation datasets.

Table 5.2. *Case study 2: list of the input variables considered in the roller compactor model (columns 1-4), and characterization of the input calibration dataset (columns 5-6).*

Input variable	ID	Symbol	Measurement unit	Mean	St. dev.
compressibility factor	1	K	[-]	9.85	2.53
roller diameter	2	D	[m]	0.40	0.07
roller width	3	W	[m]	0.13	0.02
roller speed	4	v_{roll}	[rpm]	10.24	6.43
pressure force	5	F_{roll}	[kN]	13866.67	6951.19
friction angle between solid granulate and roller compactor	6	γ_{FR}	[rad]	27.51	8.78
effective friction angle	7	γ_{EFF}	[rad]	48.17	31.76
springback factor	8	F_{sb}	[-]	0.11	0.03

The historical data refer to 5 different lots of microcrystalline cellulose (Table 5.3). The raw materials properties are generated in such a way as to guarantee a meaningful physical behavior, namely positive correlation between the friction angle γ_{FR} and the effective friction angle γ_{EFF}, and negative correlation between the compressibility factor K and the springback factor F_{sb}. For each processed lot, the variability of the raw materials properties is accounted for by adding white noise with standard deviation σ_m to the average property value (Table 5.3).

Table 5.3. *Case study 2: properties of the historical raw materials lots processed in the roller compactors.*

Lot no.	K [-]	γ_{FR} [rad]	γ_{EFF} [rad]	F_{sb} [-]	σ_m
1	8.0	20.0	32.0	0.1250	0.4
2	9.0	30.0	48.0	0.1111	0.6
3	10.0	25.0	40.0	0.1000	0.7
4	14.0	40.0	64.0	0.0714	0.5
5	6.0	20.0	32.0	0.1667	0.4

Table 5.4. *Case study 2: characteristics of the roller compactors settings.*

	Roller compactor 1	**Roller compactor 2**
***W* [m]**	0.12	0.15
***D* [m]**	0.3; 0.4	0.4; 0.5
Processed materials [-]	1; 2; 3; 4	2; 3; 4; 5
v_{roll} **[rpm]**	2.0; 6.5; 15.5; 10.0; 20.0	2.0; 6.5; 15.5; 13.0; 20.0
$F_{roll} \cdot 10^{-3}$ **[kN]**	4.0; 9.0; 14.0; 17.0; 24.0	4.0; 9.0; 14.0; 20.0; 24.0

The simulations are carried out assuming that different roller compactors manufactured the historical products, where the compactors differ by their roller width *W* (two widths are admissible) and roller diameter *D* (two diameters are admissible for each roller width). As detailed in Table 5.4 not all the materials can be processed by each roller compactor and not all settings are admissible.

5.4.3 Case study 3: wet granulation

This case study considers the design of a powder product to be manufactured by a high-shear wet granulation process. Real experimental data are available from the work of Vemavarapu *et al.*(2009); details on the process are reported in the original reference.

The historical dataset includes 25 observations of 7 input material properties and of one response variable (the percent of oversize granules, i.e. the fraction of granules of dimension larger than 1.4 mm). The input variables identify the properties of the inlet pre-blend, namely solubility data (variables 1, 2 and 3), morphological characteristics of the particle size distribution (variables 4 and 5), and porosity characteristics (variables 6 and 7). A summary of the characteristics of the seven process inputs is reported in Table 5.5.

Table 5.5. *Case study 3: list of the input variables considered in the wet granulator process (columns 1-3), and characterization of the input calibration dataset (columns 4-5).*

Input variable	**ID**	**Measurement unit**	**Mean**	**Std. dev.**
H_2O solubility	1	[mg/mL]	38.97	73.30
contact angle	2	[rad]	93.64	36.26
H_2O holding capacity	3	[wt %]	5.69	8.58
Sauter mean diameter	4	[μm]	68.48	127.77
distribution span	5	[-]	14.17	11.68
surface area	6	[m^2/g]	1.20	1.54
pore volume	7	[cm^3/g]	0.0037	0.0056

5.5 Results and discussion for Case study 1

5.5.1 Development of a new product

A PLS model is first built using the calibration datasets. The number of LVs to be retained in the model is determined by the scree test (§ 2.1.1.2) in such a way as to explain a sufficiently large fraction of the variance not only of the product quality (to have good predictive power), but also of the input variables (to obtain good predictive ability also in model inversion, Jaeckle and MacGregor 2000b). Namely, using $A = 2$ LVs the model explains 96.1% of the variance of **y** (94.8% with the first LV), and 98.3% of the variance of **X** (58.5% with the first LV). Note that, since $A > \text{rank}(\mathbf{y})$, a null space exists.

The problem of developing a product with $y_{DES} = 285.23$ (not included in the historical dataset) is addressed. The true DS $\overline{\mathbf{X}}_{REAL}$ for this product is calculated from the first-principles model assuming this model is a perfect representation of the true process. $\overline{\mathbf{X}}_{REAL}$ is then projected onto the PLS model space, resulting in the green line of Figure 5.3a; in the following, it will be referred to this projection as to the true design space (TDS). Some issues deserve attention. Firstly, note that since the actual process is nonlinear, the TDS is a curve. On the other hand, since PLS is a linear modeling technique, it may have limited representativeness when the process variables are related in a strongly nonlinear way. Secondly, some of the input combinations belonging to the TDS may be projected beyond the T^2_{lim} limit or the SPE_{lim} limit of the model (e.g., in Figure 5.3a the TDS projections exceeding T^2_{lim} lie outside the confidence ellipse). These input combinations cannot be represented by PLS model inversion, regardless of the fact that the system is nonlinear or not. Finally, note that some of the input combinations projecting onto the TDS may not be achievable in practice, because of physical or operational constraints acting on the process.

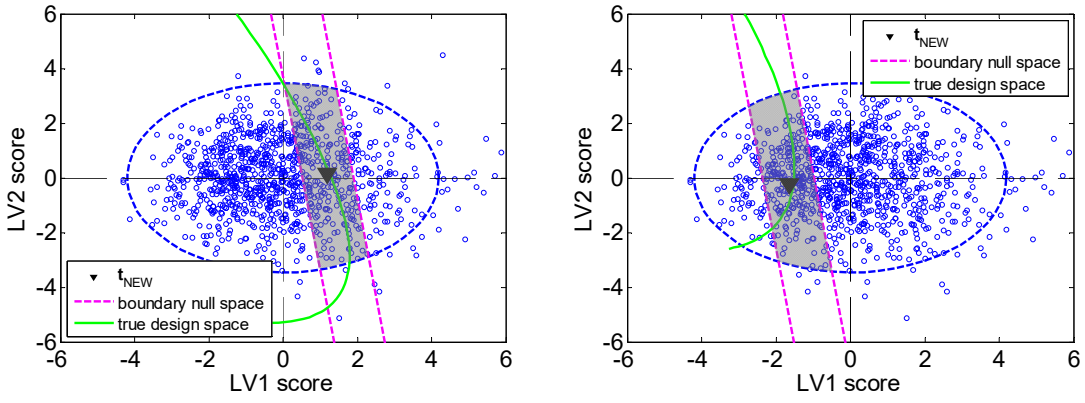

Figure 5.3. *Case study 1: designated experiment space (grey-shaded area) and projection of the true design space onto the PLS model space for the development of a product with (a) yDES = 285.23, and (b) yDES = 168.23.*

The set $\mathbf{x}_{NEW}$ of input variables that is expected to yield the desired new product is calculated by PLS model direct inversion, assuming no model prediction uncertainty, obtaining $\mathbf{x}_{NEW} = [47.56; 12.92; 2505.41; 173.33; 609.96]$. The related scores $\mathbf{t}_{NEW}$ are plotted in the model score space (triangle in Figure 5.3a). After accounting for the prediction uncertainty of the PLS model, the knowledge space is segmented and the experiment space highlighted by the grey-shaded area of Figure 5.3a is determined. It can be seen that the designated experiment space is a narrow region of the knowledge space that effectively brackets large part of the TDS; namely, the experiment space brackets the entire fraction of the TDS that lies within the knowledge space. The experiments needed to experimentally determine the design space would therefore be carried out using input combinations that project within the experiment space (not within the entire knowledge space), thus significantly reducing the required experimental effort.

Figure 5.3b shows the designated experiment space for the development of a product with $y_{DES} = 168.23$, for which $\mathbf{x}_{NEW}$ = [33.70; 8.65; 1302.50; 76.63; 265.17] is calculated. The knowledge space segmentation if effective, as only a small fraction of the TDS included within the confidence ellipse lies outside the designated experiment space, and the experiment space is a very small fraction of the entire knowledge space.

5.5.2 Effect of the dimension of the calibration dataset on the experiment space

At assigned confidence (say, 95%), the PLS model prediction uncertainty depends on the model calibration dataset, namely of the number and "quality" of the observations upon which the model is built (i.e., on the amount of variability the calibration data are able to capture). Therefore, it is interesting to study how the effectiveness of the proposed segmentation methodology changes with the number of observations that are available to build the PLS model. As an example, we consider the development of a product with $y_{DES} = 204.86$.

First, a graphical analysis is considered for three historical datasets, each comprising a different number I of samples ($I = 10$, $I = 100$ and $I = 1000$). Obviously, three different PLS models can be built from these datasets, and the designated experiment space is different in each case. Note that although the actual DS of the product does not depend on the dimension of the historical dataset, its projection onto the model latent space does, because this projection does depend on the PLS model. Figure 5.4 qualitatively shows that increasing the dimension of the historical dataset improves the knowledge space segmentation effectiveness, as a larger portion of the TDS is bracketed by the designated experiment space.

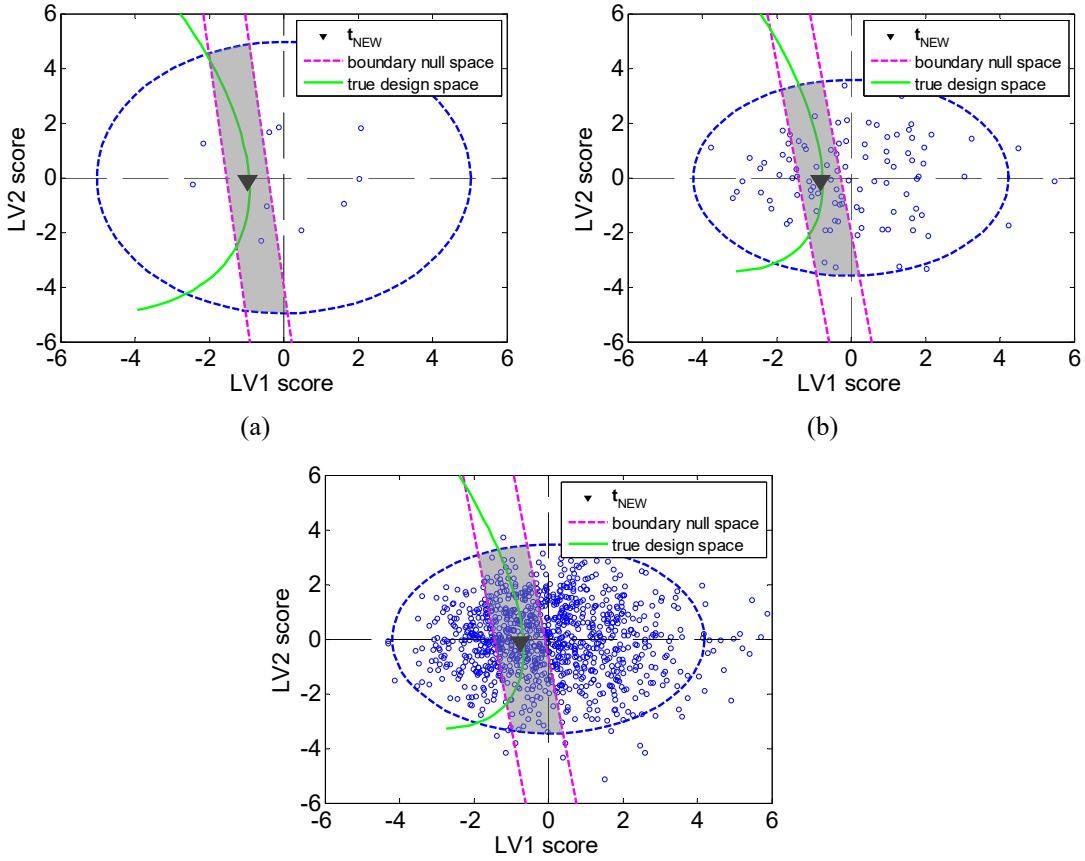

Figure 5.4. *Case study 1, y_{DES} = 204.86: designated experiment space (grey-shaded area) and projection of the true design space onto the PLS model space for historical datasets with (a) I = 10, (b) I = 100, and (c) I = 1000 samples.*

This qualitative evaluation requires knowing the DS in advance, which is obviously not possible in a real application. A quantitative evaluation, that does not require prior knowledge of the DS, can be carried out as follows.

One randomly-selected sample is removed from the historical dataset ($\mathbf{X}$; $\mathbf{y}$), and the PLS model is built without using this sample. Then, the validation dataset ($\mathbf{X}^*$; $\mathbf{y}^*$) is considered, and the experiment space is determined for all products included in the dataset. Consider a sample belonging to this dataset; the sample is characterized by a set $\mathbf{x}^*_{REAL}$ of inputs and a related product quality value y^*_{DES}. The projection $\mathbf{t}^*_{REAL}$ of $\mathbf{x}^*_{REAL}$ onto the PLS model space is obtained from Eq. (5.4) written in the form:

$$\mathbf{t}^*_{REAL} = \frac{\mathbf{x}^*_{REAL}\mathbf{W}}{\mathbf{P}^T\mathbf{W}} \quad . \tag{5.13}$$

For the experiment space designation to be effective, it is expected that (at least) $\mathbf{t}^*_{\text{REAL}}$ lies within with the designated experiment space for product y^*_{DES}. It is assumed that a wrong experiment space designation has been obtained for a given product when at least one of the following conditions is met: *i*) $T^{*2}_{\text{REAL}} < T^2_{\text{lim}}$, but $\mathbf{t}^*_{\text{REAL}}$ is outside the experiment space; *ii*) $T^{*2}_{\text{REAL}} > T^2_{\text{lim}}$; *iii*) $\text{SPE}^*_{\text{REAL}} > \text{SPE}_{\text{lim}}$. Note that this approach is somewhat conservative, as conditions *ii* and *iii* are related to inadequacy of the PLS model, rather than to ineffectiveness of the knowledge space segmentation methodology. The operation is repeated for each sample of the validation dataset. The fraction of validation samples, for which a wrong experiment space designation is obtained, represents the frequency of wrong experiment space designation for a PLS model with $(I-1)$ samples.

Then, a new iteration is carried out by removing two (instead of one) randomly-selected samples from the historical dataset, and repeating the whole calculation.

By removing one additional sample at each iteration, the results illustrated in Figure 5.5 are obtained (all PLS models related to the figure are built on 2 LVs). It can be seen that when the model is built upon only very few calibration samples, the segmentation result is ineffective. For example, if only 5 calibration samples are used, for ~86 % of the products to be designed the proposed methodology is unable to correctly designate the experiment space. However, using 15 calibration samples is enough to reduce to ~9 % the percentage of wrong experiment space designation, and this percentage does not substantially change even when a very large calibration dataset is used. In a way, this measure provides the intrinsic capability of the available historical dataset to serve as an effective source of information to bracket the design space of a new product.

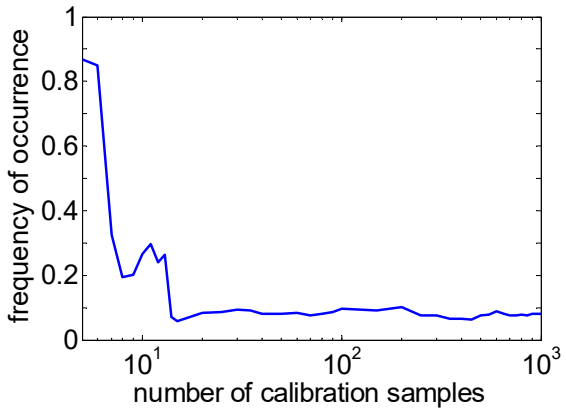

Figure 5.5. *Case study 1: effect of the number of model calibration samples on the frequency of occurrence of wrong experiment space designation.*

Note that, generally speaking, the fewer the calibration samples, the more the results depend on the quality of the calibration dataset. This means that, when too few samples are available to calibrate the PLS model, the experiment space identified by the proposed methodology is expected to be strongly dependent on each single calibration sample. To investigate this issue, we

consider the problem of developing a product with $y_{DES} = 204.86$, and two different calibration datasets: one with $I = 5$ samples and one with $I = 20$ samples (in both cases, the samples are randomly selected from the entire historical dataset). A jackknife modeling technique is used (Efron *et al*, 1983) to build one PLS model (with 2 LVs) for each of the *N* possible combinations of $I - 1$ calibration samples, leaving out one of the original calibration samples at each iteration. For comparison, the results from a model built on the entire set of *I* calibration samples are also considered.

Figure 5.6a refers to the case with $I = 5$ available calibration samples, and shows that the projection of $\mathbf{x}_{NEW}$ onto the score space (i.e., $\mathbf{t}_{NEW}$) changes significantly with the calibration dataset. If all *I* samples are used to calibrate the model, $\mathbf{x}_{NEW}$ projects onto the black triangle; however, when $I - 1$ samples are used for calibration, *I* significantly different $\mathbf{x}_{NEW}$ values are obtained, each one projecting onto different score points (open triangles).

Figure 5.6a also shows the null spaces associated to each $\mathbf{t}_{NEW}$. It is apparent that the null spaces are significantly different, implying that also the experiment spaces that can be designated are very different. Stated differently, the fact that the calibration dataset is deficient implies that the model prediction results are largely uncertain, and this in turn implies that there is a large uncertainty in the designation of the experiment space.

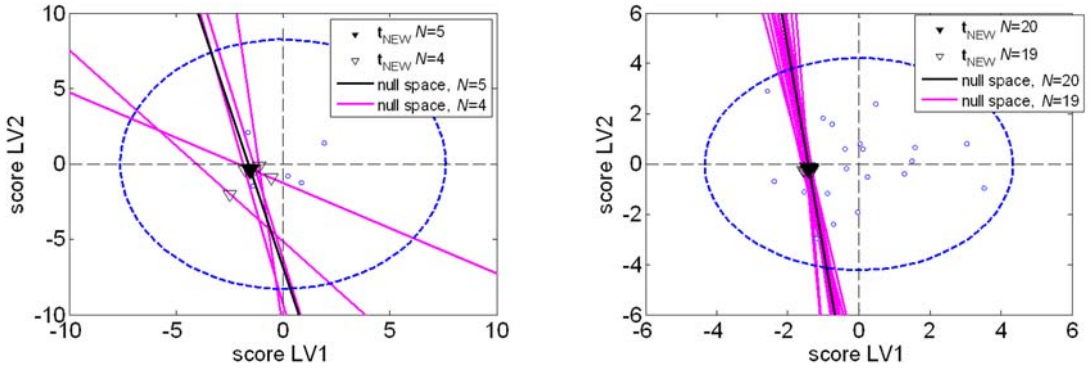

(*a*) (b)

Figure 5.6. *Case study 1, y_{DES} = 204.86: effect of the dimension of the model calibration dataset on the designation of the experiment space: (a) jackknifing with I = 5 calibration samples; (a) jackknifing with I = 20 calibration samples.*

Figure 5.6b refers instead to the calibration dataset with $I = 20$. Clearly, the $I + 1$ solutions obtained by model inversion all project very close to each other onto the score space, indicating that the model inversion results do not strongly depend on the single calibration sample. The null spaces almost overlap, implying that the experiment space designation is almost insensitive to the calibration set.

5.6 Results and discussion for Case study 2

First, the effect of the dimension of the calibration dataset on the effectiveness of the experiment space designation is studied for a PLS model with 2 LVs. The results reported in Figure 5.7 (which refer to the entire validation dataset of 22 samples) are obtained. Similar general considerations as in Case study 1 can be drawn: when the model is built on few calibration samples only, the experiment space designation is ineffective. The uncertainty in the experiment space designation decreases as more calibration samples become available. For this roller compaction process, about 30 calibration samples are needed to reduce to less than 20 % the fraction of incorrect experiment space designations; using more than 40 calibration samples reduces to ~10 % the designation errors.

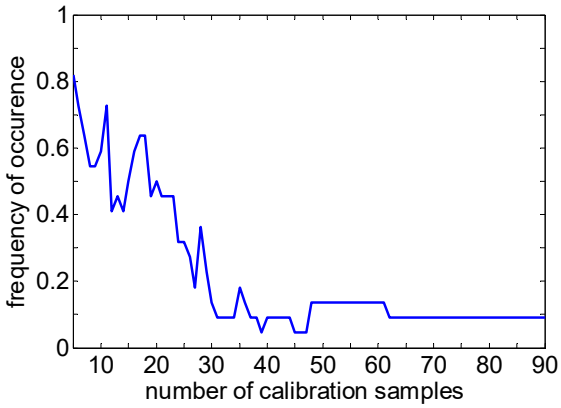

Figure 5.7. *Case study 2: effect of the number of model calibration samples on the occurrence of wrong experiment space designation.*

The design of a process for the manufacturing a granulate with intra-void fraction of the solids out of the roller compactor $y_{DES} = 0.6341$ m^3/m^3 is now considered. We assume that 40 randomly chosen samples are available to calibrate the model. For this Case study with a large number of inputs, it is impractical to determine the TDS, as several inputs take discrete (rather than continuous) values. For these reasons, the true inputs combinations that lead to the desired product (i.e., the input combinations belonging to the DS) are found by trial-and-error. However, because of the complexity of the problem, it is not possible to guarantee that all the input combinations that can lead to y_{DES} are found, the results obtained appear consistent with the knowledge that is available from the historical database.

After building a PLS model with 2 LVs, application of the proposed methodology provides the results of Figure 5.8 The knowledge space segmentation is effective: the designated experiment space is a small fraction of the knowledge space and includes the TDS projections onto the score space (green circles). The fact that these projections are clustered in a relatively narrow region of the knowledge space reflects the fact that a product with the desired quality can be obtained by processing only some of the available input materials with only some of the potential roller

compactor settings. Note that, notwithstanding the fact that the system is subject to a large number of inputs, a clear graphical representation of the multivariate experiment space is obtained.

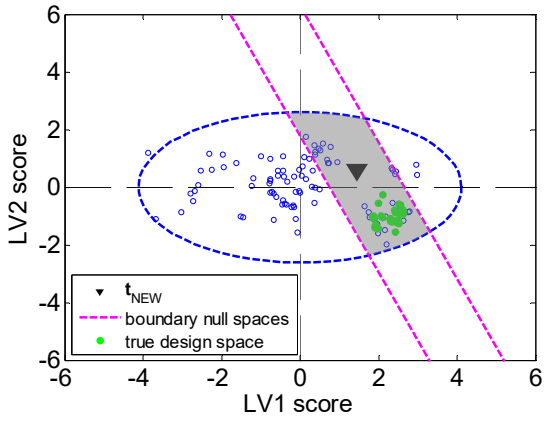

Figure 5.8. *Case study 2: designated experiment space (grey-shaded area) and projection of the true design space onto the PLS model space for the development of a product with y_{DES} = 0.6341 m^3/m^3 (40 samples are used to calibrate the model).*

5.7 Results and discussion for Case study 3

As discussed in Section 4.3, real experimental data are available for this wet granulation process. Hence, the situation closely resembles a real one, where the TDS cannot be calculated in advance. Furthermore, the available historical dataset comprises only 25 experimental samples. To attenuate the data scarceness problem, a Monte Carlo approach is followed. Namely, 100 iterations are carried out in which the available observations are split into a calibration dataset of $I = 20$ observations (randomly selected at each iteration from the entire historical dataset), whereas the remaining 5 observations are used to validate the knowledge space segmentation results. The results presented are averaged throughout all the iterations of the Monte Carlo procedure. Figure 5.9 shows that as few as 13 calibration samples are enough for this wet granulation process to reduce the occurrence of wrong experiment space designation to a negligible value.

Given the results of Figure 5.9, fifteen randomly selected samples are used to calibrate the PLS model that relates the input material properties to the percentage of oversize granules. Figure 5.10, which refers to the development of a granulate product characterized by $y_{DES} = 20$ % oversize granules, shows a typical knowledge space segmentation result. It is apparent that the proposed methodology does a good job in bracketing within the experiment space at least the projection $\mathbf{t}_{REAL}$ of the true input combination. The fact that $\mathbf{t}_{REAL}$ is close to the null space related to $\mathbf{t}_{NEW}$ provides indirect indication that the model predictions are not subject to a large uncertainty for this problem.

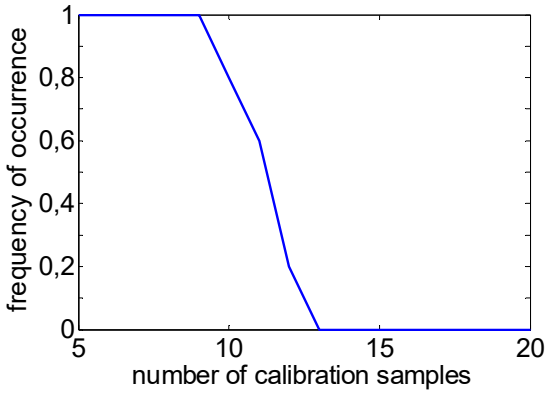

Figure 5.9. *Case study 3: effect of the number of model calibration samples on the occurrence of wrong experiment space designation; the frequency of occurrence is averaged over 100 Monte Carlo simulations.*

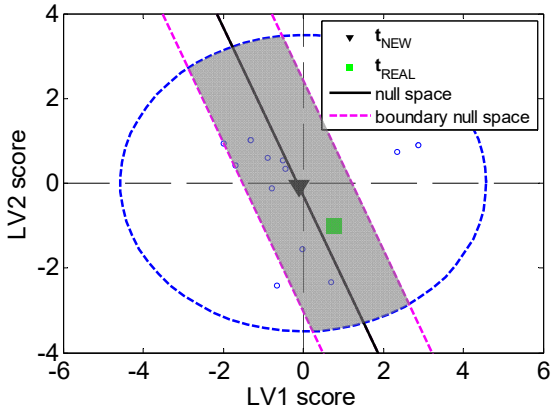

Figure 5.10. *Case study 3: designated experiment space (grey-shaded area) for the development of a product characterized by 20 % of oversize granules (15 samples are used to calibrate the model).*

5.8 Conclusions

A key element of the Quality-by-Design initiative is the determination of the design space for the manufacturing of a pharmaceutical product. When this calculation cannot be assisted by the use of a first-principles model, the DS determination heavily relies on experiments. In some cases, the DS can be found using experiments designed within a domain of input combinations (e.g. material properties and process conditions) that derive from the experience gained from products that have already been developed and are similar to the new one under development. This domain is the knowledge space and the related experimentation can be very demanding, especially if the number of process inputs is large. Since the DS is only a subspace of the knowledge space, the experimental effort could be reduced if one were able to find a narrower region within which

designing and carrying out the experiments. This region, which we call the experiment space, is inside the knowledge space and is likely to bracket the DS.

In this Chapter, a methodology has been proposed to determine the experiment space using historical data on products already developed. By means of a latent-variable model inversion approach, the knowledge space is segmented in such a way as to identify the experiment space in the latent variable space of the model. The segmentation makes use of the concept of null space and accounts for the existence of uncertainty in the model predictions.

Using three simulated case studies, the segmentation results have been shown to be effective, as the designated experiment space includes the true DS and is much narrower than the knowledge space. One additional advantage of the proposed methodology is that, being the experiment space identified in a multivariate latent variable space, its graphical representation is clear also when the number of process inputs is large.

The segmentation effectiveness is shown to depend on the number of samples available in the historical dataset, but the appropriate number of samples does not necessarily need to be very large. In this respect, a procedure has been suggested to test the intrinsic capability of the available historical dataset to serve as an effective source of information to identify the experiment space.

Future investigations should be devoted to assess the effectiveness of a design-of-experiments exercise carried out in the latent space with respect to the more common situation where the experiments are designed directly in the true input space. Additionally, although model uncertainty was explicitly accounted for, the proposed methodology only considered model prediction uncertainty. Therefore, other forms of uncertainty (such as uncertainty on the model parameters and on the calibration data) should be considered in future studies. Furthermore, this study has considered only the case of products characterized by a single quality attribute. However, quality is a truly multivariate property for many pharmaceutical products. How to extend this methodology to the multivariate case represents an area open for further investigation.

Chapter 6

Knowledge management in secondary manufacturing by pattern recognition techniques*

In this Chapter a methodology is proposed to systematically analyze large data historians of secondary pharmaceutical manufacturing systems using pattern recognition techniques. The objective is to develop an approach enabling to automatically retrieve operation-relevant information that can assist the management in the periodic review of a manufactory system. The proposed methodology allows one to automatically perform three tasks: the identification of single batches within the entire data-sequence of the historical dataset, the identification of distinct operating phases within each batch, and the characterization of a batch with respect to an assigned multivariate set of operating characteristics. The approach is tested on two six-month datasets of a commercial-scale granulation/drying system, where several millions of data entries are recorded.

The Chapter is organized as follows: first, after the introduction of the problem, the proposed methodology and the units analyzed are presented, then each step of the methodology is explained in detail using one of the two available datasets, in order to demonstrate the practical application of the methodology when no information about the products processed is available (section A). Finally (Section B), the analysis is performed for both datasets also accounting for the information available about the product manufacturing recipes.

6.1 Introduction

In the last decade, the pharmaceutical industry has been faced with unprecedented business scenario changes. Many blockbuster drugs have been crossing the period of patent expiry and fewer blockbusters are on the horizon. The development of new products is shifting towards more complex therapeutic targets, and the patient base is narrower than that of preceding blockbusters

* Excerpts from this Chapter belong to: N. Meneghetti, P. Facco, F. Bezzo, C. Himawan, S. Zomer, M. Barolo, 2016, Knowledge management in secondary pharmaceutical manufacturing by mining of data historians – A proof-of-concept study. Submitted to *Int. J. Pharm.*

(Kukura and Thien, 2011). Generic competition has become more and more aggressive (am Ende, 2011). Governments are taking radical measures to gain control over drug pricing (e.g. by changing the copayment plans; Sadat *et al*., 2014). Given this scenario, the pharmaceutical companies are striving to reduce costs to maintain competitiveness.

Primary pharmaceutical manufacturing is concerned with the production of active ingredients, whereas secondary pharmaceutical manufacturing focuses in the production of dosage forms (Bennett and Cole, 2003). Both primary and secondary manufacturing play a central role in cost allocation. However, while on the one hand the pharma industry is very effective in discovering new drugs, on the other hand its manufacturing efficiency is far behind the one of several other sectors. Poor performance in manufacturing costs the pharma industry US$90 billion per year, which is considered equivalent to the current development cost for 80–90 new drugs (The Economist, 2005; Danese and Constantinou, 2007). Based on the annual reports of 17 "big pharma" companies, it has been estimated that manufacturing costs amount to ~27% of the revenues, largely exceeding the R&D expenses that are at ~17% (am Ende, 2011). Therefore, even a fractional improvement in the quality of the manufacturing system can bring tremendous competitive advantages to a company.

Though product quality targets are very severe, pharmaceutical manufacturing processes still suffer for high variability. Continuous manufacturing is gaining more and more consideration, but most active pharmaceutical ingredients and drug products are still manufactured batchwise. Commercial manufacturing processes are often suboptimal, because they are conceived at the development stage and get frozen close to product registration, with little or no attempt to optimize them. Manufacturing cycle times are very variable, because out-of-specifications ("exceptions") during manufacturing need frequently be dealt with (Suresh and Basu, 2008). All of these factors contribute to significantly decrease productivity and increase product costs.

With the advent of fast, cheap and reliable on-line measurement devices, product manufacturing environments have now available large historical databases spanning several manufacturing years. However, while being data rich, the pharma industry is also known to be information poor (Politis and Rekkas, 2011). This is due to the fact that, due to data overload, the information embedded in data historians is hidden and therefore remains largely unexploited. Indeed, transforming data into knowledge is not a simple task. To clarify this issue, consider a typical secondary manufacturing system. The ingredients are processed by a series of batch operations, which eventually result in the final drug product. Each operation evolves through a series of phases, which may involve exchange of heat and/or mass with the surroundings and are often triggered by the operators. While a unit is processing the material, there may be short time windows where the unit is stalled (e.g. for re-setting, quick maintenance, and the like). At the conclusion of a batch, the equipment is possibly subject to maintenance and operation tests, then cleaned and set in a hold position for the next operation. Each piece of equipment is equipped with several sensors and hooked to a computer where sensor measurements (temperatures, flows,

torques, compression forces, etc.) are recorded along with some settings (position of switches, controller set-points, etc.), for a total number of recordings on the order of a few tens at each time instant per piece of equipment. Typically, the recordings are made continuously (i.e., at the frequency of one set of recordings every few seconds) across an entire production campaign, which may last several months and may possibly include different products. In most cases, the data capture systems are meant to record data in a "passive" way only, i.e. without contextualizing the operations around them. Therefore, the recordings typically include also data segments that refer to temporary stalls of the equipment, where the time profiles of the recorded signals are totally unrelated to the evolution of the operation within the equipment; not even when the equipment is not processing material is the recording interrupted. The net result is that the amount of data records that gets archived for a given production campaign is overwhelming, easily reaching several millions of data entries. Additionally, the structure of the data capture systems may be out of step with respect to the implementation of newer and increasingly sophisticated data modeling and monitoring techniques, whose requirements were possibly not factored in at the time of the systems installation. A mechanical update of the systems to this end might even produce further disruption at significant cost for production. Periodic review of the historical operational data by the company management is not easy, as the information is masked to a point that even finding the start and end point of a batch may be difficult. Yet, there are several pieces of information that are hidden in the historian and would be useful to know when reviewing a production campaign, such as how many batches have been carried out in the campaign; which factors characterize the evolution of the operating phases within each batch; whether and how these factors have changed along the campaign; whether there have been some trends/drifts along the campaign. Systematic review of these issues by science-driven methods would amount to turning data into knowledge, and this can be a decisive step toward continuous improvement of the manufacturing system. Note that, while the ultimate objective is to provide full contextualization of the entire data historians for all the potential costumers (e.g., manufacturing performance review teams, product development teams, equipment/maintenance engineers), even an incremental improvement to progressively reduce existing gaps, where data cannot be fully exploited, may lead to substantial savings.

In this Chapter, a methodology is proposed to systematically analyze large data historians of secondary manufacturing systems using data mining techniques. The objective is to develop an approach enabling to automatically retrieve operation-relevant information that can assist the management in the periodic review of a manufactory system, thus improving process understanding and contributing to reduce the occurrence of exceptions through systematic identification of the variability sources. The approach is tested on two six-month datasets of a commercial-scale granulation/drying system. The final result is an advanced process analytical technology (PAT) tool that can assist the implementation of continuous improvement paradigms within a quality-by-design framework (FDA 2004b).

6.2 Proposed framework

Following the industrial parlance, the variables registered in manufacturing historians will be named ‘tags’ in this study. The proposed methodology allows one to automatically perform the following tasks:

Task 1: batch identification; namely, isolation of single batches within the entire data-sequence of the historical dataset, depending on the characteristics of the available tags;

Task 2: phase identification; namely, identification of distinct operating phases within each batch;

Task 3: batch characterization; namely, characterization of each batch with respect to an assigned set of multivariate characteristics (e.g., length of a given phase, speed of a given device, maximum or minimum temperature achieved, etc.) The methodology is sketched in Figure 6.1. The three tasks are carried out sequentially and, depending on the characteristics of the available tags, may involve alternative scenarios. In particular, for the batch identification task (Task 2) two alternative scenarios are envisaged: Scenario 1 refers to the situation where tags are available that are directly linked to the length of a batch, whereas Scenario 2 refers to the more general case where these tags do not exist; in this case, the Task 2 operations are carried out before the Task 1 ones. Note that a preliminary exploratory analysis of the available data is suggested to select the subset of tags suitable for the subsequent tasks, as well as to analyze the data structure and the complexity of the system.

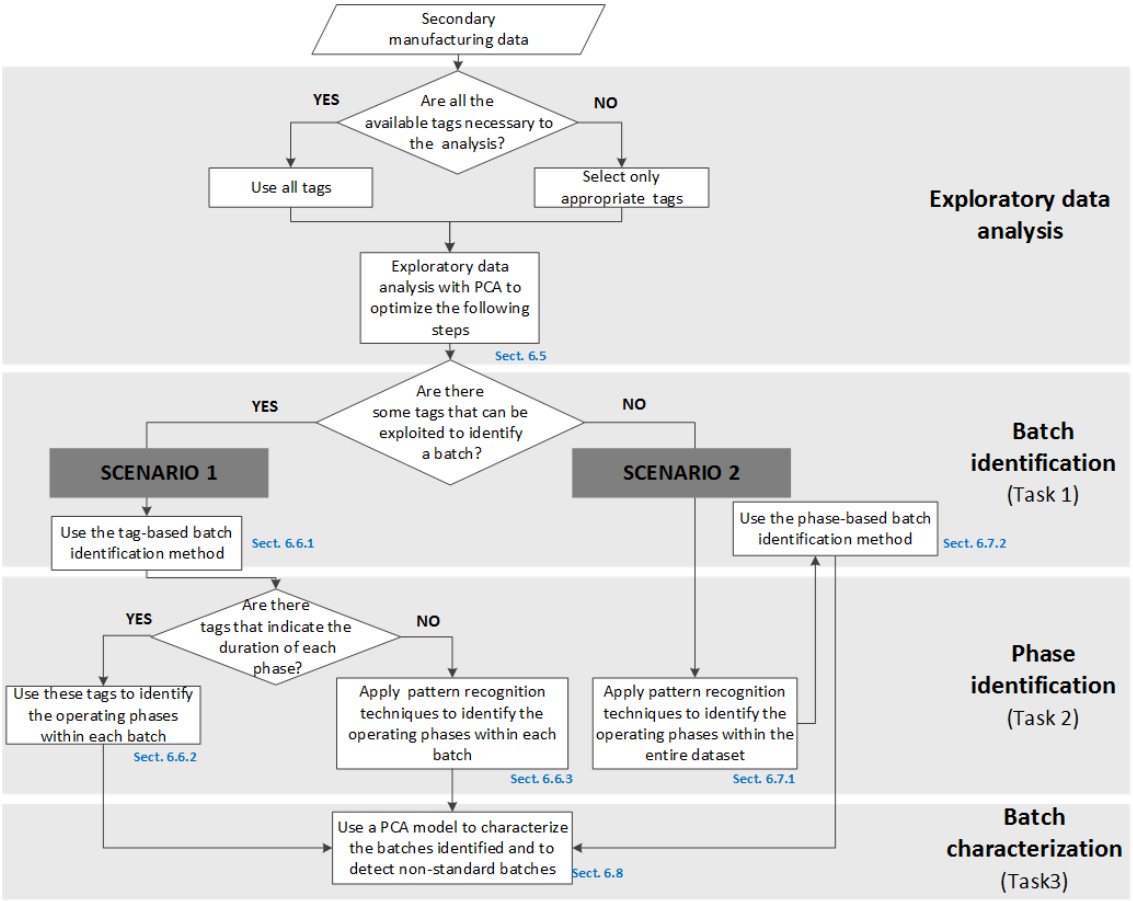

Figure 6.1 *Flowchart of the proposed approach to analyze secondary manufacturing data historians for batch systems. Each block includes a reference to the section where the block operations are discussed.*

6.2.1 Tag sources and possible data analysis scenarios

The available tags may derive from different sources, which should be clearly identified prior to the analysis; therefore, interaction with the plant experts is fundamental at this stage. In this study, four such sources were identified:

- Source 1: measurement sensors. In this case, the tag values are registered in the form of real numbers;
- Source 2: calculations involving Source 1 variables;
- Source 3: process settings (subject to operators' adjustment). The tag values are recorded in the form of integer positive numbers (0; 1; 2; …), representing the manually-driven activation of a certain operation, or the current status of a piece of equipment;
- Source 4: time span settings. The tag values are recorded in the form of real numbers indicating the time elapsed from the operator-triggered start of a given event, to the current

time instant (until event termination). Note that after the termination of a given event, the relevant time span value is often recorded as a constant value equal to the total event duration.

In general, for a given manufacturing unit the available tags may not come from all sources; additionally, the available tags may well change from unit to unit. For this reason, two possible data analysis scenarios are considered in Figure 6.1, which depend on the tags available. Scenario 1 is preferred if tags indicating the status of the unit under investigation and/or the duration of all its operating phases (Source 3 and 4 tags) are available; when such tags are not available, Scenario 2 is followed.

6.3 Manufacturing system and datasets

Two industrial secondary manufacturing units, both operating batchwise, were selected as test beds for the proposed knowledge management methodology: a high-shear wet granulator and the downstream fluid-bed dryer. Two consecutive six-month datasets were extracted from the available historians, where data were recorded at a sampling rate of one data entry every 5 s, for a total number of data entries on the order of 10^8. The available datasets are denoted as follows:

- Dataset 1 collects the data recorded in the first production period analyzed;
- Dataset 2 collects the data recorded in the second production period analyzed;

Dataset 2 presents the same number of observations as Dataset 1 (namely, 3,127,088 observations, at a sampling rate of one data entry every 5 s).

In the first part of this Chapter the methodology is tested on Dataset 1, assuming that no information is available about the product (or possibly products) manufactured. In the second part, the analysis is repeated on the same dataset, but information about the manufacturing recipe(s) is also used; additionally, Dataset 2 is also analyzed.

Note that the recorded data include time windows where a unit is in operation but temporary stalled, as well as time windows where material is not being processed. Neither of these occurrences are marked somehow in the historian. Note that the number of granulation and drying batches included in the selected time window was not known a priori (namely, it was a piece of information to be obtained by the proposed knowledge management method).

A description of each unit and a list of the tags recorded are reported in the following.

6.3.1 High-shear wet granulator: process description and operating phases

The high-shear wet granulator processes a powder feed to manufacture granular material with assigned particle size distribution. The granule formation and size increase are obtained by agglomeration, which is determined by adding a liquid combined with the action of an impeller

and a chopper. As schematically illustrated in Figure 6.2, four operating phases characterize the typical evolution of a standard granulation batch:

- Phase 1: dry mixing;
- Phase 2: water addition;
- Phase 3: wet massing;
- Phase 4: discharge.

During Phase 1, the material is slowly charged into the unit and mixed by the impeller only. In Phase 2 the aggregating agent is added and the chopper is activated. In Phase 3, changes in the granule size and porosity are observed, causing an increase in the impeller power consumption. Finally, when the granules reach an assigned size, the unit is emptied by opening a discharge valve, and the material is sent to the dryer unit (Phase 4).

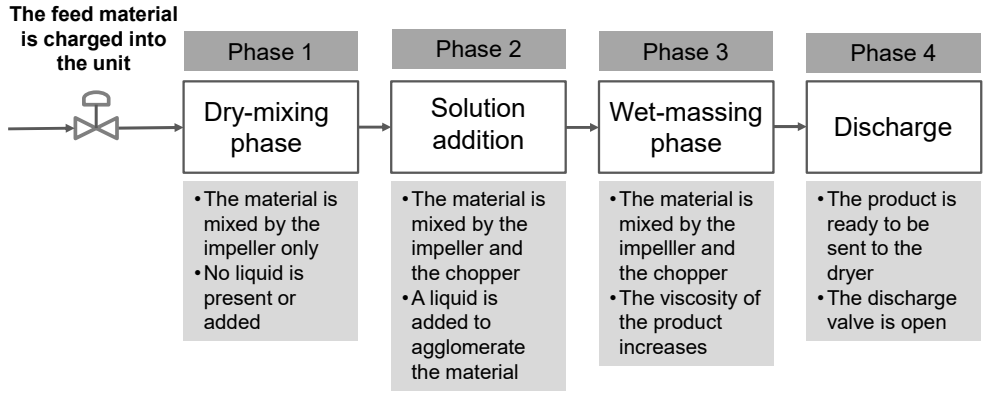

Figure 6.2 *Granulation unit: description of the four operating phases of a standard batch.*

Note that each operating phase may either represent an event related to the physical evolution of the batch (e.g., wet massing) or an event triggered by the operators (e.g., solution addition, discharge, etc.).

6.3.2 Fluid-bed dryer: process description and operating phases

The fluid bed dryer receives the material processed by the granulator as feed. The granulated material moisture content is reduced by fluidizing the particles with an air stream until the final product humidity or temperature reach a desired value. The complexity of the physical mechanisms involved in the process, and the fact that product sampling requires stopping the operation, make the analysis of the drying variable profiles more complex than that of the granulator. Six operating phases can be identified for a standard drying batch (Figure 6.3):

- Phase 1: pre-heating;

- Phase 2: charging;
- Phase 3: constant drying rate;
- Phase 4: falling drying rate;
- Phase 5: cooling down;
- Phase 6: discharge.

In Phase 1, the equipment is heated up. Then, while the material to be dried is gradually charged (Phase 2), the solvent evaporates mainly from the particle surface (Phase 3), without significant changes in the product temperature. During Phase 4, the product temperature increases due to the slow diffusion of the liquid embedded in the particles toward the particle surface. Finally, the material is cooled (Phase 5) and then discharged (Phase 6).

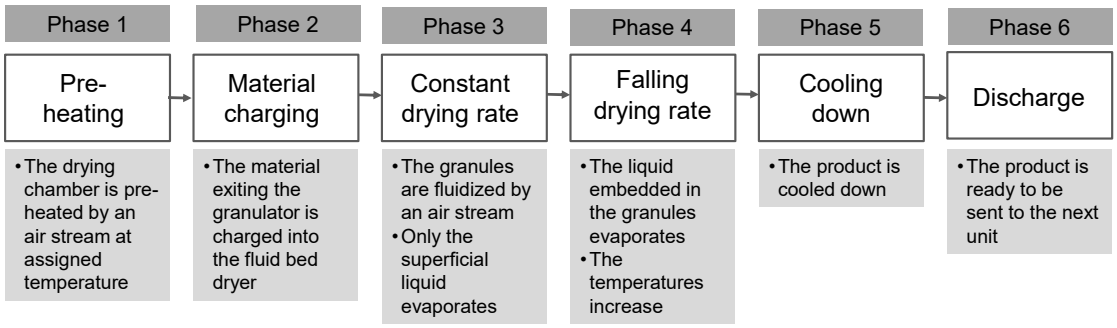

Figure 6.3. *Drying unit: description of the six operating phases of a standard batch.*

SECTION A – ANALYSIS OF DATASET 1 WITH NO PRODUCT INFORMATION AVAILABLE

6.4 Available data for Dataset 1

6.4.1 Granulation unit data

Thirty-four tags are available in the plant to monitor the granulation unit at any time instant. Before further data processing, it may be useful or necessary to remove some tags from the original dataset. The reasons for this may be different: for example, not all tags might be available for all recorded batches, some tags may have been temporarily dismissed or be under maintenance, some others may confound the analysis when used within the models that will be described later (for more details refer to Section 6.6.3). Following this rationale, 11 tags were retained to build the granulator dataset (Table 6.1), and they were organized in a granulator matrix **G** [3127088×11], where each column represents one tag and each row (observation) reports the

set of tag values recorded at a given time instant. The time profiles of the selected tags in a typical granulation batch are shown in Figure 6.4.

Table 6.1. *Granulation unit: list of the tags selected. The measurement units have been omitted to protect data confidentiality.*

Tag no.	Tag source	Tag description
1	Source 1	Granulator chopper current
2	Source 3	Granulator chopper speed
3	Source 1	Granulator impeller current
4	Source 1	Granulator impeller load
5	Source 3	Granulator impeller speed
6	Source 3	Granulator discharge valve status
7	Source 4	Granulator dry mix time
8	Source 4	Granulator solution addition time
9	Source 4	Granulator wet massing time
10	Source 1	Impeller power
11	Source 3	Granulator status

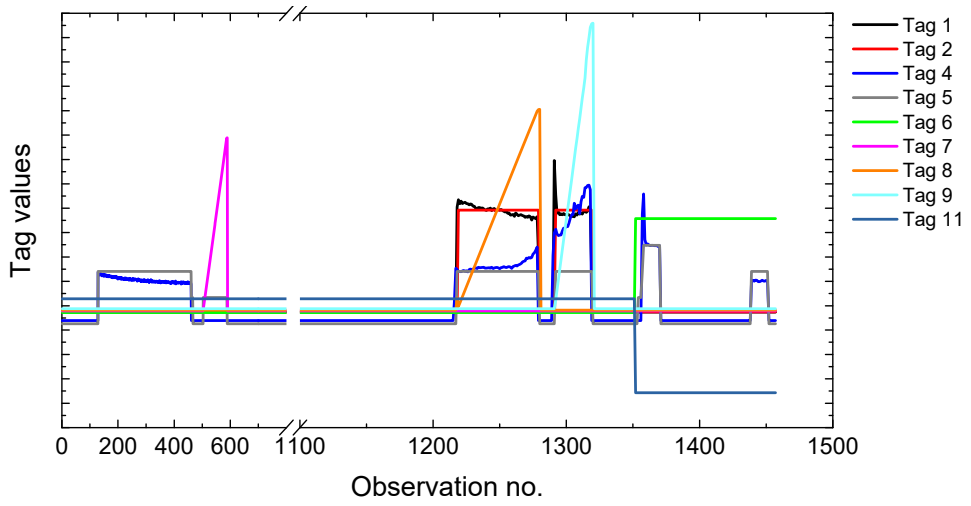

Figure 6.4. *Granulation unit: example of the trend of the tags selected for a standard batch. The y-axis scale has been masked to protect data confidentiality.*

6.4.2 Drying unit data

A set of 23 tags is available for the drying unit, and 14 of them were selected to build the drying dataset (Table 6.2.). These tags were organized in a dryer matrix **D** [3127088×14]. Typical tag profiles for a drying batch are reported in Figure 6.5.

Table 6.2. *Drying unit: list of the tags selected. The measurement units have been omitted to protect data confidentiality.*

Tag no.	Tag source	Tag description
1	Source 3	Dryer status
2	Source 1	Pressure difference
3	Source 4	Drying time
4	Source 3	Drying status
5	Source 1	Exhaust air temperature
6	Source 1	Inlet air humidity
7	Source 1	Inlet air moisture content
8	Source 1	Inlet air temperature
9	Source 1	Inlet air volume
10	Source 1	Inlet air fan speed
11	Source 1	Inlet air flap position
12	Source 1	Outlet air flap position
13	Source 4	Pre-heat time
14	Source 1	Product bed temperature

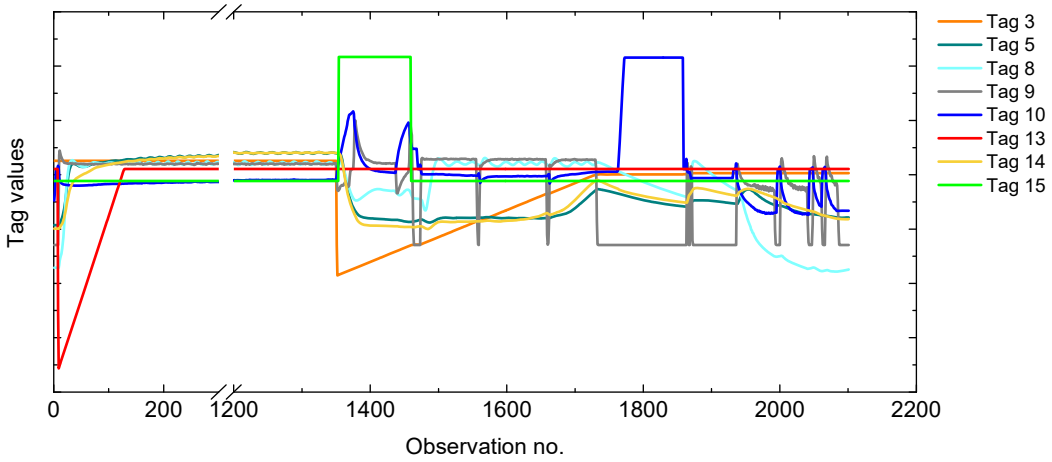

Figure 6.5. *Drying unit: example of the trend of the tags selected for a standard batch. The y-axis scale has been masked to protect data confidentiality.*

6.5 Exploratory data analysis

As a preliminary step of the proposed methodology, an exploratory data analysis is suggested to investigate the correlation structure of the available data. The analysis requires visual identification of a limited number B of batches included in the available datasets (**G** or **D**). This operation may be time consuming, as the start and end point of the batches are not known a priori, and therefore visual inspection of the datasets may be demanding. Note that, to avoid considering batches that belong to a single production campaign (i.e., to a limited time frame), the batches should be selected across the entire data historian. For generic batch b within this subset of data, the available data are collected in matrix $\mathbf{V}_b$ $[I_b \times T]$, where I_b and T are the number of historical

observations for the batch and the number of tags used, respectively. Then, the exploratory analysis can be carried out as follows.

1. One batch of this subset, recognized as "standard" according to prior process knowledge, is denoted as the reference batch, and the operating phases are visually identified for it. After data pretreatment (namely, autoscaling), a principal component analysis (PCA; Chapter 2, Section 2.1.1) model is built on the reference batch.
2. The PCA model scores are examined to extract information about the relations among the observations belonging to different operating phases. In fact, the observations belonging to the same operating phase usually locate close in the scores space to form a cluster.
3. The remaining $(B-1)$ batches, denoted as validation batches, are projected onto the PCA model space (note that each validation batch is autoscaled on its own mean and standard deviation). Information about the degree of the batch-to-batch variability can be obtained by analyzing the score patterns of the projected batches.
4. A few iterations of the procedure with different reference batches are suggested to assess the consistency of the results obtained.

6.5.1 Results for the granulation unit

A PCA model or the granulator was built as indicated in step 1. Two PCs[‡‡] (capturing ~63% of the variability of the calibration data) were considered, but more may be used if a more accurate analysis is required.

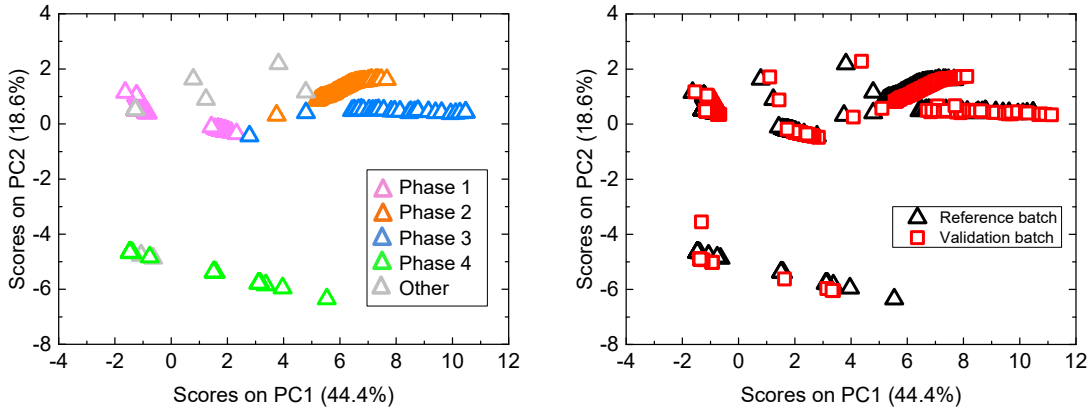

(a) (b)

Figure 6.6. *Granulation unit: (a) scores of the PCA model built on a reference batch; (b) projections of one representative validation batch onto the PCA model space. In (a), the calibration scores are marked with different colors according to the operating phase they belong to.*

[‡‡] Since the objectives of this preliminary analysis is only to evaluate how easily different operating phases can be discriminated, and whether the time trend of different batches is similar, it is suggested to use few PCs as possible. In fact, two PCs are often enough for this purpose.

The model scores are reported in Figure 6.6a: the four operating phases characterizing a granulation batch are apparent in the score space, meaning that each phase is characterized by a unique combination of tag values that can be captured by the model. The same pattern is found also for most validation batches; a projection of one representative validation batch onto the PCA model space is shown in Figure 6.6b. The main conclusion for this analysis is that the batch-to-batch variability is relatively limited for the granulation unit, even if the operators' settings change from batch to batch. Note that a standard PCA model loadings analysis (not reported here for the sake of conciseness) can be used to identify the tags that most characterize each granulation phase.

6.5.2 Results for the drying unit

The pattern of the PCA scores resulting from the PCA model of a reference drying batch (Figure 6.7a) indicates that the drying process is more difficult to analyze. In contrast to the granulation process, the clusters are not clearly distinguishable, suggesting that the identification of different operating phases using the available tags may be difficult. Additionally, the projections of different batches onto the PCA model space (a representative example is reported in Figure 6.7b) reveals a much larger batch-to-batch variability.

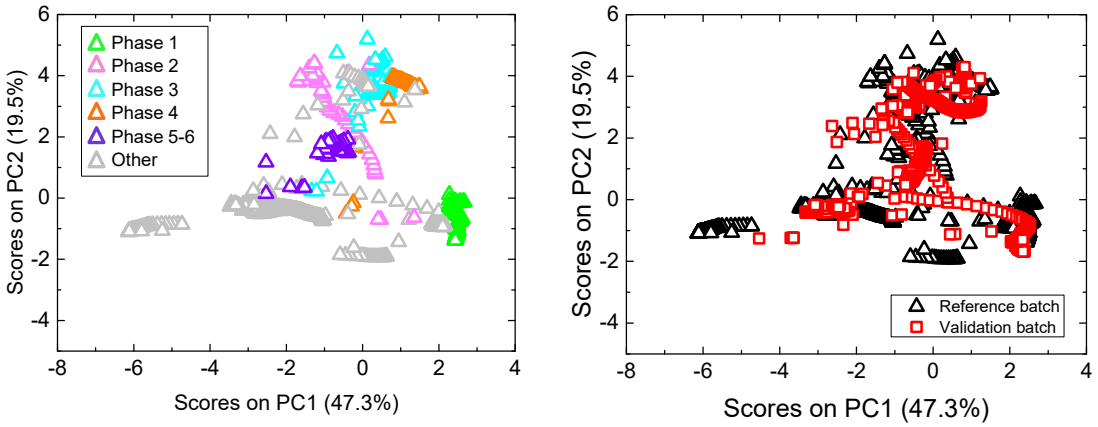

(a) (b)

Figure 6.7. *Drying unit: (a) scores of the PCA model built on a reference batch; (b) projections of one representative validation batch onto the PCA model space. In (a), the calibration scores are marked with different colors according to the operating phases they belong to.*

6.6 Batch identification and phase identification in Scenario 1

In this section, the procedure to automatically extract (from **G** or **D**) the observations belonging to *each single* batch is presented. The objective is to screen each dataset in order to identify segments of consecutive observations that all refer to the same granulation or drying batch. The

number of observations in these segments is not known a priori, and changes from batch to batch. When one such segment is identified, the related observations are rearranged into a matrix $\mathbf{O}_b$ $[I_b \times T]$ ($\mathbf{O}_{G,b}$ or $\mathbf{O}_{D,b}$ for the granulator or the drying, respectively), where the meaning of the symbols is the same as in Section 6.5 . Note that, since the true batches may be separated by data segments that are not directly related to actual product manufacturing, not all the observations in **G** or **D** will eventually belong to one of the $\mathbf{O}_b$ matrices. The procedure discussed in this section is based on direct tag analysis (Scenario 1); an alternative procedure that uses a pattern recognition technique (Scenario 2) will be presented in Section 6.7 . Once all batches in **G** and **D** have been singled out, the automatic identification of operating phases within each batch can be carried out (Task 2). A procedure for carrying out this task is also presented in this section.

6.6.1 Tag-based batch identification

The simplest method that can be employed in order to recognize a batch within an historical dataset makes use of those tags that can be directly related to the duration of the entire batch or of its operating phases. The most convenient situation (which is actually encountered both in the granulator and in the drier) is represented by the availability of one tag unambiguously indicating when the manufacturing unit is (and is not) in operation (green path in Figure 6.8).

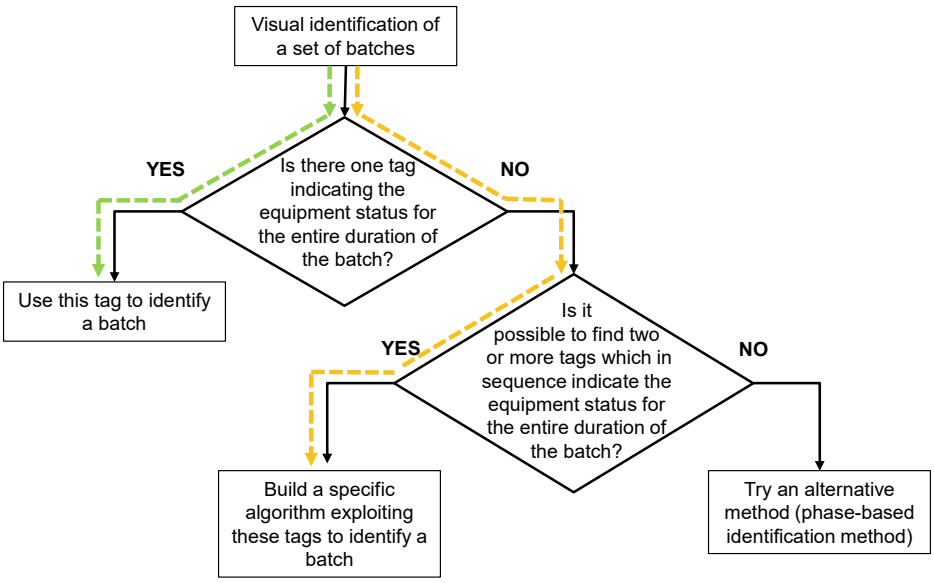

Figure 6.8. *Tag-based batch identification: different alternatives are identified depending on the sources of the available tags. The orange path indicates the procedure followed to identify a granulation batch, whereas the green path was followed to identify a drying batch.*

This tag can be directly used in a simple algorithm (not discussed here for the sake of conciseness) that, based on the values the tag takes, recognizes whether or not the unit is in operation, and

consequently extracts the relevant data segments from **G** and **D**. If such a tag is not available, alternative solutions exist as summarized by the orange path in Figure 6.8. Note that, in order to be able to choose the appropriate path, a preliminary step is necessary to visually extract a set of batches from the global dataset. To this purpose, the batches used for the preliminary exploratory analysis (Sections 6.5.1 and 6.5.2) can be used. Some implementation issues that may arise following the procedure proposed in Figure 6.8 will be discussed in Section 6.13 .

Note that, in general, not all of the batches identified can be considered as "standard", because some operating segments may be repeated twice in some batches, or they may last much longer than in other batches. Therefore, regardless the scenario followed for batch identification, an additional analysis is needed to discriminate between standard and non-standard batches (Figure 6.1). This topic (batch characterization) will be discussed in Section 6.8.

6.6.1.1 Results for the granulation unit

Since granulator Tag 11 (granulator status) indicates when the granulator is operating, this tag can in principle be used for tag-based batch identification. However, this tag is active during the first three operating phases only; therefore, an additional tag that remains active for the rest of the batch is required (orange path in Figure 6.8). This tag exists and is Tag 6 (granulator discharge valve). Therefore, a granulation batch *b* can be easily singled out from the **G** dataset using the combination of Tag 11 and Tag 6.

A graphical representation of the results from this procedure is reported in Figure 6.9a for a small subset of **G**: the grey-shaded areas correspond to the batch identified automatically. Using this tag-based identification procedure, 90 different granulation batches were eventually identified.

6.6.1.2 Results for the drying unit

Using dryer Tag 1 (dryer status) is sufficient to identify the drying batches, as this tag is active during the entire duration of the batch (green path in Figure 6.8). Eventually, ninety[§§] different drying batches were identified automatically. A graphical representation of the results of drying batch identification is shown in Figure 6.9b. Note that the three batches marked by the grey shading are separated by operational segments where all tag values (except Tag 1) change (Figure 6.9b), probably due to equipment testing; therefore, identifying the batch by analyzing the trajectories of *these* tags would not be easy.

[§§] The coincidence of this number with the number of batches identified for the granulation unit is accidental.

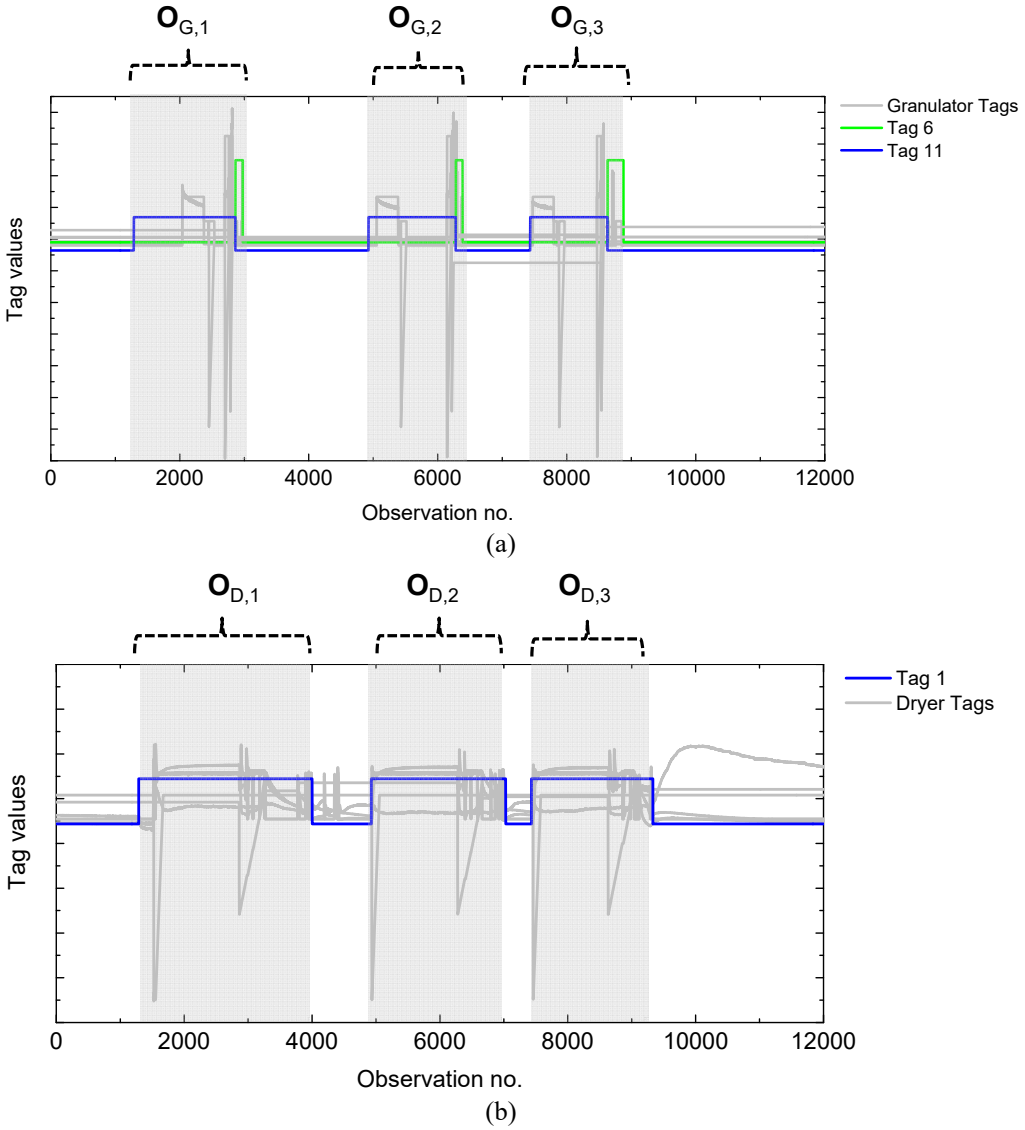

Figure 6.9. *Representative example of automatic batch identification using a tag-driven method for (a) the granulation unit and (b) the drying unit. For both units, three batches carried out in a few weeks are identified (using Tag 11 and Tag 6 for the granulation unit, and Tag 1 for the drying unit). The time profiles for the tags used to identify the batches have been marked with colors, whereas those of some other tags are reported in grey. The y-axes scales have been masked to protect data confidentiality.*

6.6.2 Phase identification by tag analysis

If tags are available that are specifically intended to mark the start/end point of an operating phase (Source 3 and Source 4 tags), they can be directly exploited to automatically identify the phases through which a batch evolves (the procedure is very simple and will not be discussed for conciseness). To be able to implement to this method, the following conditions on the available tags need to be fulfilled:

- each operating phase must be defined by a tag;
- the tags employed for phase identification must recorded for all batches.

This is the case of the granulation unit, for which phase identification can be easily done by directly exploiting the following tags:

- Tag 7 and Tag 5, indicating the duration of Phase 1;
- Tag 8, indicating the duration of Phase 2;
- Tag 9, indicating the duration of Phase 3;
- Tag 6, indicating the duration of Phase 4.

However, this solution is not applicable to the drying unit, since there is only one tag (Tag 13) that univocally marks the duration of an operating phase (namely the Pre-heating phase).

6.6.3 Phase identification by pattern recognition

In many manufacturing units, tags allowing one to easily identify the start and end instants for all the phases that characterize a batch (Source 4 and Source 3 tags) may not be available for *all* phases. In such instances, the batch phase identification problem can be transformed into a sample classification problem, which is manageable even in the absence of sufficient number of these tags. The task is therefore to assign each observation (sample) of a given batch $\mathbf{O}_b$ to a class p($p = 1,2,...,P$), the P classes being the operating phases characterizing that batch plus some "inter-phases", which are conveniently defined because on certain time periods some observations may not be assignable to any operating phases, since they simply represent the intervals occurring between two consecutive phases when ancillary operations are carried out (e.g., unit re-setting, samplings etc.).

Both unsupervised methods (PCA, Chapter 2, Section 2.2.2) and supervised methods (linear discriminant analysis; McLachlan ,2004); *k*-nearest neighbors (*k*-NN, Chapter 2, Section 2.2.1); partial least-squares discriminant analysis (Barker and. Rayens, 2003) were tested to this purpose. On average, *k*-NN showed a better performance for the case studies considered in this study, and for this reason only the results obtained with this technique will be discussed.

The *k*-NN classification method allows one to classify an observation as belonging to one class or to another, depending on the class attribution for an assigned number *k* of neighbors identified according to a given distance criterion (detailed information about *k*-NN is reported in Chapter 2, Section 2.2.1. The *k*-NN model is built from a set of calibration observations for which the class assignment is known a priori and then used to classify new observations (e.g., an entire batch not included in the calibration set). Therefore, to build the classification model one needs: *i*) defining the calibration observations; *ii*) providing the class assignment for each of them.

Given batch b, for which N_b observations have to be assigned to P classes, the *k*-NN model classification performance can be evaluated using three metrics (Ballabio and Todeschini, 2009): error rate (ER), sensitivity (Sn_p), and specificity (Sp_p):

$$\mathrm{ER} = \frac{I_b - \sum_{p=1}^{P} h_{pp}}{I_b} \quad , \tag{6.1}$$

$$\mathrm{Sn}_p = \frac{h_{pp}}{I_p} \quad , \tag{6.2}$$

$$\mathrm{Sp}_p = \frac{\sum_{j=1}^{P} (h'_j - h_j)}{I_b - I_p} \quad k \neq p, \; h'_j = \sum_{k=1}^{P} h_{pj} \quad , \tag{6.3}$$

where I_p represents the number of observations for class p, and h_{pp} represents the diagonal element of the so-called confusion matrix **H** (Ballabio and Todeschini, 2009). The confusion matrix is a square [$P \times P$] matrix whose rows represent the true class assignments, and whose columns represent the classes assigned by the k-NN model. Therefore, each element h_{pj} of the confusion matrix represents how many observations belonging to class p have been classified by the model as belonging to class j. Consequently, the diagonal elements h_{pp} represents the observations classified correctly by the model.

Basically, ER represents the average fraction of wrongly assigned observations, Sn_p represents the ability of the model to correctly recognize observations belonging to class p, and Sp_p represents the ability of class p to reject observations belonging to other classes.

6.6.3.1 Phase classification for the granulation batches

To be consistent with the assumption that tags that univocally identifies all phases do not exist, some of the tags originally included in $\mathbf{O}_{\mathrm{G},b}$ were removed. Namely, a scenario was considered by removing Tags 7, 8 and 9, which are related to phase duration. A calibration matrix $\mathbf{C}_\mathrm{G}$ [$I \times T$] was then defined that includes 7 batches, selected by a preliminary exploratory analysis among those identified automatically in Section 6.5.1. The batches selected for model calibration are reported Table 6.3. Matrix $\mathbf{C}_\mathrm{G}$, which results from the variable-wise unfolding (Kourti, 2003) of this calibration set, includes $I = 8451$ observations and $T = 9$ tags.

Table 6.3. *Granulation unit: list of the batches included in the calibration set of the k-NN classification model.*

Calibration batch no.	No. of observations
1	1688
24	1291
27	1110
38	1098
43	1101
59	985
90	1178

Note that assigning the correct class to each observation included in $\mathbf{C}_G$ is a time consuming task, because class assignment is done on the basis of a visual analysis of the time profiles of the tags available for each observation. Appropriately selecting $\mathbf{C}_G$ is therefore crucial, since $\mathbf{C}_G$ should include a limited subset of batches, which nevertheless represent well the *entire* variability of the data historian. The explorative data analysis discussed in Section 6.5 can provide useful information to this purpose.

Five classes were identified visually by analyzing the tag profiles for $\mathbf{C}_G$; an example of such visual analysis is shown in Figure 6.10. These classes (Table 6.5) include the four granulation phases (Section 6.3.1) as well as one inter-phase, which represents the interval between two different operating phases when the impeller is off. Note that the actual operation of a given phase may sometimes be different from batch to batch (e.g., depending of the product manufactured). This does not represent a problem for phase recognition, provided that all the admissible tag patterns are well represented in the calibration matrix.

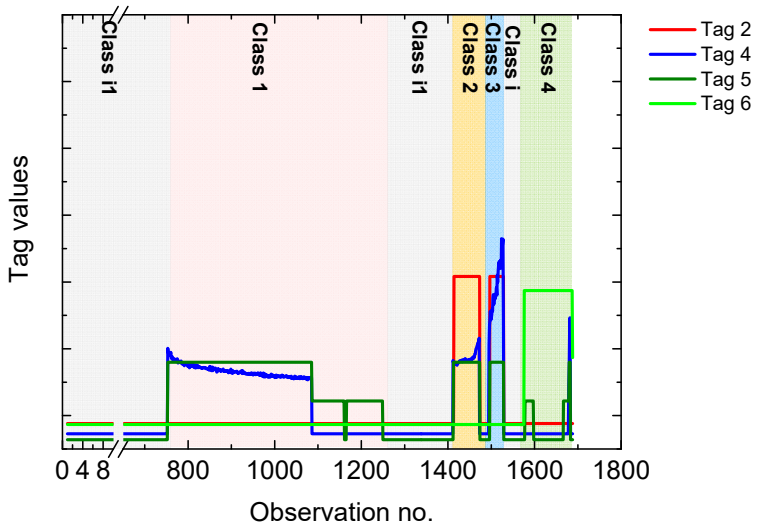

Figure 6.10. *Granulation unit: classes identified for a representative granulation batch of the calibration set (batch no.1); for clarity only a few tag profiles are indicated. The y-axes scale has been masked to protect data confidentiality.*

A vector $\mathbf{c}_G$, whose elements represent the class assigned to each observation of the calibration matrix, was defined to build the *k*-NN classification model, whose characteristics are summarized in Table 6.4. Note that, in addition to the Euclidean distance, other distance criteria were tested, with no major impact on the final results.

Table 6.4. *Granulation unit: main characteristics of the k-NN model used for batch phase identification.*

No. of neighbors (*k*)	Distance criterion	Data pre-treatment	No. of classes (*P*)
5	Euclidean distance	Autoscaling on $\mathbf{O}_b$ columns	5

Table 6.5. *Granulation unit: list of the classes identified for this process.*

Class ID	Phase Type	Phase description
i1	Inter-phase	Interval between phases
1	Phase 1	Dry-mixing phase
2	Phase 2	Solution addition phase
3	Phase 3	Wet-massing phase
4	Phase 4	Discharge of the material

A set of validation batches was then used to test the performance of the classification model. Classification results for 4 representative validation batches are reported in Table 6.4 using the performance indices discussed above. It can be concluded that:

- the error rate is well below 1%;
- the sensitivity is high for each class, meaning each class can be recognized with the same high success. It was found that most classification errors were due to the wrong identification of the *starting* observation of a given phase. However, since also the visual identification of these observation points was somewhat uncertain, it is believed that this error (which corresponds to a time shift on the order of ±5 s) may be further reduced if the start and end point of a phase for the calibration dataset can be identified with smaller uncertainty;
- the specificity is high for each class, meaning that all the classes have a similar capacity to reject the observations not belonging to that class.

Results therefore suggest that the pattern recognition approach enables a systematically correct allocation of the manufacturing phases, regardless of specific recipe adopted to manufacture different products.

Table 6.4. *Granulation unit: phase identification results for representative validation batches, in terms of error rate, sensitivity and specificity for each class.*

Valid'n batch no.	No. of obsrv'ns	ER	Sn_{i1}	Sn_1	Sn_2	Sn_3	Sn_4	Sp_{i1}	Sp_1	Sp_2	Sp_3	Sp_4
4	1372	0.004	0.999	1	0.966	0.973	1	1	0.998	0.998	0.999	1
23	1026	0.009	0.991	0.996	1	0.889	1	1	0.996	0.996	0.998	1
33	1185	0.005	0.998	0.998	0.952	0.972	1	0.996	0.996	1	1	1
44	1552	0.003	1	1	0.984	0.968	0.987	1	0.999	0.999	0.999	1

A graphical example of automatic phase identification is shown in Figure 6.11b for validation batch no.23; the tag profiles for this batch are shown in Figure 6.11a. The colored bars in Figure 6.11*b* represent the automated class assignment results, whereas the black lines are the true class assignment for each observation. Note that, as mentioned, the wrong class assignments are found

mainly at the very beginning of a true operating phase (e.g., see the blue bar around observation no. 600 in Figure 6.11b).

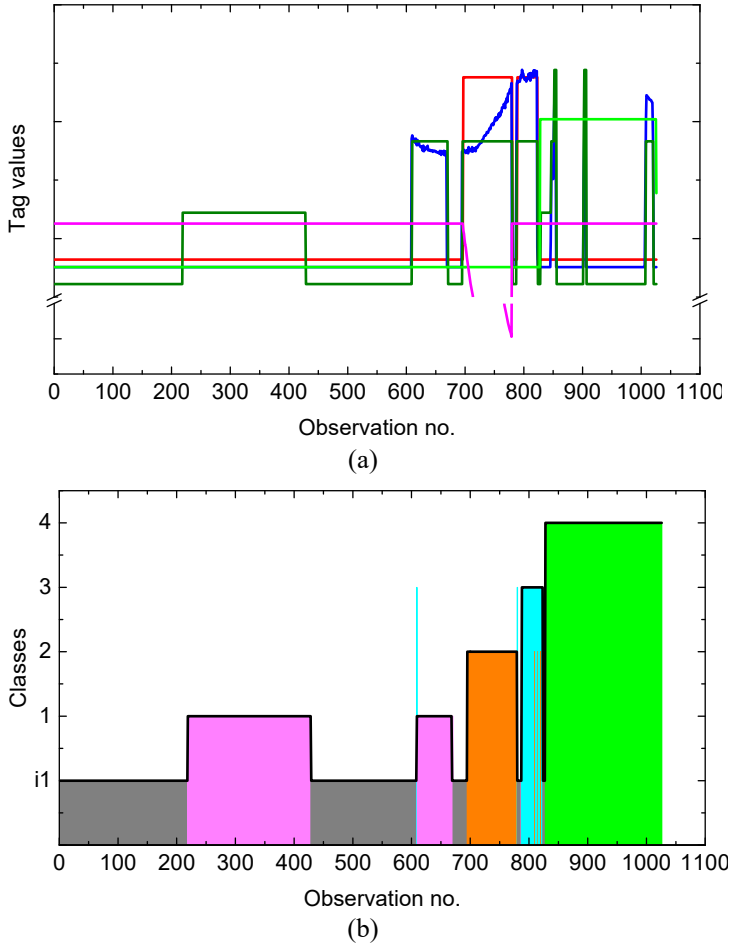

Figure 6.11. *Granulation unit, validation batch no.23: (a) representative tag profiles and (b) class assignment as obtained from the k-NN classification model. The classes assigned by the model are color-coded as indicated in the legend; the true class assignment is indicated by the black line.*

6.6.3.2 Phase classification for the drying batches

The same procedure used for the granulator was applied to the drying unit. A calibration set was defined using 8 batches among those identified in Table 6.5. Note that, since drying follows granulation, the opening of the granulator discharge valve indicates not only the end of Phase 4 for the granulation process, but also that the material is starting to be charged into the drying unit, i.e., the beginning of drying Phase 2. For this reason, Tag 6 of Table 6.1 (which is in fact pertinent to the granulation process) was added as an additional column to **D**. We mention this simple trick to stress that, although the data historian review can indeed be performed automatically, it is nevertheless very important that, prior to the design of the data mining system, the datasets are conveniently arranged according to engineering reasoning.

Table 6.5. *Drying unit: list of the batches included in the calibration set of the k-NN classification model.*

Calibration batch no.	No. of observations
5	1195
21	1760
24	2067
58	2046
75	1359
78	2058
79	1892
87	1287

By analyzing the trends of the available tags for the calibration batches, 9 classes were eventually defined as reported in Table 6.6. Five of them denote true operating phases, whereas the remaining four classes represent recurrent events (not necessarily present in all batches), which were classified as inter-phases.

Table 6.6. *Drying unit: list of the classes identified for this process.*

Class ID	Phase Type	Phase description
i1	Inter-phase	Break phase
1	Phase 1	Pre-heating phase
i2	Inter-phase	Break-phase after pre-heating phase
2	Phase 2	Charging phase
3	Phase 3	Constant-drying rate phase
4	Phase 4	Falling-drying-rate phase
i3	Inter-phase	Break phase related to the drying phase
5	Phase 5	Cooling-down and discharge phases
i4	Inter-phase	Break phase related to the cooling down phase

A graphical representation of the classes identified during model building is provided in Figure 6.12 for a typical calibration batch. Note that the discrimination between the constant drying rate phase and the falling drying rate phase was uncertain for some calibration batches. For this reason, it was assumed that the falling drying rate phase starts as soon as the temperatures of the exhaust air and of the product start to increase. Furthermore, to simplify the analysis the cooling down phase and the discharge phase were considered as a single phase. Details on the *k*-NN model built for the drying unit are reported in Table 6.7. A summary of the automatic phase identification results for four representative validation batches is reported in Table 6.8 and Table 6.9.

Table 6.7. *Drying unit: main characteristics of the k-NN model used for the phase classification.*

No. of neighbors	Distance criterion	Data pre-treatment	No. of classes
7	Euclidean distance	Autoscaling of $\mathbf{O}_b$ columns	9

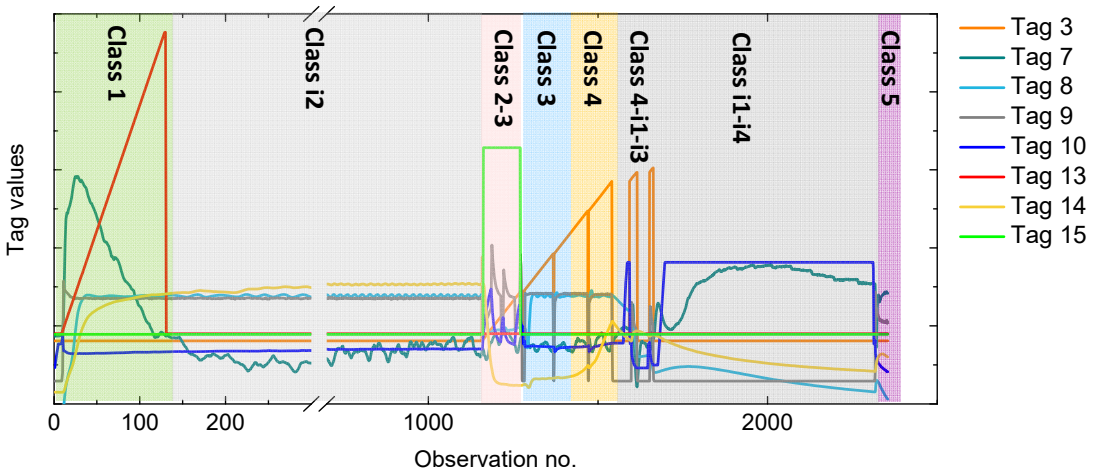

Figure 6.12. *Drying unit: classes identified for a representative drying batch of the calibration set (batch no. 58); for clarity only a few tag profiles are indicated. The y-axes scale has been masked to protect data confidentiality.*

The increase of the misclassified observations reflects the greater complexity of the phase identification problem for the drying system. As anticipated by the preliminary exploratory analysis, this is due to the larger variability experienced by the drying unit than by the granulation one. Nevertheless, the classification model still exhibits very good performance:

- the error rate ranges between 1.0% and 7.0%, with the largest ER value being obtained for a very peculiar batch (no.73; Figure 6.13b-d), which was purposely included in the validation dataset to provide a challenging test bed;
- the sensitivity index indicates that, for all batches, the model does a very good job in class attribution for classes 1, 2 3 and 5 (see Table 6.6 for class/phase correspondence). Bad model performance is limited to class 6 assignment for validation batch no.6, and to class 4 assignment for validation batch no.73. However, it was found that also the visual identification of the exact start and end point of these two phases is uncertain for both batches. Therefore, the number of such misclassifications may probably be reduced if a clearer identification of the operating phases can be provided;
- the specificity index is satisfactorily high for all classes and all batches, meaning that all the classes have the same ability to reject observations belonging to other classes.

Table 6.8. *Drying unit: phase identification results for representative validation batches, in terms of error rate and sensitivity for each class.*

Valid'n batch no.	No. of obsrv'ns	ER	Sn_{i1}	Sn_1	Sn_{i2}	Sn_2	Sn_3	Sn_4	Sn_{i3}	Sn_5	Sn_{i4}
2	2101	0.010	0.964	1	1	0.917	1	0.940	-	0.977	1
6	1269	0.021	0.996	1	1	0.989	0.947	0.125	0.949	0.956	-
38	4672	0.014	0.986	1	1	0.971	0.866	0.905	-	0.885	-
73	2371	0.070	0.979	1	0.975	0.385	0.787	0.913	-	0.925	0.964

Table 6.9. *Drying unit: phase identification results for representative validation batches, in terms of specificity for each class.*

Batch	Sp_{i1}	Sp_1	Sp_{i2}	Sp_2	Sp_3	Sp_4	Sp_{i3}	Sp_5	Sp_{i4}
2	0.997	1	0.999	1	0.997	0.999	0.998	0.999	1
6	0.988	1	0.999	0.999	0.995	0.996	1	0.999	1
38	0.997	1	0.999	1	0.998	0.998	0.995	0.999	1
73	0.952	1	1	0.987	0.998	0.983	0.992	0.997	0.996

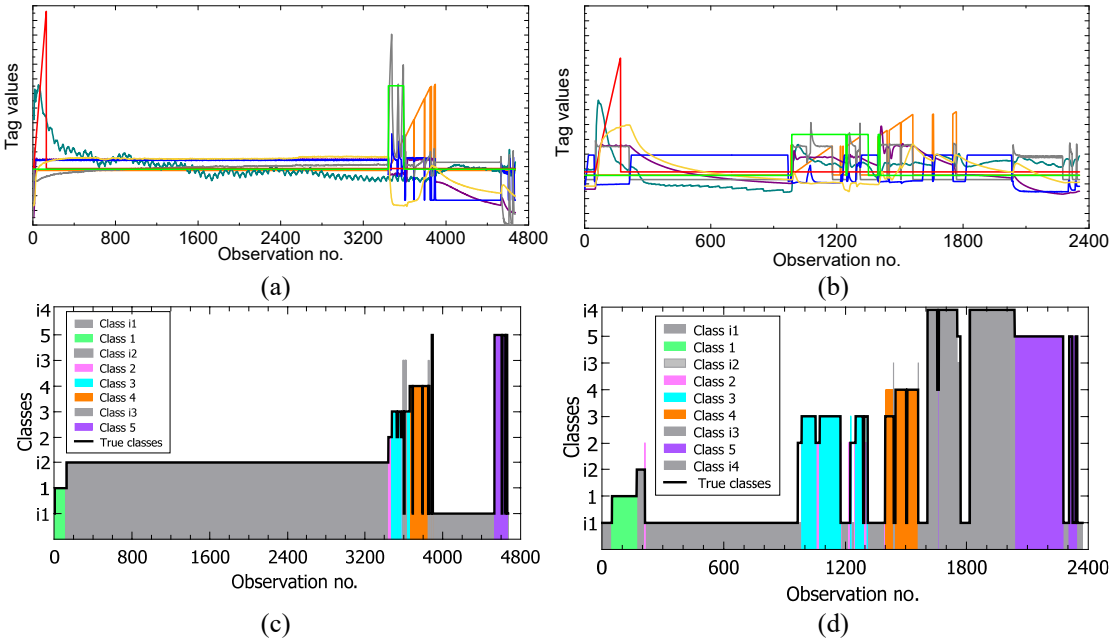

Figure 6.13. *Drying unit. Upper diagrams: representative tag profiles for validation batch (a) no.38 and (b) no.73; lower diagrams: class assignment as obtained from the k-NN classification model for validation batch (c) no.38 and (d) no. 73 (phase identification is done on the basis of Table 8). In (c) and (d), the classes assigned by the model are color-coded as indicated in the legend; the true class assignment is indicated by the black line.*

6.7 Batch identification and phase identification in Scenario 2

The availability of appropriate tags to carry out a tag-based batch identification procedure (Section 6.6.1) cannot be considered as a standard occurrence in secondary manufacturing environments. In fact, there might be units for which appropriate tags indicating the status of the unit or the duration of the operating phases are not available (Scenario 2 in Figure 6.1). In this section, an alternative methodology to identify single batches from historical datasets is presented. This methodology, which we call phase-based batch identification, works *jointly* with a phase identification procedure, and therefore requires to preliminarily identify the operating phases within the **D** or **G** datasets (Section 6.7.1). This information is then used to reconstruct the information needed to identify each single batch included in **D** or **G** (Section 6.7.2).

As a demonstration example, the methodology will be applied to the granulation unit only (even if, as discussed earlier, tag-based batch identification is actually possible for this unit).

6.7.1 Phase identification in the entire data historian

The identification of the operating phases within the data historian can be carried out using the pattern recognition technique illustrated in Section 6.6.3 even if the batch segments are not available. In fact, to build the *k*-NN classification model, one needs to *i*) visually identify the set **C** of calibration batches within the data historian (**G**), and *ii*) assign each observation of **C** to a class. Once the model is built, it can be used to classify each single observation remaining in the historian, regardless of the fact that the observation has already been attributed to a batch or not. The class assignments for all observations are then collected in vector $\hat{\mathbf{c}}$.

6.7.2 Phase-based batch identification

Since the phase identification operation is carried out observation-by-observation, by arranging the observations in chronological order, the identification of sequences of operating phases belonging to different batches can be obtained: the first observation included in $\hat{\mathbf{c}}$ that belongs to the first operating phase indicates the start of a batch, whereas the last observation classified as belonging to the last operating phase indicates the end of that batch.

6.7.2.1 Results for the granulation unit

To be consistent with the assumption that leads to follow Scenario 2[***], a different set of tags was included in a new overall dataset $\widetilde{\mathbf{G}}$. Namely, some tags (which do relate to the batch length) were removed from **G**. The tags removed are the number 7, 8, 9 and 11. Since only Tag 6 (granulator discharge valve) indicates the duration of the granulation Phase 4, this tag was not removed.

The phase-based batch identification method was then applied to $\widetilde{\mathbf{G}}$ matrix, thus identifying 315 different "batches", i.e. many more than those (90) identified using the tag-based method (Section 6.6.1). To explain this difference, it should be noted that the historical data segments include events (e.g., valve openings) that in some cases occur *during* a batch, whereas in some other are totally unrelated to the batch operation. Since in most cases the correlation between tag values are not very different in these two occurrences, phase misclassifications may well occur. This, in turn, causes the wrong identification of these events as part of granulation batches that in fact do not exist. However, the "spurious" batches can be easily detected by the batch characterization procedure presented in the next section.

[***] Scenario 2 refers to datasets for which no tags explicitly indicating the start and end observations of a batch are available. Therefore, for these datasets, the tag-based batch identification procedure of Scenario 1 cannot be implemented.

6.8 Batch characterization

The methods allowing one to identify the single batches within an overall data historian also provide the number of different batches that have been carried out along the window spanned by the historian. However, the batch identification methods cannot discriminate between "standard" batches (i.e., batches whose tag profiles conform to an assigned standard, as for example those reported in Figure 6.4 and Figure 6.5) and "non-standard" batches (i.e., batches that present a very different time evolution). There are several reasons why a batch might be classified as non-standard; among them: the presence of cleaning operations during a batch, the presence of operating segments repeated twice or lasting much longer than for other batches, partial testing on the equipment tests, or the processing of a new product. Note that the fact that a batch is denoted as non-standard is *not* related to the quality of the manufactured product, but only to the time evolution of the tags.

A method is proposed in this section to automatically detect those batches that present a time evolution that is significantly different from the standard ones. The method can also be used to characterize each batch depending on a set of features of industrial interest (e.g., duration of a given operating phase, load to an impeller, etc.). This may be a simple way to further verify that the manufactured product or associated process did not unexpectedly change characteristics over time. As such, the proposed procedure may contribute to periodic product quality reviews.

6.8.1 Batch characterization by PCA and k-NN modeling

The method requires building a feature matrix $\mathbf{F}^{\dagger\dagger\dagger}$ $[B \times V]$, where B is the total number of batches identified for a given operation, and V is the number of feature variables purposely defined for the unit where that operation is carried out. Each of these variables represents a specific feature of the batch set (e.g., the duration of an operating phase, or the time-integral or average value of some selected tags), which summarizes the dynamic evolution of the tags. Note that the values of some feature variables may be the outcome of Task 1 or Task 2 calculations.

The characterization of a batch can be obtained through the following procedure:

1. **F** is split into two matrices, a calibration matrix ($\mathbf{F}_{cal}$) and a validation matrix ($\mathbf{F}_{val}$);
2. a PCA model is built from $\mathbf{F}_{cal}$;
3. the model scores and loadings are analyzed in order to identify groups (clusters) of batches with similar characteristics (see Chapter 2, Section 2.2.2). Each cluster is assigned to a different class; the characteristics of each cluster can be highlighted by coupling a loadings plot analysis to a visual inspection of the tag profiles for the batches included in the cluster;

††† Note that, in this Chapter **F** is used to denote the feature matrix and not the residual matrix **F** as in the previous Chapters.

4. a *k*-NN classification model is built using the scores of the PCA model and the classes defined at step 3;
5. $\mathbf{F}_{val}$ is projected onto the PCA model, and the position of each batch of the validation set is analyzed in the score space. The batches that appear not to belong to any of the clusters identified at step 3 are denoted as "non-standard";
6. automatic characterization of the standard batches included in $\mathbf{F}_{val}$ is carried out using the *k*-NN model.

Next, application of this procedure is discussed with reference to the granulation unit. Similar results were obtained also for the drying unit.

6.8.1.1 Results for the granulation unit

The feature matrix $\mathbf{F}_G$ was built using the features indicated in Table 6.10, where $\mathbf{f}_{G,v}$ [B×1] indicates the v-th feature variable (v = 1, 2, …, V). Note that, although $\mathbf{f}_{G,8}$ is expected to always be zero, this variable was purposely included in the feature matrix in order to detect possible inconsistencies in the recorded tag values.

Table 6.10. *Granulation unit: feature variables defined for batch characterization.*

Feature variable name	Feature variable description
$\mathbf{f}_{G,1}$	Duration of Phase 1
$\mathbf{f}_{G,2}$	Duration of Phase 2
$\mathbf{f}_{G,3}$	Duration of Phase 3
$\mathbf{f}_{G,4}$	Duration of Phase 4
$\mathbf{f}_{G,5}$	Average impeller speed in Phase 1
$\mathbf{f}_{G6}$	Average impeller speed in Phase 2
$\mathbf{f}_{G,7}$	Average impeller speed in Phase 3
$\mathbf{f}_{G,8}$	Average chopper speed in Phase 1
$\mathbf{f}_{G,9}$	Average chopper speed in Phase 2
$\mathbf{f}_{G10}$	Average chopper speed in Phase 3
$\mathbf{f}_{G,11}$	Maximum impeller load

It is important to remark that different sets of features may be defined and included in **F**, according to the information that one wishes to extract from the available dataset.

A PCA model was built using a subset of $\mathbf{F}_G$ that includes 83 batches; the model used 2 PCs, capturing more than 73% of the data variability. The remaining 7 batches were used for model validation.

Figure 6.14a shows that most granulation batches (circles) are clustered in similar areas of the scores plane, with the exception of batches no. 51, 18, and possibly 69, which locate away from the main clusters. These three calibration batches are therefore different from the other ones, and as such they were denoted as non-standard. Analysis of the tag profiles for these batches revealed that the non-standard designation was truly justified by operational reasons, namely:

- batch 51 presented tag profiles that are strongly different from those usually found in standard granulation operations;
- in batch 18, Phase 1 was extremely prolonged;
- in batch 69, Phase 1 was repeated twice.

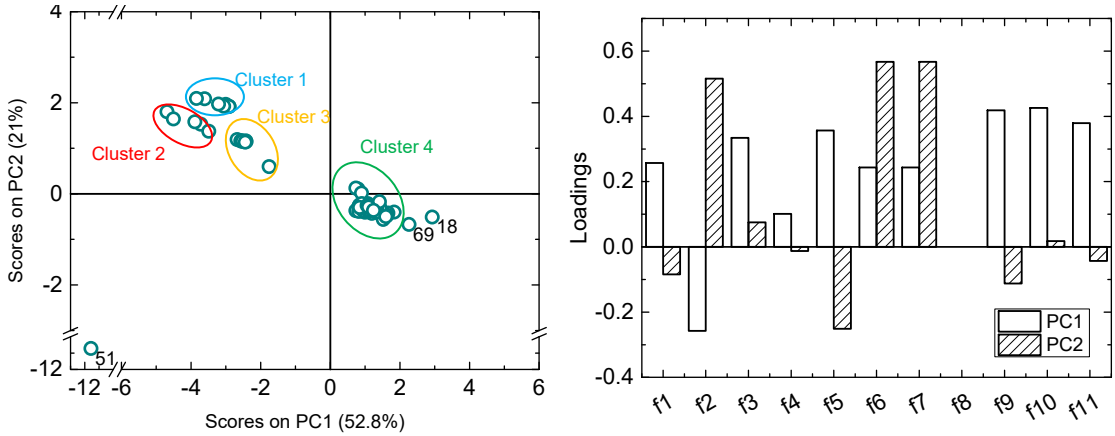

(a) (b)

Figure 6.14. *Batch characterization in the granulation unit: (a) loadings and (b) scores of the PCA model built on the calibration feature matrix. The numbers in the symbols indicate the batch number.*

The remaining calibration batches, which are visually grouped in four different clusters, were denoted as standard. Analysis of the PCA model loadings (Figure 6.14b) provided the following general considerations:

- the position of a batch along PC1 is mainly related to the impeller speed, the chopper speed, the duration of Phase 1 and the duration of Phase 3;
- the position of a batch along PC2 is mainly related to the duration of Phase 2 and to the impeller load.

Consequently, the main characteristics of each cluster were identified as reported in Table 6.11 The clusters (and related characteristics) served as the basis for the automatic characterization of the validation batches.

Table 6.11. *Granulation unit: characteristics of the 4 clusters defined to classify the calibration batches.*

	Batches included	**Batch characteristics**
Cluster 1	15, 45, 46, 47,65, 84, 85, 89,	Very long phase 2, low chopper speed, low impeller load
Cluster 2	38, 39, 81, 82, 83	Long phase 2, low chopper speed, low impeller load
Cluster 3	4, 5, 6, 23, 24, 78, 79, 80	Intermediate phase 2, low chopper speed, low impeller load
Cluster 4	All the other batches	Short phase 2, high chopper speed, high impeller load, different duration of phase 1

Projection of the validation data $\mathbf{F}_{val,G}$ onto the PCA model resulted in the red triangles of Figure 6.15.

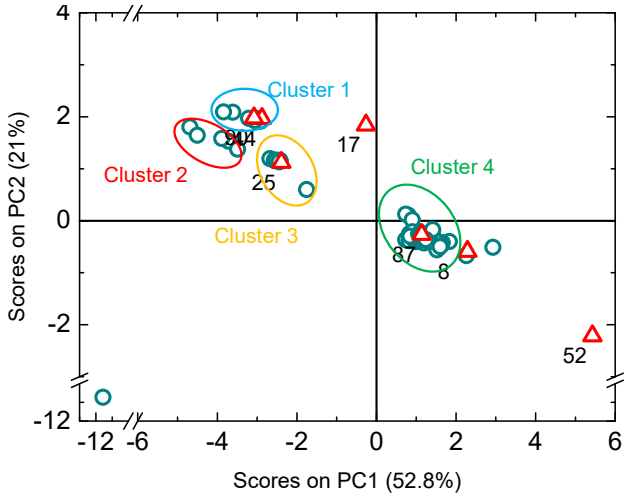

Figure 6.15. *Batch characterization in the granulation unit: projections on the scores plane of the 7 validation batches (red triangles). The numbers in the symbols indicate the batch number.*

Three non-standard validation batches were identified, namely batches no. 52, 17, and possibly 8. Inspection of the relevant tag profiles confirmed that:

- batch 52 presented tag profiles that are very different from those found in standard granulation operations;
- in batch 17, some operating phases were repeated twice;
- in batch 8, Phase 1 was very long.

Note that, although class assignment for the standard validation batches was done by visual inspection, assignment of these batches to the clusters identified in Figure 6.15 can be achieved also *automatically*, by simply building a classification model (e.g., a *k*-NN one) for the scores of the PCA model shown in Figure 6.15, and then using this classification model with the standard validation batches. Excellent classification results were indeed obtained by using this approach.

SECTION B – COMPARISON OF DIFFERENT PRODUCTION PERIODS USING RECIPE INFORMATION

6.9 Objectives of Section B

In the following Sections the analysis is carried out for both datasets assuming that information about the products manufactured is available in the form of *number* of products and manufacturing *recipe*.

In this second section, the same tags reported in Section 6.4.1 have been selected for the granulation unit. For the drying unit instead, Tag no. 3, 6 and 7 have been removed from the set reported in Section 6.4.2, and one more tag (related to the pressure difference) has been added, in order to improve the classification performance (Section 6.11). For each dataset *i*, the observations of the two datasets are arranged into two matrices ($\mathbf{G}_i$ and $\mathbf{D}_i$) whose characteristics are reported in Table 6.12. In the two production periods analyzed, four different products were manufactured. Using the available information about the manufacturing recipes may be appropriate to better tune the data review activity. In this section of the analysis, the methodology has been improved (Figure 6.16) using this new piece of information by modifying the batch characterization step.

Table 6.12. *Characteristics of the 2 datasets analysed in Part 2 for the granulation and the drying unit.*

	$\mathbf{G}_1$	$\mathbf{D}_1$	$\mathbf{G}_2$	$\mathbf{D}_2$
Unit	Granulation	Drying	Granulation	Drying
Dataset	Dataset 1	Dataset 1	Dataset 2	Dataset 2
Size	3127088×11	3127088×12	3127088×11	3127088×12

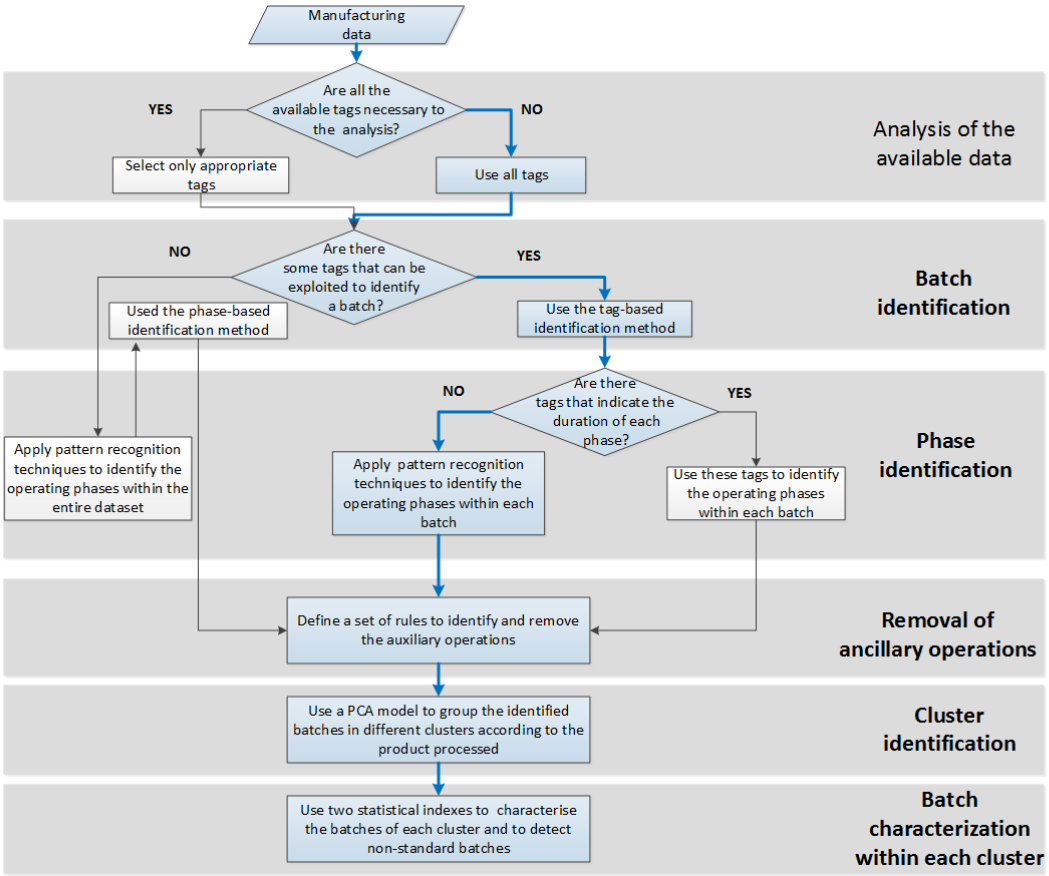

Figure 6.16. *Flowchart of the modified approach to analyze historical manufacturing data. In this study, only the steps following the blue path have been considered.*

Namely, three additional steps have been considered (Figure 6.16) with the purpose of:

- removing all the data segments that do not refer to actual drying/granulation batches (ancillary operation removal);
- grouping the identified batches in different clusters according to the product processed (cluster identification);
- characterizing each batch within each cluster in order to detect non-standard batches (batch characterization within each cluster).

The objectives of this section are the following: *i*) testing the performance of the methodology by also using the batch *recipes* as an information source (path marked in blue in Figure 6.16); *ii*) evaluating the consistency of the two available datasets, namely assessing whether the features characterizing a given batch operation have changed throughout the production periods analyzed.

6.10 Batch identification

Depending on the characteristics of the available tags, two methods were proposed (Section 6.2) to automatically recognize the start and end points of each batch within an historical dataset: tag-based batch identification and phase-based batch identification. In this study, the tag-based batch identification is used to identify the batches included in $\mathbf{G}_2$ and $\mathbf{D}_2$ using the same methodology employed for $\mathbf{G}_1$ and $\mathbf{D}_1$ in Section 6.6.1. The observations belonging to a single drying or granulation batch b are extracted and arranged into a new matrix $\mathbf{O}_b$ [$N_b \times T$], where the meaning of the symbols is the same as in Section 6.6.1.

6.10.1 Adjustments introduced in the tag-based batch identification

The tags available in $\mathbf{G}_2$ and $\mathbf{D}_2$ allow implementing the tag-based batch identification method for both units. In fact, one or more tags exist that unambiguously indicate when the equipment is (and is not) in operation.

In general, it is known a priori that some operations identified as single batches simply correspond to equipment tests or cleaning operations. Thanks to the information acquired in the analysis of Dataset 1 (Section 6.8) and to the new information available from the recipes, an additional analysis has been included in the proposed methodology to discriminate between these auxiliary operations and actual drying/granulation batches. This topic will be discussed in Section 6.12.1 .

For Dataset 1, an exploratory analysis of the batches identified by the tag-based batch identification procedure in Dataset 1 revealed that some of the operations, which had originally been recognized as *separate* batches, actually corresponded to *the same* batch that was interrupted for a short time period. For this reason, a post-batch identification procedure was implemented in Section 6.6.1 (both for the granulation unit and for the drying unit) in order to collect in the same matrix $\mathbf{O}_b$ only the observations that can be considered as belonging to the same operation. For

Dataset 2 this post-batch identification procedure cannot be applied, since there are some cases for which the gap between two consecutive data segments is less than a given threshold, but these segments do refer to truly different operations (usually a drying/granulation batch and a test/cleaning operation). Therefore, in order to apply the same procedure for both datasets, the post-batch identification was not applied to Dataset 1. As a consequence the number of batches identified in the following sections is different from those reported in Section 6.6.1.1 and 6.6.1.2

6.10.2.1 Results for the granulation unit

For the granulator, a granulation batch b can be easily singled out using the combination of Tag 11 and Tag 6. The relevant data were collected in matrix $\mathbf{O}_{G1,b}$ and $\mathbf{O}_{G2,b}$. Using this tag-based identification procedure, 99 different granulation batches were identified in $\mathbf{G}_1$ and 215 in $\mathbf{G}_2$.

6.10.2.2 Results for the drying unit

In this case, a single tag (Tag 1) is sufficient to recognize different drying operations, as this tag is active during the entire duration of the batch. Eventually, 99 different $\mathbf{O}_{D1,b}$ matrices and 214 $\mathbf{O}_{D2,b}$ matrices were defined for $\mathbf{D}_1$ and for $\mathbf{D}_2$ respectively.

6.11 Phase identification

In this section, the classification method employed to automatically recognize the operating phases characterizing a typical granulation/drying batch is tested on the batches identified within $\mathbf{G}_2$ and $\mathbf{D}_2$. In particular the k-NN models used in Section 6.6.3 for the granulation and the drying unit have been enhanced based on the information provided by the recipes of the product manufactured during the time windows under investigation, thus permitting to relax some assumptions previously considered for both units. Furthermore, in order to improve the reliability of the results, the performance of these classification models are tested on larger validation sets with respect to the validation sets considered above. Therefore, the objectives of this section are mainly two: *i*) assessing the performance of the new classification models, thus defining the limit of the analysis thanks to the availability of larger validation sets; *ii*) testing the ability of recognizing different operating phases in batches carried out in different time windows.

For both units, a k-NN model, which is the same for all products, was defined to classify the observations included in each $\mathbf{O}_b$ as belonging to one of the classes defined for each unit. The classification model is built from a set of calibration observations belonging to Dataset 1 for which the class assignment is known and therefore can be set a priori. The model is then used to classify new observations, i.e. the observations included in the batches of Dataset 2 (or of Dataset 1, but

not included in the calibration set). A subset[‡‡‡] of these batches (validation set) is then selected for each unit to test the model performance. The *k*-NN model classification performance is evaluated using the three metrics defined in Section 6.6.3.

6.11.1 Phase identification in the granulation unit

6.11.1.1 Design of the classification model

The *k*-NN model used to recognize different operating phases in the granulation batches of Dataset 1 has been updated according to the recipes provided for each of the four products manufactured during the six months investigated. In particular, six classes (Table 6.13) were considered instead of five as shown in Figure 6.17. These classes include the four operating phases that characterize the granulation process and two inter-phases. The new inter-phase has been introduced to better characterize the first part of the process, which differs according to the product processed. A calibration matrix $\mathbf{C}_G$ is defined by collecting 7 batches of Dataset 1 selected by a preliminary exploratory analysis, including at least one batch for each of the 4 products considered in this work. Note that, thanks to the availability of the recipes, a representative batch for each manufactured product can be included in the calibration matrix. Matrix $\mathbf{C}_G$ includes $I = 8451$ observations (each observation corresponds to 5 s) and $T = 11$ variables (tags). The classification model characteristics are summarized in Table 6.14.

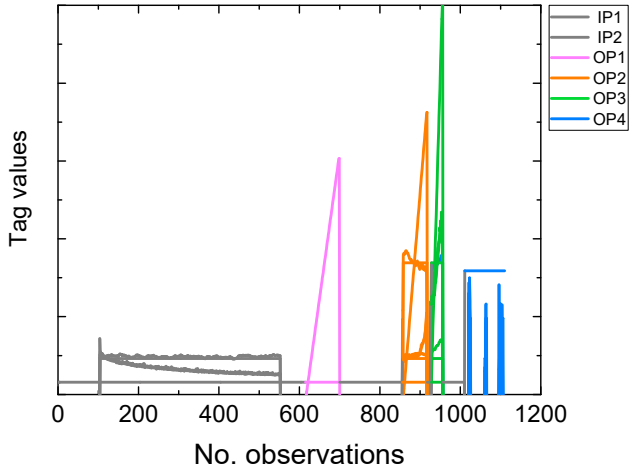

Figure 6.17. *Granulation unit: classes identified for a representative granulation batch of the calibration set. The four operating phases (OPs) are coloured respectively in pink, orange, blue and green, whereas the inter-phases (IPs) are marked in grey. For clarity, a few tags only are reported. The y-axis scale has been masked to protect data confidentiality.*

[‡‡‡] Assigning the correct class to each single observation included in both calibration and validation dataset is a time consuming task, because class assignment is done on the basis of a visual analysis of the time profiles of the tags available for each observation. For this reason only a subset of the available batches is selected.

Table 6.13. *Granulation unit: main characteristics of the k-NN model used for phase identification.*

No. of neighbours	Distance criterion	Data pre-treatment	No. of classes
5	Euclidean distance	Autoscaling on $\mathbf{O}_b$ columns	6

Table 6.14. *Granulation unit: list and description of the classes identified for this process.*

Class no.	Phase type	Description
i1	Inter-phase	Interval between phases
i2	Inter-phase	Pre-Phase 1
1	Phase 1	Dry-mixing phase
2	Phase 2	Solution addition phase
3	Phase 3	Wet-massing phase
4	Phase 4	Discharge of the material

6.11.1.2 Phase identification for the validation batches

Only minor changes have been implemented in the classification model defined for the granulation unit, so the results achieved for Dataset 1 are very similar to those presented in Section 6.6.3.1 . Hence, for the sake of conciseness, only the results obtained testing the classification model on a set of batches of the new dataset (Dataset 2) are reported.

A set of 8 validation batches of Dataset 2 is used to test the performance of the classification model. The classification results obtained for each validation batch are reported in Table 6.15, whereas in Figure 6.18 a graphical representation of the results is provided by grouping all the batches that present similar classification errors. The results obtained are very similar to those achieved for Dataset 1 in Section 6.6.3.1 , where the wrong class assignments are found mainly at the very beginning of a true operating phase. The error rate ER never exceeds 1%, meaning that only an average of about 5 observations out of 990 are assigned to a wrong class. Moreover, both the sensitivity and the specificity (the values calculated for this index have not been reported here for conciseness) are high for each class.

Table 6.15. *Granulation unit: phase identification results for the validation batches (Dataset 2), in terms of error rate and sensitivity for each class.*

Valid'n batch no.	No. of obsrv'ns	ER	Sn_{i1}	Sn_{i2}	Sn_1	Sn_2	Sn_3	Sn_4
101	635	0.008	0.994	-	1	0.991	0.920	1
112	1722	0.002	1	0.999	0.988	0.984	0.977	1
132	2742	0.001	1.000	0.998	0.988	1	0.971	1
145	906	0.004	0.995	0.997	1	1	0.949	1
156	1172	0.003	0.998	1	0.988	0.984	0.971	1
178	1053	0.003	1	-	0.984	1	0.950	1
244	746	0.008	1	-	0.936	1	0.926	1
281	936	0.009	0.999	-	0.920	1	0.920	1

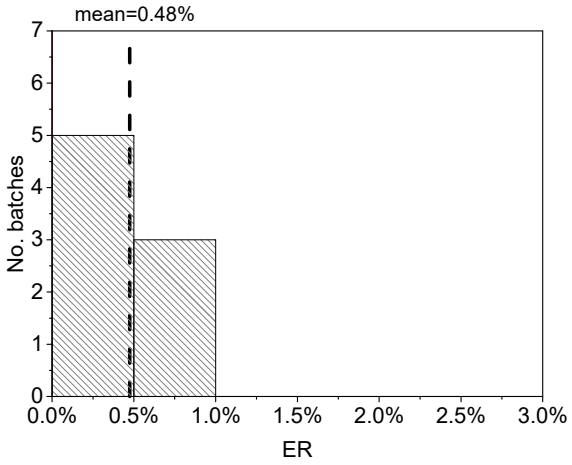

Figure 6.18. *Granulation unit: distribution of the classification errors calculated for 10 validation batches of Dataset 2.*

6.11.2 Phase identification in the drying unit

6.11.2.1 Design of the classification model

The availability of the recipes for the four products manufactured during the time windows under investigation strongly contributes to improve the identification of the operating phases that characterize the drying unit, allowing one to:

- discriminate between the cooling and discharge phase (Phase 5 and 6);
- consider the presence of an additional inter phase related to the final phase of the batch;
- recognize the different time evolution of the batches depending on the product manufactured.

However, no information is available to clearly discriminate between the falling and constant drying rate, whose starting points remains uncertain.

The *k*-NN model used to identify the operating phases for the batches of Dataset 1 has been modified considering a different number of classes and a different calibration set. In fact, by analyzing the trends of the available tags jointly with the information included in the recipes (duration of some phases, values of some tags), 10 classes were eventually defined as reported in Table 6.16. Six of them denote true operating phases, whereas the remaining four classes represent recurrent events (not necessarily present in all batches), which were classified as inter-phases. A calibration matrix $\mathbf{C}_D$ including 7 batches purposely selected to consider all the products manufactured has been defined. This matrix includes $I = 13886$ observations (each observation corresponds to 5 s) and $T = 13$ variables (tags), selected by engineering reasoning in such a way as to minimize the classification errors.

Table 6.16. *Drying unit: list and description of the classes identified for this process.*

Class no.	Phase type	Description
i1	Inter-phase	Break phase
1	Phase 1	Pre-heating phase
i2	Inter-phase	Break phase after the pre-heating phase
2	Phase 2	Charging phase
3	Phase 3	Constant-drying rate phase
4	Phase 4	Falling-drying rate phase
i3	Inter-phase	Break phase
5	Phase 5	Cooling-down
6	Phase 6	Discharge
i4	Inter-phase	Break phase related to the filter shaking

A graphical representation of the classes identified during model building is provided in Figure 6.19 for a typical calibration batch. Note that all tags related to phase duration were modified as done for the granulation data. Details on the *k*-NN model built for the drying unit are reported in Table 6.17.

Table 6.17. *Drying unit: main characteristics of the k-NN model used for the phase classification.*

No. of neighbours	Distance criterion	Data pre-treatment	No. of classes
5	Euclidean distance	Autoscaling of $\mathbf{O}_b$ columns	10

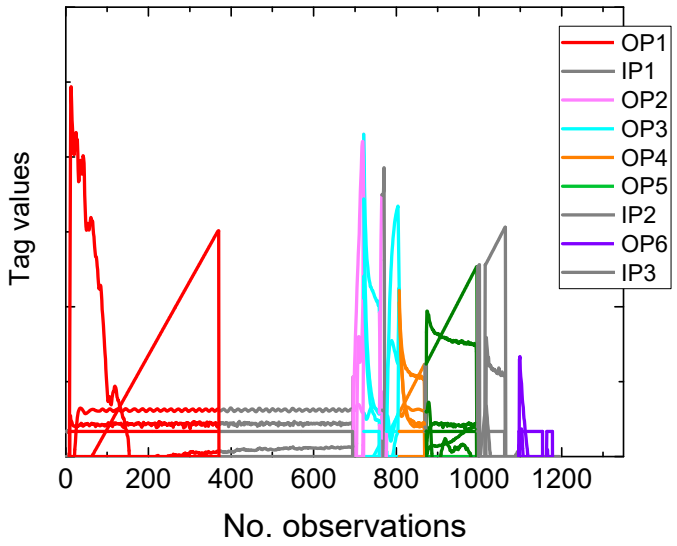

Figure 6.19. *Drying unit: classes identified for a representative drying batch of the calibration set. The six operating phases (OPs) are coloured respectively in red, pink, blue, orange, green and purple whereas the inter-phases (IPs) are marked in grey. For clarity, a few tags only are reported. The y-axis scale has been masked to protect data confidentiality.*

6.11.2.2 Phase classification for the validation batches of Dataset 1

The new *k*-NN model built for the drying unit is tested on a validation set of 10 batches belonging to Dataset 1 in order to assess the effects of the adjustments introduced. A summary of the phase identification results is reported in Table 6.18, from which it can be observed that:

- the error rate ER ranges from 0.7% to 6.7%, with an average value of 2.4%, namely about 47 observations out of 2160 are assigned to a wrong class. A graphical representation of the results obtained for this index is provided in Figure 6.20 by grouping all the batches that present similar classification errors;
- the sensitivity index Sn_p indicates that, for all batches, the model does a very good job in classifying classes 1, 2, 3, 7, 8 and 9 (see Table 6.16 for class/phase correspondence). For some batches the model is not able to correctly recognize the observations belonging to class 4, 5, 6 and 10. Anyway, it should be highlighted that for the batches that present a low value of sensitivity index related to class 4, actually Phase 4 is very short and the temperature increasing is not significant. The model is not able to correctly identify Phase 4 for all batches with the same characteristics;
- the specificity index has not been reported since it was observed that in general the values of this index are satisfactorily high for all classes and all batches.

Table 6.18. *Drying unit: phase identification results for the validation batches of Dataset 1, in terms of error rate and sensitivity for each class.*

Valid'n batch no.	No. of obsrv'ns	ER	Sn_{i1}	Sn_1	Sn_{i2}	Sn_2	Sn_3	Sn_4	Sn_{i3}	Sn_5	Sn_6	Sn_{i4}
5	1195	0.016	0.976	0.997	1.000	0.886	1.000	0.903	-	0.984	0.975	0.963
6	1269	0.027	0.988	1.000	1.000	0.979	1.000	0.125	-	0.895	0.956	0.882
16	1845	0.020	0.966	0.976	1.000	0.985	0.881	1.000	-	-	1.000	0.783
26	2663	0.010	0.997	0.984	1.000	1.000	0.995	0.879	-	-	0.983	0.889
27	1760	0.016	0.986	0.992	1.000	1.000	0.900	0.952	1.000	-	1.000	-
35	1500	0.067	0.994	1.000	1.000	0.983	0.637	0.980	-	-	0.987	0.074
44	4672	0.014	0.996	0.992	1.000	0.971	0.819	0.983	-	-	0.966	0.381
82	2371	0.037	0.994	0.984	0.905	0.682	0.848	0.982	0.986	-	0.969	0.958
87	2058	0.026	0.927	0.997	1.000	0.957	0.936	0.043	-	0.976	1.000	0.581
92	2269	0.007	1.000	0.992	1.000	0.977	1.000	0.939	-	-	0.974	0.840

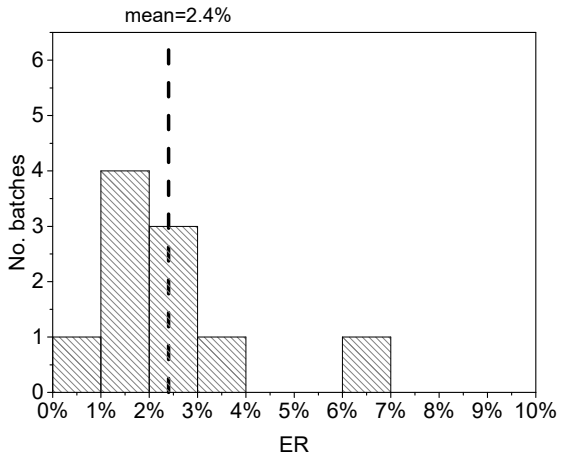

Figure 6.20. *Drying unit: distribution of the classification errors calculated for 10 validation batches of Dataset 1.*

6.11.2.3 Phase classification for the validation batches of Dataset 2

The same classification model is then used to recognize different operating phases in 13 batches belonging to Dataset 2. A summary of the results is reported in Table 6.19. The error rate (Table 6.19) ranges from 2.1% to 12.5%. The average value (5.5%) is significantly higher than for the batches of Dataset 1. Particularly, note that for some batches the sensitivity index is very low for class 5 (Sn_3) and 10 (Sn_{i4}).

Table 6.19. *Drying unit: phase identification results for the validation batches of Dataset 2, in terms of error rate and sensitivity for each class.*

Valid'n batch no.	No. of obsrv'ns	ER	Sn_{i1}	Sn_1	Sn_{i2}	Sn_2	Sn_3	Sn_4	Sn_{i3}	Sn_5	Sn_6	Sn_{i4}
113	1609	0.037	0.939	1.000	1.000	0.972	0.869	0.988	-	-	0.747	-
119	938	0.125	0.893	0.777	1.000	0.950	1.000	0.645	-	-	0.927	0.632
125	1617	0.073	1.000	0.779	1.000	1.000	0.734	0.971	-	-	0.790	0.667
131	755	0.096	0.926	0.967	1.000	0.968	0.376	0.988	-	-	0.695	0.000
136	2793	0.069	0.806	0.992	1.000	0.960	0.474	0.990	0.920	-	0.500	1.000
176	1768	0.027	0.937	0.964	1.000	0.985	1.000	0.875	-	0.886	0.964	0.750
190	1882	0.049	0.892	0.992	0.998	1.000	0.710	0.991	0.968	-	0.957	0.667
209	2195	0.045	0.982	0.989	1.000	0.985	0.633	0.966	-	-	0.968	0.476
213	1421	0.043	0.948	0.992	1.000	1.000	1.000	0.797	0.357	-	0.964	0.500
231	1236	0.047	0.862	1.000	1.000	1.000	0.989	0.818	-	-	0.987	0.810
237	2133	0.045	0.919	0.857	1.000	0.965	0.917	0.990	0.996	-	0.784	0.231
243	2011	0.038	0.971	0.833	0.997	0.977	1.000	0.892	-	-	0.906	0.826
261	1506	0.021	0.962	0.992	1.000	1.000	1.000	0.846	-	-	0.944	0.962

In order to improve the results, a new classification model has been defined, considering a different calibration matrix $\mathbf{C}_{D,2}$. Namely, the new $\mathbf{C}_{D,2}$ [10372×13] includes 7 batches of Dataset

2 and the same tags of $\mathbf{C}_D$. Details on the *k*-NN model built for the drying unit are reported in Section 2.2.1. Note that $k = 9$ neighbours were used.

Table 6.20. *Drying unit: main characteristics of the k-NN model used for the phase classification of Dataset 2.*

No. of neighbours	Distance criterion	Data pre-treatment	No. of classes
9	Euclidean distance	Autoscaling of $\mathbf{O}_b$ columns	10

A comparison of the results reported in Table 6.19 (referring to the classification performed with the *k*NN model built considering a calibration set of Dataset 1) and Table 6.21 (referring to the classification performed with the *k*NN model built considering a calibration set of Dataset 2) demonstrate that the use of a different calibration set significantly improves the classification performance[§§§]:

- using $\mathbf{C}_{D,2}$ the error rate ER (Table 6.21) ranges from 1.3% to 4.9% , with an average value of 3.3%, namely about 59 observations out of 1760 are assigned to a wrong class. The ER calculated using $\mathbf{C}_{D,2}$ results to be smaller for all the batches considered in the validation set, apart from batch 113 and 237.
- the comparison of the sensitivity index Sn_p indicates that with the new classification model the classification errors for class 3 decrease but slightly increase for class 4 (note that for batch 176 in Table 6.21, Sn_4 is low for the same reason of batches 6 and 86 of Dataset 1). This result suggests that the calibration set could be optimized to reduce this error. Finally the classification errors for class 10 remains high, indicating that the new model is also unable to recognize this phase exactly. Note that usually this is a very short phase, where the variable trend is very irregular.

These results lead to the conclusion that, across the time windows analyzed in this study, the drying operation displays a higher variability than the granulation operation. Therefore, for certain process, a classification model built on the basis of the batches performed in a given time window may not be appropriate to reliably classify batches belonging to different time windows. A graphical comparison of the ER calculated for each batch of the validation set of Dataset 2 is reported in Figure 6.21.

[§§§] The specificity index has not been reported for the same reasons explained for Dataset 1.

Table 6.21. *Drying unit: phase identification results for the validation batches, in terms of error rate and sensitivity for each class.*

Valid'n batch no.	No. of obsrv'ns	ER	Sn_{i1}	Sn_1	Sn_{i2}	Sn_2	Sn_3	Sn_4	Sn_{i3}	Sn_5	Sn_6	Sn_{i4}
113	1609	0.049	0.946	1.000	1.000	0.958	0.983	0.548	-	-	0.716	-
119	938	0.044	0.982	0.893	1.000	0.950	0.930	0.984	-	-	0.891	0.632
125	617	0.046	1.000	0.836	1.000	0.983	0.828	0.895	-	-	0.967	0.533
131	1755	0.042	0.957	0.950	1.000	0.968	0.794	0.963	-	-	0.841	0.000
136	2793	0.047	0.806	0.959	1.000	0.960	0.805	0.893	0.977	-	0.630	1.000
176	1768	0.019	0.969	1.000	1.000	0.955	1.000	0.313	-	0.935	0.973	0.750
190	1882	0.041	0.946	0.984	0.998	0.982	0.988	0.550	0.988	-	0.968	0.733
209	2195	0.013	0.994	0.989	1.000	0.985	0.982	0.980	-	-	0.952	0.619
213	1421	0.030	0.960	0.992	1.000	1.000	1.000	0.967	0.000	-	0.982	0.467
231	1236	0.023	0.962	0.992	1.000	1.000	0.928	1.000	-	-	0.974	0.810
237	2133	0.049	0.958	0.845	1.000	0.947	0.989	0.542	0.996	-	0.938	0.231
243	2011	0.016	0.987	0.975	0.997	0.977	0.944	0.985	-	-	0.943	0.826
261	1506	0.013	0.984	0.992	1.000	1.000	1.000	0.915	-	-	0.963	0.923

In Figure 6.22 the results of the phase classification performed with the new classification model are reported for a batch that presents a very low value of ER (batch no. 261, Figure 6.22a) and for a batch which presents an high value of ER (batch no.125, Figure 6.22b). Note that batch 125 presents a very peculiar variable trend: for this reason, some batches which present a similar anomalous trend were purposely included in the validation set.

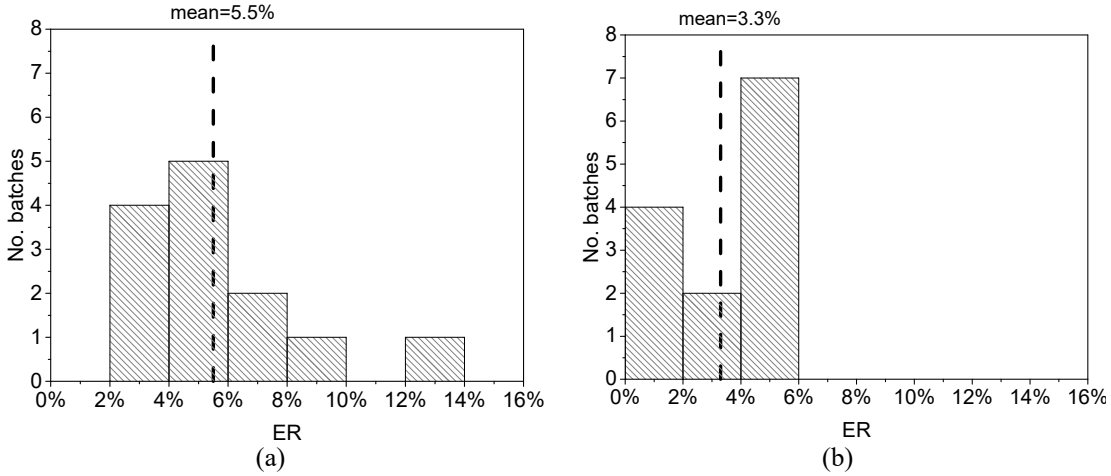

Figure 6.21. *Drying unit: distribution of the classification errors calculated for 13 batches of Dataset 2: (a) using a k-NN model built on* $\mathbf{C}_D$ *and (b) using a k-NN model built on* $\mathbf{C}_{D,2}$.

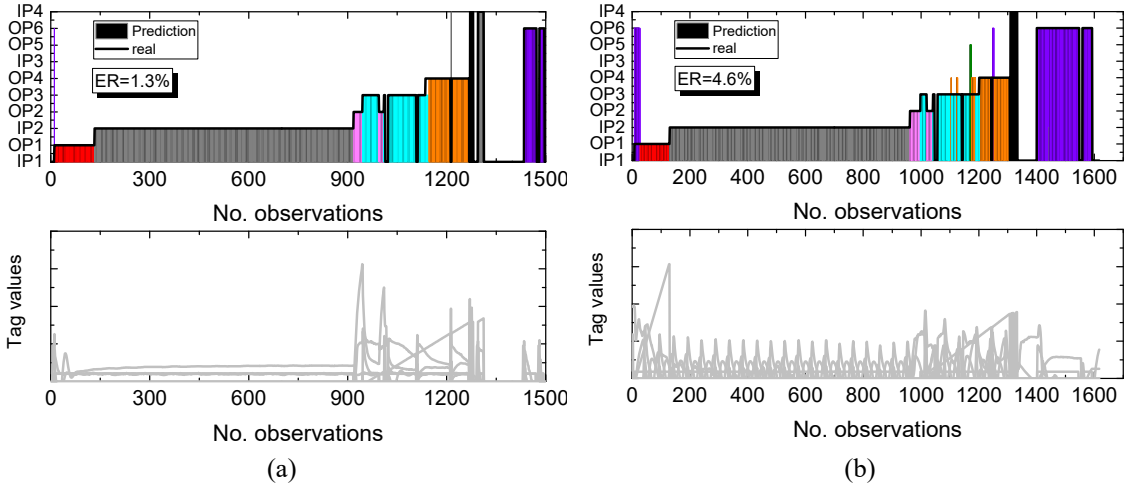

Figure 6.22. *Drying unit: representative tag profiles and class assignment as obtained from the k-NN classification model for (a) validation batch no.261 and (b) validation batch no.125.*

6.12 Batch characterization

In Section 6.8 , principal component analysis was used to characterize each batch depending on a set of features of industrial interest and to automatically detect those batches that present different characteristics from the standard ones; these batches were denoted as “non-standard” batches (i.e., batches that present a very different time evolution with respect to those recognized as standard). The term “non-standard” has been used with reference to cleaning operations and equipment tests, as well as for anomalous drying/granulation batches. However, a discrimination between these two categories appears more appropriate, since the recipe availability can help one to clearly discriminate between these two categories. Therefore, in this section the term ‘non-standard’ will be used to refer only to those batches that present a different behavior from a standard batch, but which are still recognizable as drying/granulation batches. For this reason, an additional step has been introduced in the overall methodology to remove from the dataset to be characterized all the operations that are not actual batches (Section 6.12.1).

In the two sections to follow, a batch characterization methodology is presented that can be applied separately to the granulation unit and to the drying unit. In particular, PCA is used for different purposes: *i*) to recognize different clusters of batches, each of which referring to one of the products manufactured during the time window under investigation (*cluster identification*, Section 6.12.2); *ii*) to characterize each batch with respect to the batches of the same cluster (*batch characterization within each cluster*, Section 6.12.3).

6.12.1 Removal of non-drying/granulation batches

The characterization (provided in Section 6.8) of batches within the overall historical databases **G** and **D** reveals the presence of operations that are not actual drying or granulation batches, but are instead short batch segments or possibly auxiliary operations (such as cleaning or test runs). A preliminary analysis of the batches included in Dataset 2 revealed the presence of a significant number of operations with the same characteristics. Therefore, since these operations are not relevant for the aim of this analysis, an additional step has been introduced in the overall methodology in order to identify and automatically remove all of them from the investigated datasets. To this purpose a set of rules have been defined for both units, based on the information extracted from the available recipes, to remove these operations. Therefore, the number of different batches that were carried out during the six-month window investigated in this study are reported in Table 6.1[****].

Table 6.22. *Number of real batches and number of ancillary operations removed from included in each datasets analyzed.*

	G_1	G_2	D_1	D_2
Number of batches	89	141	88	142
Number of ancillary operations	10	74	11	72
Total number of operations	99	215	99	214

The rules are based on the identification of the most common features that discriminate a real drying/granulation batch from a different operation, but false negatives (drying/granulation batches recognized as different operations) may occasionally exist, as well as false positives (tests/ cleaning operations recognized as actual drying/granulation batches).

6.12.2 Cluster identification

A feature matrix **F** [$B \times V$] is defined, where B is the total number of batches identified for a given operation, and V is the number of feature variables defined for each unit. Since the aim of this analysis is to cluster the batches according to the product manufactured, only a subset of $\overline{V}$ variables is selected out of the total number V. These variables should contain the information needed to differentiate the batches according to the product processed; on the other hand, including additional information able to discriminate between batches within the same cluster is not required at this point (that is the purpose of Section 6.12.3). Regardless of the unit, the classification of a batch can be obtained following the same procedure presented in Section 6.8.1, where the calibration matrix ($\overline{\mathbf{F}}_{cal}$) and a validation matrix ($\overline{\mathbf{F}}_{val}$) are built considering respectively the batches of Dataset 1 and Dataset 2.

[****] Note that the identification numbers of the granulation and drying batches reported in the following, change from those reported in Section 6.11, as a consequence of the removal of the ancillary operations from the entire dataset.

6.12.3 Batch characterization within each cluster

A procedure is proposed in this section to automatically discriminate between "standard" batches and "non-standard" batches within each cluster (where "non-standard" batches are those presenting a different time evolution with respect to those recognized as standard). Regardless of the unit, the characterization of a batch within each cluster can be obtained through the following procedure:

1. a calibration matrix ($\mathbf{F}_{cal}^{cluster\_n}$) and a validation matrix ($\mathbf{F}_{val}^{cluster\_n}$) are built for each *n*-th cluster, using all the batches of Dataset 1 and Dataset 2 available for that given cluster. The *entire* set of features *V* defined for the unit under investigation is considered;
2. a PCA model is built from each $\mathbf{F}_{cal}^{cluster\_n}$, selecting a number of principal components (PCs) able to appropriately describe the variability of the dataset;
3. each $\mathbf{F}_{val}^{cluster\_n}$ is projected onto the correspondent PCA model.
4. the model scores are analyzed visually in order to identify batches with similar characteristics;
5. two indices, namely the Hotelling's T^2 and the similarity factors (Krzanowski, 1979) are used to characterize each batch within each cluster, in order to discriminate batches that display different characteristics compared to the others. In particular, the Hotelling T^2 of each batch is used to isolate batches that have different features values. On the other hand, the similarity factors are used to compare the correlation structure of the measurements of a given batch to a reference one within the same cluster[††††]. Therefore, small values of the similarity factors and large values of the the Hotelling T^2 can serve as indicators of non-standard batches. In this study, the similarity factor formulation suggested by Gunther *et al*. (2009) is used (Eq. 6.4). Given a reference batch (*Ref*) and a generic batch *b*, the similarity factor $S_{Ref,b}$ indicates how similar the two batches (*Ref* and *b*) are with respect to the correlation structure characterizing their observations. Each $S_{Ref,b}$ can be calculated by comparing the loadings of the PCA model built on the reference batch to those of the PCA model built for batch *b* (with the two models being built on the same number *A* of PCs) as:

$$S_{Ref,b} = \frac{\text{trace}\left[\left(\mathbf{P}_{Ref}\right)^T\left(\mathbf{P}_b\right)\left(\mathbf{P}_{Ref}\right)^T\left(\mathbf{P}_b\right)\right]}{\sum_{a=1}^{A}\lambda_{Ref,a}\lambda_{b,a}} \quad , \tag{6.4}$$

where $\mathbf{P}_{Ref}$ and $\mathbf{P}_b$ are the loadings matrices respectively for the reference batch and for batch *b*, and λ_{Ref} and λ_b are the eigenvalues of the *a*-th principal component.

[††††] Within each cluster, the batch presenting low values of Hotelling's T^2 and SPE is selected as the reference batch for the evaluation of the similarity factors.

6.12.4 Results for the granulation unit

A set of features were identified to characterize the product manufactured by the granulation process, as reported in Table 6.23.

Table 6.23. *Granulation unit: feature variables defined for batch characterization.*

Feature variable name	Feature variable description
$\mathbf{f}_{G,1}$	Duration of Phase 1
$\mathbf{f}_{G,2}$	Duration of Phase 2
$\mathbf{f}_{G,3}$	Duration of Phase 3
$\mathbf{f}_{G,4}$	Duration of Phase 4
$\mathbf{f}_{G,5}$	Average impeller speed in Phase 1
$\mathbf{f}_{G6}$	Average impeller speed in Phase 2
$\mathbf{f}_{G,7}$	Average impeller speed in Phase 3
$\mathbf{f}_{G,8}$	Maximum impeller load
$\mathbf{f}_{G,9}$	Duration of the entire batch

6.12.4.1 Cluster identification

A subset of the above features, namely $\mathbf{f}_{G,1}$, $\mathbf{f}_{G,2}$, $\mathbf{f}_{G,3}$, $\mathbf{f}_{G,5}$, $\mathbf{f}_{G,6}$, and $\mathbf{f}_{G,7}$, are selected to build a calibration matrix $\overline{\mathbf{F}}_{cal,G}$ [89×6] and a validation matrix $\overline{\mathbf{F}}_{val,G}$ [142×6]. According to the available recipes, each feature assumes *different* and *specific* values for each product manufactured. Then, $\overline{\mathbf{F}}_{cal,G}$ was used to build a PCA model using 2 PCs, which captured more than 86% of the data variability. Figure 6.23a shows how the granulation batches (circles) with similar characteristics are located in the same area of the scores plane, forming four main clusters.

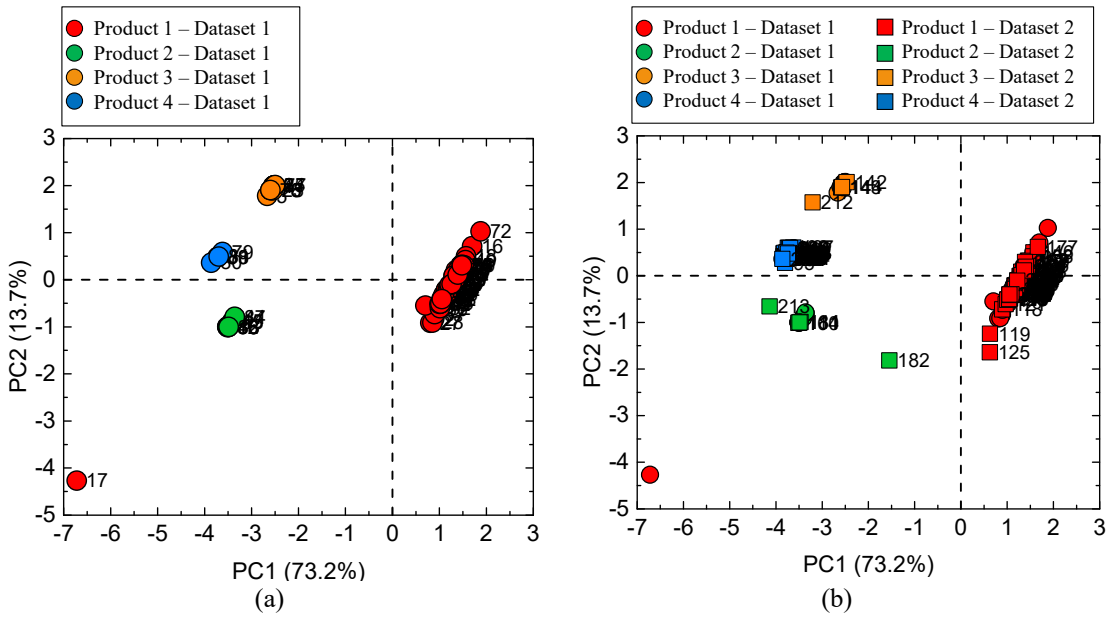

Figure 6.23. *Batch characterization in the granulation unit: (a) scores of the PCA model built on the calibration feature matrix, and (b) projections of the validation feature matrix.*

After building the PCA model, the batches included in $\overline{\mathbf{F}}_{val,G}$ were projected onto it, obtaining the scores projections shown in Figure 6.23b as squares. It is clear that batch 17 of Dataset 1 (Figure 6.23a) and batch 182 from Dataset 2 (Figure 6.23b) present different characteristics with respect to the other batches. Especially for batch 17, its location suggests a strong difference from the other batches.

A *k*-NN classification model was then built using the calibration scores obtained by the PCA model grouped according to the classes corresponding to the 4 clusters identified in Figure 6.23. After that, the scores resulting from the projections of the validation batches were classified *automatically* using the *k*-NN model.

6.12.4.2 Batch characterization within each cluster

For each cluster a new PCA model was built, considering the entire set of features defined for the granulation unit. The PCA model was built by considering a new calibration matrix for each cluster, $\mathbf{F}_{cal,G}^{cluster\text{-}n}$, including the batches of Dataset 1. Then, each validation matrix $\mathbf{F}_{val,G}^{cluster\text{-}n}$ has been projected on the latent space defined for each cluster. An example of the projections obtained for Cluster 1 (for which $\mathbf{F}_{cal,G}^{cluster1}$ includes 65 batches and $\mathbf{F}_{val,G}^{cluster1}$ includes 76 batches) is reported in Figure 6.23a, whereas in Figure 6.23b the same batches are plotted according to the values of the Hotelling T^2 and similarity factor calculated for each of them. In order to discriminate those batches tat present very different characteristics from the others, the threshold values of the two indices, namely 0.7 for the similarity factor, and the 95% limit for T^2 are indicated (anyway note that different values can be selected).

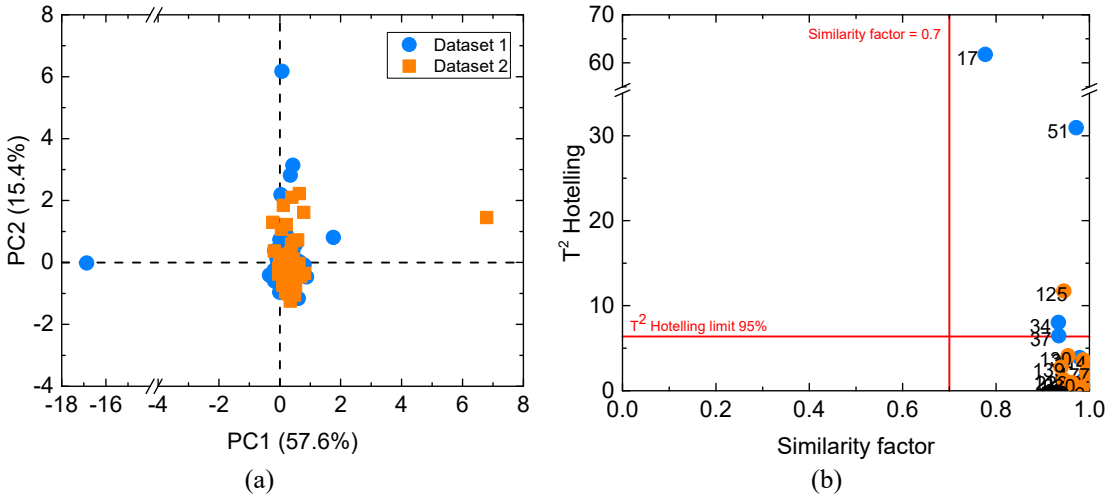

Figure 6.24. *Batch characterization within each cluster for the granulation unit: (a) comparison of the scores of Dataset 1 and 2 for cluster 1 and (b) values of the Hotelling's T^2 and similarity factors for each batch of the same cluster.*

The results for the first cluster (Figure 6.23b) suggest that the four batches that present large T^2 values, are non-standard batches. A-posteriori analysis of the tag profiles of these batches, carried out to investigate on the possible causes of the non-standard behavior, confirms that they actually present some anomalies respect to the batches of the same cluster. Finally, in Figure 6.23*a* the scores of Dataset 2 locate close to the scores of Dataset 1, indicating that the correlation structure of the two datasets is very similar; stated differently, for each product the granulation process conditions appear consistent across the investigated time frames.

6.12.5 Results for the drying unit

Similarly to the granulation unit, a set of features was defined to characterize the drying process (Table 6.24).

Table 6.24. *Drying unit: feature variables defined for batch characterization.*

Feature variable name	Feature variable description
$\mathbf{f}_{D,1}$	Duration of Phase 1
$\mathbf{f}_{D,2}$	Duration of Phase 2
$\mathbf{f}_{D,3}$	Duration of Phase 3
$\mathbf{f}_{D,4}$	Duration of Phase 4
$\mathbf{f}_{D,5}$	Duration of Phase 5
$\mathbf{f}_{D,6}$	Average inlet air temperature before Phase 2
$\mathbf{f}_{D,7}$	Average inlet air temperature during Phase 3
$\mathbf{f}_{D,8}$	Maximum value of product bed temperature during Phase 4
$\mathbf{f}_{D,9}$	Average inlet air volume before Phase 2
$\mathbf{f}_{D,10}$	Duration of Phase 2+ Phase 3+ Phase 4+ Phase 5
$\mathbf{f}_{D,11}$	Duration of the entire batch

6.12.5.1 Cluster identification

A subset of the feature variables were selected to recognize different products, namely no. $\mathbf{f}_{D,1}$, $\mathbf{f}_{D,6}$, $\mathbf{f}_{D,7}$, $\mathbf{f}_{D,8}$, and $\mathbf{f}_{D,9}$. A calibration matrix $\mathbf{F}_{cal,D}$ [88×5] was built considering the batches of Dataset 1, whereas a validation matrix $\mathbf{F}_{val,D}$ [142×5] was built considering the batches of Dataset 2. The first one was used to build a PCA model considering 2 PCs (which captured more than the 75% of the variability of the data). Figure 6.25a shows that, like in the granulation unit, the batches cluster in 4 clusters (i.e., 4 different products are identified). The projections of the validation batches onto the PCA model are shown in Figure 6.25b as squares. The Dataset 2 batches locate close to the four clusters identified for Dataset 1. As observed also for the granulation unit, some batches locate far from the others, and this happens for both datasets. Anyway, the investigation of how many and which batches present some anomalies respect to the others is the purpose of the batch characterization analysis within each cluster (Section .6.12.3.4).

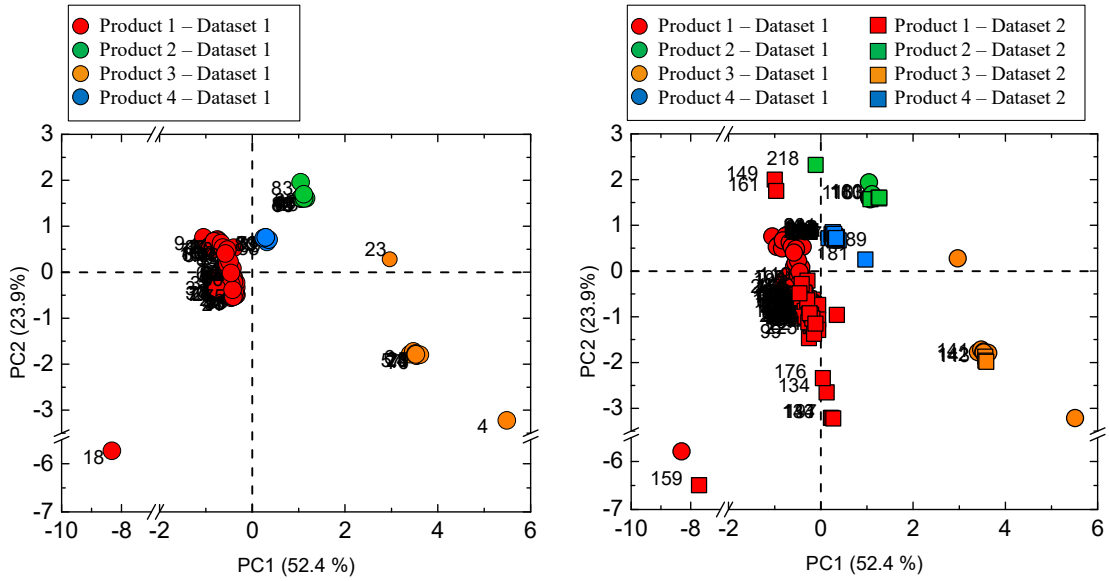

Figure 6.25. *Batch characterization in the drying unit: (a) scores of the PCA model built on the calibration feature matrix and (b) projections of the validation feature matrix.*

6.12.5.2 Batch characterization within each cluster

Using Dataset 1, a PCA model was built for each cluster (i.e., product) using a new calibration matrix ($\mathbf{F}_{cal,D}^{cluster-n}$) for each cluster. The projections of the $\mathbf{F}_{val,D}^{cluster-n}$ matrices on the model space built for each cluster, reveal the presence of a shift between the batches of the two datasets, which is particularly apparent for cluster 1 (Figure 6.26a, where $\mathbf{F}_{cal,D}^{cluster1}$ includes 65 batches and $\mathbf{F}_{val,D}^{cluster1}$ includes 75 batches). By analyzing the model parameters and the feature values, it is possible to identify the reasons of the shift observed that are mainly related to a different execution of the drying phases.

The results obtained by pairing the indices used to identify non-standard batches (Figure 6.26b, where the threshold for both indices is indicated) demonstrate the presence in cluster 1 of batches presenting large T^2 values and/or small similarity factor values. Actually, the analysis of the tag profiles of these batches reveals that all of them, except for batch 159, present anomalous trends and/or a different duration of an operating phase. Batch 159 does not present anomalies: it has been erroneously recognized as a non-standard batch due to the misclassification of some samples of phase 6.

The results obtained demonstrate the potential of the proposed methodology in revealing the presence of some differences between the datasets analyzed, and in disclosing the causes of these differences. However, some improvements should be considered further in order to prevent that some batches are identified as non-standard when they are actually standard batches and vice verse.

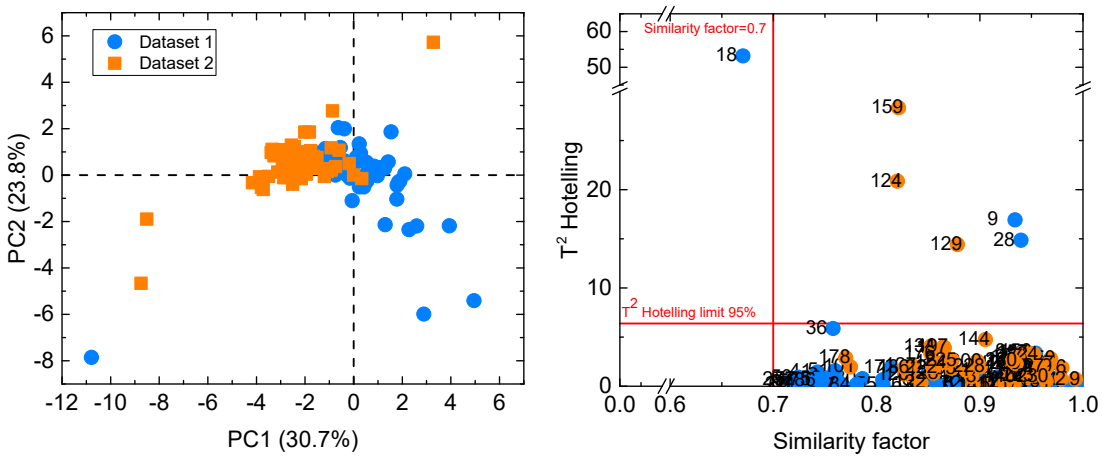

Figure 6.26. *Batch characterization within each cluster for the drying unit: (a) comparison of the scores of Dataset 1 and 2 for cluster 1 and (b) values of the Hotelling's T^2 and similarity factors for each batch of the same cluster.*

6.13 Implementation issues

Application of the proposed methodology to industrial historians may give rise to practical design and implementation issues. While providing a comprehensive list of issues that one may be required to face in an industrial environment is obviously impossible, we nevertheless believe that some issues are quite general and can be tackled by appropriate modeling assumptions. In this respect, note that the flowchart presented in Figure 6.1 describes a methodology that can be undertaken regardless of the specific nature of the unit operation under consideration.

Table 6.25 lists some implementation issues that are encountered frequently; suggested actions that may be taken to fix them are also indicated.

Table 6.25. *Possible solutions and recommendations to support the implementation of the suggested methodology.*

Issue	Suggested action
Preliminary analysis	
A tag is not recorded for the entire dataset.	• If the tag is not helpful to identify an operating phase (Task 2), remove it from the dataset. • If the tag is helpful to visually identify an operating phase, keep the tag only to perform the visual identification of phases, then remove it from the dataset.
A tag is very noisy	Filter its value; alternatively, remove the tag from the dataset if there are other tags providing similar information.
Task 1: batch identification	
Some consecutive batches isolated by the tag-based batch identification method actually correspond to the same batch.	This is usually due to temporary stall of the unit. Adjust the batch identification algorithm so as to cross-check the values of identification-relevant tags, and disregard from the analysis the data segments that, following tag cross-check, can be attributed to stalled operation.
Task 2: phase identification	
The classification results of the *k*-NN model are not satisfactory.	• Select a different distance criterion or a different value for *k.* • Assess whether removing one or more tags or tag segments improves the *k*-NN model performance (this may be helpful especially for very noisy tags).
During model building, it is apparent that the tag profiles that refer to a given batch phase change across the dataset.	This usually corresponds to different manufactured products. Include all these products in the calibration dataset.
A true operating phase is difficult to be identified.	Consider including this phase with the previous or successive one.
The start/end point of a phase in a unit cannot be detected accurately by visual inspection.	If the unit (Unit A) follows or precedes a different unit (Unit B), try to exploit a tag of Unit B to mark the phase start/end point in Unit A.
How many inter-phases should be considered?	The inter-phases correspond to operational segments presenting visually different combinations of the tag profiles.
Task 3: batch characterization	
The clusters identified by the PCA model are not representative of the true batch differences.	• Consider using more PCs. • Consider using different features in **F**.
How can a batch be marked as standard or non-standard?	An appropriate batch distance criterion may be considered (e.g., using *k*-NN modeling) to discriminate between standard and non-standard batches.
A group of batches has been wrongly recognized as non-standard.	Consider updating the calibration model including these batches.

6.14 Conclusions

In this Chapter, a methodology has been developed to retrieve operation-relevant information from historical secondary manufacturing databases. The methodology allows one to automatically perform three tasks: the identification (isolation) of single batches within the entire historical data sequence, the identification of distinct operating phases within each batch, and the characterization of a batch with respect to an assigned multivariate set of operating characteristics. Fulfilment of these tasks can allow a company to increase the fraction of historical data that is appropriately contextualized in full, which may lead to substantial savings in the life-cycle of a product. Because the proposed methodology aims at assessing the consistency of operations over a given time window(s) (e.g. monthly/quarterly) by providing visual diagnostics, it is naturally positioned to rapidly identify potential areas of improvements. For example, the presence of atypical phases in a unit operation, or in a more extreme case their absence, might relate either to operators not following the correct procedure or to the system not responding as expected. Similarly, the automated comparison between an extended number of batches might reveal subtler offsets, e.g. relating to the effect of changes in the supply line for one of the ingredients over time, which may not be immediately obvious otherwise. Conclusions drawn from the diagnostic charts can therefore be used to assess the need to implement ameliorative activities or corrective and preventing actions to avoid recurrence of undesirable events.

The methodology has been tested on two six-month datasets (Dataset 1 and Dataset 2) coming from two industrial manufacturing units: a high-shear wet granulator and a fluid-bed dryer. First, Dataset 1 has been analyzed demonstrating the potential of the methodology in handling different type of data and units, using no information about the products processed. Then, the methodology has been improved and tested on both datasets using new information coming from the recipes of the products manufactured during the time windows investigated. The results demonstrate that the methodology allows one to correctly recognize different operating phases for both units and to correctly classify batches according to the product processed. Finally, the application of the methodology permits also to reveal the presence of some differences in the process settings across the two available datasets. Additional improvements may be considered in future applications: *i*) a different metric/index may be identified to more properly detect anomalies in the batch evolution and to avoid a wrong classification of actual standard batches as non-standard batches; *ii*) the classification model may be enhanced by considering a larger calibration set; *iii*) the rules defined to discriminate a true drying/granulation batch from a different (“ancillary”) operation may be enhanced in order to reduce false negatives and false positives. However, the quality of results and the generality of the approach indicate that there is a strong potential for extending the method to larger historical datasets and different operations, thus making it an advanced PAT tool that can assist the implementation of continuous improvement paradigms, targeting consistent operation quality and easy monitoring of the entire manufacturing proces

Conclusions and future perspectives

Traditionally, the pharmaceutical industry has been subject to different attraction forces that led to the development of a bipolar character along the years: if on the one hand more and more cutting edge solutions were provided to respond to the rapid society evolution, on the other hand the manufacturing environment fossilized on well-known experience-based procedures, minimizing the interaction with the regulatory Agencies. Recently, market requirements have forced a radical change in the pharmaceutical sector, which is moving towards a more efficient industrial organization, based on a technologically advanced approach and on a more open attitude with respect to academic collaborations and new markets. A decisive contribution to this improvement has been provided by the new strategy adopted by the regulatory Agencies, which realized the importance of fostering pharmaceutical innovation by the introduction of *Quality-by-Design* (QbD) paradigms and by facilitating effective collaboration with the companies. The QbD approach aims to build quality *into* a product by using a thorough understanding of the product and process features and risks and by implementing appropriate strategies to control those risks. The implementation of QbD paradigms relies on the use of a systematic scientific-based approach that should support all the activities that characterize a pharmaceutical process; the knowledge acquired during these activities should represent the base for continual process and product improvement. From an engineering perspective, this represents the opportunity to adapt and expand to the pharmaceutical applications the knowledge acquired in more mature sectors, especially regarding process modeling activities (both knowledge-driven or data-driven). However, the rapidly expansion of the use advanced modeling tools is somewhat limited by the peculiar features of the pharmaceutical industry. The greater product complexity, low volume multi-product productions and the strict regulatory oversight that characterize this sector, all contribute to make the application of these advanced tools more challenging.

In this context, data-driven (DD) models have been demonstrated to be an optimal opportunity to address several problems that characterize pharmaceutical development and manufacturing. In this Dissertation, the potential of DD modeling, in particular of latent variable modeling and pattern recognition techniques, has been exploited to develop general methodologies that aim to strengthen the use process modeling (for example by facilitating first-principles model diagnosis) and foster the use of the historical available data. Their application may support the practical implementation of some fundamental elements of the QbD philosophy, from the definition of the design space to the use of knowledge acquired throughout product lifecycle.

Table 1 summarizes the main achievements of the Dissertation, with indication of the application considered and the data origin, as well as a reference to related papers that have been published or submitted to journal or conferences.

Table 1. *Summary of the main achievements of this Dissertation, with indication of the considered application, data origin and relevant references.*

Chapter	Main achievement	Application	Data origin	Reference
Chapter 3	General methodology to diagnose process/model mismatch in first-principles models for steady-state systems	• Continuous-stirred jacketed tank reactor • Milling	Simulated	Meneghetti, N., P. Facco, F. Bezzo, M. Barolo (2014). A methodology to diagnose process/model mismatch in first-principles models. *Ind. Eng. Chem. Res.*, **53**, 14002-14013. Meneghetti, N., P. Facco, F. Bezzo, M. Barolo (2014). Diagnosing process/model mismatch in first-principles models by latent variable modeling. In: *Computer-Aided Chemical Engineering 33* (J.J. Klemeš, P.S. Varbanov, P.Y. Liew, Eds.), Elsevier, Amsterdam (The Netherlands) 1897-1902.
Chapter 4	General methodology to diagnose process/model mismatch in first-principles models for dynamic systems	• Drying • Penicillin fermentation	Simulated	Meneghetti, N., P. Facco, S. Bermingham, D. Slade, F. Bezzo, M. Barolo (2015). First-principles model diagnosis in batch systems by multivariate statistical modeling. In: *Computer-Aided Chemical Engineering 37* (K.V. Gernaey, J.K. Huusom, R. Gani, Eds.), Elsevier, Amsterdam (The Netherlands), 437-442.
Chapter 5	Methodology to speed-up design space identification	• Nonlinear one-equation model • Dry granulation by roller compaction • Wet granulation	Simulated and laboratory (Vemavarapu *et al.*, 2009)	Facco, P., F. Dal Pastro, N. Meneghetti, F. Bezzo, M. Barolo (2015). Bracketing the design space within the knowledge space in pharmaceutical product development. *Ind. Eng. Chem. Res.*, **54**, 5128–5138.
Chapter 6	Methodology to automatically retrieve operation-relevant information in secondary manufactory system	• Granulation unit • Drying unit	Industrial	Meneghetti N., P. Facco, F. Bezzo, C. Himawan, S. Zomer, M. Barolo, 2015, Knowledge management in secondary pharmaceutical manufacturing by mining of data historians – A proof-of-concept study, submitted to: *Int. J. Pharm.* Meneghetti N., P. Facco, F. Bezzo, C. Himawan, S. Zomer, M. Barolo, 2016, Automated Data Review in Secondary Pharmaceutical Manufacturing by Pattern Recognition Techniques, to be presented at: ESCAPE 26, 26th European Symposium on Computer-Aided Process Engineering (Portorož, Slovenia, 12-15 June 2016).

With respect to **first-principles models diagnosis**, in Chapter 3 a methodology has been proposed to improve first-principles steady-state models designed to describe steady-states systems for which the presence of a process/model mismatch (PMM) has been observed. The aim of the methodology is to diagnose the cause of the PMM by exploiting only the historical and simulated data used to detect the presence of the PMM for the system under investigation, without carrying out any additional experiment. A PCA model is used to compare the correlation structure of two matrices, built considering a set of auxiliary variables calculated using the historical and a simulated data. Appropriate diagnostic indices permit one to pinpoint the model equations or model parameters that most contribute to the observed PMM.
In Chapter 4 the methodology has been modified to deal with dynamic models and to also consider systems with strongly correlated variables. Different simulated case studies were used to assess the effectiveness of the proposed methodology. The results obtained demonstrated that the methodology is effective in diagnosing the model sections affected by modeling errors. By facilitating the diagnosis of the PMM root causes, any additional experimental effort, which may be needed to enhance the first-principles model performance, can be targeted much more appropriately, and the overall need for experimental campaigns can therefore be reduced.

One of the main results of product and process understanding activities promoted by Quality-by-Design initiative is the determination of the **design space** (DS) for the manufacturing of a pharmaceutical product. The DS can be defined using first-principles models, when available, alternatively, its determination relies on experiments. In Chapter 5 a methodology has been proposed to support the determination of the design space using the historical data (e.g. material properties and process conditions) on products already developed that are similar to the new one under development; these historical data are often said to represent the knowledge space of the system. The methodology aims to find a narrower region within the knowledge space, called experiment space, within which the experiments needed to define the DS can be designed and carried out, thus reducing the experimental effort usually required. By means of a latent-variable model inversion approach, the knowledge space is segmented in such a way as to identify the experiment space in the latent variable space of the model. The segmentation makes use of the concept of null space and accounts for the existence of uncertainty in the model predictions.
Using three simulated case studies, it has been demonstrated that: *i*) the segmentation results are effective; *ii*) the segmentation effectiveness depends on the number of samples available in the historical dataset, but the appropriate number of samples does not necessarily need to be very large; *iii*) the graphical representation of the experiment space identified in a multivariate latent variable space is clear also when the number of process inputs is large.

Finally, in Chapter 6 a methodology was proposed to support the implementation of continual improvement paradigms, by the **periodic review of large manufacturing databases**. In order to

retrieve operation-relevant information from historical secondary manufacturing databases, the proposed methodology allows one to automatically carry out four tasks: *i*) the identification (isolation) of single batches within the entire historical data sequence, *ii*) the identification of distinct operating phases within each batch, *iii*) the characterization of a batch with respect to an assigned multivariate set of operating characteristics, and *iv*) the comparison of batches carried out in different time windows. Fulfilment of these tasks can allow a company to increase the fraction of historical data that is appropriately contextualized in full in order to monitor the evolution of the manufacturing campaigns over time and to detect possible exceptions, which may lead to substantial savings in production. The methodology has been tested on two historical datasets of two industrial manufacturing units (a high-shear wet granulator and a fluid-bed dryer). The quality of results and the generality of the approach indicate that there is a strong potential for extending the method to even larger historical datasets and to different operations.

In summary this Dissertation has shown how LVMs can be considered as an advanced flexible tool whose potential can be exploited in many different applications. Thanks to their multivariate nature, the possibility to handle large amount of data regardless their source and the ability of investigate their correlation structure, DD models have been demonstrated to be a fundamental PAT tool to support the implementation of QbD paradigms.

One of the main contributions of this Dissertation is the demonstration of the ‘‘power’’ of the pharmaceutical process data. Manufacturing data should be considered not only as a means to monitor the quality of product or the real-time performance of a manufacturing system, but also as a fundamental source of information about the history of the process itself. This information can be extracted and exploited to accomplish many objectives that lead to the realization of a pharmaceutical quality system.

The studies carried out in this Dissertation have opened further perspectives, which could be addressed in future research. For example, an interesting area open to **further investigation** is the improvement of the methodology used to identify a PMM in Chapters 3 and 4. First, a general procedure to systematically select proper auxiliary variables should be defined, as well as appropriate confidence limits when the residuals distribution is found to be not normal. Additionally, different diagnostic indices might be considered to better deal with the problem of correlated auxiliary variables. Finally, the effectiveness of the proposed methodology should be assessed for a *combination* of parametric and structural mismatches, and the methodology itself should be challenged against real-world systems.

In the definition of the experiment space (Chapter 5), future studies should consider not only the prediction uncertainty, but also other forms of uncertainty (such as uncertainty on the model parameters and on the calibration data), as well as the manufacturing of products characterized by a *multivariate* quality profile. Finally, future investigations should be devoted to assess the

effectiveness of a design-of-experiments exercise carried out in the latent space with respect to the more common situation where the experiments are designed directly in the true input space. Finally, the methodology developed to review large historical datasets (Chapter 6) can be further improved according to different directions: *i*) a different metric/index might be identified to more properly detect anomalies in the batch evolution and to avoid a misclassification of true standard batches; *ii*) the rules defined to discriminate a true process batch from a different operation might be enhanced in order to reduce false negatives and false positives.

Appendix A

On the interpretation of the latent variable model parameters

This Appendix reports some details on the interpretation of the parameters of a latent variable model (LVM). In particular, some indications are provided on how to interpret the loading and score diagrams in order to get information from the data (largely based on the Dissertations of Tomba 2013 and Ottavian, 2014). The interpretation of the loading plots of the case study considered in Chapter 6 is used as an example.

A.1 Interpretation of the scores and loading plots

PCA and PLS models (Chapter 2) are usually built not only for facilitate the analysis of large multivariate datasets, by identifying a reduced number of latent variables describing the system, but also to enhance understanding of the system itself. This can be achieved by analyzing the correlation between variables and the similarities between samples. The advantage in using LVMs to this purpose is due to the fact that the model parameters allow to interpret the correlation structure in a straightforward way, facilitating also the identification of the mechanisms acting on the system. Therefore, under a practical point of view, the analysis of the PCA and PLS parameters is fundamental and it is done by considering plots of the scores and of the loadings of the model. Although these plots can be reported in several ways, according to common practice (which is adhered to in this Dissertation), the scores are reported as scatter plots, in which the scores on a PC (or on a LV indifferently) are reported versus the scores on another PC. This is usually done for the scores on the first LVs found by the model, because they explain most part of the variability in the data. Bi-dimensional plots are usually used as they are easier to visualize than three-dimensional ones. Figure A.1b reports an example of a score plot.

Loadings are usually reported as bar plots or as scatter plots. In the first case (which is the way used in this Dissertation) a bar plot of the loadings of the original variables on each PC is reported, as in Figure A.1a.

In general, loading plots are useful for two important reasons: *i*) understanding which are the variables related to the data variability and which are not; *ii*) understanding if there are correlations among the variables. Recalling the meaning of loadings in PCA and weights in PLS

(Chapter 2, Section 2.1.1 and Section 2.1.2), a measured variable which shows a high loading or weight has a significant importance on the related PC/LV, thus being responsible of a significant part of the variability in the data. Therefore, loadings in PCA and weights in PLS help in identifying the "most important" variables for the system under study, and to rank them by importance order. If this information is combined with physical knowledge on the system, one can obtain additional physical insights on the system under investigation, by understanding which are the driving forces linked to physical phenomena that drive the system. When two variables have similar loadings on a PC, they are said to be correlated. If the loading absolute values are similar but the values are opposite, they are said to be inversely related (or anti - correlated). This means that it is expected that, considering the data used to build the model, an increase in one variable results in a decrease of the other variable.

Figure A.1a gives an example of this occurrence. For example, considering PC1 it can be clearly seen that variable f_9, f_{10} and variable f_{11} are the most significant variables on this direction, followed by f_1, f_3 and f_5, and they are inversely related to f_2 as their loadings are opposite.

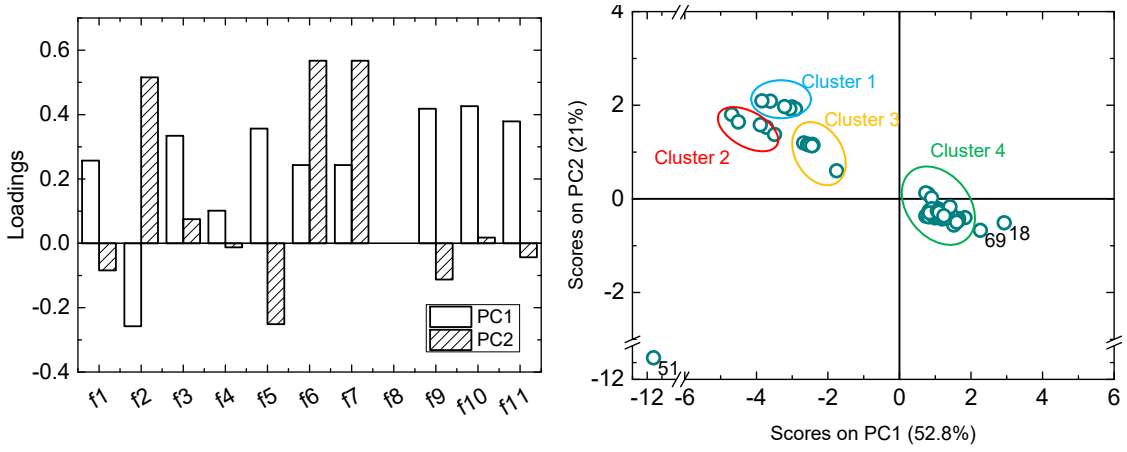

(a) (b)

Figure 6.27. *Batch characterization in the granulation unit: (a) loadings and (b) scores of the PCA model built on the calibration feature matrix. The numbers in the symbols indicate the batch number.*

Differently, on the second latent direction, PC2, f_2, f_6 and f_7 have the highest loading and looks inversely related to f_5, which has a lower importance. Note that the PCA loadings and the PLS weights on each PC/LV are independent. Therefore, the information obtained from the analysis of one latent component is not contrasting with the other ones, but it simply provides a different type of information (namely, it identifies a different driving force for the process).

Score plots as the one reported in Figure A.1b are useful to identify similarities between samples. This means that samples with similar characteristics fall in the same region of the score plot. Moreover, the pattern observed in a score plot reflects the correlation structure identified by the variable loadings. For example, in Figure A.1b four main clusters can be observed. Samples are

therefore grouped according to their similarities or differences in the variables that have the highest loading on PC1 and PC2. By analyzing the loading plot, one can identify which these variables are. Considering for example the first direction, samples having a high positive score on PC1 as those included in cluster 4 will have higher values of f_9, f_{10} and f_{11} and lower f_2 values on average. The situation is opposite in the case of samples with negative PC1 scores. A similar analysis can be done also for the other PCs.

Appendix B

Details on the simulated processes analyzed in Chapter 3

This Appendix reports some details on the generation of the data used in the two examples considered in Chapter 3: the CSTR system and the milling unit. For the second example, the diagnostics of the MPCA model built for the first case study analyzed are also reported.

B.1 Generation of the historical dataset for Example 1

This Section provides the nominal values (Table B.1) of the parameters used to generate the historical dataset for the CSTR system ("process Π") analyzed in Example 1 (Section 3.3). The ranges of the measured variables included in this dataset are also reported (Table B.2).

Table B.1. *Nominal values of the parameters used to generate the historical dataset for Example 1.*

Parameters	Values
$A_{1,\Pi}$	20 kmol/(m^3·s)
$A_{2,\Pi}$	10 kmol/(m^3·s)
$c_{P,\Pi}$	4.186 kJ/(kg·K)
$c_{P,w,\Pi}$	3.137 kJ/(kg·K)
$E_{a1,\Pi}$	69.7 kJ/mol
$E_{a2,\Pi}$	72 kJ/mol
S_Π	32.98 m^2
$V_{R,\Pi}$	26.15 m^3
$\Delta H_{1,\Pi}$	-59·10^3 J/mol
$\Delta H_{2,\Pi}$	-10·10^3 J/mol
$\rho_{w,\Pi}$	1000 kg/m^3
ρ_Π	800 kg/m^3

Table B.2. *Ranges of the measured variables included in the historical dataset for Example 1.*

Measured variables	Values
$C_{A,\Pi}^{in}$	[3 - 9] kmol/m^3
$C_{A,\Pi}^{out}$	[2.897 - 8.814] kmol /m^3
$C_{B,\Pi}^{in}$	[2 - 5] kmol /m^3
$C_{B,\Pi}^{out}$	[1.791 - 4.829] kmol /m^3
$C_{C,\Pi}^{in}$	0 kmol /m^3
$C_{C,\Pi}^{out}$	[0.181 - 1.778] kmol /m^3
$C_{D,\Pi}^{in}$	0 kmol /m^3
$C_{D,\Pi}^{out}$	[$2.701 \cdot 10^{-4}$ - $2.186 \cdot 10^{-2}$] kmol /m^3
$F_{j,\Pi}$	[0.236 - 0.257] m^3/s
U_{Π}	[0.2923 - 0.3035] kJ/(m^2·s·K)
T_{Π}^{in}	[292 - 298] K
T_{Π}^{out}	[293.7 - 315.7] K
$T_{j,\Pi}^{in}$	[287.5 - 292.5] K
$T_{j,\Pi}^{out}$	[287.6 - 292.7] K
$F_{j,\Pi}$	[0.236 - 0.257] m^3/s

B.2 Generation of the historical dataset and diagnostics of the MPCA model for Example 2

This Section provides the nominal values (Table B.3 and B.4) of the parameters used to generate the historical dataset for the mill system ("process Π") analyzed in Example 2 (Section 3.4), and the eigenvalues λ, the explained variance R^2 and its cumulated value R^2_{cum} for each PC of the MPCA model (Table B.5) built for Case study 2.A (Section 3.4.2.1).

Note that all parameters included in Table S3 (but k_{Π} and y'_{Π}) are material-dependent. The ranges of the measured variables included in this dataset are also reported.

Table B.3. *Ranges of the measured variables included in the historical dataset for Example 2.*

Measure variables	Values
$\rho_{bulk,\,\Pi}$	[320-450] kg/m^3
Din_{Π}	[3-6]·10^{-3} m
$\sigma_{in,\,\Pi}$	[0.6-1]·10^{-3} m
v_{Π}	[30-80] m/s

Table B.4. *Nominal values of the parameters used to generate the historical dataset for Example 2. The values in curly brackets refer to different materials. The values reported for parameter $W_{m,\mathrm{kin},\Pi}$ refer to the range taken by the parameter for the entire set of materials.*

Parameters	Values
c_{Π}	{–0.052; –0.0422; –0.0325; –0.0226} [-]
d_{Π}	{4.42; 5.898; 5.51; 8.01} [-]
$f_{\mathrm{Mat},\Pi}$	{0.059; 0.095; 0.115; 0.125} [-]
k_{Π}	1 [-]
y'_{Π}	$2 \cdot 10^{-5}$ m
$W_{m,\mathrm{kin},\Pi}$	[1376.4 - 3808.9] J/kg
$W_{m,\min,\Pi}$	{2.957; 3.427; 3.5; 3.541} Jm/kg

Table B.5. *Case study 2.A. Diagnostics of the MPCA model on $\underline{\mathbf{X}}_M$.*

PC number	Eigenvalue of cov($\mathbf{X}_M$)	R^2	R^2_{cum}
1	83.84	42.56	42.56
2	68.28	34.66	77.22
3	20.13	10.22	87.44
4	11.93	6.05	93.49
5	5.57	2.83	96.32
6	3.01	1.53	97.84
7	1.68	0.85	98.69
8	1.24	0.63	99.33
9	0.76	0.39	99.71
10	0.31	0.16	99.87
11	0.15	0.08	99.94
12	0.08	0.04	99.99
13	0.02	0.01	99.99
14	0.01	0.01	100.00

Appendix C

An improved method to diagnose the cause of a process/model mismatch: preliminary results

As highlighted in Chapter 3 and 4, strongly correlated auxiliary variables make the identification of the mismatch particularly difficult, in the analysis of the residuals and/or of the score shifts. For this reason, in this Appendix a preliminary solution to deal with strongly correlated variables is presented, which exploits the methodology proposed by Rato and Reis (2015b) for fault diagnosis purposes. A preliminary example of the results obtained is provided for the two examples analyzed in Section 4.3 for the fermentation process.

C.1 An alternative approach to diagnose the cause of a PMM

The alternative approach proposed in this Appendix to identify which term of a first-principles model might lead to a PMM is based on the use of partial correlation coefficients. The basic idea in the use of partial correlation coefficients is to remove the effect of third-party variables before checking for an association between the two designated variables. Therefore, considering 3 variables (x_1, x_2 and x_3) the correlation between the first two is quantified, after conditioning upon (i.e., controlling for, or holding constant) the third one, namely after the removal of the common effect of x_3 on x_1 and x_2 (Rato and Reis, 2014a).

Rato and Reis (2014a, 2014b, 2015a and 2015b) provide a detailed description and several examples of the use of partial correlation coefficients for process monitoring purposes. In particular, they suggest a number of sensitivity enhancing data transformations (SET) that can maximize the detection ability of all monitoring procedures based on (partial or marginal) correlation (Rato and Reis, 2014a). In their studies, they state that ‘‘even though partial correlations do not provide information about the variables causality direction, they are still able to discern if such connectivity does exist and in what degree it has changed. This characteristic, coupled with their easy computation, makes them suitable for fault detection and diagnosis purposes at the structural level’’. For this reason, the alternative approach proposed in this Appendix to diagnose which term of a model is mostly related to the observed mismatch is based on the fault diagnosis procedure introduced by Rato and Reis (2015b) with the purpose of

identifying a reduced set of variables that are closely related with the fault root cause. The authors exploit the partial correlations ability to remove the effects of faulty variables in the data, under the assumption that if a change on the variables relationships occurs, it is expected that the partial correlation coefficients controlled by the variables associated with the root cause of the fault remain close to their normal values, since the source of variability is being removed in such circumstances (Rato and Reis, 2015b).

It should be highlighted that, the methodology proposed by Rato and Reis (2015b) refers to continuous systems. In order to apply this methodology (only minor adjustments have been introduced) to the purpose of our analysis, only the final measurements of N different batches are considered, and for each of them B observations are simulated, which differ only for white noise. Each batch has been carried out with different initial conditions for C_s, P, F_s, f_g (for the meaning of the symbols refer to Section 4.1). Appropriate solutions to consider the whole batch trajectories are still under investigation.

The procedure proposed in this Appendix has been adapted from the one proposed by Rato and Reis (2015b) and it is composed by 7 steps:

1. a set of V variables that represent only some measured variables (namely, the outputs of the most important model equations) is defined. The measurements available for this set of variables are collected in a historical matrix $\underline{\mathbf{X}}_{\Pi}$ [$N \times M \times B$] and a simulated matrix $\underline{\mathbf{X}}_{M}$ [$N \times V \times B$];
2. for each sample $\mathbf{x}_M$ [$V \times B$], the first-order partial correlation coefficients are calculated considering all possible combination of pairs of variables in $\underline{\mathbf{X}}_{M}$ (for example, $\mathbf{x}_i$ and $\mathbf{x}_j$) controlled by a third variable (for example $\mathbf{x}_k$) as:

$$r_{\mathbf{x}_i\mathbf{x}_j,\mathbf{x}_k} = \frac{r_{\mathbf{x}_i\mathbf{x}_j} - r_{\mathbf{x}_i\mathbf{x}_k} \cdot r_{\mathbf{x}_j\mathbf{x}_k}}{\sqrt{\left(1-r_{\mathbf{x}_i\mathbf{x}_k}{}^2\right)\left(1-r_{\mathbf{x}_j\mathbf{x}_k}{}^2\right)}} \quad , \tag{C.1}$$

3. each partial correlation coefficient is normalized as:

$$w_r = \frac{\sqrt{N-q-1}\cdot\left(r-\rho\right)}{1-\rho^2} \quad , \tag{C.2}$$

   where ρ represents the population mean, N the number of samples, and q the order of the partial correlation coefficient. In this analysis, q=1;
4. step 2 and 3 are repeated for $\underline{\mathbf{X}}_{\Pi}$, but normalizing each $r_{i,j}$ based on the ρ calculated for $\underline{\mathbf{X}}_{M}$;
5. a matrix $\mathbf{D}$[‡‡‡‡] [$V \times V$] is defined, where each row corresponds to a control variable, whereas the j-th element of the k-th row is calculated as:

‡‡‡‡ Note that, in this Appendix matrix **D** assumes a different meaning respect to matrix **D** used in Chapter 6.

$$d_{k,j} = \sum_{k \neq i, k \neq j} f(w(r_{ji,k})) \quad , \tag{C.3}$$

where $f(r_{ji,k}) = 1$ if $|w_r(r)| > CL$, and 0 otherwise. Since, thanks to the transformation of Eq. (D.2), each $w_r(r)$ is normally distributed, therefore the *CL* (confidence limit) is calculated as:

$$CL = \sigma(w_r) \cdot z(\alpha / 2) \quad , \tag{C.4}$$

with z =2.58, corresponding to a threshold of 99%;

6. the squared norm of each row and column of matrix **D** is calculated to mark each variable as RED, ORANGE and YELLOW, according to the rules reported in Table C.1. A variable is RED when it presents the smallest value of the squared norm of the rows of **D**, and the largest value of the norm of the columns of **D**. A variable is ORANGE when it presents the smallest value of the squared norm of the rows of **D**, but the value of the norm of its column is smaller than the largest one. Finally a variable is YELLOW when presents the largest value of the squared norm the columns of **D**, but the value of the norm its row is larger than the smallest one;

Table C.1. *Rules proposed by Rato and Reis (2015b) to marked a variable i as RED, ORANGE or YELLOW.*

	$\|\mathbf{D}(i,:)\|^2 = \min\left(\|\mathbf{D}(i,:)\|^2\right)$	$\|\mathbf{D}(:,i)\|^2 = \max\left(\|\mathbf{D}(:,i)\|^2\right)$
RED	yes	yes
ORANGE	yes	no
YELLOW	no	yes

7. steps from 2-6 are repeated considering a new set of *V* variables composed by the terms of the model involved in the calculation of the measured variables that demonstrated to be mostly related to the mismatch.

According to Rato and Reis (2015b), when the variable related to the mismatch is controlled for, the partial correlations calculated for the remaining pairs of variables should remain within the control limits (low values of the norm of the columns of **D**). On the other hand, a variable presenting high values of the norm of the rows of **D** indicates that it has suffered many changes in correlation with the other variables. For this reason it is expected that most of the times, when a variables is marked as red, it should be directly related with the cause of the mismatch, even if also variables marked as ORANGE or YELLOW should also be checked.

The procedure proposed in the previous Section has been applied first considering only the measured variables (C_x, C_p, C_s, C_l,), and then considering the terms of the model involved in the calculation of the variables marked as RED or ORANGE.

C.1.1 Example 1

In this first example, it is assumed that a mismatch is forced by introducing an error in the calculation of mass transfer coefficient k_{la}, as done in Example 2.A in Chapter 4 (Section 4.3.2). In this case, N = 69 batches and B = 300 observations are considered. The results obtained by the analysis of the partial correlation coefficients calculated for the measured variables C_x, C_p, C_s, C_l are reported in Figure C.1*a*. It can be observed that the variable that seems mostly related to the cause of the mismatch is C_l, although also C_x and C_p should be considered in the following step. Therefore, the terms of the model (Eq. 4.10-14 in Chapter 4) that relate C_l with C_x and C_p are considered in the second step. In particular, the analysis of the partial correlation coefficients described in the previous section has been repeated considering the following 4 auxiliary variables:

$$\begin{aligned} x_1(n,t) &= \mu_{pp} \cdot C_x \\ x_2(n,t) &= \mu \cdot C_x \\ x_3(n,t) &= C_p \\ x_4(n,t) &= k_l a \cdot \left(C_l^* - C_l\right) \end{aligned} \quad . \tag{C.5}$$

The results obtained (Figure C.1*b*) confirms the effectiveness of the analysis performed by the partial correlation coefficients comparison in recognizing the term of the model actually responsible of the PMM. For all the samples (batches) considered, variable no. 4 has been marked as RED.

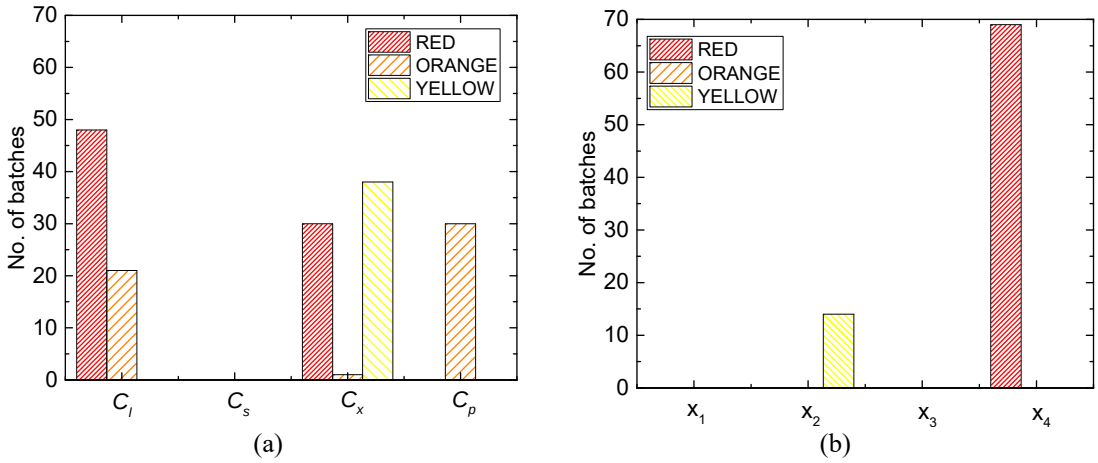

Figure C.1. *Example 1. Number of batches (samples) for which each variable considered in the analysis has been marked as RED, ORANGE or YELLOW, considering (a) only the available measured variables and (b) a set of auxiliary variables.*

C.1.2 Example 2

In this second example, it is assumed that a mismatch is forced by changing the parameter $Y_{s/x}$ (from 0.45 [-] to 0.2 [-]), as done in Example 2.B in Chapter 4 (Section 4.2.5). In this case $N = 50$ batches and $B = 200$ observations are considered. The results of the analysis of the partial correlations coefficients calculated for the available measured variables are reported in Figure C.2a. In this case, only C_x appears to be the measured variable mostly related with the mismatch, whereas the relations with C_l does not appear to be affected by the mismatch. For this reason, in the second step of the analysis the relations of C_x with C_s and C_p are investigated. Therefore the new set of variables selected for the analysis is:

$$\begin{aligned} x_1(n,t) &= \mu_{pp} \cdot C_x \\ x_2(n,t) &= \mu \cdot C_x \\ x_3(n,t) &= C_p \\ x_4(n,t) &= C_s \end{aligned} \quad . \tag{C.6}$$

The results obtained are reported in Figure C.2b. Since the amount of time that μ is marked as RED is greater than for μ_{pp}, and since the correlation coefficients which involves C_s seems to be affected by error more than those involving C_p, the results obtained suggest that the cause of the mismatch is possibly due to the relation of x_2 and x_4, namely to $Y_{s/x}$.

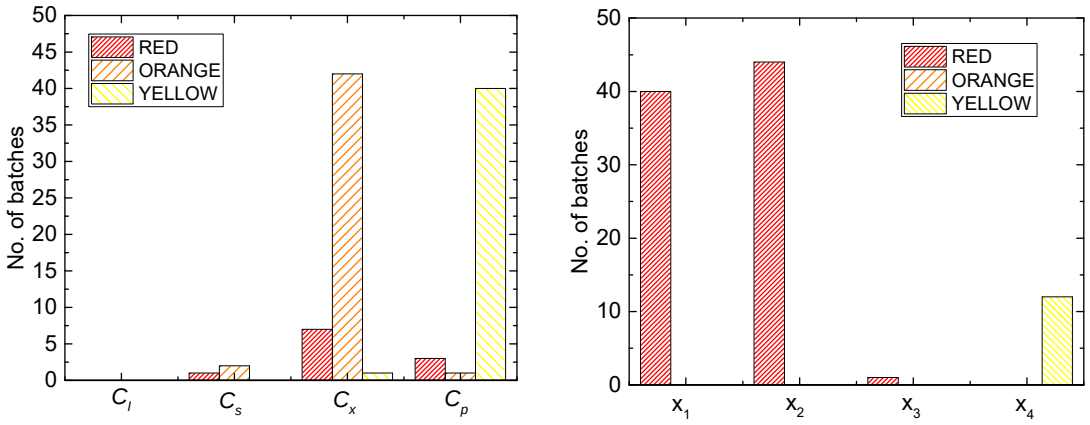

Figure C.2. *Example 2. Number of batches (samples) for which each variable considered in the analysis has been marked as RED, ORANGE or YELLOW, considering (a) only the available measured variables and (b) a set of auxiliary variables.*

Although in this section only preliminary results are presented, a significant margin of improvement is expected upon further investigation. The final objective is to provide a robust tool that, by exploiting the entire trajectory of the batches analyzed, is able to detect the cause of the mismatch even with strongly correlated variables. To this purpose, further investigation is now

focused on: *i*) adapting the solutions suggested by Rato and Reis (2015b) to enhance the accuracy of the detection of a change in the correlation structure of the variables analyzed, especially with time-dependent variables; *ii*) developing a robust procedure to identify appropriate sets of auxiliary variables that can be analyzed with partial correlation coefficients; *iii*) analyzing the effect of the number of available samples and of their features on the effectiveness of the methodology.

References

am Ende, D.J., K. S. Bronk, J. Mustakis, G. O'Connor, C.L. Santa Maria, R. Nosal and T.J.N. Watson (2007). API Quality by Design example from the Torcetrapib manufacturing process. *J. Pharm. Innov.*, **2**, 71-86.

am Ende, D.J. (2011). Chemical engineering in the pharmaceutical industry: an introduction. In: am Ende, D.J. (Ed.), *Chemical Engineering in the Pharmaceutical Industry. R&D to Manufacturing*. John Wiley & Sons, Inc. New York, NJ.

Anderson, T. W., D. A. Darling (1952). Asymptotic Theory of Certain "Goodness of Fit" Criteria Based on Stochastic Processes. *Ann. Math. Stat.*, **23**, 193–212.

Badwe, A. S., R. D. Gudi, R. S. Patwardhan, S. L. Shah, S. C. Patwardhan (2009). Detection of Model-Plant Mismatch in MPC Applications. *J. Process Control*, **19**, 1305–1313.

Ballabio D., R. Todeschini (2009). Multivariate classification for qualitative analysis. In *Infrared Spectroscopy for Food Quality Analysis and Control*. Sun, D.W., Ed. Elsevier, Burlington, MA, USA, pp. 83–104.

Barker M., W. Rayens (2003). Partial least squares for discrimination, *J. Chemometr.*, **17**, 166–173.

Bennett B. and G. Cole (2003). *Pharmaceutical production: an engineering guide*, IChemE, Rugby, UK.

Birol, G., C. Ündey, and A. Çinar (2002). A modular simulation package for fed - batch fermentation: penicillin production. *Computers Chem. Eng.*, **26**, 1553-1565.

Bishop C.M. (2006). *Pattern recognition and machine learning*, Springer, New York (U.S.A.).

Boukouvala, F., F.J. Muzzio and M. Ierapetritou (2010). Design space of pharmaceutical processes using data-driven-based methods. *J. Pharm. Innov.*, **5**, 119-137.

Box, G. E. P., and N. R. Draper (2007). *Response surfaces, mixtures, and ridge analysis*. Hoboken, NJ Wiley.

Bu, D., B. Wan, G. McGeorge (2013). A Discussion on the Use of Prediction Uncertainty Estimation of NIR Data in Partial Least Squares for Quantitative Pharmaceutical Tablet Assay Methods. *Chemom. Intell. Lab. Syst.*, **120**, 84.

Burgschweiger J., E. Tsotsas (2002). Experimental investigation and modelling of continuous fluidized bed drying under steady-state and dynamic conditions, *Chem. Eng. Sci.*, **57**, 5021–5038.

Burnham, A, R. Viveros and J.F. MacGregor (1996). Frameworks for latent variable multivariate regression. *J. Chemom.*, **10**, 31-45.

Burnham, A.J., J.F. MacGregor and R. Viveros (1999). Latent variable multivariate regression modeling. *Chemom. Intell. Lab. Syst.*, **48**, 167-180.

Burt, J.L., A.D. Braem, A. Ramirez, B. Mudryk, L. Rossano, S. Tummala, (2011). Modelguided design space development for a drug substance manufacturing process. *J. Pharm. Innov.* **6**, 181–192.

Chatzizacharia, K. A., D. T. Hatziavramidis (2014). Design Space Approach for Pharmaceutical Tablet Development. *Ind. Eng. Chem. Res.*, **53**, 12003.

Choi S. W. and I. B. Lee (2005). Multiblock PLS-based localized process diagnosis, *J.Process Control*, **15**, 295-306.

Çinar, A., S.J. Parukelar, C. Ündey, G. Birol (2003). *Batch fermentation – Modeling, monitoring and control*. Marcel-Dekker, New York, NJ.

Close, E. J., J. R. Salm, D. G. Bracewell, E. Sorensen (2014). A Model Based Approach for Identifying Robust Operating Conditions for Industrial Chromatography with Process Variability. *Chem. Eng. Sci.*, **116**, 284.

Conlin, A.K., E.B. Martin and A.J. Morris (2000). Confidence limits for contribution plots. *J. Chemom.*, **14**, 725-736.

Cook, J., M. T. Cruañes, M. Gupta, S. Riley, and J. Crison (2013). Quality-by-Design: Are We There Yet?, *AAPS PharmSciTech*, **15**, 140-148.

Cover, T. M., P.E. Hart (1967). Nearest neighbor pattern classification. *IEEE Tran. Inf. Theory*, **13**, 21-27.

Danese, J., D. Constantinou (2007). Lean practices in a life sciences organization. *Contract Pharma*. Available at: http://shows.contractpharma.com/articles/2007/10/lean-practices-in-a-life-sciences-organization (Last accessed 26/01/2016).

Deloitte, (2015) Global life sciences outlook - Adapting in an era of transformation Deloitte Touche Tohmatsu Limited's life science and health care (DTTL LSHC), Available at: http://www2.deloitte.com/it/it/pages/life-sciences-and-healthcare/articles/2015-global-life-sciences-outlook.html (Last accessed 26/01/2016).

Dong, D. and T.J. McAvoy (1996), Nonlinear principal component analysis based on principal curves and neural networks, *Computers Chem. Eng.*, **20**, 65-78.

Doymaz, F., J. Chen, J. A. Romagnoli, A. Palazoglu (2001). A Robust Strategy for Real-Time Process Monitoring. *J. Process Control*, **11**, 343–359.

Duda, R.O., P.E. Hart, D. G. Stork (2001). *Pattern classification*, 2nd Ed., John Wiley & Sons, Inc., New York (U.S.A.).

Efron, B., G. Gong (1983). A Leisurely Look at the Bootstrap, the Jackknife, and Cross-Validation. *Am. Stat.*, **37**, 36.

Eigenvector Research, (2015). PLS_Toolbox 8.0.2, Eigenvector Research, Inc., Wenatchee, WA, USA.

Eriksson, L., E. Johansson, N. Kettaneh-Wold, J. Trygg, C. Wikström and S. Wold (2006). *Multi- and megavariate data analysis. Part I. Basic principles and applications*. Umetrics AB, Umeå (Sweden).

EvaluatePharma (2015), EvaluatePharma World Preview 2015 Outlook to 2020, Evaluate^{TM} Ltd. Available at: http://www.evaluategroup.com/public/EvaluatePharma-Overview.aspx (Last accessed 26/01/2016).

Faber, K., B. R. Kowalski (1997). Propagation of Measurement Errors for the Validation of Predictions Obtained by Principal Component Regression and Partial Least Squares. *J. Chemom.*, **11**, 181.

Faber, N. (Klaas) M. (2002). Uncertainty Estimation for Multivariate Regression Coefficients. *Chemom. Intell. Lab. Syst.*, **64**, 169.

FDA (2004a). Pharmaceutical CGMPs for the 21st century – A risk based approach. Final report. *U.S. Department of Health and Human Services*. *U.S. Food and Drug Administration*.

FDA (2004b). Guidance for industry. PAT - A framework for innovative pharmaceutical development, manufacturing and quality assurance. *Center for Drug Evaluation and Research, U.S. Food and Drug Administration*, Rockwille (MD), USA.

FDA (2006). Guidance for Industry - Quality Systems Approach to Pharmaceutical CGMP Regulations. *U.S. Department of Health and Human Services*. *U.S. Food and Drug Administration.*

Fernández Pierna, J. A., L. Jin,, F. Wahl, N. M. Faber, D. L. Massart (2003). Estimation of Partial Least Squares Regression Prediction Uncertainty When the Reference Values Carry a Sizeable Measurement Error. *Chemom. Intell. Lab. Syst.*, **65**, 281.

Flores-Cerillo, J. and J.F. MacGregor (2004). Control of batch product quality by trajectory manipulation using LV models. *J. Process Control*, **14**, 539-553.

Franceschini, G., S. Macchietto (2008). Model-Based Design of Experiments for Parameter Precision: State of the Art. *Chem. Eng. Sci*., **63**, 4846–4872.

Gabrielsson, J., N.-O. Lindberg and T. Lundstedt (2002). Multivariate methods in pharmaceutical applications. *J. Chemom.*, **16**, 141-160.

Gani, R. Modelling for PSE and Product-Process Design. In *Computer-Aided Chemical Engineering*; Proceedings of the 10th International Symposium on Process Systems Engineering: Part A, Salvador de Bahia, Brazil, August 16-27, 2009; Brito Alves, R. M., Oller Nascimento, C. A., Biscaia Jr, E. C., Eds.; Elsevier, 2009; **27**, 7–12.

García-Muñoz S., S. Dolph and H.W. Ward II (2010). Handling uncertainty in the establishment of a design space for the manufacture of a pharmaceutical product. *Computers Chem. Eng.*, **34**, 1098-1107.

García-Muñoz, S., T. Kourti, J.F. MacGregor, A.G. Mateos and G. Murphy (2003). Troubleshooting of an industrial batch process using multivariate methods. *Ind. Eng. Chem. Res.*, **42**, 3592-3601.

García-Muñoz, S., T. Kourti, J.F. MacGregor, F. Apruzzese and M. Champagne (2006). Optimization of batch operating policies. Part I. Handling multiple solutions. *Ind. Eng. Chem. Res.*, **45**, 7856-7866.

García-Muñoz, S., J.F. MacGregor and T. Kourti (2005). Product transfer between sites using Joint-Y PLS. *Chemom. Intell. Lab. Syst.*, **79**, 101-114.

García-Muñoz, S., J.F. MacGregor, D. Neogi, B.E. Letshaw and S. Mehta (2008). Optimization of batch operating policies. Part II. Incorporating process constraints and industrial applications. *Ind. Eng. Chem. Res.*, **47**, 4202-4208.

García-Muñoz, S. and C.A. Oksanen (2010). Process modeling and control in drug development and manufacturing. *Computers Chem. Eng.*, **34**, 1007-1008.

García-Muñoz, S., L. Zhang and M. Cortese (2009). Root cause analysis during process development using Joint-Y PLS. *Chemom. Intell. Lab. Syst.*, **95**, 101-105.

Gautam, A., Pan, X. The changing model of big pharma: impact of key trends, Drug Discov Today (2015), in Press. DOI: 10.1016/j.drudis.2015.10.002.

Gernaey, K.V., A.E. Cervera-Padrell and J.M. Woodley (2012). A perspective on PSE in pharmaceutical process development and innovation. *Computers Chem. Eng.*, **42**, 15-29.

Gernaey, K.V., R. Gani (2010). A model-based systems approach to pharmaceutical product-process design and analysis. *Chem. Eng. Sci*., **65**, 5757-5769.

Geladi, P. and B. Kowalski (1986). Partial least-squares regression: a tutorial. *Anal. Chim. Acta.*, **185**, 1-17.

Gunther, J. C., J. Baclaski, D. E. Seborg and J. S. Conner (2009). Pattern Matching in Batch Bioprocesses - Comparisons Across Multiple Products and Operating Conditions. *Computers Chem. Eng.,* **33**, 88-96.

Höskuldsson, A. (1988). PLS regression methods. *J. Chemom.*, **2**, 211-228.

Hotelling, H. (1933). Analysis of a complex of statistical variables into principal components. *J. Educ. Psycol.*, **24**, 417-441.

Huang, J., G. Kaul, C. Cai, R. Chatlapalli, P. Hernandez-Abad, K. Ghosh, A. Nagi (2009). Quality by design case study: an integrated approach to drug product and process development. *Int. J. Pharm.*, **382**, 23-32.

ICH (1999). ICH harmonised tripartite guide. Specifications: test procedures and acceptance criteria for new drug substances and new drug products: chemical substances. Q6A.

ICH (2005). ICH harmonised tripartite guide. Quality risk management Q9.

ICH (2008). ICH harmonised tripartite guide. Pharmaceutical quality system Q10.

ICH (2009). ICH harmonised tripartite guide. Pharmaceutical development Q8(R2).

ICH (2010). Quality implementation working group on Q8, Q9 and Q10. Questions & Answers (R4).

ICH (2011). ICH quality implementation working group. Points to consider (R2). ICH-endorsed guide for ICH Q8/Q9/Q10 implementation.

Jackson, J. E (1991). *A user's guide to principal components*. John Wiley & Sons, Inc., New York (U.S.A.).

Jaeckle, C.M. and J.F. MacGregor (1998). Product design through multivariate statistical analysis of process data. *AIChE J.*, **44**, 1105-1118.

Jaeckle, C.M. and J.F. MacGregor (2000a). Industrial application of product design through the inversion of latent variable models. *Chemom. Intell. Lab. Syst.*, **50**, 199-210.

Jaeckle, C.M. and J.F. MacGregor (2000b). Product transfer between plants using historical process data. *AIChE J.*, **46**, 1989-1997.

Johanson, J. R. (1965).A Rolling Theory for Granular Solids. *J. Appl. Mech.*, *32*, 842.

Johnson, R.A. and D. W. Wichern (2007). *Applied multivariate statistical analysis (6th ed.).* Pearson Education, Inc., Upper Saddle River, NJ, (U.S.A).

Juran, JM. (1992). Juran on quality by design: the new steps for planning quality into goods and services. New York: The Free Press, New York, (U.S.A.).

Kapsi, S.G., L.D. Castro, F.X. Muller, T.J. Wrzosek (2012). Development of a design space for a unit operation: illustration using compression-mix blending process for the manufacture of a tablet dosage form. *J. Pharm. Innov*., **7**, 19-29.

Kashid, M. N., D. W. Agar and S. Turek (2007). CFD modelling of mass transfer with and without chemical reaction in the liquid–liquid slug flowmicroreactor. *Chem. Eng. Sci*., **62**, 5102–5109.

Ketterhagen, W.R., M.T. am Ende, B.C. Hancock (2009). Process modeling in the pharmaceutical industry using the discrete element method. *J Pharm Sci.,* **98**, 442-470.

Kiparissides, A., C. Georgakis, A. Mantalaris, E. N. Pistikopoulos (2014). Design of In Silico Experiments as a Tool for Nonlinear Sensitivity Analysis of Knowledge-Driven Models. *Ind. Eng. Chem. Res*., **53**, 7517−7525.

Klatt, K.-U., W. Marquardt, (2009). Perspectives for process systems engineering-Personal views from academia and industry. *Computers Chem. Eng*., **33**, 536-550.

Kourti, T. (2003). Multivariate Dynamic Data Modelling for Analysis and Statistical Process Control of Batch Processes, Start –Ups and Grade Transitions, *J. Chemom.*, **17**, 93-109.

Kourti, T. (2005). Application of latent variable methods to process control and multivariate statistical process control in industry. *Int. J. Adapt. Control.,* **19**, 213-246

Kourti, T. (2006). Process analytical technology beyond real-time analyzers: the role of multivariate analysis. *Crit. Rev. Anal. Chem.*, **36**, 257-278.

Kourti, T., B. Davis (2012). The Business Benefit of Quality by Design (QbD). *Pharm. Eng. Off. Magazine of ISPE*., **32**,1-10.

Krämer, N., M. Sugiyama (2011). The Degrees of Freedom of Partial Least Squares Regression. *J. Am. Stat. Assoc.*, **106**, 697.

Kremer, D.M. and B.C. Hancock (2006). Process simulation in the pharmaceutical industry: a review of some basic physical models. *J. Pharm. Sci.*, **95**, 517-529.

Krzanowski, W. J. (1979). Between-Groups Comparison of Principal Components. *J. Am. Stat. Assoc*., **74**, 703-707.

Kukura, J.L., M.P. Thien (2011). Current challenges and opportunities in the pharmaceutical industry. In: am Ende, D.J. (Ed.), *Chemical Engineering in the Pharmaceutical Industry. R&D to Manufacturing*. John Wiley & Sons, Inc., New York, NJ, 21–27.

Laínez, J.M., E. Schaefer, G.V. Reklaitis (2012). Challenges and opportunities in enterprise-wide optimization in the pharmaceutical industry. *Computers Chem. Eng,* **47**, 19-28.

Lavine, B. K., C.E. Davidson (2006). *Classification and Pattern Recognition, in Practical guide to chemometrics*, edited by Paul Gamperline, 2nd Edition, CRC press Taylor & Francis Group, Boca Raton, FL, U.S.A.

López-Negrete de la Fuente, R., S. García-Muñoz and L.T. Biegler (2010). An efficient nonlinear programming strategy for PCA models with incomplete data sets. *J. Chemom.*, **24**, 301-311.

Lourenço, V., D. Lochmann, G. Reich, J.C. Menezes, T. Herdling, J. Schewitz (2012). A quality by design study applied to an industrial pharmaceutical fluid bed granulation. *Euro. J. Pharm. Biopharm*. **81**, 438–447.

Luyben, W. L., *Chemical Reactor Design and Control*, Wiley, New York , NJ, 2007.

MacGregor, J.F. and M-.J. Bruwer (2008). A framework for the development of design and control spaces. *J. Pharm. Innov.*, **3**, 15-22.

MacGregor, J.F. and T. Kourti (1995). Statistical process control of multivariate processes. *Control Eng. Pract.,* **3**, 403-414.

Magnus J.R. and H. Neudecker (1999). *Matrix Differential Calculus with Applications in Statistics and Econometrics*, Revised Ed., John Wiley & Sons Inc., Chichester, (U.K.)

Mardia, K.V., J.T. Kent and J.M. Bibby (1979). *Multivariate analysis*. Academic Press Limited, London (U.K.).

Marquardt, W., J. Morbach, A. Wiesner and A. Yang (2010). OntoCAPE: A re-usable ontology for chemical process engineering. Springer-Verlag Berlin, Heildeberg.

Marquardt, W. (2005). Model-Based Experimental Analysis of Kinetic Phenomena in Multi-Phase Reactive Systems. *Chem. Eng. Res. Des*., **83**, 561–573.

Martens, H., M. Martens (2000). Modified Jack-Knife Estimation of Parameter Uncertainty in Bilinear Modelling by Partial Least Squares Regression (PLSR). *Food Qual. Prefer.*, **11**, 5.

Martin, E. B., A. J. Morris (1996). Non-Parametric Confidence Bounds for Process Performance Monitoring Charts. *J. Process Control*, **6**, 349–358.

Mathworks (2015). Matlab 8.6. (R2015b). The MathWorks Inc., Natick, MA (U.S.A.).

McLachlan G. J. (2004). *Discriminant Analysis and Statistical Pattern Recognition*, John Wiley & Sons, Inc., Hoboken, New Jersey, (U.S.A.)

Meyer, C.D. (2000). *Matrix analysis and applied linear algebra*. SIAM, Philadelphia, PA (U.S.A.).

Mika, S., B. Scholkopf, A.J. Smola, K.-R. Muller, M. Scholz, G. Ratsch (1999). Kernel PCA and de-noising in feature spaces. *Adv. Neural. Inf. Process. Syst.*, **11**, 536–542.

Montgomery, D.C. (2005). *Design and analysis of experiments. 6th edition*. John Wiley & Sons, Inc., New York (U.S.A.).

Morbach, J., A. Yang and W. Marquardt (2007). OntoCAPE – A large-scale ontology for chemical process engineering. *Eng. Appl. Artif. Intel.* **20**, 147–161.

Muteki, K., J.F. MacGregor and T. Ueda (2006). Rapid development of new polymer blends: the optimal selection of materials and blend ratios. *Ind. Eng. Chem. Res.*, **45**, 4653-4660.

Nomikos, P. and J.F. MacGregor (1994). Monitoring Batch Processes Using Multiway Principal Component Analysis. *AIChE J.*, **40**, 1361–1375.

Nomikos, P. and J.F. MacGregor (1995). Multivariate SPC charts for monitoring batch processes. *Technometrics*, **37**, 41-59.

Ottavian, M. (2014). Latent Variable Modeling to Assist Product Quality Characterization in the Food and Pharmaceutical Industries. *PhD Thesis*, University of Padova (Italy).

Ottavian, M., E. Tomba, M. Barolo (2016). Advanced process decision making using multivariate latent variable methods. In: *Process Simulation and Data Modeling in Solid Oral Drug Development and Manufacturing* (M. G. Ierapetritou and R. Ramachandrean, Eds.), Springer, New York (NJ), 159-189.

Pal, S. K. and P. Mitra, (2004) *Pattern Recognition Algorithms for Data Mining*, Chapman & Hall CRC Press, Boca Raton, FL (U.S.A.).

Pantelides, C. C., M. Pinto, S. K. Bermingham (2010). *Design Space Characterization Using First-Principles Models*. In; (Salt Lake City, UT), p paper no. 358b.

Pantelides, C. C. and J. G. Renfro (2013). The Online Use of First-Principles Models in Process Operations: Review, Current Status and Future Needs. *Comput. Chem. Eng.,* **51**, 136–148.

Pantelides, C. C., N. Shah, C. S. Adjiman (2009).*Comprehensive Quality by Design in Pharmaceutical Development and Manufactur*e. In; Nashville (TN, U.S.A), p 417f.

Pantelides, C., Z. E. Urban (2004). Process Modeling Technology: A Critical Review of Recent Developments. *Proceedings of the 6th International Conference on Foundations of Computer-Aided Process Design*, Princeton, NJ, July 11-16, 2004; Floudas, C. A., Agrawal, R., Eds.; CACHE Corp.: New York, 2004.

Peterson, J. J. (2008). A Bayesian Approach to the ICH Q8 Definition of Design Space. *J. Biopharm. Stat.*, **18**, 959.

Politis, S. N. and Rekkas D. M. (2001). The Evolution of the Manufacturing Science and the Pharmaceutical Industry, *Pharm. Res*., **28**, 1779–1781.

Pomerantsev, A.L. and O.Y. Rodionova (2012). Process analytical technology: a critical view of the chemometricians. *J. Chemom*., **26**, 299-310.

Process Systems Enterprise Ltd. (2013) gSOLIDS®, version 3.0; Process Systems Enterprise Ltd: London, UK.

Process Systems Enterprise Ltd. (2014) gSOLIDS®, version 4.0; Process Systems Enterprise Ltd: London, UK.

Rafols, I., M. M. Hopkins, J. Hoekman, J. Siepel, A. O'Hare, A. Perianes-Rodríguez, P. Nightingale (2012). Big Pharma, little science? A bibliometric perspective on Big Pharma's R&D decline. *Technol. Forecast. Soc.*, **81**, 22–38.

Rantanen J. and Khinast J. (2015). The Future of Pharmaceutical Manufacturing Sciences. *J. Pharm. Sci*., **104**, 3612–3638.

Realpe, A. and C. Velázquez (2006). Pattern recognition for characterization of pharmaceutical powders. *Powder Technol.,* **169***,* 108-113.

Reis, M.S. and P. M. Saraiva (2005). Integration of Data Uncertainty in Linear Regression and Process Optimization. *AIChE J.*, **51**, 3007.

Reis, M.S. and P. M. Saraiva (2012). Prediction of Profiles in the Process Industries. *Ind. Eng. Chem. Res.*, **51**, 4254.

Rajalahti, T. and O.M. Kvalheim (2011). Multivariate data analysis in pharmaceutics: a tutorial review. *Int. J. Pharm.,* **417**, 280-290.

Rato, T. J. and M. S. Reis (2014a). Sensitivity enhancing transformations for monitoring the process correlation structure, *J. Process Control*, **24**, 905-915.

Rato, T. J. and M. S. Reis (2014b). Non-causal data-driven monitoring of the process correlation tructure: A comparison study with new methods, *Computers Chem. Eng.*, **71**, 307-322.

Rato, T. J. and M. S. Reis (2015a). On-line process monitoring using local measures of association: Part I — Detection performance, *Chemom. Intell. Lab. Syst*., **142**, 307-322.

Rato, T. J. and M. S. Reis (2015b) On-line process monitoring using local measures of association. Part II: Design issues and fault diagnosis, *Chemom. Intell. Lab. Syst*., **142**, 265-275.

Rogers, A. and M. Ierapetritou (2015). Challenges and opportunities in modeling pharmaceutical manufacturing processes, *Comput. Chem. Eng.*, **81**, 32-39.

Roggo, Y., P. Chalus, L. Maurer, C. Lema-Martinez, A. Edmond, N. Jent (2007). A review of near infrared spectroscopy and chemometrics in pharmaceutical technologies, *J. Pharmaceut. Biomed.*, **44**, 683-700.

Rousseeuw, P.J. (1987) Silhouettes: A graphical aid to the interpretation and validation of cluster analysis, *J. Comput. Appl. Math.*, **20**, 53-65.

Sadat, T., R. Russell, M. Stewart (2014). Shifting paths of pharmaceutical innovation: Implications for the global pharmaceutical industry. *Int. J. Knowl. Innov. Entrep.,* **2**, 6-31.

Saltelli, A., S. Tarantola, F. Campolongo (2000). Sensitivity Analysis as an Ingredient of Modeling. *Stat. Sci*., **15**, 377–395.

Saltelli, A., M.Ratto, T. Andres, F. Campolongo, J. Cariboni, D.Gatelli, M. Saisana, S. Tarantola (2008). *Global Sensitivity Analysis: The Primer*. John Wiley and Sons, Ltd, Chichester, (U.K).

Schölkopf, B., S. Mika, C.J.C. Burges, P. Knirsch, Müller, G. Rätsch, , A.J. Smola (1999). Input space versus feature space in kernel-based methods. *IEEE T. Neural Networ.*, **10**, 1000–1016.

Simon L. L. *et al*., 2015. Assessment of Recent Process Analytical Technology (PAT) Trends: A Multiauthor Review, *Org. Process Res. Dev*., **19**, 3−62.

Singh, R., K. V. Gernaey and R. Gani (2010). An ontological knowledge based system for selection of process monitoring and analysis tools. *Computers Chem. Eng.*, **34**, 1137–1154.

Souihi, N., M. Josefson, P. Tajarobi, B. Gururajan, J. Trygg (2013). Design space estimation of the roller compaction process. *Ind. Eng. Chem. Res*., **52**, 12408–12419.

Stephanopoulos, G. and G. V. Reklaitis (2011). Process Systems Engineering: From Solvay to Modern Bio- and Nanotechnology: A History of Development, Successes and Prospects for the Future. *Chem. Eng. Sci*., **66**, 4272–4306.

Streefland, M., P.F.G. Van Herpen, B. Van de Waterbeemd, L.A. Van der Pol, E.C. Beuvery, J. Tramper, D.E. Martens, M. Toft (2009). A practical approach for exploration and modeling of the design space of a bacterial vaccine cultivation process. *Biotechnol. Bioeng*., **104**, 492–504.

Suresh, P. and P.K. Basu, (2008). Improving Pharmaceutical Product Development and Manufacturing: Impact on Cost of Drug Development and Cost of Goods Sold of Pharmaceuticals. *J. Pharm. Innov*., **3**, 175-187.

The Economist. *Quality manufacturing: a blockbuster opportunity for pharmaceuticals*. The Economist Intelligence Unit: London; 2005. Available at: http://graphics.eiu.com/files/ad_pdfs/eiu_ORACLE_PHARMA_WP.pdf (Last accessed 07/27/2015).

Thirunahari, S., P. Shan Chow and R.B.H. Tan (2011). Quality by Design (QbD)-based crystallization process development for the polymorphic drug tolbutamide. *Cryst. Growth Des.*, **11**, 3027-3038.

Tomba, E., M. Barolo and S. García-Muñoz (2012). General framework for latent variable model inversion for the design and manufacturing of new products. *Ind. Eng. Chem. Res*., **51**, 12886-12900.

Tomba, E. (2013). Latent Variable Modeling Approaches to Assist the Implementation of Quality-by-Design Paradigms in Pharmaceutical Development and Manufacturing. *PhD Thesis*, University of Padova (Italy)

Tomba, E., P. Facco, F. Bezzo, M. Barolo (2013a). Latent variable modeling to assist the implementation of Quality-by-Design paradigms in pharmaceutical development and manufacturing: A review. *Int. J. Pharm,* **457**, 283-297.

Tomba, E., P. Facco, F. Bezzo, S. García-Muñoz (2013b). Exploiting historical databases to design the target quality profile for a new product. *Ind. Eng. Chem. Res*. **52**, 8260–8271.

Tomba, E., M. Barolo, S. García-Muñoz (2014). In silico product formulation design through latent variable model inversion. *Chem Eng Res Des*, **92**,534–544.

Troup, G. M. and C. Georgakis (2013). Process Systems Engineering Tools in the Pharmaceutical Industry. *Comput. Chem. Eng.*, **51**, 157.

Valle, S., W. Li and S.J. Qin (1999). Selection of the number of principal components: the variance of the reconstruction error criterion with a comparison to other methods. *Ind. Eng. Chem. Res.*, **38**, 4389-4401.

Van der Voet, H. (1999). Pseudo-Degrees of Freedom for Complex Predictive Models: The Example of Partial Least Squares. *J. Chemom.*, **13**, 195.

Vanlaer, J., G. Gins, J. F. M. Van Impe (2013). Quality Assessment of a Variance Estimator for Partial Least Squares Prediction of Batch-End Quality. *Comput. Chem. Eng.*, **52**, 230.

Varmuza K., P. Filmozer (2009). Classification, Chapter 5. In*: Introduction to Multivariate Statistical Analysis in Chemometrics*. CRC press Taylor & Francis Group, Boca Raton, FL, U.S.A.

Vemavarapu, C., M. Surapaneni, M. Hussain, S. Badawy (2009). Role of Drug Substance Material Properties in the Processibility and Performance of a Wet Granulated Product. *Int. J. Pharm.*, **374**, 96.

Venkatasubramanian, V., C. Zhao, G. Joglekar, A. Jain, L. Hailemariam, P. Suresh, et al. (2006). Ontological informatics infrastructure for pharmaceutical product development and manufacturing. *Computers Chem. Eng*., **30**, 1482–1496.

Vogel, L. and W. Peukert (2005). From Single Particle Impact Behaviour to Modelling of Impact Mills. *Chem. Eng. Sci*., **60**, 5164–5176.

Wang H., Q. Liu, Y. Tu, (2005). Interpretation of partial least-squares regression models with VARIMAX rotation, *Comput. Stat. Data Anal.*, **48**, 207-219.

Wang, H., L. Xie, Z. Song (2012). A Review for Model Plant Mismatch Measures in Process Monitoring. *Chin. J. Chem. Eng*., **20**, 1039–1046.

Wassgren, C. and J. S. Curtis (2006). The application of computational modeling to pharmaceutical materials science. *MRS Bulletin*, **31**, 900–904.

Wise, B. M. and N. B. Gallagher (1996). The Process Chemometrics Approach to Process Monitoring and Fault Detection. *J. Process Control*, **6**, 329–348.

Wise, B.M., N.B. Gallagher, R. Bro, J.M. Shaver, W. Windig and R. Scott Koch (2006). *PLS_Toolbox Version 4.0 for use with MATLAB™*. Eigenvector Research, Inc., Wenatchee, WA (U.S.A.).

Wold, H. (1966). Estimation of principal components and related models by iterative least squares. In *Multivariate analysis*, Academic Press Limited, New York (U.S.A.).

Wold, S. (1978). Cross-validatory estimation of the number of components in factor and principal component models. *Technometrics*, **20**, 397-405.

Wold, S., H. Martens and H. Wold (1983). The multivariate calibration problem in chemistry solved by the PLS method. *Lecture Notes in Math.*, **973**, 286-293.

Woo, X.Y., R.B.H. Tan and R.D. Braatz (2009). Modeling and computational fluid dynamics - population balance equation - micromixing simulation of impinging jet crystallizers. *Cryst. Growth Des.*, **9**, 156-164.

Woodcock J., (2013). FDA Check Up: Drug Development and Manufacturing Challenges. Available at: http://www.fda.gov/NewsEvents/Testimony/ucm378343.htm (Last accessed 26/01/2016).

Yacoub, F. and J.F. MacGregor (2004). Product optimization and control in the latent variable space of nonlinear PLS models. *Chemom. Intell. Lab. Syst.*, **70**, 63-74.

Yacoub, F. and J.F. MacGregor (2011). Robust processes through latent variable modeling and optimization. *AIChE J.*, **57**, 1278-1287.

Ye, J. (1998). On Measuring and Correcting the Effects of Data Mining and Model Selection. *J. Am. Stat. Assoc.*, **93**, 120.

Yu, L. X., G. Amidon, M. A. Khan, S. W. Hoag, J. Polli, G. K. Raju, J. Woodcock (2014). Understanding Pharmaceutical Quality by Design. *The AAPS Journal*, **16**, 771-783.

Yu L. X. and J. Woodcock (2015). FDA pharmaceutical quality oversight. *Int. J. Pharm.*, **491**, 2-7.

Zacour, B.M., J.K. Drennen III and C.A. Anderson (2012a). Development of a statistical tolerance-based fluid bed drying design space. *J. Pharm. Innov.*, **7**, 151-162.

Zacour, B.M., J.K. Drennen III and C.A. Andreson (2012b). Development of a fluid bed granulation design space using critical quality attribute weighted tolerance intervals. *J. Pharm. Sci.*, **101**, 2917-2929.

Zhang, L. and S. García-Muñoz (2009). A Comparison of Different Methods to Estimate Prediction Uncertainty Using Partial Least Squares (PLS): A Practitioner's Perspective. *Chemom. Intell. Lab. Syst.*, **97**, 152.

Zomer, S., M. Gupta and A. Scott (2010). Application of multivariate tools in pharmaceutical product development to bridge risk assessment to continuous verification in a quality by design environment. *J. Pharm. Innov.*, **5**, 109-118.

Acknowledgements

There are many people to whom I would like to express my gratitude for their support and/or contribution to this project during these three years.
First, I would like to thank my supervisor, Prof. Massimiliano Barolo, for his guidance, support, encouragement, and especially for his patience. He helped me in my scientific, as well as, in my professional and personal growth. I am also grateful to Prof. Fabrizio Bezzo and Dr. Pierantonio Facco, for all the helpful discussions that enriched this Dissertation, which would not have been possible without their fundamental contribution.
Thanks to Dr. Sean Bermingham for his support during my visit at Process Systems Enterprise, and to all the kind colleagues I had the chance to meet and work with there. I am especially grateful to Dr. David Slade, for his patience and his assistance in this work.
Thanks to Dr. Simeone Zomer for his support and enthusiasm during our collaboration.

Un enorme grazie a tutti gli amici del Cape-Lab e non: Riccardo, Andrea e Junaid, i migliori compagni d'ufficio di sempre, grazie per la pazienza e lunghi e fruttuosi discorsi; Myriam, grazie per il tuo entusiasmo e la capacità di farci sentire tutti uniti; Filippo, grazie non solo per il tuo contributo in questa tesi, ma anche per darmi sempre un motivo per una genuina risata; Pierantonio (di nuovo), grazie per tutte le nostre discussioni e per il grande esempio che mi offri ogni giorno; grazie ad Amir, per il suo contributo in questo lavoro, e a tutti gli studenti del Cape-Lab. Grazie a Chiara, Elena, Barbara, Elia, Ricardo, Martina e a tutti i magnifici amici che mi hanno accompagnato in questa esperienza. Grazie a Matteo ed Emanuele, il vostro esempio è stato molto utile per la mia formazione.

Grazie a Elisa e Mario, il vostro supporto e la vostra comprensione sono stati fondamentali in questa esperienza. Grazie a Romina, Patrick e Grace, perché mi avete sempre fatto sentire la vostra presenza e il vostro supporto.

Infine grazie Federico, non potevo trovare persona migliore per affrontare piccole e grandi sfide di ogni giorno.